Dissertation
submitted to the
Combined Faculties of the Natural Sciences and Mathematics
of the Ruperto-Carola-University of Heidelberg,
Germany
for the degree of
Doctor of Natural Sciences

Put forward by
Shahpoor Saeidian
born in Bijar (Iran)
Oral examination: June 18th 2008

Scattering resonances of ultracold atoms in confined geometries

Referees: Prof. Dr. Peter Schmelcher
Prof. Dr. Jochen Schirmer

Zusammenfassung

Streuresonanzen ultrakalten Atomen in eingeschlossen Geometrien

Thema dieser Doktorarbeit ist sowohl die Untersuchung der Dynamik im quantenmechanischem Regime von ultrakalten Atomen in eingeschlossen Geometrien. Wir diskutieren das Verhalten von Grundzustandsatomen in einem dreidimensionalen magnetischen Quadrupolfeld. Solche Atome können für schwache Felder näherungsweise wie neutrale Punktteilchen betrachtet werden. Ergänzend zu den bekannten Resonanzen für positive Energien weisen wir die Existenz kurzlebiger Resonanzen im negativen Energiebereich nach, wobei letztere ihren Ursprung in einer fundamentalen Symmetrie des zugrundeliegenden Hamilton-Operators haben. Desweiteren leiten wir eine Abbildung für die beiden Zweige des Spektrums ab. Außerdem analysieren wir die atomaren Hyperfeinresonanzen in einem magnetischen Quadrupolfeld. Dies entspricht dem Fall, für welchen sowohl die Hyperfein- als auch Zeemanwechselwirkung von vergleichbarer Größenordnung sind und beide berücksichtigt werden müssen. Schließlich entwickeln wir für die Mehrkanalstreuung von zwei Atomen in einem zweidimensionalen harmonischen Einschluss eine allgemeine Gittermethode. Mit unserem Ansatz analysieren wir transversale An-/Abregungen im Zuge von Streuprozessen (unterscheidbare oder identische Atome), wobei alle wichtigen Partialwellen und deren Kopplung aufgrund von gebrochener Kugelsymmetrie in Betracht gezogen werden. Besondere Aufmerksamkeit wird einer nicht-triviale Erweiterung der CIR-Theorie gewidmet, welche ursprünglich nur für das Einmodenregime und den Grenzfall der Grundzustandsenergie entwickelt wurde.

Abstract

Scattering resonances of ultracold atoms in confined geometries

Subject of this thesis is the investigation of the quantum dynamics of ultracold atoms in confined geometries. We discuss the behavior of ground state atoms inside a 3D magnetic quadrupole field. Such atoms in enough weak magnetic fields can be approximately treated as neutral point-like particles. Complementary to the well-known positive energy resonances, we point out the existence of short-lived negative energy resonances. The latter originate from a fundamental symmetry of the underlying Hamiltonian. We drive a mapping of the two branches of the spectrum. Moreover, we analyze atomic hyperfine resonances in a magnetic quadrupole field. This corresponds to the case for which both the hyperfine and Zeeman interaction, are comparable, and should be taken into account. Finally, we develop a general grid method for multichannel scattering of two atoms in a two-dimensional harmonic confinement. With our approach we analyze transverse excitations/deexcitations in the course of the collisional process (distinguishable or identical atoms) including all important partial waves and their couplings due to the broken spherical symmetry. Special attention is paid to suggest a non-trivial extension of the CIRs theory developed so far only for the single-mode regime and zero-energy limit.

CONTENTS

1. INTRODUCTION AND OUTLINE OF THE THESIS

1.1 Introduction

Ultracold atomic gases offer a wealth of opportunities for studying quantum phenomena at mesoscopic and macroscopic scales [64, 65, 66, 67, 68]. Laser and evaporative cooling in conjunction with the application of magnetic and/or electric fields allows for a precisely control over the external atomic degree of freedom below temperatures of one micro-Kelvin. Eventually, this makes it possible experimental observation of some fascinating phenomena, Bose-Einstein-Condensation (BEC) of alkali-metal atoms being one of the most prominent examples [64, 65, 68, 67]. The resulting coherent matter waves exhibit a wealth of intriguing properties and phenomena ranging from nonlinear excitation such as solitons and vortices to an amazingly controllable and beautiful many-body dynamics. The later manifests itself e.g. in the recently discovered Mott-insulator phase transition [91] and BEC-BCS crossover [92].

Ultracold atomic gases, have also shown their potential for modelling solid states systems. Periodic potentials which are usually found in crystalline matter can be mimicked by optical lattices [91]. Gauge potentials which are reminiscent of electromagnetic field coupling can be introduced into the many-body Hamiltonian by rotating the atomic gases [98]. Moreover, the capability of adjusting the two-body coupling via Feshbach resonances [99] allows for modelling any kind of many-particle Hamiltonian.

The possibility to control over the properties of many-body systems has opened a new opportunity for studying and understanding of many-body phenomena in solid state physics, such as quantum-phase transition [91, 56], the quantum Hall effect [100, 98] or the BEC-BCS crossover [92]. The latter takes place in gases of fermionic atoms, which depending on their mutual interaction, either form Bose-Einstein condensate (BEC) of tightly bound molecules or strongly correlated Cooper pairs (BCS-regime), a regime which has also been found within superconductors although it is hidden from the view of the outside world.

Ultracold atom gases also display interesting features of many-body systems when their dynamics are confined to one-dimension. By employing optical dipole traps [15] and atom chips [16, 17, 18] it is possible to fabricate mesoscopic structures in which the atoms are freezed to occupy a single or a few lowest quantum states of a confining potential such that in one or more dimensions the characteristic length possesses the order of the atomic de Broglie wavelength. These configurations can be well described by effective one-dimensional sys-

tems. Well-known examples are quantum wires and atom waveguides or quasi two-dimensional systems such as 2D electronic gases. The quantum dynamics of such systems is strongly influenced by the geometry of the confinement. These systems are expected to play an important role for example in Atom Interferometries, Quantum Computing applications, ultrasensitive detectors of accelerators , and gravitational anomalies as well as to provide an opportunity to study novel 1D many-body states.

The spin-statistics theorem, according to which identical particles with integer spin are bosons whereas those with half-integer spin are fermions, breaks down in low-dimensional systems. The "Fermi-Bose duality" which is a very general property of identical particles in 1D, maps strongly interacting bosons to weakly-interacting fermions and vice versa. In recent years this esoteric subject has become highly relevant through experiments on ultracold atomic vapors in atom waveguides.

Almost all phenomena discussed above are outcome of scattering events. This explain the importance of studying quantum scattering theory in these systems. Of particular interests are the scattering resonances. In Ref. [1], the resonance has been defined as the *most striking phenomenon in the whole range of scattering experiments*. When the lifetime of the particle-target system in the region of interaction is larger than the collision time in a direct collision process we call the phenomenon a resonance phenomenon. Scattering theory in confined geometries are completely different from the free space. In a confined geometry we may observe some resonances leading to strange phenomena which never happen in free space. For example, two particles with strong coupling in free space may pass through without any interaction in a confined geometry. This stimulated the development of quantum scattering theory in confined geometries.

The work in this thesis studies scattering resonances in confined geometries in low-energy limit.

1.2 Outline of the Thesis

In this work we study scattering resonances of atoms in confined geometries including 3D magnetic quadrupole field as well as 2D harmonic confining potential.

Atom waveguides or 2D optical latices are well-known examples of quasi-1D systems, which are very applicable in quantum optics, especially to produce 1D Bose-Einstein condensate. These systems can be approximated for example by assuming a 2D transverse potential (harmonic or unharmonic) as a confinement, while along the third dimension the particles move freely.

Inhomogeneous fields (e.g., 3D magnetic quadrupole field) is another example which find its application in ultracold atomic physics for the purpose of trapping and confinement.

The basic idea behind the control of ultracold atoms via inhomogeneous magnetic fields is very simple. The neutral atoms couple to the magnetic field

via their magnetic moment. In the case of enough weak gradient field, when the spatial variations of the field is small enough, it can be considered homogeneous over the size of an atom, therefore the atom can be assumed as a point-like particle. For ground state atoms, this assumption is in general justified.

In the case of strong hyperfine interactions (compared to the magnetic interactions) the atomic magnetic moment is due to the total angular momentum (being composed of the electronic and nuclear angular momentum), which remains constant. Therefore the atom can be treated as a point-like particle with total angular momentum $\mathbf{F}$. However, in the case of small hyperfine interactions and/or strong gradient fields (e.g., for electronically excited atoms) this simplification fails and an admixture of different hyperfine states F due to the field interaction has to be expected. In this case F is not a constant of motion.

The thesis is divided into three parts. The first part is dedicated to give an overview of scattering theory in free space, which is necessary to describe the systems considered in next parts, along with the numerical methods which have been used during this work.

In part II we study scattering of two particles under a 2D confining potential. Chapter 4 gives an overview of the works which have been done already to describe such systems. In chapter 5 we develop a general grid method for multichannel scattering of two atoms confined by a transverse harmonic potential. the method allows us to consider a rich spectral structure where several different partial waves are participating in the scattering process. With our approach we analyze transverse excitations and deexcitations in the course of the collisional process (distinguishable or identical) including all important partial waves and their coupling due to the broken spherical symmetry. Special attention is paid to the analysis of the CIRs in the multimode regimes for non-zero collision energies, i.e., to suggest a non-trivial extension of the CIRs theory developed so far only for the single-mode regime and zero-energy limit.

In part III we analyze quantum dynamics of atoms in a magnetic quadrupole field. Chapter 6 gives an overview of the quadrupole magnetic field, and the works which have been done already to analyze the dynamics of atoms in such a field. In chapter 7 we present an analysis of the quantum dynamics of ground state atoms in magnetic quadrupole fields. The internal atomic structure is not resolved and consequently the atoms can be treated as if they were neutral fermions or bosons. Complementary to the well-known positive energy resonances, it is shown that there exist short-lived negative energy resonances, which originate from a fundamental symmetry of the underlying Hamiltonian. We drive a mapping of the two classes. In chapter 8 we study the case for which both interactions, the hyperfine and the field interaction, have to be taken into account on equal level for the description of the neutral atoms in the field. We focus on atoms possessing a single active valence electron with spin $S = 1/2$ and a nucleus with spin $I = 3/2$.

Part I

SCATTERING THEORY AND NUMERICAL METHODS

2. SCATTERING THEORY: A BRIEF REMINDER

Probably much of our information about the interaction between particles being derived from scattering experiments. In this chapter we study in brief the scattering theory and derive some important relations which will be needed in the next chapters. Here we follow [1-4].

Let us consider an experiment in which a particle is scattered from a target. The particle can be, for example, an electron, an elementary particle, an atom or a molecule and the target can be a nucleus, an atom, a molecule, a flat or curved surface. In an *elastic* scattering experiment the energy of the particle is conserved. In a *non-elastic* scattering experiment there is an energy exchange between the particle and intrinsic degrees of freedom of the target, and the final energy of the particle in its *out* asymptote limit can be smaller or larger than the initial energy of the particle in its *in* asymptote limit. In a *reactive* scattering experiment the particle and the target undergo a change during the rearrangement collision and become different species. The time-dependent description of quantum scattering has a natural and instructive parallel in classical mechanics and we begin with a first description of this classical theory. Figure 2.1 shows a typical classical scattering of a particle by some fixed target. Even in the simple case of elastic scattering three possibilities may be considered. The first possibility, presented in Fig. 2.1(a), is that of a particle which comes in from infinity, gets caught in a spirally orbit and never emerges out of the attractive potential well. As time passes the potential energy of the trapped particle drops down to $-\infty$ whereas the kinetic energy increases to $+\infty$. This *black hole* phenomenon is avoided when the interaction potential at the origin is less attractive than $V(r) = -r^{-2}$.

In order to obtain a free particle in the *in* and *out* asymptotes, $V(r)$ should fall of quicker than r^{-3} at infinity. A direct scattering event is illustrated in Fig. 2.1(b). One should add to these two, a 3^{th} possibility, that is, due to multiple-scattering events, the particle is temporarily trapped by the target [Fig. 2.1(c)]. When the lifetime of the particle-target system in the region of interaction is larger than the collision time in the direct collision process we call the phenomenon a resonance phenomenon.

If the potential fall off faster than r^{-3} at infinity, the trajectory can be roughly divided into three parts: (1) the approach of the particle along an almost straight orbit until it reaches its region of interaction with the target, (2) the possibly very complicated orbit and (3) the departure of the particle along some other approximately straight orbit.

Although these three divisions are only roughly defined, it is clear that, in

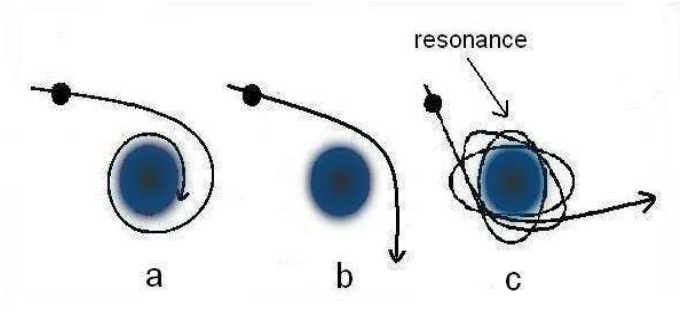

Fig. 2.1: Different possible scattering orbits.

atomic scales, the region of interaction is certainly no longer than a few atomic diameters and so is, in practice, completely unobservable. All that will be visible is a pair of straight tracks corresponding to the free motion before and after the collision. Therefore, in seeking a mathematical description of the scattering process, we shall try (as far as possible) to suppress the precise details of the orbit in the neighborhood of the target and concentrate on the relation between the asymptotically free incoming and outgoing trajectories.

For every *in* or *out* asymptote, one may reasonably expect there will be a corresponding actual orbit $X(t)$. Although our principal interest is in the *in* and *out* asymptote, we must recognize that the correspondence between them is defined by the actual orbit, that is, the correspondence has the form

$$\begin{aligned} X(t) &\xrightarrow[t \to -\infty]{} X_{in}(t) \\ X(t) &\xrightarrow[t \to +\infty]{} X_{out}(t) \end{aligned} \tag{2.1}$$

Although the condition of asymptotic free motion is expressed mathematically by the limits t tends to infinity, this does not mean that one really has to wait an infinite time to observe the asymptotic, free motion. Quite the contrary; even for a very slow projectile (e.g., a thermal neutron) incident on a large target (some big molecule) the total collision time will normally not exceed $10^{-10}s$; this means that if the collision is centered on $t = 0$ then for times before $t \approx -10^{-10}s$ and after $t \approx 10^{-10}s$ the motion is experimentally indistinguishable from free motion; that is in practice t becomes *infinite* at $t \approx \pm 10^{-10}s$. The reason is that, for any given orbit, even if there is no finite time beyond which $X(t)$ is exactly equal to $X_{out}(t)$, nevertheless our measuring devices have some minimum resolutions, and there is a finite time beyond which the difference between $X(t)$ and $X_{out}(t)$ is smaller than we can resolve.

In our discussion of quantum scattering we shall establish limits that are to be interpreted in exactly the same way - that for times more than some small amounts (usually $10^{-10}s$ or less) before or after the collision, the motion is experimentally indistinguishable from free motion.

In the following the scattering of a single particle in free space by a fixed target situated at the origin (or equivalently relative motion of two-body colli-

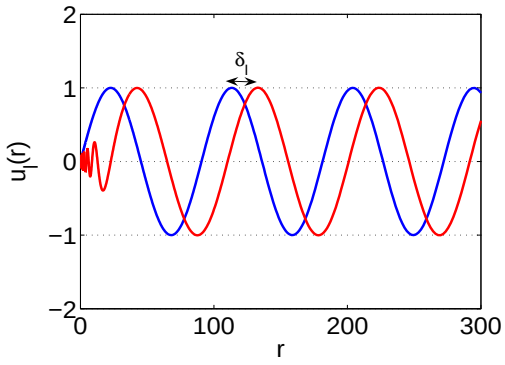

Fig. 2.2: The effect of the short-range scattering potential on the radial function u_l.

sion in the center of mass frame) will briefly be discussed. For more details, we refer the reader to appendices A and B.

2.1 Scattering by a Spherical Potential

Scattering by a spherical potential probably is one of the easiest example of 3D scattering. In this case the scattering potential $V(r)$ depends only on the magnitude of the distance between the particle and the target. Since no internal degrees of freedom of the particle and/or target can be excited by such an interaction, they may be ignored. Only *elastic* scattering will be possible in this model.

The time-independent Schrödinger equation, in spatial representation looks like

$$\frac{\hbar^2}{2\mu}\nabla^2\psi(\mathbf{x}) + [E - V(r)]\psi(\mathbf{x}) = 0 \tag{2.2}$$

It is convenient to consider a restricted class of potentials that vanish [or at least become negligible compared to the centrifugal term $\hbar^2 l(l+1)/2\mu r^2$] for $r > a$. This does not include e.g. Coulomb potential, for which $V(r) \propto r^{-1}$, requires some special treatment.

If the scattering potential were identically zero, the unique (apart from normalization) solution would be

$$\psi(\mathbf{x}) = \psi_{in}(\mathbf{x}) = e^{i\mathbf{k}\cdot\mathbf{x}} = \sum_l (2l+1) i^l j_l(kr) P_l(\cos\theta) \tag{2.3}$$

where $k = |\mathbf{k}| = \sqrt{2\mu E/\hbar^2}$, j_l is a spherical Bessel function, P_l is a Legendre polynomial, and θ is the angle between $\mathbf{k}$ and $\mathbf{x}$. Considering the solution to Schrödinger equation (2.2), including the scattering potential, for scattering of an incoming plane wave, the total wave function beyond the range of the

potential has the form

$$\psi_{\mathbf{k}}(\mathbf{x}) = e^{i\mathbf{k}\cdot\mathbf{x}} + f(k,\theta,\varphi)\frac{e^{ikr}}{r} \tag{2.4}$$

where $f(k,\theta,\varphi)$ is the scattering amplitude which for a spherical symmetric potential is given by (see appendix A)

$$f(k,\theta,\varphi) = f(k,\theta) = -\frac{\mu}{2\pi\hbar^2}\int d^3x' e^{-i\mathbf{k}_f\cdot\mathbf{x}'}V(r')\psi_{\mathbf{k}}(\mathbf{x}'),\ \mathbf{k}_f = k\widehat{\mathbf{x}} \tag{2.5}$$

Let us write the full solution in the form

$$\psi(\mathbf{x}) = \sum_l (2l+1)i^l A_l R_l(kr)P_l(\cos\theta) \tag{2.6}$$

where the radial function $R_l(r)$ satisfies the partial wave equation

$$\frac{\hbar^2}{2\mu}\frac{1}{r^2}\frac{d}{dr}r^2\frac{d}{dr}R_l(r) + \left[E - V(r) - \frac{\hbar^2}{2\mu}\frac{l(l+1)}{r^2}\right]R_l(r) = 0 \tag{2.7}$$

For $r > a$, where $V(r) = 0$, the solution of (2.7) must be a linear combination of spherical Bessel functions $j_l(kr)$ and $n_l(kr)$, we shall write as

$$R_l(r) = \cos\delta_l j_l(kr) - \sin\delta_l n_l(kr), \quad r \geq a \tag{2.8}$$

Since the differential equation is real, the solution $R_l(r)$ may be chosen real, and so δ_l is real.

The asymptotic forms of the spherical Bessel functions in the limit $kr \to \infty$ are

$$j_l(kr) \to \frac{\sin(kr - \frac{1}{2}\pi l)}{kr} \tag{2.9}$$

$$n_l(kr) \to \frac{-\cos(kr - \frac{1}{2}\pi l)}{kr} \tag{2.10}$$

Therefore the corresponding limit of $R_l(r)$ is

$$R_l(r) \to \frac{\sin(kr - \frac{1}{2}\pi l + \delta_l)}{kr} \tag{2.11}$$

If the scattering potential were exactly zero, the form (2.11) would be valid all the way to $r = 0$. But the function $n_l(kr)$ has a singularity at $r = 0$, which is not allowed in a state function, so we would have $\delta_l = 0$ if $V(r) = 0$ for all r. Comparing the asymptotic limit of the zero-scattering solution $j_l(kr)$, with (2.11), we see that the only effect of the short-range scattering potential that appears at large r is the phase shift of the radial function by δ_l (see Fig. 2.2). Since the differential cross section is entirely determined by the asymptotic form of the state function, it follows that the cross section must be expressible in terms of these phase shifts.

If we substitute the series (2.3) and (2.6) into (2.4) , and replace the Bessel functions with their asymptotic limits, we obtain

$$\sum_l (2l+1) i^l P_l(\cos\theta) A_l \frac{\sin(kr - \frac{1}{2}\pi l + \delta_l)}{kr} = \sum_l (2l+1) i^l P_l(\cos\theta) \times \frac{\sin(kr - \frac{1}{2}\pi l)}{kr} + \frac{f(k,\theta) e^{ikr}}{r} \quad (2.12)$$

By using $\sin x = \frac{e^{ix} - e^{-ix}}{2i}$ and equating the coefficients of e^{-ikr} in the above equation one obtains

$$\sum_l (2l+1) i^l P_l(\cos\theta) A_l e^{i(\frac{1}{2}\pi l - \delta_l)} = \sum_l (2l+1) i^l P_l(\cos\theta) e^{i\frac{1}{2}\pi l}. \quad (2.13)$$

This equality must hold term by term, since the Legendre polynomials are linearly independent, so we have

$$A_l = e^{i\delta_l}. \quad (2.14)$$

Equating the coefficients of e^{ikr} in (2.13) and using (2.14) then yields

$$f(k,\theta) = \sum_l (2l+1) f_l(k) P_l(\cos\theta) \quad (2.15)$$

Here the partial amplitude f_l is defined as

$$f_l(k) = \frac{e^{i\delta_l(k)} \sin\delta_l(k)}{k} = \frac{1}{k\cot\delta_l(k) - ik} \quad (2.16)$$

The phase shift δ_l for a scattering potential $V(r)$ that may be nonzero for $r < a$, but which vanishes for $r > a$, is obtained by solving (2.7) for the radial function $R_l(r)$ in the region $r \leq a$ and matching it to the form (2.8) at $r = a$. There are two linearly independent solutions to (2.7), but only one of them remains finite at $r = 0$; so the solution for $R_l(r)$ in the interval $0 \leq r \leq a$ is unique except for normalization. At $r = a$ both R_l and $\frac{dR_l}{dr}$ must be continuous. For our purposes it is sufficient to impose continuity on the logarithmic derivative, $\frac{d}{dr} log(R_l) = \frac{1}{R_l}\frac{dR_l}{dr}$ which is independent of the arbitrary normalization. This yields the condition

$$\gamma_l = \frac{k[\cos\delta_l j_l'(ka) - \sin\delta_l n_l'(ka)]}{\cos\delta_l j_l(ka) - \sin\delta_l n_l(ka)} \quad (2.17)$$

where a prime indicates differentiation of a function with respect to its argument, and γ_l denotes the logarithmic derivative evaluated at $r = a$ from the interior. The phase shift is then given by

$$\tan\delta_l = \frac{kj_l'(ka) - \gamma_l j_l(ka)}{kn_l'(ka) - \gamma_l n_l(ka)} \quad (2.18)$$

If the scattering potential is not identically zero for $r > a$, but is still of *short range*, it is possible to define phase shifts as the limit of (2.17) as $a \to \infty$,

remembering that γ_l depends on a. This limit will exist provided the potential falls off more rapidly than r^{-1}.

It has been shown that for sufficiently large values of l the phase shift δ_l decreases as the reciprocal of the factorial of l (see [3], Sec.19). This is very rapid decrease, being faster than exponential, and it is ensures that series (2.15) is convergent. However this *sufficiently large* value of l may be very large, and the phase shift series is practical only if it converges in a small number of terms. It can be shown that the phase shift δ_l will be small provided that $ka \ll l$. Therefore the real usefulness of the phase shift series is for the case $ka \ll l$ and lies, in the fact that while only the complete set $\{\delta_l\}$ gives an *exact* description of the scattering process, in practice the sum in (2.15) has significant contributions from merely a few waves. Practically, this is clear since higher partial waves are expelled from the core by the centrifugal barrier. They are only able to penetrate and hence "feel" the potential if their momentum k is large enough. Hence this method applies to low-energy scattering in the first place.

2.2 Cross Section

The angular distribution of scattered particles in a particular process is described in terms of a *differential cross section*. Suppose that a flux of J_{in} particles per unit area per unit time is incident on the target. The number of particles per unit time scattered into a narrow cone of solid angle $d\Omega$, outside the incident beam centered about a direction specified by the angles θ and φ, at a sufficiently large distance r from the target, is proportional to the incident flux J_{in} and it might be written as $J_{in}d\sigma(\theta,\varphi)$. Dividing this number by the area of the solid angle $d\Omega$, we obtain the flux of scattered particles in the direction (θ,φ),

$$J_{out} = J_{in}\frac{d\sigma(\theta,\varphi)}{r^2 d\Omega} \tag{2.19}$$

The factor $d\sigma/d\Omega$ is known as the differential cross section, and can be written as

$$\frac{d\sigma}{d\Omega}(\theta,\varphi) = \frac{r^2 J_{out}}{J_{in}} \tag{2.20}$$

from which it is apparent that it has the dimension of an area. Its value is independent of the distance r from the target, because J_{out} is inversely proportional to r^2. This expression is convenient because the fluxes J_{out} and J_{in} are measurable quantities and can be calculated theoretically. The probability flux is given by

$$\mathbf{J} = \frac{\hbar}{\mu} Im(\psi^* \nabla \psi) \tag{2.21}$$

The incident beam can be described by $\psi_{in} = Ae^{i\mathbf{k}\cdot\mathbf{x}}$, for which the flux

$$\mathbf{J}_{in} = |A|^2 \frac{\hbar\mathbf{k}}{\mu} \tag{2.22}$$

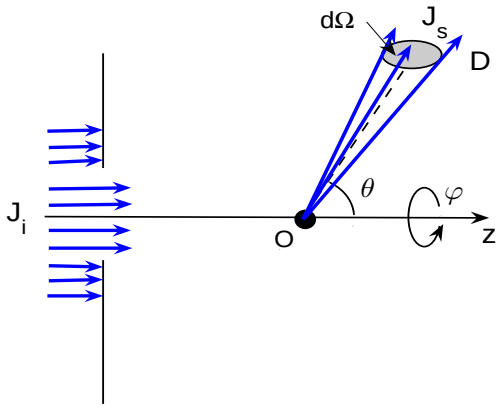

Fig. 2.3: The scattering of a beam of particles by a target situated at the origin O.

is uniform. The outgoing spherical wave at large r has the asymptotic form $\psi_{out} = Af(k,\theta,\varphi)e^{ikr}/r$, for which the radial component of the flux is

$$(\mathbf{J}_{out})_r = \frac{\hbar}{\mu} Im(\psi_s^* \frac{\partial \psi_{out}}{\partial r}) = |A|^2 \frac{\hbar k}{\mu} \frac{|f(k,\theta,\varphi)|^2}{r} \tag{2.23}$$

Substituting (2.22) and (2.23) into (2.20) yields the differential cross section to be

$$\frac{d\sigma}{d\Omega}(\theta,\varphi) = |f(k,\theta,\varphi)|^2 \tag{2.24}$$

Since we have neglected any internal degrees of freedom of the particles, we have implicitly restricted our solution to the case of *elastic scattering*. The result (2.24) will be modified when we treat inelastic scattering.

The total cross-section is defined as

$$\sigma = \int \frac{d\sigma}{d\Omega} d\Omega \tag{2.25}$$

For spherically symmetric potential we have

$$\begin{aligned} \sigma &= 2\pi \int_0^\pi |f(k,\theta)|^2 \sin\theta d\theta \\ &= 2\pi \int_0^\pi |\sum_{l=0}^{\infty} (2l+1) f_l(k) P_l(\cos\theta)|^2 \sin\theta d\theta \end{aligned} \tag{2.26}$$

Now using the normalization of the Legendre polynomials

$$\int_0^\pi [P_l(\cos\theta)]^2 \sin\theta d\theta = \frac{2}{2l+1} \tag{2.27}$$

we obtain for the total cross section

$$\begin{aligned}\sigma &= 4\pi \sum_{l=0}^{\infty} (2l+1)|f_l(k)|^2 \\ &= \frac{4\pi}{k^2} \sum_{l=0}^{\infty} (2l+1)\sin^2\delta_l \end{aligned} \tag{2.28}$$

so the total cross section is the sum of the cross-section for each l. It is easy to prove the *optical theorem* for a spherically symmetric potential: Just take the imaginary part of each side of (2.15) at $(\theta = 0)$, and using $P_l(1) = 1$ we obtain

$$Imf(k, \theta = 0) = \frac{1}{k} \sum (2l+1)\sin^2\delta_l(k) \tag{2.29}$$

or

$$\sigma = \frac{4\pi}{k} Imf(k, \theta = 0) \tag{2.30}$$

2.3 Low Energy Scattering

The potential in the radial Schrödinger equation (2.7) is for s-wave $(l = 0)$ only the interaction potential $V(r)$, whereas for other partial waves, this potential is superimposed with the centrifugal barrier $\hbar^2 l(l+1)/2\mu r^2$. At low energies (the energy E has to be lower than the resulting barrier) partial waves for higher l are not important. Classically this is clear, because a particle at such low energies will not penetrate the barrier, but simply be reflected by it and therefore the potential inside has no effect. Thus we expect qualitatively that the scattering due to $V(r)$ goes to zero for all partial waves $l \neq 0$, when the energy is sufficiently low. We can expand (2.18) for low energy, i.e., small k, using the behavior of $j_l(x)$ and $n_l(x)$ for $x \to 0$

$$j_l(x) \approx \frac{x^l}{(2l+1)!!},\ n_l(x) \approx \frac{(2l-1)!!}{x^{l+1}} \tag{2.31}$$

where $(2l+1)!! = 1.3.5. \cdots .(2l+1)$ such that we obtain for $k \to 0$

$$\tan\delta_l(k) \approx \frac{(2l+1)}{[(2l+1)!!]^2} \frac{l - a\gamma_l}{l+1+a\gamma_l} (ka)^{2l+1} \tag{2.32}$$

If we also take the expansion of the tangent into account, we will obtain

$$\delta_l(k) \propto k^{2l+1} \pmod{\pi} \quad \text{when } k \to 0 \tag{2.33}$$

This is known as *threshold behavior* and makes it clear that at low energy, with a potential, which decreases rapidly enough, partial waves with $l \geq 1$ do not contribute to the scattering process. We have pure s-wave scattering. Now we consider extremely low energies $(k \approx 0)$. Outside the range of the potential the radial Schrödinger equation (2.7) satisfies

$$\frac{d^2u}{dr^2} = 0 \tag{2.34}$$

where we took for simplicity $rR_{k=0,l=0}(r) = u_{k=0,l=0}(r) \equiv u(r)$. The solution of this equation is

$$u(r) = \text{const}(r - a_0) \tag{2.35}$$

On the other hand, the usual asymptotic wavefunction for the $l = 0$ case, is

$$u_{k,l=0} = rR^{>}_{k,l=0}(r) \propto \sin(kr + \delta_0) \tag{2.36}$$

Noting that

$$\lim_{k\to 0} \sin(kr + \delta_0) = \lim_{k\to 0} \sin\left[k\left(r + \frac{\delta_0}{k}\right)\right] \approx k\left(r + \frac{\delta_0}{k}\right) \tag{2.37}$$

which looks like (2.35) - for low energies $\delta_0(k) \propto k$ such that $\delta_0(k)/k$ =const - and therefore we can understand (2.35) as an infinitely long wavelength limit of the usual outside wavefunction (2.36). Furthermore we have

$$\frac{u'_{k,l=0}}{u_{k,l=0}} = k \cot\left[k\left(r + \frac{\delta_0}{k}\right)\right] \tag{2.38}$$

If we expand this quantity for very small k and then set $r = 0$, we obtain

$$\lim_{k\to 0} k \cot \delta_0(k) = -\frac{1}{a_0} \tag{2.39}$$

where the quantity a_0 is called the *scattering length*. A better result can be obtained by keeping the next term in this expansion

$$k \cot \delta_0(k) \approx -\frac{1}{a_0} + \frac{1}{2} R_0 k^2 \tag{2.40}$$

Here R_0 is called the effective range of the potential.

The physical meaning of the scattering length a_0 is clear. The asymptotic wave function (2.36) has a series of zeros $r_n(k) = (-\delta_0(k) + n\pi)/k$, $n = 0, \pm 1, \pm 2, \cdots$. When k goes to zero, all $r_n(k)$ go to $\pm\infty$, except for one which tends to a_0 (which can be either positive or negative).

Figure 2.4 shows the s-wave scattering length a_0 as a function of the potential depth for the screened Coulomb potential

$$V(r) = -\frac{V_0}{r} e^{-r} \tag{2.41}$$

When the potential has no bound state, as illustrated in Fig. 2.5, a repulsive potential gives $a > 0$ [Fig. 2.5(a)], and an attractive potential gives $a < 0$ [Fig. 2.5(b)]. When there are bound states in an attractive potential, however, the scattering length can be positive or negative [Fig. 2.5(d-f)]. If we increase continuously the well depth, we find that the scattering length goes to infinity in some discrete values of V_0. Each divergence corresponds to appearance of a bound state (Levinson theorem). When V_0 is slightly lower than the threshold for the appearance of a new bound state, the scattering length is large and

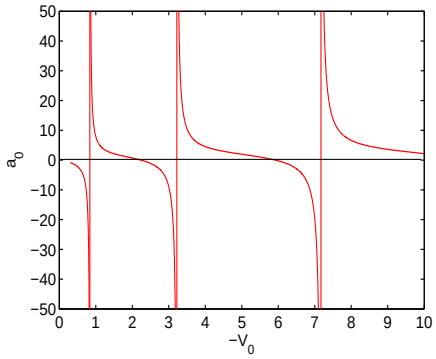

Fig. 2.4: S-wave scattering length as a function of the potential depth V_0 for the potential (4.111).

negative [Fig. 2.5(c)]; while if V_0 is slightly larger than this threshold, it is large and positive [Fig. 2.5(d)]. The above results are quite general and can be shown for other kind of potentials.

One of the exciting recent developments in ultracold atomic physics is that the scattering length can be tuned, from $-\infty$ to $+\infty$, by changing an external magnetic field, through the Feshbach resonance [7]. This realizes the usual thought experiment of changing the coupling constant in the Hamiltonian.

It should be emphasized that a is a parameter that describes scattering in 3D in the limit of zero energy, where the shape of the potential is irrelevant. At higher energies, the shape of the potential does make a difference, and one must include other parameters, such as the effective range.

We can obtain another relation for scattering length which is useful for identifying the scattering amplitude. To do this we divide (2.40) by k, differentiate it with respect to k and take the limit $k \to 0$

$$\lim_{k\to 0}\left[-(1+\cot^2\delta_0(k))\frac{\partial\delta_0(k)}{\partial k}\right] = \lim_{k\to 0}\left(\frac{1}{a_0k^2}+\frac{R_0}{2}\right) \tag{2.42}$$

Now we use (2.40) again

$$-\frac{\partial\delta_0(k)}{\partial k} = \lim_{k\to 0}\left[\frac{1/a_0+R_0k^2/2}{k^2+(-1/a_0+R_0k^2/2)^2}\right] = a_0 \tag{2.43}$$

Thus we see, that another possibility of defining the scattering length consistently is

$$a_0 = -\lim_{k\to 0}\frac{\partial\delta_0(k)}{\partial k} \tag{2.44}$$

Therefore we can implicitly deduce that

$$f_0(k) = -\frac{1}{1+ika_0} \tag{2.45}$$

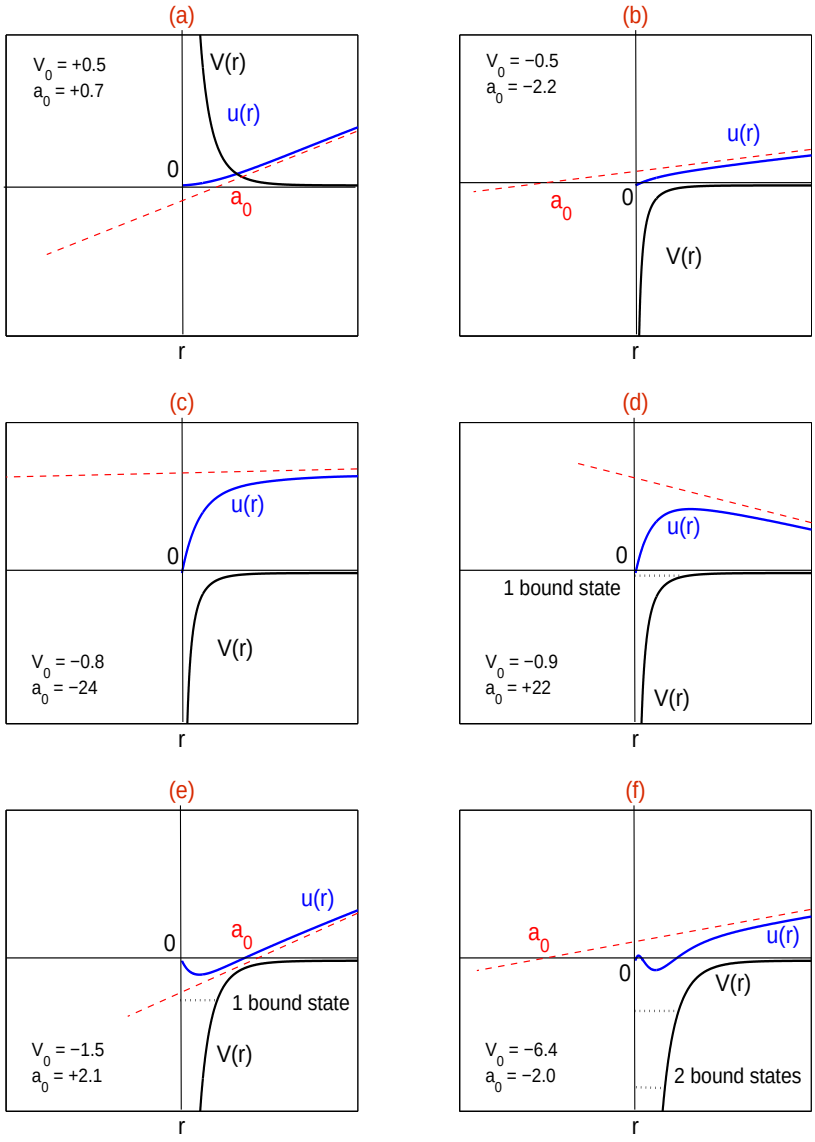

Fig. 2.5: Scattering length a_0 for the potential (4.111). The number of nodes of the wavefunction u in the effective range of the potential coincides with the number of bound states of the potential.

The solution of the scattering problem at ultra-low energies is therefore equivalent to the determination of a single quantity: the scattering length a_0.

In the limit $k \to 0$ the total cross section is

$$\sigma = \sigma_0 = 4\pi \lim_{k\to 0} \left| \frac{1}{k \cot \delta_0(k) - ik} \right|^2 = 4\pi a_0^2 \tag{2.46}$$

For bosons we have to take the symmetry into account and we get $8\pi a_0^2$. Due to $\sigma_l(k) \propto \frac{\sin^2 \delta_l}{k^2} \propto k^{4l}$ for $k \to 0$ and the fact that only odd l contribute to the scattering process for fermions, the scattering cross section for polarized fermions tends to zero at low temperatures, i.e., the polarized fermions do not "see" each other at low temperatures. This makes the evaporative cooling of a fermi gas difficult.

To obtain an implicit definition for l-wave scattering length a_l let study the analytical properties of $f_l(k)$, for small k. Using the lowest-order Born approximation, we replace $\psi_{\mathbf{k}}(\mathbf{r}')$ in (2.5) by

$$e^{i\mathbf{k}\cdot\mathbf{x}'} = \sum_l i^l (2l+1) j_l(kr') P_l(\cos\theta') \tag{2.47}$$

to obtain

$$\begin{aligned} f(k,\theta) &= -\frac{\mu}{2\pi\hbar^2} \int d^3x' e^{-i\mathbf{k}_f\cdot\mathbf{x}'} V(r') e^{i\mathbf{k}\cdot\mathbf{x}'} \\ &= -\frac{\mu}{2\pi\hbar^2} \int d^3x' e^{-i\mathbf{k}_f\cdot\mathbf{x}'} V(r') \sum_l i^l (2l+1) j_l(kr') P_l(\cos\theta') \end{aligned} \tag{2.48}$$

Labelling the angle between $\mathbf{k}_f$ and $\mathbf{x}'$ by γ, we have

$$e^{-i\mathbf{k}_f\cdot\mathbf{x}'} = \sum_l (-i)^l (2l+1) j_l(kr') P_l(\cos\gamma) \tag{2.49}$$

Now using the theorem

$$P_l(\widehat{X}\cdot\widehat{Y}) = \frac{4\pi}{2l+1} \sum_{m=-l}^{l} Y_{lm}^*(\widehat{X}) Y_{lm}(\widehat{Y}) \tag{2.50}$$

and taking $\widehat{X} = (\theta', \varphi')$ and $\widehat{Y} = (\theta, \varphi)$ as the direction of $\mathbf{x}'$ and $\mathbf{k}_f$ respectively, we obtain

$$P_l(\gamma) = \frac{4\pi}{2l+1} \sum_{m=-l}^{l} Y_{lm}^*(\theta', \varphi') Y_{lm}(\theta, \varphi) \tag{2.51}$$

By inserting (2.49) and (2.51) into (2.48), and integrating over θ' and φ', the nonzero m terms give zero, in fact the only nonzero term is that with the same l as the term in the $\psi_{\mathbf{k}}(\mathbf{x}')$ expansion, giving

$$f(k,\theta) = -\frac{2\mu}{\hbar^2} \sum_{l=0}^{\infty} (2l+1) P_l(\cos\theta) \int_0^{\infty} r^2 dr V(r) [j_l(kr)]^2 \tag{2.52}$$

or

$$f_l(k) \simeq -\frac{2\mu}{\hbar^2}\int dr V(r)[rj_l(kr)]^2$$
$$= -\frac{2\mu}{\hbar^2}\int dr V(r) r^2 \left[\frac{(kr)^l}{(2l+1)!!}\left(1+\mathcal{O}[(kr)^2]\right)\right]^2 \quad (k\to 0) \qquad (2.53)$$

Assuming uniform convergence, one may interchange the limits and conclude the general momentum dependence $f_l(k) = \mathcal{O}(k^{2l})$ as $k \to 0$. Via $f_l(k) \sim 1/k \cot\delta_l(k)$ (2.16), one can reformulate this in terms of the phase shifts. Eventually, that leads to

$$k^{2l+1}\cot\delta_l(k) = -\frac{1}{(a_l)^{2l+1}} + \frac{1}{2}R_l k^2 + O(k^4), \quad a_l \neq 0,\, R_l \in \mathcal{R} \qquad (2.54)$$

or

$$\frac{\tan\delta_l(k)}{k^{2l+1}} = -(a_l)^{2l+1} + \mathcal{O}(k^2) \qquad (2.55)$$

which is an implicit definition of the l-wave scattering length a_l and the *effective* range R_l. It is only for s-wave scattering ($l = 0$) that the amplitude does not vanish for low energies (or, alternatively, the slope of the phase shift). In that limit, a_0 is the only relevant parameter, no matter what the shape of the potential. It makes sense, in the wider scheme of things, because as $k \to 0$, the wavelength λ becomes much larger than the potential's range and thus cannot probe its short-scale structure.

2.4 Scattering Resonances

The scattering cross sections as a function of energy, may exhibit some sharp peaks superimposed on a smooth background. These peaks correspond to resonance states and occur when one of the phase shifts passes rapidly through $\pi/2$. In Ref.[1], the resonances has been defined as the *most stricking phenomenon in the whole range of scattering experiment.* When the lifetime of the particle-target system in the region of interaction is larger than the collision time in a direct collision process we call the phenomenon a resonance phenomenon. A resonance state is defined as a long-lived state of a system which has sufficient energy to break-up into two or more subsystems. In elastic and inelastic scattering experiments the subsystems are associated with the scattering particle and the target. Resonances are observed in atomic, nuclear and particle physics. There are many different theoretical approaches to the resonance phenomenon, all of them having in common that the sharp variation of the cross section at a resonant energy E_r, is in some way related to the existence of a nearly bound state of the projectile-target system with energy E_r. When the projectile is sent in with energy E_r it can be temporarily captured into this *meta-stable* state; and it is this possibility that is considered the cause of violent variations in cross section.

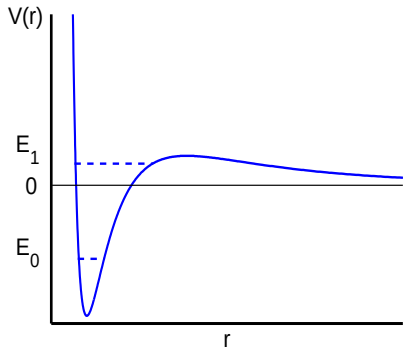

Fig. 2.6: Schematic representation of a spherically symmetric potential which supports shape-resonances.

2.4.1 Shape (Breit-Wigner) resonances

An illustrative plot of spherically symmetric potential which supports resonances, $V(r)$, is given in Fig. 2.6. Such potential describing for example decay of radioactive nuclei or of unstable particles [8]. Naturally, we shall refer to the nucleus as the target in this case. r is, for example, the distance between an α particle and the nucleus. E_0 and E_1 represent bound and resonance energies respectively.

A very similar potential can describe both the molecular interaction in a diatom for which the total angular momentum, j, is much larger than zero and gives rise to a centrifugal potential barrier [9], and the scattering of an electron from a neutral diatom [10]. In such cases, the lifetime of the metastable resonance states can vary from femtoseconds (e.g. $\sim 10^{-15}s$ for the autoionization of H_2^- in its ground state) to millions of years (e.g. $4.5 \times 10^9 y$ for the decay of the ^{238}u isotope to Thorium). In all of these cases the temporarily trapping of

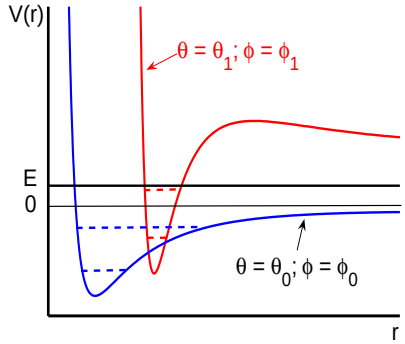

Fig. 2.7: Schematic representation of two couples adiabatic potentials.

the *particle* inside the potential well is a quantum phenomenon which is known as the tunnelling phenomenon. The quantum equation of motion are reduced to the classical one as $\hbar \to 0$. While $\hbar$ is taken to zero, the penetration probability of the quantum particle through the potential barrier (into the well or out of it) is reduced and in the limit of $\hbar = 0$ no resonance states will be observed. These kind of resonances are known as shape-type resonances. The temporarily trapping of the particle inside the potential well can occur also when the energy of the particle is larger than the height of the potential barrier or even in the absence of a potential barrier (e.g. scattering of a Gaussian wave packet from a finite square well [5]).

Let's consider scattering by a spherical potential and neglect any internal degrees of freedom of the particles. In order for δ_l to achieve the value $\pi/2$, which maximizes contribution to the cross section from the partial wave l, it is necessary for the denominator of (2.18) to vanish. Suppose this happens at the energy $E = E_r$. Then in a neighborhood of $E = E_r$, we may write, approximately, $\gamma_l \approx c - b(E - E_r)$, where $c = kn_l'(ka)/n_l(ka)$. It is clear that the approximation can be valid only if $n_l(ka) \neq 0$. In the neighborhood of $E = E_r$, (2.18) becomes

$$\begin{aligned} \tan\delta_l &\approx \frac{kj_l'(ka) - \gamma_l j_l(ka)}{n_l(ka)b(E - E_r)} \\ &\approx \frac{kj_l'(ka) - cj_l(ka)}{n_l(ka)b(E - E_r)} \\ &= \frac{k[j_l'(ka)n_l(ka) - n_l'(ka)j_l(ka)]}{n_l^2(ka)b(E - E_r)} \end{aligned} \tag{2.56}$$

this expression can be simplified by means of the Wronskian relation, $j_l'(z)n_l(z) - n_l'(z)j_l(z) = -z^{-2}$, which follows directly from the differential equation satisfied by the Bessel functions. Thus we obtain

$$\tan\delta_l \simeq \frac{\frac{1}{2}\Gamma}{E_r - E} \tag{2.57}$$

where $\frac{1}{2}\Gamma = (ka^2b[n_l(ka)]^2)^{-1}$ and $\hbar^2k^2/2\mu = E_r$. Without further approximation this yields

$$\sin\delta_l exp(i\delta_l) = \frac{\Gamma}{2(E_r - E) - i\Gamma}. \tag{2.58}$$

The contribution of this resonant partial wave l to the total cross section is

$$\sigma_l = \frac{4\pi(2l+1)}{k^2}\frac{\Gamma^2}{4(E_r - E)^2 + \Gamma^2} \tag{2.59}$$

This is the famous Breit-Wigner formula. Although we obtained this result for a spherical potential, it is also correct in more general cases.

If Γ is small, this term will produce a sharp narrow peak in the total cross section.

2.4.2 Feshbach-Fano resonances

Let us consider a non-spherical symmetric interaction potential, between the particle and the target. In this case it may happen that a bound state of the particle-target system in a fixed orientation (e.g. a square integrable eigenfunction of the one-dimensional time-independent Schrödinger equation

$$H(r, \theta_0, \varphi_0)|\psi\rangle = E|\psi\rangle \tag{2.60}$$

for fixed polar coordinates θ_0 and φ_0 of the relative motion) is embedded in the continuum of the system in another orientation when $\theta = \theta_1$ and $\varphi = \varphi_1$. The two adiabatic potentials are schematically presented in Fig. 2.7.

Due to the coupling of the r-coordinate with the angle θ and φ the bound state which is pushed up into the continuum becomes a resonance state. These kind of resonances are known as Feshbach-Fano type resonances and can also be obtained in classical calculations. Unlike the shape-type resonances, the lifetime of the Feshbach metastable states get nonzero value as $\hbar$ is taken to the limit of $\hbar = 0$.

For a Feshbach-Fano resonance, in contrast with a shape resonance, the corresponding profile in the cross-section has the so-called Fano shape, i.e. it can be fitted with a function proportional to

$$\frac{(q\Gamma + 2(E - E_r))^2}{4(E - E_r)^2 + \Gamma^2} \tag{2.61}$$

The E_r and Γ parameters are the standard Breit-Wigner parameters (position and width of the resonance, respectively). The so-called Fano parameter, q is interpreted as the ratio between the resonant and background scattering probability. In the case the background scattering probability is vanishing, the q parameter becomes infinite and the Fano formula is boiling down to the usual Breit-Wigner formula.

Within a method is named as the Feshbach-Fano partitioning theory one can partitions the wave function (and therefore the associated quantities like cross section and phase shift) into the resonant and the background components

$$|\psi\rangle = P|\psi\rangle + Q|\psi\rangle \tag{2.62}$$

with asymptotic conditions

$$\lim_{r\to\infty} \langle \mathbf{x}|P|\psi\rangle = \frac{1}{(2\pi)^{3/2}} \left(e^{i\mathbf{k}\cdot\mathbf{x}} + [f_P(k, \theta, \varphi) + f_Q(k, \theta, \varphi)] \frac{e^{ikr}}{r} \right) \tag{2.63}$$

and

$$\lim_{r\to\infty} \langle \mathbf{x}|Q|\psi\rangle = 0 \tag{2.64}$$

Here f_P and f_Q are the background and the resonance scattering amplitude respectively. P and Q are projectors on the background and the resonant subspace respectively. The subspaces onto which P and Q project are sets of states obeying the continuum and the bound state boundary conditions respectively.

In this method the Schrödinger equation governing the whole scattering process (defined by the Hamiltonian H) is solved in two steps: First by solving the scattering problem ruled by the background Hamiltonian PHP

$$PHP|\phi\rangle = E|\phi\rangle \tag{2.65}$$

with asymptotic condition

$$\lim_{r\to\infty}\langle \mathbf{x}|\phi\rangle = \frac{1}{(2\pi)^{3/2}}\left(e^{i\mathbf{k}\cdot\mathbf{x}} + f_P(k,\theta,\varphi)\frac{e^{ikr}}{r}\right) \tag{2.66}$$

It is often supposed that the solution of this problem is trivial or at least fulfilling some standard hypotheses which allow to skip its full resolution. Second by solving the resonant scattering problem corresponding to the effective complex (energy dependent) Hamiltonian

$$H^{eff}(E) = QHQ + QHP\frac{1}{E+i0-PHP}PHQ \tag{2.67}$$

where $E + i0 = \lim_{\eta\to 0^+} E + i\eta$. One can show that

$$Q|\psi\rangle = \frac{1}{E - H^{eff}(E)}QHP|\phi\rangle \tag{2.68}$$

and

$$P|\psi\rangle = |\phi\rangle + \frac{1}{E+i0-PHP}PHQ\frac{1}{E-H^{eff}(E)}QHP|\phi\rangle \tag{2.69}$$

By taking the limit $r \to \infty$ of $\langle r|P|\psi\rangle$ and comparing with (2.63) one can easily calculate the resonance scattering amplitude f_Q.

The resonance positions are the solutions (in the lower complex-E plane) of the so-called implicit equation

$$det[H^{eff}(E) - E] = 0 \tag{2.70}$$

with $E = \epsilon - i\Gamma/2$.

2.4.3 Decay of a resonant state

The physical nature of a resonance scattering state can be understood by examining its behavior in time. Instead of a stationary (monoenergetic) state, we now consider a time-dependent state involving a spectrum of energies that is much broader

$$\psi(\mathbf{x},t) = \int A(\mathbf{k})\psi^{(+)}_{\mathbf{k}}(\mathbf{x})e^{-iEt/\hbar}d^3k \tag{2.71}$$

where $E = \hbar^2k^2/2\mu$. The function $A(\mathbf{k})$ should be nonzero only for values of $\mathbf{k}$ that are collinear with the initial beam. This state function can be divided into

an incident wave and a scattered wave [see (2.4)], the scattered wave will be of the form

$$\psi_{out}(\mathbf{x},t) \sim \int A(\mathbf{k}) f(k,\theta,\varphi) \frac{e^{ikr}}{r} e^{-iEt/\hbar} d^3k \tag{2.72}$$

in the limit of large r.

Suppose now that all phase shifts δ_l are small except for $l = l'$ which is a resonant. Then the scattering amplitude will be dominated by l', and using (2.15) and the resonance approximation (2.58) we obtain

$$\psi_{out}(\mathbf{x},t) = (2l+1)P_l(\cos\theta) \int A(\mathbf{k}) \frac{e^{ikr}}{kr} \frac{\Gamma}{[2(E_r - E) - i\Gamma]} e^{-iEt/\hbar} d^3k \tag{2.73}$$

here θ is the angle of $\mathbf{x}$ relative to the incident beam. This integral can most conveniently be analyzed by going to polar coordinates and using $E = \hbar^2 k^2/2\mu$ as a variable of integration, so we put

$$d^3k = k^2 d\Omega_k dk = \frac{\mu}{\hbar^2} d\Omega_k k dE \tag{2.74}$$

This yields

$$\psi_{out}(\mathbf{x},t) \sim \frac{\mu}{\hbar^2}(2l+1)P_l(\cos\theta)\frac{F(r,t)}{r} \tag{2.75}$$

where

$$F(r,t) = \int_0^\infty \alpha(E)\Gamma \frac{exp[i(kr - Et/\hbar)]}{2(E_r - E) - i\Gamma} dE \tag{2.76}$$

and

$$\alpha(E) = \int A(\mathbf{k}) d\Omega_k \tag{2.77}$$

The precise time dependence of $F(r,t)$ is determined by the details of the initial states through the function $\alpha(E)$ and can be quite complicated. We assume $\alpha(E)$ to be a smooth function of energy, nearly constant over an energy range Γ, and so it is reasonable to replace $\alpha(E)$ by $\alpha(E_r)$ in the integral. In the resonance approximation, the integral is dominated by contribution in the energy range $E_r \pm \Gamma$. Therefore we replace k in the exponential by its Taylor series $k \approx k_r + \mu(E - E_r)/\hbar^2 k_r$ where $E_r = \hbar^2 k_r^2/2\mu$. Introducing a dimensionless variable of integration, $z = (E - E_r)/\Gamma$, and a retarded time $\tau = t - r/v_r$, where $v_r = \hbar k_r/\mu$, we can rewrite (2.76) as

$$F(r,t) = -\alpha(E_r)\Gamma exp(ik_r r - iE_r t/\hbar) \int_{-E_r/\Gamma}^\infty \frac{exp(-i\tau\Gamma z/\hbar)}{2z + i} dz \tag{2.78}$$

If $\Gamma \ll E_r$, the lower limit can be replaced by $-\infty$. The integral then can be evaluated for positive τ by closing the counter of integration with an infinite semicircle in the lower half of the complex $z-$plane. From the residue of the pole at $z = -i/2$ we obtain the time dependence $exp(-\tau\Gamma/2\hbar)$. For negative τ, the counter must be closed in the upper half-plane, where there are no poles,

and so the integral vanishes. Thus the time dependence of the scattered wave (2.73) at large distance will be

$$\begin{aligned} \psi_{out}(\mathbf{x},t) &\propto e^{-\Gamma t/2\hbar} \quad \text{for} \quad t > r/v_r \\ \psi_{out}(\mathbf{x},t) &= 0 \quad \text{for} \quad t < r/v_r \end{aligned} \tag{2.79}$$

It is zero before $t = r/v_r$ because that is the time needed for propagation from the scattering region to the detector. For times greater than this, the detection probability decay exponentially.

2.4.4 Virtual bound states

The physical picture of a scattering resonance that we derive from the above analysis is of a particle being temporarily captured by the scattering potential in a virtual bound state whose mean lifetime is $\hbar/\Gamma$. It is possible to exhibit a closer connection between bound states and resonances. Suppose that the potential supports a bound state at the negative energy $E = -E_b$. As the strength of the potential is reduced the binding energy E_b will decrease and eventually vanish. As the potential strength is further reduced, a resonance or virtual bound state, appears at positive energy. Further reduction in the potential strength results in Γ increasing, so that the virtual bound state has so short a lifetime that it is no longer significant.

We shall illustrate this connection only for $E = 0$, which is the boundary between bound states and scattering states. It is apparent from (2.18) that in the limit $k \to 0$ we have $\tan\delta_l \to 0$ for almost all values of the logarithmic derivative γ_l. The exception occurs if the denominator vanishes, in which case the phase shift has the zero energy limit $\pi/2$, and we have a zero-energy resonance. In this case, we must have $\gamma_l = kn_l'(ka)/n_l(ka) \to -(l+1)/a$ in the limit $k \to 0$.

3. NUMERICAL METHODS

3.1 The Complex Scaling Method

In the previous chapter a resonance state, has been defined as a non-stationary (or quasi-bound) state with a lifetime long enough to be well characterized, and long enough to make its explicit recognition of experimental and theoretical importance. The simplest, and most naive, mathematical description of such states is that they resemble bound stationary states in that they are *localized* in space (at t = 0) and their time evolution is given by

$$\psi^{res}(\mathbf{x},t) = e^{-iE_r t/\hbar}\phi^{res}(\mathbf{x}) \tag{3.1}$$

which is the usual stationary state time dependence, except that now the energy, E_r, of the resonant state is complex:

$$E_r = \epsilon - i\frac{\Gamma}{2} \tag{3.2}$$

where ϵ and Γ are real, and $\Gamma \geq 0$. The presence of the $-i\frac{\Gamma}{2}$ forces the probability density

$$|\psi^{res}(\mathbf{x},t)|^2 = |\phi^{res}(\mathbf{x})|^2 e^{-\Gamma t/\hbar} \tag{3.3}$$

to decay exponentially to zero as time passes at a constant r. Therefore the *particles* disappear from any given point in the coordinate space. From this point of view, one needs to solve the time-dependent schrödinger equation to obtain the lifetime of a resonance state. Nevertheless it is also possible to estimate the resonance lifetime from time-independent calculation. In [6] it has been shown that the resonance phenomenon as obtained in a scattering experiment are associated with the poles of the scattering matrix S in fourth-quarter of the complex k-plane (i.e., $Re(k) > 0$, $Im(k) < 0$), where k is the wavevector given by

$$E - E_t = \frac{(\hbar k)^2}{2\mu} \tag{3.4}$$

with E_t being the threshold energy, which for resonance state is a complex number. These resonance poles are complex eigenvalues of the Hamiltonian H

$$H(\mathbf{x})\phi_n^{res}(\mathbf{x}) = E_n\phi_n^{res}(\mathbf{x}), \quad E_n = \varepsilon_n - \frac{i}{2}\Gamma_n, \tag{3.5}$$

where ε_n is the resonance position above the threshold, $\Gamma/2$ is the inverse lifetime. Equation (3.5) is the basic equation in the resonance theory for time-independent Hamiltonian. The resonances are associated with complex eigenvalues of the Hamiltonian which describes the physical systems. One may expect that, the Hamiltonian of a physical system should be Hermitian, with real eigenvalues. However a physical Hamiltonian is hermitian only when it acts on bounded functions (not necessarily square integrable) or, when box normalization is used, on a functional space of all possible square integrable functions (i.e., Hilbert space) [6]. The ϕ^{res} which are associated with complex eigenvalues are not in the Hermitian domain of the Hamiltonian (i.e., not in the Hilbert space) as at asymptotic region they diverges exponentially

$$\phi^{res}(\mathbf{x} \to \infty) \sim e^{i\mathbf{k}\cdot\mathbf{x}} + S(k)e^{ikr} \to \infty, \quad (r = |\mathbf{x}|) \tag{3.6}$$

Due to (3.3) and (3.6) the number of particles is conserved only when both the reaction coordinate r and the time t, approach the limit of infinity.

Most of the computational algorithms in quantum mechanics, such as variational methods, have been developed for Hermitian operators, and they can not be used to solve (3.5), even for the $1D$ case. During the past decays there has been rapid development and application of a theory variously known as complex scaling, complex coordinates, coordinate-rotation, and dilatation analyticity, to problems of resonances in atomic and molecular physics and in chemistry. One of the major purposes of the introduction of complex scaling theory is to extend the variational principle and of other well-known theorems in quantum mechanics to non-Hermitian operators by carrying out similarity transformation $\mathbf{S}$ which makes the resonance wavefunctions ϕ^{res}, square integrable functions. That is

$$(\mathbf{S}H\mathbf{S}^{-1})(\mathbf{S}\phi^{res}) = E(\mathbf{S}\phi^{res}), \quad E = \varepsilon - \frac{i}{2}\Gamma \tag{3.7}$$

such that $\mathbf{S}\phi^{res} \to 0$ as $r \to \infty$ and thus satisfy our feeling that resonances are localized, at least at complex values of the coordinates. One example for the complex scaling operator is

$$\mathbf{S} = e^{i\eta r\partial/\partial r} \tag{3.8}$$

such that

$$\mathbf{S}f(r) = f(re^{i\eta}) \tag{3.9}$$

for any analytical function $f(r)$. As it has been illustrated in figure 3.1, bound states and scattering thresholds (corresponding to the possibility of fragmentation of different subsystems in differing states of excitation) are independent under the dilatation transformation. However the segments of continua beginning at each scattering threshold rotate by an angle 2η into the lower half plane ($\eta \geq 0$), each about its individual threshold. This follows from the fact that due to (3.4), ϕ^{res} becomes square integrable only for the complex wavevector $k = |k|e^{-i\eta}$ and since for finite range potential a continuum is related to the kinetic energy $E \propto k^2/2$ and not to the potential, it rotates like

$$E \propto \frac{k^2}{2} \to e^{-2i\eta}\frac{k^2}{2}. \tag{3.10}$$

As the continua rotate, new, complex, discrete eigenvalues of $H(\eta)$ may appear in the lower half complex energy plane, such that once revealed , maintain their positions. These eigenvalues correspond to poles of the $S-$matrix which we associate with resonances. They are *hidden* on a higher sheet if $\eta = 0$, and will be exposed if the cuts pass through the angle

$$\theta = 2\eta = \arctan\left[\frac{\Gamma}{2(\varepsilon - E_t)}\right] \tag{3.11}$$

where as before ε is the resonance position above the threshold and $\Gamma/2$ is the inverse lifetime.

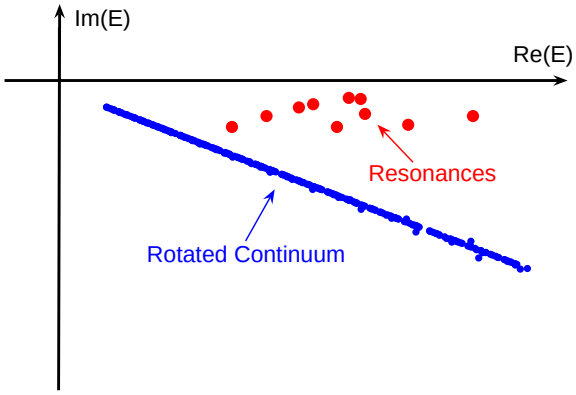

Fig. 3.1: Schematic representation of the eigenvalues of the rotated Hamiltonian.

Since resonance states of the complex scaled Hamiltonian are square integrable the linear variational principle can be applied. An eigenstate $|E\rangle$ of the stationary Schrödinger equation can now be expanded in terms of a set of basis-functions

$$|E\rangle = \sum_i c_i |\chi_i\rangle \tag{3.12}$$

leading to the generalized spinor eigenvalue problem

$$\overline{H}(\eta)\mathbf{c} = E\mathcal{S}\mathbf{c} \tag{3.13}$$

which yields the complex eigenvalues E_i, and the complex vectors $\mathbf{c}_i$. $\mathcal{S}$ is the corresponding matrix representation of the overlap matrix

$$(\mathcal{S})_{ij} = \langle\chi_i|\chi_j\rangle \tag{3.14}$$

The basis set must be chosen in such a way that the exact wave function can be approximated to a sufficient degree of accuracy by as small as possible number of functions. Therefore the form of the basis set must be adapted to the

geometry and the symmetries of the system. We note once that as $\overline{H}(\eta)$ is not Hermitian, its spectral resolution involves both its left and right eigenfunctions. However, elementary manipulation gives the results that the left eigenfunction $\mathbf{d}_i$ corresponding to eigenvalue E_i is just $\mathbf{c}_i^T$ where T is the transpose. (Note that the transpose is not the usual Hermitian conjugate, which is the transpose complex conjugate.) Thus

$$\overline{H}(\eta) = \sum_i E_i \mathbf{c}_i \mathbf{c}_i^T \tag{3.15}$$

This is a bi-orthogonal expansion, and $\mathbf{c}_i^T \mathbf{c}_j = \delta_{ij}$ (rather than the usual for Hermitian problems.)

3.1.1 The c-product for time-independent Hamiltonian

The inner product is defined in quantum mechanics as the scaler product, that is

$$\langle f|g\rangle = \int_{\text{all space}} f^* g d\tau \tag{3.16}$$

where f, g are functions in the Hilbert space. When f and g are exponentially divergent functions (as the resonance eigenfunctions of H are) they are not in the Hilbert space, and they are NOT in the Hermitian domain of H. By scaling the coordinates in the time-independent Schrödinger equation by a complex factor, the exponentially divergent resonance states become square integrable. However, in spite of the fact that the complex-scaled resonance states are in the generalized Hilbert space, they are not associated with an Hermitian operator [$H(re^{i\eta})$ is non-Hermitian] and the above scaler Hermitian product should be replaced by a generalized inner product (the so-called c-product). In the c-product, the complex conjugate of the terms in the function which are complex not as a result of the complex scaling are taken. In the c-product first the complex conjugate of the function is taken and only then the coordinates or momentum are analytically continued into the complex plan. If for example, the eigenfunctions of the unscaled Hamiltonian are real and the COMPLEX eigenfunctions of the complex-scaled Hamiltonian are expanded in terms of REAL functions (as it is the case in our calculation of resonances of an atom in external magnetic field), then the inner product is given by

$$(f|g) \equiv \langle f^*|g\rangle = \int_{\text{all space}} f g d\tau \tag{3.17}$$

Knowing the resonance eigenfunctions of the complex-scaled Hamiltonian one can calculate corresponding expectation value of an arbitrary observable A within the generalized inner c-product

$$\langle A\rangle = \frac{(\mathbf{S}\phi^{res}|A|\mathbf{S}\phi^{res})}{(\mathbf{S}\phi^{res}|\mathbf{S}\phi^{res})}. \tag{3.18}$$

The expectation value which is obtained in this way is in general complex. The real part represents the average value, whereas the imaginary part can be interpreted as the uncertainty of our observable in a measurement when the system is prepared in the corresponding resonance state [6].

3.2 The Linear Variational Principle

The quantum mechanical problems, can not be solved exactly, except for some special cases. Therefore we need to use some methods of approximation. One important tool is the linear variational principle which allows for solving the stationary Schrödinger equation

$$H|\psi_j\rangle = E_j|\psi_j\rangle \tag{3.19}$$

In this method, a set of normalized basis functions $\{|\phi_i\rangle\}$ is employed to construct the trial wavefunction $|\psi\rangle$ as

$$|\psi\rangle = \sum_i c_i|\phi_i\rangle \tag{3.20}$$

with the expansion coefficient c_i serving as variational parameters. The basis set could in general be non orthonormal. Introducing the column vector $\mathbf{c}$ with component c_i, we find for a normalized $|\psi\rangle$

$$1 = \langle\psi|\psi\rangle = \sum_{i,j} c_i^* c_j \langle\phi_i|\phi_j\rangle = \sum_{i,j} c_i^* c_j \mathcal{S}_{ij} = \mathbf{c}^\dagger \mathcal{S}\mathbf{c}. \tag{3.21}$$

$\mathcal{S}$ is the so-called overlap matrix, which in the case of an orthonormal set of basis functions, is just the unity matrix. The expectation value of H is given by

$$\langle H\rangle = \langle\psi|H|\psi\rangle = \sum_{i,j} c_i^* c_j \langle\phi_i|H|\phi_j\rangle = \sum_{i,j} c_i^* c_j \mathcal{H}_{ij} = \mathbf{c}^\dagger \mathcal{H}\mathbf{c} \tag{3.22}$$

According to the variational principle finding the optimum variational parameters is equivalent to finding the minimum of the expectation value $\langle H\rangle$ under the constraint (3.21), which is equivalent to minimize the function $\mathcal{L}$, defined by

$$\mathcal{L} = \sum_{i,j} c_i^* c_j \mathcal{H}_{ij} - \chi[\sum_{i,j} c_i^* c_j \mathcal{S}_{ij} - 1] \tag{3.23}$$

here χ is the corresponding Lagrange parameter. Evaluating the derivative of $\mathcal{L}$ with respect to c_i^* and putting it equal to zero we obtain a set of equations whose solution yields the optimal expansion coefficient c_i:

$$\frac{\partial \mathcal{L}}{\partial c_i^*} = \sum_i [\mathcal{H}_{ij} - \chi \mathcal{S}_{ij}] c_j = 0. \tag{3.24}$$

They can be written more compactly as a single matrix equation:

$$\mathcal{H}\mathbf{c} = \chi \mathcal{S}\mathbf{c}. \tag{3.25}$$

Therefore the task of finding the optimum parameters reduces to a generalized algebraic eigenvalue problem. In order to illuminate the actual meaning of the generalized eigenvalues χ, let's consider the matrix element

$$\langle\psi_i|H|\psi_j\rangle = \mathbf{c}_i{}^\dagger\mathcal{H}\mathbf{c}_j = \chi_j\mathbf{c}_i^\dagger\mathcal{S}\mathbf{c}_j = \chi_j\langle\psi_i|\psi_j\rangle = \chi_j\delta_{ij} \tag{3.26}$$

This shows that χ_j is the energy expectation value of the state $|\psi_j\rangle$, or, on the other words, it can be considered as an approximation for the eigenenergy E_j of the Hamiltonian H. In the case of a complete basis functions, $|\phi_j\rangle$, χ_j would represent the exact eigenenergies. Usually for the systems which will be considered in this work, we need infinite set of basis functions, and since in practice any computation can involve only a finite set of basis functions, the eigenvalue χ_j represent only upper bounds of the exact eigenvalues such that:

$$E_1 \leq \chi_1 \leq E_2 \leq \chi_2 \leq E_3 \leq \chi_3 \leq ... \leq E_N \leq \chi_N$$

N is the number of the basis functions $\{|\phi_i\rangle\}$. This is known as the Hylleraas-Undheim theorem whose prove is presented in the following section.

3.2.1 The Hylleraas-Undheim theorem

Let assume $\mathcal{H}'$ and $\mathcal{H}$ to be the representations of the Hermitian operator H in the subspace spanned by the basis $\mathcal{M}' = \{|\phi_1\rangle, ..., |\phi_{N-1}\rangle\}$ and $\mathcal{M} = \mathcal{M}' \cup \{|\phi_N\rangle\}$, respectively. Then the real eigenvalues $\lambda'_1 \leq \lambda'_2 \leq .. \leq \lambda'_{N-1}$ of $\mathcal{H}'$ and $\lambda_1 \leq \lambda_2 \leq .. \leq \lambda_N$ of $\mathcal{H}$ satisfy the relation

$$\lambda_1 \leq \lambda'_1 \leq \lambda_2 \leq \lambda'_2 \leq ... \leq \lambda_{N-1} \leq \lambda'_{N-1} \leq \lambda_N$$

For proving we follow Ref. [11]. Without loss of generality, the basis $\mathcal{M}'$ is chosen such that $\mathcal{H}'$ is diagonal with its eigenvalues being the diagonal elements in ascending order, i.e. $\lambda'_i \leq \lambda'_{i+1}$. Then $\mathcal{H}$ takes the form

$$\mathcal{H} = \begin{pmatrix} & & & \mathcal{H}_{1N} \\ & \mathcal{H}' & & \mathcal{H}_{2N} \\ & & & \vdots \\ \mathcal{H}_{N1} & \mathcal{H}_{N2} & \cdots & \mathcal{H}_{NN} \end{pmatrix} \tag{3.27}$$

The eigenvalues λ_i of the matrix $\mathcal{H}$ are the zeros of the determinant

$$\begin{aligned} f(\lambda) = \det(\mathcal{H} - \lambda 1) &= \begin{vmatrix} \lambda'_1 - \lambda & 0 & \cdots & \mathcal{H}_{1N} \\ 0 & \lambda'_2 - \lambda & \cdots & \mathcal{H}_{2N} \\ \vdots & \vdots & \ddots & \vdots \\ \mathcal{H}_{N1} & \mathcal{H}_{N2} & \cdots & \mathcal{H}_{NN} - \lambda \end{vmatrix} \\ &= (\mathcal{H}_{NN} - \lambda)\prod_{n=1}^{N-1}(\lambda'_n - \lambda) - \sum_{m=1}^{N-1}|\mathcal{H}_{mN}|^2\prod_{n\neq m}^{N-1}(\lambda'_n - \lambda) \end{aligned} \tag{3.28}$$

Evaluating $f(\lambda)$ at the points $\lambda = \lambda'_k$ yields

$$f(\lambda) = -|\mathcal{H}_{kN}|^2 \prod_{n\neq k}^{N-1} (\lambda'_n - \lambda'_k) \begin{array}{l} \leq 0 \\ \geq 0 \end{array} \begin{array}{lll} \text{if} & k & \text{odd} \\ \text{if} & k & \text{even} \end{array} \tag{3.29}$$

One then finds the following behavior for $f(\lambda)$

$$f(\lambda) \rightarrow \quad (\pm)^N \infty \quad \text{if} \quad \lambda \rightarrow \mp\infty \tag{3.30}$$

which is obvious when writing $f(\lambda)$ in the form

$$f(\lambda) = \prod_{n=1}^{N-1} (\lambda_n - \lambda) \left[(\mathcal{H}_{NN} - \lambda) - \sum_{m=1}^{N-1} \frac{|\mathcal{H}_{mN}|^2}{(\lambda_m - \lambda)} \right] \tag{3.31}$$

from (B.80) it follows that there is an odd number of zeros between two distinct eigenvalues of $\mathcal{H}'$. On the other hand $f(\lambda)$ has exactly N real zeros $\lambda_1, \lambda_2, ..., \lambda_N$ and therefore the λ'_i must be ordered according to

$$\lambda_1 \leq \lambda'_1 \leq \lambda_2 \leq \lambda'_2 \leq ... \leq \lambda_{N-1} \leq \lambda'_{N-1} \leq \lambda_N$$

Hence, the eigenvalues λ' constitute upper bounds for the λ.

3.3 Solving the Algebraic Eigenvalue Problem

By employing the variational principle, solving the stationary Schrödinger equation (3.19) is reduced to an generalized eigenvalue problem (3.25),which can be solved by means of the Arnoldi method, a numerical procedure designed for solving large scale eigenvalue problem. In conjunction with Arnoldi method, we use the so-called shift-invert procedure which allows for the calculation of eigenvalues lying in arbitrary regions of the spectrum without the need to find the entire bottom up. For the numerical implementation of these two methods, the routines from the software packages ARPACK [12], and superLU [13] have been used. The latter has been designed to solve large inhomogeneous linear system of equations, performing an LU-decomposition of the corresponding matrices.

3.3.1 The Arnoldi method

The idea of the Arnoldi method is to reduce a large-scale eigenvalue problem

$$\mathcal{A}\mathcal{X} = \lambda \mathcal{S}\mathcal{X} \tag{3.32}$$

to one with a significantly lower dimension, which is then soluble with comparatively little effort. The basis for this procedure is the so-called Arnoldi decomposition. By representing a matrix $\mathcal{A} \in C^{n\times n}$ in the so-called Krylov-space $K_k(\mathcal{A}, v) := Span\{v, \mathcal{A}v, ..., \mathcal{A}^{k-1}v\}$, where $v \in C^n \backslash \{0\}$ is an arbitrary vector, we obtain a so-called k-step Arnoldi decomposition of the form

$$\mathcal{A}\mathcal{V}_k = \mathcal{V}_k \mathcal{H}_k + f_k e_k^T \tag{3.33}$$

here the matrix $\mathcal{V}_k \in C^{n\times k}$ has orthonormal columns, obeys $\mathcal{V}_k^T f_k = 0$ and the matrix $\mathcal{H}_k \in C^{k\times k}$ is an upper Hessenberg matrix with non-negative subdiagonal elements. In the case of a Hermitian matrix $\mathcal{A}$, $\mathcal{H}_k$ is reduced to a real, symmetric and tri-diagonal matrix, and (3.33) is referred to as k-step Lanczos Factorization. Given vector s satisfying the eigenvalue equation

$$\mathcal{H}_k s = \theta s \tag{3.34}$$

the vector $u = \mathcal{V}_k s$ satisfies

$$\|\mathcal{A}u - \theta u\| = \|(\mathcal{A}\mathcal{V}_k - \mathcal{V}_k\mathcal{H}_k)s\| = \|f_k\||e_k^T s| \tag{3.35}$$

The pair (u, θ) is denoted as a Ritz pair representing an approximate eigenpair of the matrix $\mathcal{A}$. The accuracy degree of this approximation can be measured by the so-called Ritz estimate $\|f_k\||e_k^T s|$. If this value drops below a given threshold (commonly machine precision), the Ritz pair (u, θ) is considered a solution of the eigenvalue problem (3.34). If necessary the value of k should be increased to establish convergence.

In summary, the eigenvalue problem should only be solved for k-dimensional Hessenberg matrix $\mathcal{H}_k$ with k being much smaller than the dimension of the matrix $\mathcal{A}$ ($\mathcal{H}_k$ is even symmetric and tridiagonal if $\mathcal{A}$ is Hermitian), for which efficiently working algorithms are available. The method converges firstly for those eigenvalues of the matrix $\mathcal{A}$ which are the largest or smallest in magnitude. Thus, it can be most efficiently used to calculate the extermal eigenvalues of $\mathcal{A}$.

3.3.2 The Shift-Invert method

For physical problems with high dimensionality it is not possible to calculate the entire spectrum of the Hamiltonian. Employing the shift-invert method, in the case we need to calculate the eigenvalues just in a certain region of the spectrum, we can transfer the initial Matrix, such that those eigenvalues which we are interested in be the first to converge. For this purpose we perform the transformation

$$\begin{aligned} \mathcal{H}c = \epsilon\mathcal{S}c \leftrightarrow (\mathcal{H} - \sigma\mathcal{S})c &= (\epsilon - \sigma)\mathcal{S}c \\ \leftrightarrow (\mathcal{H} - \sigma\mathcal{S})^{-1}\mathcal{S}c &= \lambda c \end{aligned} \tag{3.36}$$

where $\lambda = 1/(\epsilon - \sigma)$. The eigenvector c remains unchanged. The old eigenvalues ϵ_i are related to the new ones λ_i by

$$\epsilon_i = \sigma + 1/\lambda_i. \tag{3.37}$$

According to this relation, the eigenvalues lying close to σ correspond to eigenvalues of the operator $(\mathcal{H} - \sigma s)^{-1}\mathcal{S}$ with largest magnitude and thus converge first.

3.3.3 Convergence of the eigenvalues

Given an operator H, the eigenvalues ϵ_i obtained from the linear variational method, constitute upper bounds of the exact eigenenergy E_i of H, thus E_i can be approximated by ϵ_i. As the number of basis functions increases, the accuracy of this approximation increases. To obtain a measure of the convergence behavior, of the eigenvalues, we introduce the convergence parameter K_i as

$$K_i = \left| \frac{\epsilon_i^{G_1} - \epsilon_i^{G_2}}{\epsilon_i^{G_1} - \epsilon_{i-1}^{G_1}} \right| \tag{3.38}$$

which is a measure of the difference of the same eigenvalue ϵ_i for two different basis set size G_1 and G_2 ($G_2 > G_1$) relative to the difference to the next lower eigenvalue ϵ_{i-1}. During the computation an eigenvalue $\epsilon_i^{G_2}$ is considered as converged once the corresponding convergence parameter K_i is found to be smaller than a certain value (e.g., 0.01).

3.4 The Discrete Variable Representation Method

The essence of all numerical schemes in solving differential equations and integration is in the discretization of the continuous variables, that is the spatial coordinates and/or time. Let us assume the simple case of a single-variable function $f(x)$. The first order derivative of this function around a point x is defined from the limit

$$f'(x) = \lim_{\Delta x \to 0} \frac{f(x + \Delta x) - f(x)}{\Delta x} \tag{3.39}$$

if it exists. Now if we divide the space into discrete points x_k with an evenly spaced interval $h = x_{k+1} - x_k$ and label the function at the lattice points as $f_k = f(x_k)$, we obtain the simplest expression for the first-order derivative

$$f'_k = \frac{f_{k+1} - f_k}{h} + \mathcal{O}(h) \tag{3.40}$$

The above formula is referred to as the *two-point formula* for the first-order derivative; it can be easily derived by taking the Taylor expansion of f_{k+1} around x_k. The accuracy can be improved if we expand f_{k+1} and f_{k-1} around x_k and take the difference

$$f_{k+1} - f_{k-1} = 2hf'_k + \frac{h^3}{6} f_k^{(3)} + \cdots \tag{3.41}$$

After a simple rearrangement, we have

$$f'_k = \frac{f_{k+1} - f_{k-1}}{2h} + \mathcal{O}(h^2) \tag{3.42}$$

which is commonly known as the *three-point formula* for the first-order derivative. The accuracy of the expression will increase to even higher orders in h if

more points are used. For example a *seven-point formula* (what we have used in our calculations) can be derived by including the expansions of f_{k+3}, f_{k-3}, f_{k+2} and f_{k-2} around x_k. After some combinations one obtains [14]

$$f'_k = \frac{1}{60h}(-f_{k-3} + 9f_{k-2} - 45f_{k-1} + 45f_{k+1} - 9f_{k+2} + f_{k+3}) + \mathcal{O}(h^6) \quad (3.43)$$

The approximate expressions for the second-order derivative can be obtained with different combinations of f_i. The *three-point formula* for the second-order derivative is given by the combination

$$f_{k+1} - 2f_k + f_{k-1} = h^2 f''_k + O(h^4) \quad (3.44)$$

with the Taylor expansions of $f_{k\pm1}$ around x_k. The above equation gives the second-order derivative as

$$f''_k = \frac{f_{k+1} - 2f_k + f_{k-1}}{h^2} + \mathcal{O}(h^2) \quad (3.45)$$

With the similar method one obtains in the *seven-point approximation* to the second order derivative

$$f''_k = \frac{1}{180h^2}(2f_{k-3} - 27f_{k-2} + 270f_{k-1} - 490f_k + 270f_{k+1} - 27f_{k+2} + 2f_{k+3}) + \mathcal{O}(h^6) \quad (3.46)$$

Let us turn to numerical integration. In general, we want to obtain the numerical value of an integral defined in the region $[a, b]$ as

$$S = \int_a^b f(x)dx \quad (3.47)$$

We can divide the region $[a, b]$ into n slices with an evenly spaced interval h. If we take the lattice points as x_k with $k = 0, 1, \ldots, n$, we can write the integral as a summation of integrals over all the slices

$$\int_a^b f(x)dx = \sum_{k=0}^{n-1} \int_{x_k}^{x_{k+1}} f(x)dx \quad (3.48)$$

Of course, if we can develop a numerical scheme that evaluates the integral over several slices accurately, we will have solved the problem. Let us first consider each slice separately. The simplest quadrature is obtained if we approximate $f(x)$ in the region $[x_k, x_{k+1}]$ linearly, that is, $f(x) \simeq f_k + (x - x_k)(f_{k+1} - f_k)/h$. After integration every slice with this linear function, we have

$$S = \frac{h}{2} \sum_{k=0}^{n-1} (f_k + f_{k+1} + \mathcal{O}(h^2) \quad (3.49)$$

where $\mathcal{O}(h^2)$ comes from the error in the linear interpolation of the function. The above quadrature is commonly referred to as the *trapezoid rule*, which has an overall accuracy up to $\mathcal{O}(h^2)$.

We can obtain a quadrature with a higher accuracy by working on two slices together. If we apply the Lagrange interpolation to the function $f(x)$ in the region of $[x_{k-1}, x_{k+1}]$ we have

$$f(x) = \frac{(x-x_k)(x-x_{k+1})}{(x_{k-1}-x_k)(x_{k-1}-x_{k+1})} f_{k-1} + \frac{(x-x_{k-1})(x-x_{k+1})}{(x_k-x_{k-1})(x_k-x_{k+1})} f_k + \frac{(x-x_{k-1})(x-x_k)}{(x_{k+1}-x_{k-1})(x_{k+1}-x_k)} f_{k+1} + \mathcal{O}(h^3) \quad (3.50)$$

If we carry out the integral for every pair of slices together with the integrand given from the above equation, we have [14]

$$S = \frac{h}{3} \sum_{l=0}^{n/2-1} (f_{2l} + 4f_{2l+1} + f_{2l+2}) + \mathcal{O}(h^4) \quad (3.51)$$

which is known as the *Simpson rule*. The third-order term vanishes because of cancellation. In order to pair up all the slices, we have to have an even number of slices.

Part II

QUANTUM SCATTERING UNDER 2D CONFINING POTENTIAL

4. ANALYTICAL DESCRIPTION OF ATOMIC SCATTERING AND CONFINEMENT-INDUCED RESONANCES IN WAVEGUIDES

Recently the field of ultracold few-body confined systems has progressed remarkably. By employing optical dipole traps [15] and atom chips [16, 17, 18] it is possible to fabricate mesoscopic structures in which the atoms are frozen to occupy a single or a few lowest quantum states of a confining potential such that in one or more dimensions the characteristic length possesses the order of the atomic de Broglie wavelength. These configurations can be well described by effective low-dimensional systems. The quantum dynamics of such systems is strongly influenced by the geometry of the confinement. This situation is encountered ,e.g., in certain quantum wires for electronic transport, or in atomic waveguides or optical lattices for ultracold atoms. Atom waveguides are fundamental component of atom optics, and are expected to play an important role for example in atom interferometry, quantum computing applications, ultrasensitive detectors of accelerators , and gravitational anomalies as well as to provide an opportunity to study novel 1D many-body states. To ensure proper coherence (long-range order) as atomic beams propagate through the waveguides, effort should be made to avoid decoherence -inducing mechanism such as collisional losses and collisional phase shifts. This clearly requires a detailed understanding of the effects of quasi-one-dimensional confinement on atom-atom collisions (see Refs. [19-45] and references therein). In particular, we will see that in the few-mode regime, necessary for coherent propagation, the free-space estimate of the collisional effects are no longer valid and a waveguide-specific theory is needed. This stimulated the development of quantum scattering theory in low dimensions. The spin-statistics theorem, according to which identical particles with integer spin are bosons whereas those with half-integer spin are fermions, breaks down in low-dimensional systems. The "Fermi-Bose duality" is a very general property of identical particles in 1D, maps strongly interacting bosons to weakly-interacting fermions and vice versa. In recent years this esoteric subject has become highly relevant through experiments on ultracold atomic vapors in atom waveguides.

Of particular interest is the single-mode regime, where only the ground state with respect to the confining direction can be actually populated. This occurs for a sufficiently dilute gas in a regime of low temperatures and densities under a sufficiently strong transverse confinement, when both the chemical potential and the thermal energy k_BT are less than the transverse oscillator level spac-

ing $\hbar\omega$. In this case the two-body scattering properties are strongly modified and short-range correlation are greatly enhanced. The dynamics of such system can then be mapped to an effective one-dimensional (1D) Hamiltonian with zero-range interactions. With this assumption, the dynamics of ultracold atoms in low-dimensional structures, e.g., tight waveguides has been studied using the simplification that the atoms occupy only the ground state of the transverse confining potential. Nevertheless, the virtual transverse excitations in the course of the collision process can play a crucial role in the scattering leading to the so-called confinement-induced resonances (CIRs), predicted by Olshanii [27, 28]. It was shown [27, 28] that CIRs appear if the binding energy of the pseudopotential, approximating the two-atom molecular state in the presence of the confinement, coincides with the energy spacing between the levels of the transverse harmonic potential. In the vicinity of the CIR the coupling constant g_{1D} can be tuned from $-\infty$ to $+\infty$ by varying the strength of the confining potential over a small range. This can result in a total atom-atom reflection, thereby creating a gas of impenetrable bosons. CIRs have also been studied for the three-body [29, 30] and the four-body [31] scattering under confining potential, as well as for a pure p-wave scattering of fermions [32]. Experimental evidence for the CIRs for bosons [33, 34] and fermions [35] has recently been reported.

A general analytical treatment of low-energy scattering under action of a general cylindrical confinement involving all partial waves and their coupling, was first provided in Ref. [36] for a spherically symmetric short-range potential. The effect of the CM motion on the s-wave collision of two distinguishable atoms (i.e. a two-species mixture) in a harmonic confinement as well as for two identical atoms in a non-parabolic confining potential has been investigated in Ref. [37] in the zero-energy limit neglecting the s and p wave mixing. A detailed study including the effect of the CM nonseparability and taking into account the s and p wave mixing for harmonic confinement was performed in the single-mode regime in Ref. [40]. Recently a so-called dual-CIR was discovered [38, 39, 40], which is characterized by a complete transmission (suppression of quantum scattering) in the waveguide due to destructive interference of s and p waves although the corresponding collisions in free space involve strong interactions.

The problem of atomic pair collisions under the action of a harmonic trap in the multimode regime when the energy of the atoms exceeds the level spacing of the transverse trapping potential is much more intricate than the single-mode regime due to several open transverse channels. It demands the development of a multichannel scattering theory accounting for the possible transitions between the levels of the confining potential. Using as a starting point the formalism for scattering in restricted geometries suggested in Refs. [41, 42], the multichannel scattering problem for bosons in a harmonic confining potential has been analyzed analytically by Olshanii et al. [43] in the s-wave pseudopotential approximation and the zero-energy limit. Without detailization of the interatomic interaction but using only two input parameters - the s-wave two-body scattering length in free space and the trap frequency - they have derived an ap-

proximate formula for the scattering amplitude describing two boson collisions confined by transverse harmonic trap in the multi-mode regime.

In [45], a general grid method has been developed for multichannel scattering of two atoms confined by a transverse harmonic trap with a single frequency for both atoms. The method applies to arbitrary atomic interactions, permitting a rich spectral structure where several different partial waves are participating in the scattering process, or even the case of an anisotropy of the interaction. Using this method the transverse excitations and deexcitations in the course of the collisional process (distinguishable or identical atoms) has been analyzed including all important partial waves and their couplings due to the broken spherical symmetry. Special attention has been paid to the analysis of the CIRs in the multimode regimes for non-zero collision energies.

In this chapter we study scattering theory of identical as well as distinguishable atoms confined by a transverse harmonic trap and discuss the scattering parameters and the transition probabilities characterizing the two-body collisions in the trap. Special attention is paid to the analysis of the CIRs in zero collision- energies.

4.1 Hamiltonian and Two-body Scattering Problem in a Waveguide

Let us consider collisions of two atoms under the action of the transverse harmonic confinement. We address both cases, distinguishable and indistinguishable atoms under the action of the same confining potential, i.e. the trap is characterized by a single frequency ω for every atom. The corresponding Hamiltonian is given by

$$H = -\frac{\hbar^2}{2m_1}\nabla_1^2 - \frac{\hbar^2}{2m_2}\nabla_2^2 + \frac{1}{2}m_1\omega^2\rho_1^2 + \frac{1}{2}m_2\omega^2\rho_2^2 + V(\mathbf{x}_1 - \mathbf{x}_2) \tag{4.1}$$

where m_i is the mass of the ith atom, $V(\mathbf{x}_1 - \mathbf{x}_2)$ is the two-body potential describing the interaction between two colliding atoms in free space, and $\mathbf{x}_i = (\rho_i, z_i) = (r_i, \theta_i, \varphi_i)$ is the coordinate of the ith atom.

The Hamiltonian is separable with respect to the relative/CM coordinate and momenta $\mathbf{x}$, $\mathbf{X}$ and $\mathbf{p}$, $\mathbf{P}$ variables. This can be done by the canonical transformation

$$\begin{pmatrix} \mathbf{X} \\ \mathbf{x} \\ \mathbf{P} \\ \mathbf{p} \end{pmatrix} = \frac{1}{M}\begin{pmatrix} m_1 & m_2 & 0 & 0 \\ M & -M & 0 & 0 \\ 0 & 0 & M & M \\ 0 & 0 & m_2 & -m_1 \end{pmatrix}\begin{pmatrix} \mathbf{x}_1 \\ \mathbf{x}_2 \\ \mathbf{p}_1 \\ \mathbf{p}_2 \end{pmatrix} \tag{4.2}$$

where $M = m_1 + m_2$ is the total mass. The transformed Hamiltonian takes the form

$$H = H_{CM} + H_{rel} \tag{4.3}$$

where

$$H_{CM} = -\frac{\hbar^2}{2M}\nabla_{\mathbf{X}}^2 + \frac{1}{2}M\omega^2 R_\perp^2 \tag{4.4}$$

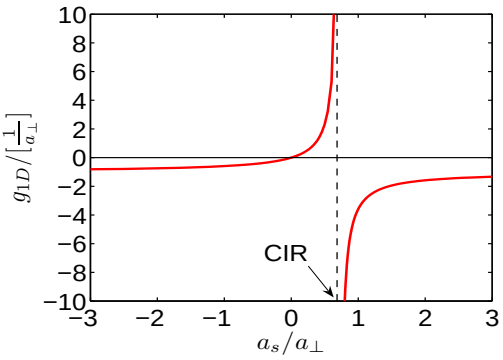

Fig. 4.1: The effective quasi-1D coupling constant g_{1D} as a function of the s-wave scattering length a_s for single-channel scattering of two bosons under a harmonic confinement.

and

$$H_{rel} = -\frac{\hbar^2}{2\mu}\nabla^2_{\mathbf{x}} + \frac{1}{2}\mu\omega^2\rho^2 + V(\mathbf{x}) \tag{4.5}$$

Here $\mu = m_1 m_2/(m_1+m_2)$ is the reduced mass, and ρ and $\mathbf{R}_\perp$ are the relative and center of mass radial coordinates respectively. The center of mass Hamiltonian is that of a simple harmonic oscillator whose solution is known, hence the problem, reduces to scattering of a single effective particle with the reduced mass μ and collision energy $E > \hbar\omega$, off a scatterer $V(\mathbf{x})$ at the origin, under transverse harmonic confinement with frequency ω, $U(\rho) = \frac{1}{2}\mu\omega^2\rho^2$

$$\left[-\frac{\hbar^2}{2\mu}\nabla^2_{\mathbf{x}} + U(\rho) + V(r)\right]\psi(\mathbf{x}) = E\psi(\mathbf{x}) \tag{4.6}$$

Here the energy of the relative two-body motion $E = E_\perp + E_\parallel$ is a sum of the transverse $E_\perp$ and longitudinal collision $E_\parallel$ energies. Due to our definition of the confining potential, the transverse excitation energies $E_\perp$ can take the possible values $E_\perp = E - E_\parallel = \hbar\omega(2n+|m|+1) > 0$ of the discrete spectrum of the 2D oscillator $\frac{1}{2}\mu\omega^2\rho^2$.

Determining the eigenstates of this Hamiltonian, in particular within the s-wave scattering approximation for $V(\mathbf{x})$, is the central goal of this section.

4.2 s-wave Scattering Regime: the Reference T-Matrix Approach

The T-matrix formulation allows for a self-consistent description of the low-energy part of the spectrum that uses the *free-space* low-energy scattering properties of the interaction potential as the *only* input. In addition the low-energy (s-wave) limit is isolated to a single well-defined approximation without requiring the ad-hoc introduction of regularization via a pseudo-potential. This

self-consistent low-energy treatment has been outlined first in [43]. In their work, they also solved for the T-matrix using the standard Huang-Fermi pseudo-potential, showing that the pseudo-potential reproduces the exact result in this situation.

In this section we follow [43] and [44]. Let the unperturbed Hamiltonian H be a Hamiltonian for a single nonrelativistic particle in presence of a trapping potential U

$$\langle \mathbf{x}|H|\psi\rangle = \left[\frac{-\hbar^2\nabla_{\mathbf{x}}^2}{2\mu} + U(\mathbf{x})\right]\langle \mathbf{x}|\psi\rangle \tag{4.7}$$

Assume also that the particle is 'perturbed' by a scatterer given by

$$\langle \mathbf{x}|V|\psi\rangle = V(\mathbf{x})\langle \mathbf{x}|\psi\rangle \tag{4.8}$$

localized around $\mathbf{x} = \mathbf{0}$. In what follows we will derive a *low-energy approximation* for the T-matrix of the scatterer V in presence of H. By making use of the Lupu-Sax formula (A.119), one can drive the correct form of the T-matrix in the low-energy s-wave regime. We begin our derivation by first specifying a "reference" background Hamiltonian H' as

$$\langle \mathbf{x}|H'|\psi\rangle = \left[\frac{-\hbar^2\triangle_{\mathbf{x}}}{2\mu} + E\right]\langle \mathbf{x}|\psi\rangle \tag{4.9}$$

This Hamiltonian is that of a free particle, but with an explicit energy dependence included so that the eigenstates have zero wavelength at all energies. We note that this reference Hamiltonian agrees with the free-space Hamiltonian in the zero-energy limit. While this Hamiltonian may seem strange, it is a valid reference Hamiltonian which turns out to be useful because the resulting T-matrix is energy independent for any scattering potential. The Green's function for this Hamiltonian is given by

$$\langle \mathbf{x}|G_{H'}(E)|\mathbf{x}'\rangle = -\frac{\mu}{2\pi\hbar^2}\frac{1}{|\mathbf{x}-\mathbf{x}'|} \tag{4.10}$$

as can be derived by direct substitution into $[E - H']G_{H'}(E) = I$. In turn the T-matrix of the interaction potential V in presence of H' is independent of energy and can therefore be expressed as

$$\langle \mathbf{x}|T_{H',V}(E)|\mathbf{x}'\rangle = gD(\mathbf{x},\mathbf{x}') \tag{4.11}$$

where the kernel D is defined as normalized to unity,

$$\int d\mathbf{x}d\mathbf{x}'D(\mathbf{x},\mathbf{x}') = 1 \tag{4.12}$$

The normalized coefficient g is then related, through the zero-energy scattering amplitude, to the three-dimensional scattering length a_s according to

$$g = \frac{2\pi\hbar^2 a_s}{\mu} \tag{4.13}$$

Imagine that the kernel $D(\mathbf{x}, \mathbf{x}')$ is well localized within some radius R. In perturbative expansion at low energies this kernel only participates in convolutions with slow (as compared to R) functions, in which case it can be approximated by a δ-function,

$$D(\mathbf{x}, \mathbf{x}') \approx \delta(\mathbf{x})\delta(\mathbf{x}') \tag{4.14}$$

This straightforward approximation is the key to the s-wave scattering approximation. This effectively replaces the exact reference T-matrix by its long-wavelength limit, so that the reference T-matrix assumes the form

$$\langle \mathbf{x}|T_{H',V}(E)|\mathbf{x}'\rangle \approx g\delta(\mathbf{x})\delta(\mathbf{x}') \quad [k, k' \ll 1/R] \tag{4.15}$$

which is equivalent to

$$T_{H',V}(E) = g|0\rangle\langle 0| \tag{4.16}$$

where $|0\rangle$ is the position eigenstate corresponding to the location of the scatterer. In expression (4.15) k and k' refer to the wavevectors of any matrices which multiply the T-matrix from the left and right, respectively.

If we now substitute the above expression for the reference T-matrix into the Lupu-Sax formula (A.119) for the T-matrix under the background Hamiltonian H we arrive at

$$\begin{aligned} T_{H,V}(E) &= \sum_{n=0}^{\infty} \left[g|0\rangle\langle 0|G_{H'}(E)\right]^n g|0\rangle\langle 0| \\ &= \left[1 - g\langle 0|G_H(E)|0\rangle + g\langle 0|G_{H'}(E)|0\rangle\right]^{-1} g|0\rangle\langle 0| \end{aligned} \tag{4.17}$$

Making use of (4.10), we introduce the function $\chi(\epsilon)$, defined as

$$\chi(E) = \lim_{\mathbf{x}\to 0}\left[\langle \mathbf{x}|G_H(E)|0\rangle + \frac{\mu}{2\pi\hbar^2|\mathbf{x}|}\right] \tag{4.18}$$

from which we obtain the following simple expression for the T-matrix of the scatterer V in presence of the trap

$$\langle \mathbf{x}|T_{H,V}(E)|\psi\rangle \approx \frac{g\delta(\mathbf{x})}{1 - g\chi(E)}\langle \mathbf{x}|\psi\rangle \quad [E \ll \hbar^2/\mu R^2] \tag{4.19}$$

From comparing the equations the free-space and bound Green's functions obey, one can show that the singularity in bound Green's function is the same as that in the free-space Green's function. Hence, $\chi(E)$ is the value of the regular part of the bound Green's function at the origin.

4.2.1 Eigenstates of the waveguide Hamiltonian

The Hamiltonian for the relative motion of two atoms in a harmonic waveguide contains two parts, the longitudinal free Hamiltonian H_z and the transverse confinement Hamiltonian $H_\perp$,

$$H = H_z + H_\perp \tag{4.20}$$

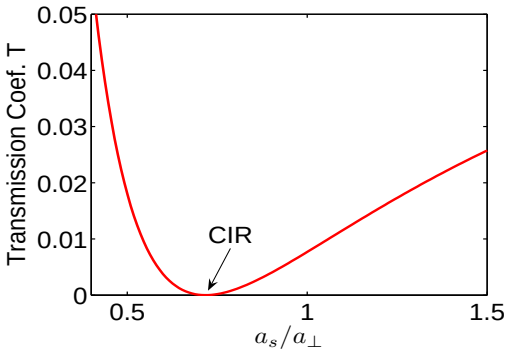

Fig. 4.2: The Transmission Coefficient T as a function of the s-wave scattering length a_s for single-channel scattering of two bosons under a harmonic confinement.

where

$$H_z = -\frac{\hbar^2}{2\mu}\frac{\partial^2}{\partial z^2} \tag{4.21}$$

and

$$H_\perp = -\frac{\hbar^2}{2\mu}(\frac{\partial^2}{\partial \rho^2} + \frac{1}{\rho}\frac{\partial}{\partial \rho} + \frac{1}{\rho^2}\frac{\partial^2}{\partial \varphi^2}) + \frac{1}{2}\mu\omega^2\rho^2 \tag{4.22}$$

The eigenstates of the transverse Hamiltonian, denoted by $|nm\rangle$, are well known and satisfy both

$$H_\perp|nm\rangle = \hbar\omega(2n + |m| + 1)|nm\rangle \tag{4.23}$$

as well as

$$L_z|nm\rangle = \hbar m|nm\rangle \tag{4.24}$$

where L_z is the operator for angular momentum along the z-axis. We note that in this representation the radial and the azimuthal quantum numbers n and m independently take the values

$$n = 0, 1, 2, ...\infty \tag{4.25}$$

and

$$m = 0, \pm 1, \pm 2, ... \pm \infty \tag{4.26}$$

The eigenfunctions are given in spatial-representation by

$$\langle \rho\varphi|nm\rangle = \left[\frac{\pi a_\perp^2 (n + |m|)!}{n!}\right]^{-1/2} (\frac{\rho}{a_\perp})^{|m|} e^{-\rho^2/(2a_\perp^2)} L_n^{|m|}(\rho^2/a_\perp^2) e^{im\varphi} \tag{4.27}$$

Here $L_n^m(x)$ are the generalized Laguerre polynomials and $a_\perp = \sqrt{\hbar/\mu\omega}$, is the transverse oscillator length. Lastly we note that the value of $|nm\rangle$ at the origin is given by

$$\langle 0|nm\rangle = \frac{\delta_{m,0}}{\sqrt{\pi}a_\perp} \tag{4.28}$$

which is independent of n.

4.2.2 The Green's function for the relative motion of two particles in a harmonic waveguide

For the case of transverse harmonic confinement function we can evaluate $\chi(E)$ by expanding the matrix element $\langle \mathbf{x}|G(E)|0\rangle$ onto the set of states

$$|nmz\rangle = |nm\rangle \otimes |z\rangle \tag{4.29}$$

where $|nm\rangle$ is the eigenstate of the transverse potential given by (4.27) and $|z\rangle$ is the eigenstate of the operator z, satisfying $\langle z|z'\rangle = \delta(z - z')$. For simplicity we take $G_H(E) \leftrightarrow G(E)$,

$$\langle \mathbf{x}|G(E)|0\rangle = \sum_{n,m,n',m'} \langle \rho\varphi|nm\rangle\langle nmz|G(E)|n'm'0\rangle\langle n'm'0|0\rangle \tag{4.30}$$

In the other hand the bound Green's function is the solution to the equation

$$[E - H_\perp - H_z]G(E) = I \tag{4.31}$$

where I is the identity matrix. Expanding this equation onto the set of states (4.29) gives

$$\left[E - \hbar\omega(2n + |m| + 1) + \frac{\hbar^2}{2\mu}\frac{\partial^2}{\partial z^2}\right]\langle nmz|G(E)|n'm'z'\rangle = \langle nmz|n'm'z'\rangle$$
$$= \delta_{n,n'}\delta_{m,m'}\delta(z - z') \tag{4.32}$$

We proceed by making the ansatz for the Green's function

$$\langle nmz|G(E)|n'm'z'\rangle = \delta_{n,n'}\delta_{m,m'}\alpha_{nm}e^{i\gamma_{nm}|z-z'|} \tag{4.33}$$

Differentiating (4.33) twice with respect to z and substituting the result into (4.32) gives

$$\left[E - \hbar\omega(2n + |m| + 1) - \frac{\hbar^2\gamma_{nm}^2}{2\mu}\right]\langle nmz|G(E)|n'm'z'\rangle$$
$$+i\frac{\hbar^2\gamma_{nm}\alpha_{nm}}{\mu}\langle nmz|n'm'z'\rangle = \langle nmz|n'm'z'\rangle \tag{4.34}$$

This equation is satisfied provided that

$$\gamma_{nm}^2 = \frac{2\mu}{\hbar^2}[E - \hbar\omega(2n + |m| + 1)] \tag{4.35}$$

and

$$\alpha_{nm} = -i\frac{\mu}{\hbar^2\gamma_{nm}} \tag{4.36}$$

Equation (4.35) is quadratic, and therefore has in general two solutions. We should choose the solutions which propagate outwards from $z = z'$.

By introducing the dimensionless energy

$$\varepsilon = \frac{E}{2\hbar\omega} - \frac{1}{2} \tag{4.37}$$

we find that retarded Green's function can be expressed as

$$\langle nmz|G(\varepsilon)|n'm'z'\rangle = -i\frac{\mu a_\perp}{2\hbar^2}\frac{e^{i\frac{2}{a_\perp}\sqrt{\varepsilon-n-\frac{|m|}{2}}|z-z'|}}{\sqrt{\varepsilon-n-\frac{|m|}{2}}}\delta_{n,n'}\delta_{m,m'} \tag{4.38}$$

With this expression for the bound Green's function and using the value of $|n,m\rangle$ at the origin (4.28) which is independent of n, we obtain for the matrix element $\langle \mathbf{x}|G(\varepsilon)|0\rangle$

$$g\langle \mathbf{x}|G(\varepsilon)|0\rangle = -\sqrt{\pi}a_s\sum_{n=0}^{\infty}\langle\rho\varphi|n0\rangle\frac{e^{-\frac{2}{a_\perp}\sqrt[\downarrow]{n-\varepsilon}|z|}}{\sqrt[\downarrow]{n-\varepsilon}} \tag{4.39}$$

where the modified complex square root $\sqrt[\downarrow]{}$ is defined for an arbitrary complex number c as

$$\sqrt[\downarrow]{|c|e^{i\phi}} = \sqrt{|c|}e^{i\phi/2} \quad -2\pi < \phi \leq 0$$

note that the usual square root is defined as

$$\sqrt[\downarrow]{|c|e^{i\phi}} = \sqrt{|c|}e^{i\phi/2} \quad 0 \leq \phi < 2\pi$$

Now by inserting (4.39) and (4.13) into (4.18) we arrive at the expression

$$g\chi(\varepsilon) = \lim_{\mathbf{x}\to 0}\left[-\sqrt{\pi}a_s\sum_{n=0}^{\infty}\langle\rho\varphi|n0\rangle\frac{e^{-\frac{2}{a_\perp}\sqrt[\downarrow]{n-\varepsilon}|z|}}{\sqrt[\downarrow]{n-\varepsilon}} + \frac{a_s}{|\mathbf{x}|}\right] \tag{4.40}$$

While both terms in (4.40) diverges in the limit $\mathbf{x}\to 0$, their difference remains finite and leads to an expression for $\chi(\varepsilon)$ in terms of a generalized Zeta function.

To proof this we assume, that the directional single-variable limits $\mathbf{x} = s\mathbf{n}, s\to 0$ exist for all directions $\mathbf{n}$ and they are all equal to each other. This assumption allows us to deal with the limit along the z-axis only

$$g\chi(\varepsilon) = -\lim_{|z|\to 0}\left[\frac{a_s}{a_\perp}\sum_{n=0}^{\infty}\frac{e^{-\frac{2}{a_\perp}\sqrt[\downarrow]{n-\varepsilon}|z|}}{\sqrt[\downarrow]{n-\varepsilon}} - \frac{a_s}{|z|}\right] \tag{4.41}$$

where we have used the identity (4.28). We proceed by first replacing the $a_s/|z|$ term in (4.41) with an integral expression via the identity

$$\frac{a_s}{|z|} = \frac{a_s}{a_\perp}\int_\varepsilon^\infty dn\frac{e^{-\frac{2}{a_\perp}\sqrt{n-\varepsilon}|z|}}{\sqrt{n-\varepsilon}} \tag{4.42}$$

This allows us to write

$$g\chi(\varepsilon) = -\frac{a_s}{a_\perp} \lim_{|z|\to 0} \lim_{N\to\infty} \left[\sum_{n=0}^{N} \frac{e^{-\frac{2}{a_\perp}\sqrt[4]{n-\varepsilon}|z|}}{\sqrt[4]{n-\varepsilon}} - \int_{\varepsilon}^{N} dn \frac{e^{-\frac{2}{a_\perp}\sqrt{n-\varepsilon}|z|}}{\sqrt{n-\varepsilon}} \right] \tag{4.43}$$

It is now tempting to interchange the limit signs and thus get rid of the coordinate dependence. In order to be able to do that one have to prove the uniformity with respect to $|z|$ of the $N \to \infty$ convergence of the expression in the square brackets $\Xi(N, |z|)$, i.e., to prove that for every ϵ there exists N^*, the same for all $|z|$, such that $\Xi(N, |z|) - \lim_{N\to\infty} \Xi(N, |z|) < \epsilon$ for all $N > N^*$. Such a proof does exist, although we do not exhibit it here.

We arrive at the following expression for $\chi(\varepsilon)$

$$g\chi(\varepsilon) = -\frac{a_s}{a_\perp} \lim_{N\to\infty} \left[\sum_{n=0}^{N} \frac{1}{\sqrt[4]{n-\varepsilon}} - 2\sqrt{N-\varepsilon} \right] \tag{4.44}$$

One can now make use of the following theorem involving the Hurwitz Zeta function, an analytic generalized Zeta function described in the mathematical literature [46]

$$\zeta(s,\alpha) = \lim_{N\to\infty} \left[\sum_{n=0}^{N} \frac{1}{(n+\alpha)^s} - \frac{1}{1-s} \frac{1}{(N+\alpha)^{s-1}} \right] \tag{4.45}$$
$$Re(s) > 0, \quad -2\pi < arg(n+\alpha) \leq 0$$

In particular,

$$\zeta(1/2,\alpha) = \lim_{N\to\infty} \left[\sum_{n=0}^{N} \frac{1}{\sqrt[4]{n+\alpha}} - 2\sqrt{N+\alpha} \right] \tag{4.46}$$

While this expression, valid for any N, may be taken as a definition of the Hurwitz Zeta function, it does not constitute an efficient method for computation. With this definition and taking $s = 1/2$ we arrive at

$$g\chi(\varepsilon) = -\frac{a_s}{a_\perp} \zeta(1/2, -\varepsilon) \tag{4.47}$$

By substituting this expression into (4.19) we arrive at the final expression for the long-wavelength T-matrix in the waveguide

$$T(\varepsilon) = \frac{g|0\rangle\langle 0|}{1 + \frac{a_s}{a_\perp}\zeta(1/2, -\varepsilon)} \tag{4.48}$$

4.2.3 Multichannel scattering amplitudes and transition rates

From equations (A.118) and (4.48) we find that the scattered wavefunction takes the form

$$\langle nmz|\psi_{out}(\varepsilon)\rangle = g \frac{\langle nmz|G(\varepsilon)|0\rangle}{[1 + \frac{a_s}{a_\perp}\zeta(1/2, -\varepsilon)]} \langle 0|\psi_0(\varepsilon)\rangle \tag{4.49}$$

Now the matrix element $\langle nmz|G(\varepsilon)|0\rangle$ can be determined by making use of (4.28) and (4.38), yielding

$$\begin{aligned}\langle nmz|G(\varepsilon)|0\rangle &= \sum_{n',m'}\int dz'\langle nmz|G(\varepsilon)|n'm'z'\rangle\langle n'm'z'|0\rangle \\ &= -i\frac{\mu}{2\sqrt{\pi}\hbar^2}\delta_{m,0}\frac{e^{i\frac{2}{a_\perp}\sqrt{\varepsilon-n}|z|}}{\sqrt{\varepsilon-n}}\end{aligned} \tag{4.50}$$

Inserting this expression into (4.49) then gives

$$\langle nmz|\psi_{out}(\varepsilon)\rangle = -i\frac{\sqrt{\pi}a_s}{[1+\frac{a_s}{a_\perp}\zeta(1/2,-\varepsilon)]}\delta_{m,0}\frac{e^{i\frac{2}{a_\perp}\sqrt{\varepsilon-n}|z|}}{\sqrt{\varepsilon-n}}\langle 0|\psi_0(\varepsilon)\rangle \tag{4.51}$$

Let us now assume that the incident wave has the longitudinal wave vector k and the transverse quantum numbers n and m, according to

$$\langle \mathbf{x}|\psi_0(\varepsilon)\rangle = \langle \rho\varphi|nm\rangle e^{ikz} \tag{4.52}$$

where the relation

$$\varepsilon = \left(\frac{a_\perp k}{2}\right)^2 + n + \frac{|m|}{2} \tag{4.53}$$

gives the dependence of the scaled energy ε on the incident wave vector k. This incident wave is nonzero at the origin only for $m = 0$, hence only incident waves with zero angular momentum will scatter. The value of the $m = 0$ incident wave at the origin conveniently takes the n-independent value,

$$\langle 0|\psi_0(\varepsilon)\rangle = \frac{\delta_{m,0}}{\sqrt{\pi}a_\perp} \tag{4.54}$$

Assuming henceforth $m = 0$, we can now express (4.51) as

$$\langle n'm'z'|\psi_{out}(\varepsilon)\rangle = -i\frac{\delta_{m',0}}{[\frac{a_\perp}{a_s}+\zeta(1/2,-\varepsilon)]}\frac{e^{i\frac{2}{a_\perp}\sqrt{\varepsilon-n}|z|}}{\sqrt{\varepsilon-n}} \tag{4.55}$$

From this expression it follows that the full wavefunction of the relative motion in s-wave regime takes the form

$$\langle \mathbf{x}|\psi(\varepsilon)\rangle = \sum_{n'=0}^{\infty}\langle \rho\varphi|n'0\rangle\left[\delta_{n',n}e^{ikz} + f^e_{nn'}e^{ik_{n'}|z|}\right] \tag{4.56}$$

Here we have introduced the even-wave *transversely inelastic scattering amplitudes* $f^e(k_{n'} \leftarrow k_n)_{n'\leftarrow n} = f^e_{nn'}$, given by

$$f^e_{nn'} = -\frac{2i}{a_\perp k_{n'}}\frac{1}{\left[\frac{a_\perp}{a_s}+\zeta(1/2,-\left(\frac{a_\perp k_n}{2}\right)^2-n)\right]} \tag{4.57}$$

and the outgoing wave vector for the mode $|n'0\rangle$

$$k_{n'} = \frac{2}{a_\perp}\sqrt{\left(\frac{a_\perp k_n}{2}\right)^2 + n - n'} \tag{4.58}$$

from which the desired scattering probabilities can be computed. One can show easily that the number n_e of open excited transverse channels -the maximum value of n' for which $k_{n'}$ in (4.58) is real- coincides with the integer part of the dimensionless energy ε. For $n > n_e$, $K_{n'}$ is purely imaginary number which results in a decaying wave, thus this channels are asymptotically closed. The interatomic interaction $V(\mathbf{r})$ mixes different transversal channels and leads to transitions $n \to n'$ between the open channels $n, n' \leq n_e$, i.e., to transverse excitation and deexcitation processes during the collisions.

One can now easily compute the elastic and inelastic transition probabilities for collisions under transverse harmonic confinement. We begin by considering the asymptotic forms of the total wavefunction given by (4.56), which are given by

$$\lim_{z\to\infty}\langle n'0z|\psi(\varepsilon)\rangle = \delta_{n',n}e^{ikz} + \Theta[\varepsilon - n']f^e_{nn'}e^{ik_{n'}z} \tag{4.59}$$

$$\lim_{z\to-\infty}\langle n'0z|\psi(\varepsilon)\rangle = \Theta[\varepsilon - n']f^e_{nn'}e^{ik_{n'}z} \tag{4.60}$$

where $\Theta(x)$ is the Heavyside step function. Because of energy conservation, an inelastic collision results in a change in the longitudinal momentum $k_n \to k_{n'}$, so that the introduction of inelastic transmission and reflection coefficients must be based on conservation of total incident and outgoing probability current. Using the asymptotic wavefunctions (4.59) and (4.60) and the total current conservation one obtains

$$\sum_{n'=0}^{n_e}(T_{nn'} + R_{nn'} - \delta_{nn'}) = 0 \tag{4.61}$$

for the inelastic transmission (reflection) coefficients $T_{nn'}$ ($R_{nn'}$). k_n ($k_{n'}$) is the initial (final) relative wave vector and n (n') the transverse excitation number according to (4.58). We have [43]

$$T_{nn'} = \Theta[\varepsilon - n']\frac{k_{n'}}{k_n}|\delta_{n,n'} + f^e_{nn'}|^2 \tag{4.62}$$

$$R_{nn'} = \Theta[\varepsilon - n']\frac{k_{n'}}{k_n}|f^e_{nn'}|^2 \tag{4.63}$$

The transition probability $W_{nn'}$, characterizing the transverse excitation and deexcitation, into a particular channel n' from the initial state n is given by the sum of the corresponding transmission and reflection coefficients

$$W_{nn'} = T_{nn'} + R_{nn'} \tag{4.64}$$

Due to the time reversal symmetry of the Hamiltonian we have $T_{nn'} = T_{n'n}$, $R_{nn'} = R_{n'n}$ and $W_{nn'} = W_{n'n}$. The total transmission (reflection) coefficient $T = \sum_{n'} T_{nn'}$ ($R = \sum_{n'} R_{nn'}$) is given by the sum of the transmission (reflection) coefficients of all the open channels. Equation (4.61) leads to $T + R = 1$.

4.2.4 *Single-channel scattering and effective one-dimensional interaction potential*

Let us now consider the special case of a single-channel scattering

$$0 \leq \varepsilon < 1, \quad n_e = 0 \tag{4.65}$$

In this case we have

$$g\chi(\varepsilon) = -\frac{a_s}{a_\perp}\zeta(1/2, -\varepsilon) = -\frac{a_s}{a_\perp}\left[\zeta(1/2, 1-\varepsilon) + \frac{i}{\sqrt{\varepsilon}}\right] \tag{4.66}$$

Using an alternative representation for $\zeta(1/2, 1-\varepsilon)$

$$\zeta(1/2, 1-\varepsilon) = \lim_{N\to\infty}\left[\sum_{n=1}^{N}\frac{1}{\sqrt[1]{n-\varepsilon}} - 2\sqrt{N}\right] \tag{4.67}$$

and making use of the expansion in powers of ε,

$$\frac{1}{\sqrt{n-\varepsilon}} = \frac{1}{\sqrt{n}} + \sum_{j=1}^{\infty}\frac{(2j-1)!!}{2^j j! n^{j+1/2}}\varepsilon^j \tag{4.68}$$
$$|\varepsilon| < 1, \quad n > 0$$

allows to write

$$\zeta(1/2, 1-\varepsilon) = \zeta(1/2) + \mathcal{L}(\varepsilon) \tag{4.69}$$

where

$$\mathcal{L}(\varepsilon) = \sum_{j=1}^{\infty}\frac{(2j-1)!!\zeta(j+1/2)}{2^j j!}\varepsilon^j \tag{4.70}$$

which clearly separates the zero energy limit from the finite energy corrections.

According to (4.57) this leads to

$$f^e(k) = -\frac{1}{\left[1 - i\frac{a_\perp}{2}\left[\frac{a_\perp}{a_s} + \zeta(1/2)\right]k - i\frac{a_\perp k}{2}\mathcal{L}\left(\frac{a_\perp^2 k^2}{4}\right)\right]} \tag{4.71}$$

where $f^e(k) = f^e(k_0 \leftarrow k_0)_{0\leftarrow 0}$ is the even single-channel scattering amplitude and $\zeta(1/2) = -1.4603\ldots$.

It is now tempting to introduce an effective one-dimensional interaction potential in such a way that its scattering amplitude, introduced through the one-dimensional scattering solution as

$$\psi_{1D}(z) = e^{ikz} + \left[f^e(k) + sgn(z)f^o(k)\right]e^{ik|z|} \tag{4.72}$$

matches (4.71), i.e., solve the corresponding one-dimensional inverse scattering problem. It turns out that this problem is ill-posed due to the presence of open channels unaccessible within the one-dimensional model. Nevertheless one may pose the following problem: find a one-dimensional potential, whose scattering

amplitude reproduces the exact one (4.71) with the relative error $\mathcal{O}(k^3)$. Such an object does exist, and it is represented by a zero-range scatterer

$$v_{1D}(z) = g_{1D}\delta(z) \tag{4.73}$$

A straightforward calculation shows that the scattering amplitude $f_\delta^e(k)$ of the one-dimensional potential (4.73) has a form

$$f_\delta^e(k) = -\frac{1}{1 + ika_{1D}} \tag{4.74}$$

where the one-dimensional scattering length a_{1D} is related to the potential strength by

$$g_{1D} = -\frac{\hbar^2}{\mu a_{1D}} \tag{4.75}$$

Comparison of the scattering amplitudes (4.71) and (4.74) leads to a conclusion that the waveguide scattering amplitude (4.71) at low velocities can be reproduced by a delta-potential (4.73) of a scattering length

$$a_{1D} = -\frac{a_\perp}{2}\left[\frac{a_\perp}{a_s} + \zeta(1/2)\right] \tag{4.76}$$

It follows from (4.75) and (4.76) that

$$g_{1D} = \frac{2\hbar^2 a_s}{\mu a_\perp^2}\frac{1}{(1 - Ca_s/a_\perp)} \tag{4.77}$$

which has a resonant form showing a Confined Induced Resonance (CIR) at $a_s = a_\perp/C$, where $C = -\zeta(1/2) = 1.4603\ldots$ (Fig. 4.1). Hence the whole range of 1D coupling constants from $-\infty$ to $+\infty$ is experimentally achievable by tuning a_s over a narrow range in the neighborhood of the 1D resonance. This can result in a total atom-atom reflection, thereby creating a gas of impenetrable bosons (see Fig. 4.2 for the transmission coefficient as a function of the scattering length). The effect was recently [28] interpreted in terms of Feshbach resonance between ground and excited vibrational manifolds.

It was shown in [28] that at low longitudinal energies $ka_\perp \ll 1$ the 1D scattering amplitude generated by the interaction $g_{1D}\delta(z)$ reproduces the exact 3D scattering amplitude in the waveguide to within a relative error $\mathcal{O}(k^3)$. The relation between g_{1D} and the 1D scattering amplitude may be found by substituting (4.72) into 1D Schrödinger equation

$$\left[-\frac{\hbar^2}{2\mu}\frac{\partial^2}{\partial z^2} + g_{1D}\delta(z) + \hbar\omega\right]\psi_{1D}(z) = E\psi_{1D}(z) \tag{4.78}$$

which gives

$$g_{1D} = \lim_{k\to 0}\frac{\hbar^2 k}{\mu}\frac{Re[f^e(k)]}{Im[f^e(k)]} \tag{4.79}$$

To establish the physical origin of the CIR, we follow [28]. We show that the CIR is in fact a zero-energy Feshbach resonance, occurring when the energy of a bound state of the asymptotically closed channels (i.e., the excited transverse modes) coincides with the continuum threshold of the open channel (lowest transverse mode).

This explanation is best verified by artificially serving the coupling between the ground transverse mode and the manifold of excited modes. If a bound state of the decoupled excited manifold exists, then a zero-energy Feshbach resonance will occur when this bound-state energy coincides with the continuum threshold of the ground transverse mode. To determine the relevant bound-state energies, we assume the standard Huang-Fermi peudopotential

$$V_{pseudo} = \frac{2\pi\hbar^2 a_s}{\mu}\delta^3(\mathbf{x})\frac{\partial}{\partial r}(r.) \tag{4.80}$$

which supports a single bound state in free space at $E = \hbar^2/\mu a_s^2$ for the case $a_s > 0$. To determine the location of the CIR, we need to ask what happens to the energy of this bound state if a single transverse mode is projected out of the Hilbert space. We therefore proceed by formally splitting the Hamiltonian onto "ground," "excited," and "ground-excited coupling" parts according to

$$\begin{aligned} H &= H_g + H_e + H_{g-e} \\ &= P_g H P_g + P_e H P_e + (P_e H P_g + H.c.) \end{aligned} \tag{4.81}$$

where $P_g = |0\rangle\langle 0|$, $P_e = \sum_{n=1}^{\infty} |n\rangle\langle n|$, are the corresponding projection operators, $|n\rangle$ being the eigenstate of the transverse two-dimensional harmonic oscillator with *radial* quantum number n and zero axial angular momentum.

The ground Hamiltonian has a 1D coordinate representation of the form

$$H_g = -\frac{\hbar^2}{2\mu}\frac{\partial^2}{\partial z^2} + g_{1D}\delta(z) + \hbar\omega \tag{4.82}$$

corresponding to the motion of a one-dimensional particle in the presence of a δ barrier with the coupling constant g_{1D} is defined via

$$g_{1D}\delta(z) = \int 2\pi\rho d\rho |\phi_0(\rho)|^2 \frac{2\pi\hbar^2 a_s}{\mu}\delta^3(\mathbf{r}) \tag{4.83}$$

which gives

$$g_{1D} = \frac{2\hbar^2 a_s}{\mu a_\perp^2} \tag{4.84}$$

The spectrum of H_g is continuous for energies above the threshold energy $E_{c,g} = \hbar\omega$. Likewise, the spectrum of the excited Hamiltonian is clearly continuous for energies $E_{c,e} = 3\hbar\omega$ but, as we will see below, H_e supports one bound state of energy $E_{b,e} < E_{c,e}$ for all values of the $3D$ scattering length, a_s.

According to the Feshbach scheme, one would predict a resonance in the renormalized g_{1D} for a set of parameters, such that the energy of the bound

state of H_e coincides with the continuum threshold of H_g. Thus, the CIR condition can be expressed as $E_{b,e} = E_{c,g}$. As we will see below, this scheme indeed predicts a position of the CIR *exactly*.

The energy $E_{b,e}$ of the bound state of H_e can be found using the following two step procedure. First, we identify the bound-state energy of the full Hamiltonian H as a pole of the scattering amplitude on the physical Riemann sheet. Second, we make use of the peculiar property of the two-dimensional harmonic oscillator that the excited Hamiltonian H_e and the full Hamiltonian H can be transformed to each other via a simple unitary transformation. This leads to a simple relation between their bound-state energies.

The even-wave one-dimensional scattering amplitude f^e at an energy E ($E_{c,g} \leq E < E_{c,e}$), is given by (4.71) which can be written as

$$f^e(k) = -\frac{2i}{ka_\perp \left[\frac{a_\perp}{a_s} + \zeta(1/2, -(ka_\perp/2)^2)\right]} \tag{4.85}$$

where the wave vector k is given by

$$E = E_{c,g} + \frac{\hbar^2 k^2}{2\mu} \tag{4.86}$$

The bound state energies of the full Hamiltonian H will be given by the poles, $\overline{k}$, on the *positive imaginary* axis of the analytical continuation of $f^e(k)$:

$$E_b = -\frac{\hbar^2 Im(\overline{k}^2)}{2\mu} \tag{4.87}$$

One can see that, in order to avoid crossing the branch cuts of the zeta function, the continuation should be performed inside the $0 \leq Arg(k) \leq \pi/2$ quadrant of the complex plane. In the end, we find a single pole corresponding to the following implicit equation for the bound-state energy

$$\zeta\left(\frac{1}{2}, -\varepsilon\right) = -\frac{a_\perp}{a_s} \tag{4.88}$$

which we have expressed through the dimensionless energy $\varepsilon_b = \frac{E_b}{2\hbar\omega} - \frac{1}{2}$. Now the full Hamiltonian H and the excited Hamiltonian H_e are connected via a simple transformation

$$H_e = A^\dagger H A + 2\hbar\omega I \tag{4.89}$$

where

$$A^\dagger = \sum_{n=0}^{\infty} |n+1\rangle\langle n| \tag{4.90}$$

This can be proved as follows:

$$\begin{aligned} A^\dagger H A &= \left(\sum_{n=0}^{\infty} |n+1\rangle\langle n|\right) H \left(\sum_{n'=0}^{\infty} |n'+1\rangle\langle n'|\right)^\dagger \\ &= \sum_{n=0,n'=0}^{\infty} |n+1\rangle\langle n| H_z^0 + H_\perp^0 + V |n'\rangle\langle n'+1| \end{aligned}$$

Here $H_z^0 = -\frac{\hbar^2\partial^2}{2\mu\partial z^2}$, $H_\perp^0 = -\frac{\hbar^2}{2\mu}\nabla_\perp + \frac{1}{2}\mu\omega^2\rho^2$ and V is given through (4.80). On the other hand we have

$$\begin{aligned}\langle n|H_z^0 + H_\perp^0 + V|n'\rangle &= \delta_{nn'}H_z^0 + \delta_{nn'}\hbar\omega(2n'+1) + \langle n|V|n'\rangle \\ &= \langle n+1|H_z^0|n'+1\rangle + \langle n+1|(H_\perp^0 - 2\hbar\omega)|n'+1\rangle \\ &\quad + \langle n+1|V|n'+1\rangle\end{aligned}$$

For the last term we have used the fact that the $m = 0$ eigenfunctions of the two-dimensional harmonic oscillator all have the same value at the origin. The 3D δ interaction thus has the same matrix elements between all the harmonic oscillator states; hence, the interaction matrix is unaffected by the shift operator. Now one can write

$$\begin{aligned}A^\dagger HA &= \sum_{n=0,n'=0}^{\infty} |n+1\rangle\langle n+1|H_z^0 + H_\perp^0 - 2\hbar\omega + V|n'+1\rangle\langle n'+1| \\ &= \sum_{n=1}^{\infty} |n\rangle\langle n|(H_z^0 + H_\perp - 2\hbar\omega I + V)\sum_{n'=1}^{\infty}|n'\rangle\langle n'| \\ &= P_e H P_e - 2\hbar\omega I = H_e - 2\hbar\omega I\end{aligned}$$

Here I is the unit operator in the Hilbert space of the excited Hamiltonian H_e.

From the above, we conclude that the rescaled bound-state energies $\varepsilon_{b,e}$ of the excited Hamiltonian and ε_b of the full Hamiltonian are related to each other via

$$\varepsilon_{b,e} = \varepsilon_b + 1 \tag{4.91}$$

and thus satisfies the equation

$$\zeta\left(\frac{1}{2}, -\varepsilon_{b,e} + 1\right) = -\frac{a_\perp}{a_s} \tag{4.92}$$

The CIR condition can now be explicitly formulated as

$$\zeta\left(\frac{1}{2}, -\varepsilon_{c,g} + 1\right) = -\frac{a_\perp}{a_s} \tag{4.93}$$

Using $\varepsilon_{c,g} = 1$, we finally arrive at the exact CIR condition $a_\perp/a = -\zeta(1/2, 1) = -\zeta(1/2, 0) = C$. A similar effect is associated with resonance behavior in harmonically confined 2D scattering for $a < 0$ [47]. This resonance would most likely be observed via changes in the macroscopic properties of the ground state of a many-atom system, e.g., the density distribution, as described in detail in [48].

We note that, While in free space a weakly bound state exists only for $a > 0$, we see that in the waveguide such a state exists for all a. These bound states may be of significant interest, allowing the formation of dimers via a modulation of the waveguide potential at the frequency $(E_{c,g} - E_b)/\hbar$. This may lead to an atom-waveguide based scheme for forming ultracold molecules, as well as the possibility to use molecular spectroscopy as a sensitive probe of the atomic field inside the waveguide.

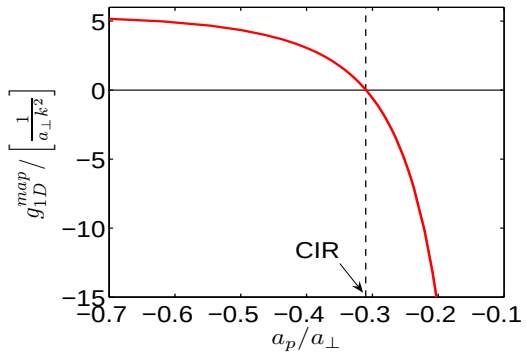

Fig. 4.3: The *mapped coupling constant* g_{1D}^{mapp} as a function of the p-wave scattering length a_p for single-channel scattering of two fermions under a harmonic confinement.

4.3 Remarks on p-wave Scattering

The results obtained for quasi-1D bosons leads us to the following question: **How do two spin-polarized *fermions* under quasi-1D confinement behave?** Attempting to carry through a program analogous to the above for the case of p-wave scattering between polarized fermions meet numerous (hopefully technical) obstacles: Most of the limiting procedures become mutually nonuniformly convergent and no clear way to identify a correct order is visible. In any case the closest candidate for the p-wave analog of the free-space three-dimensional T-matrix is the pseudopotential introduced in [49]

$$\langle\chi|T_{H,V}(E)|\psi\rangle = \frac{27\pi\hbar^2 V_p}{\mu}\nabla\chi^*(0)\cdot\nabla\psi(0) \tag{4.94}$$

that can be shown to reproduce correctly the low-energy behavior of the p-wave scattering amplitude. Here V_p is the p-wave scattering volume, that defines the low-energy behavior of the p-wave scattering phase via [50]

$$V_p = -\lim_{k\to 0}\tan\delta_p(k)/k^3 \tag{4.95}$$

An elegant way around these difficulties has been found recently by Granger and Blume [32], who used a K-matrix technique that does not explicitly involve any zero-range objects.

Application to identical fermions shows that confinement modifies the free-space scattering properties of two fermions significantly; i.e., spin-polarized fermions can have infinitely strong effective interactions for a finite 3D scattering volume V_p when confined to a quasi-1D geometry.

Similar to bosons, we can drive an effective 1D Hamiltonian that describes many of the low energy properties of two spin-polarized fermions in a waveguide.

Importantly, the 1D zero-range potential $g_{1D}\delta(z)$, which has been very successful in treating bosons, cannot be used *directly* since it results in an unphysical scattering amplitude for fermions. One way around this difficulty would be to map the effective fermionic 1D K-matrix to a bosonic 1D K matrix (along with the corresponding wave functions). Mappings between fermions and bosons are important in theoretical treatments of 1D *many body* systems, as they allow one to understand systems of strongly interacting 1D bosons (fermions) by mapping them to weakly interacting systems of 1D fermions (bosons) [51, 52] (For a briefly review of the mapping theorem see appendix D).

Application of mapping theorem to effective 1D two-fermion scattering , results in an equivalent system of two 1D bosons interacting through the potential $g_{1D}^{map}\delta(z)$, with the "mapped coupling constant"

$$\frac{g_{1D}^{map}}{a_\perp \hbar\omega} = -\frac{a_\perp^3}{6V_p}\left[1 - 12\frac{V_p}{a_\perp^3}\zeta\left(-\frac{1}{2}, -\varepsilon + 1\right)\right] \tag{4.96}$$

This remarkable result implies that two spin-polarized quasi-1D fermions with *infinitely strong* interactions when the scattering volume V_p has the critical value

$$\frac{V_p^{crit}}{a_\perp^3} = \left[12\zeta\left(-\frac{1}{2}, -\varepsilon + 1\right)\right]^{-1} \tag{4.97}$$

can be mapped to a system of *noninteracting* bosons (see Fig. 4.3); the converse of the Bose-Fermi mapping [52].

4.4 Beyond the s-wave Approximation

So far we have studied scattering of two particles under 2D confining potential by considering the lowest nonzero angular momentum component (i.e., s-wave for bosons and p-wave for fermions) and neglecting the higher components. For atomic systems, both the s and p waves can be brought into play, although separately, by means of magnetic Feshbach resonances [53]. In the additional presence of electrostatic fields, however, both component are predicted to arise simultaneously, despite the low energies involved [54]. In this latter case, a *simultaneous* resonance in the s- and p-wave scattering occurs such that the reflection coefficient $R \approx 0$. This so-called dual-CIR first observed numerically in [38] predicts the possibility of suppressing the effective two-body interaction in a quasi-1D cylindrical geometry, in spite of a strong interaction in free 3D space. This effect arises from the quantum interference of even and odd contribution to the scattering amplitude, may provide effectively a quasi-1D gas of noninteracting atoms or a free flow of carriers in a quantum wire. Recently this low dimensionality effect has analytically been modelled by applying a previous formalism [36] to quantum scattering processes under cylindrical confinement. This analytic formalism has been improved in order to account colliding between two distinguishable particles including both s and p waves [55].

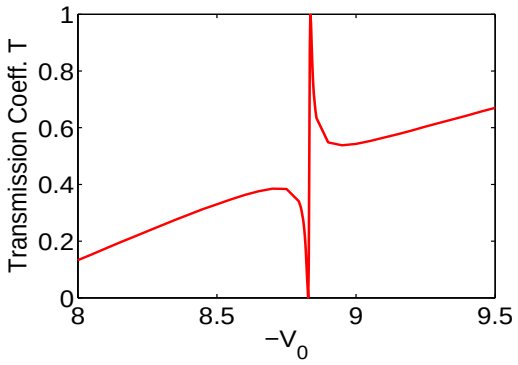

Fig. 4.4: Transmission coefficient T as a function of the depth $-V_0$ of the potential (4.111) for scattering of two distinguishable atoms under a harmonic confinement.

Following [55] the equation describing the relative motion between two distinguishable colliding particles of reduced mass μ and interacting through a central potential $V(r)$ can be written as

$$[\nabla^2 - u(\rho) + k^2]\psi(\mathbf{x}) = v(r)\psi(\mathbf{x}) \tag{4.98}$$

Here $E \equiv \hbar^2 k^2/2\mu$ is the total energy, $v(r) \equiv 2\mu V(r)/\hbar^2$, $u(\rho) \equiv 2\mu U(\rho)/\hbar^2$ and $U(\rho) = \frac{1}{2}\mu\omega^2\rho^2$ is the harmonic confining potential. A general solution to this equation can be written as

$$\psi(\mathbf{x}) = \psi_{in}(\mathbf{x}) - \int d^3\mathbf{x}' G_u(\mathbf{x}, \mathbf{x}')v(r')\psi(\mathbf{x}') \tag{4.99}$$

where $\psi_{in}(\mathbf{x})$ describes an incident wave and $G_u(\mathbf{x}, \mathbf{x}')$ is the scattering Green function under confinement satisfying

$$[\nabla^2 - u(\rho) + k^2]G_u(\mathbf{x}, \mathbf{x}') = -\delta^3(\mathbf{x} - \mathbf{x}') \tag{4.100}$$

The correct boundary condition on $G_u(\mathbf{x}, \mathbf{x}')$ should recover the form of $\psi(\mathbf{x})$ far from the scattering region where $v(r)$ is negligible, i.e., for $r \gg R_V$ with R_V being the range of $v(r)$, which can be assumed in many cases to be short-ranged in the sense that $R_V \ll R_U$, R_U is the range of $u(\rho)$.

This form can be deduced from an explicit expansion of $\psi(\mathbf{x})$ in the orthonormalized basis $\{\phi_n\}$ of eigenstates of the confining potential $U(\rho)$.

For solutions $\psi(\mathbf{x})$ that are cylindrically symmetric, the φ' integration over G_u in (4.99) can be carried out and it suffices to work with Green function under confinement

$$2\pi G_c(\mathbf{x}, \mathbf{x}') \equiv \int d\varphi' G_u(\mathbf{x}, \mathbf{x}') \tag{4.101}$$

and with the basis $\phi_n = \phi_n(\rho)$, $n = 0, 1, \ldots$, having zero angular momentum component along z and eigenvalues $E_n \equiv \hbar^2 q_n^2/2\mu$, with ϕ_0 being the ground

state and q_n, the respective transverse linear momenta. By comparison with (4.99) and with an expansion of the type $\psi(\mathbf{x}) = \sum_n \psi_n(z)\phi_n(\rho)$, an expression for $G_c(\mathbf{x}, \mathbf{x}')$ which holds for all $\mathbf{x}, \mathbf{x}'$ follows thus

$$G_c(\mathbf{x}, \mathbf{x}') = \sum_{n=0}^{\infty} \phi_n(\rho)\phi_n^*(\rho')G_n(z - z') \tag{4.102}$$

where $G_n(z) = -e^{ik_n|z|}/2ik_n$ is the purely 1D Green function, with longitudinal momentum $k_n = \sqrt{k^2 - q_n^2}$ for $0 \leq n \leq n_e$ and $k_n = i\sqrt{q_n^2 - k^2}$ for $n > n_e$, n_e denoting the highest "open channel" for a given total momentum k, i.e., the largest integer n_e such that $E_{n_e} < E < E_{1+n_e}$. Although formally exact, this decomposition in the basis $\{\phi_n\}$ is best suited for the region $r, r' \gg R_V$, where the cylindrical symmetry prevails. Without loss of generality, we may assume from now on that these cylindrically symmetric functions $\phi_n(\rho)$ are real.

In the region $r \ll R_U$ where $u(\rho)$ is negligible, however, a spherical basis should better describe the solution $\psi(\mathbf{x})$. In this regard, it has been discussed in [36] that, when $r, r' \ll R_U$ (i.e., in the absence locally of any confinement), G_u should approach a certain free space 3D Green function G. Using then (4.101), it turns out that G_c should be well approximated by [36]

$$\begin{aligned} G_c(\mathbf{x}, \mathbf{x}') &\approx \int \frac{d\varphi'}{2\pi} G(\mathbf{x}, \mathbf{x}') + \Delta_c(\mathbf{x}, \mathbf{x}') \\ &= \int \frac{d\varphi'}{2\pi} \left(\gamma_+ \frac{e^{ik|\mathbf{x}-\mathbf{x}'|}}{4\pi|\mathbf{x} - \mathbf{x}'|} + \gamma_- \frac{e^{-ik|\mathbf{x}-\mathbf{x}'|}}{4\pi|\mathbf{x} - \mathbf{x}'|} \right) + \Delta_c(\mathbf{x}, \mathbf{x}') \end{aligned} \tag{4.103}$$

where $\gamma_\pm \equiv (1 \pm \gamma)/2$, such that $\gamma_+ + \gamma_- = 1$, and γ is the prefactor of the imaginary part of G. The function Δ_c should stem from the homogeneous part of the solution G_u, i.e., that without the delta function $\delta(\mathbf{x} - \mathbf{x}')$. It should account, together with the factor γ, for the correct boundary condition given by (4.102) and relates only to the low lying levels $n \leq n_e$, for which their quantum nature is most pronounced. The upper levels for $n > n_e$, in turn, are summed up to yield, in the region $r, r' \ll R_U$, G itself. This indicates that the form of (4.103) requires only that $u(\rho)$ vanishes as $\rho \ll R_U$, being thus a property qualitatively independent of the particular basis $\{\phi_n\}$, i.e., of whether $u(\rho)$ is parabolic or not [36].

A first estimate of γ and Δ_c [see Eq. (16) in [36]] reproduces previous results on quasi-1D scattering that are obtained when $v(r)$ is replaced by zero-ranged and regularized pseudopotentials of the type $\delta(\mathbf{x})\partial_r(r.)$. This neglects all angular momentum components except the first $l = 0$, the so-called s-wave approximation. Other treatments to extend the scattering process (in free space) to higher values of l but still using zero-ranged pseudopotentials can be found in the Refs. [56, 57].

4.4.1 Effective quasi-1D scattering amplitudes

Far from the scattering region where the interaction potential $v(r)$ is negligible, the degrees of freedom under geometrical confinement should be "frozen"

into the ground state of the confining potential $u(\rho)$ (or at most into a few excited states, depending on the total energy) and only the unconfined variable, z, should reflect the overall dynamics occurring in the region around $v(r)$. Indeed, substituting G_c in the form of (4.102) into (4.99) and neglecting the exponentially decaying terms $n > n_e$ for large $|z|$ yields

$$\psi(\mathbf{x}) \approx \sum_{n=0}^{n_e} \left(b_n e^{ik_n z} + f_n^{\pm} e^{ik_n |z|} \right) \phi_n(\rho) \tag{4.104}$$

The effective quasi-1D scattering amplitudes f_n^+ and f_n^-, for $n \leq n_e$ and $z > 0$ and $z < 0$, respectively, are then given by [38]

$$\begin{aligned} f^{\pm} &= \frac{1}{2ik_n} \int d^3\mathbf{x}' \left[e^{\pm ik_n z'} \phi_n(\rho') \right]^* v(r') \psi(\mathbf{x}') \\ &= \sum_l (\pm 1)^l \frac{4\pi(2l+1)\alpha_{ln}}{2ik_n} T_l \\ &\equiv f_n^g \pm f_n^u \end{aligned} \tag{4.105}$$

where $f_n^{g(u)}$ contains only the matrix elements T_l of even (odd) angular momenta l. Here the incident state is assumed to populate only the open channels and to be of the form

$$\psi_{in}(\mathbf{x}) = \sum_{n=0}^{n_e} b_n e^{ik_n z} \phi_n(\rho) \tag{4.106}$$

for some weights b_n. $i^l(2l+1)\alpha_{ln}$ are the coefficients of the expansion of each term $e^{ik_n z}\phi_n(\rho)$ on the basis $\{j_l, P_l\}$, for $l = 0, 1, 2, \ldots$ and the "scattering matrix" element T_l is defined by

$$T_l \equiv (1/i^l 4\pi) \int d^3\mathbf{x}' [j_l(kr') P_l(\cos\theta')] v(r') \psi(\mathbf{x}') \tag{4.107}$$

j_l and P_l are the spherical Bessel functions and Legendre polynomials respectively.

4.4.2 Comparison with the unconfined 3D case. The inclusion of p-waves

As a definite example of the above improved formalism, it can be used, for example, to model analytically the remarkable effect of a dual-CIR, which was first observed in [38] numerically by solving fully the Schrödinger equation (4.98). In spite of a strong interaction from $v(r)$, which shows a resonant 3D scattering in both s and p waves with large scattering phase shifts δ_0 and δ_1, respectively, the confinement $u(\rho)$ is able paradoxically to suppress the effective action of $v(r)$ on the unconfined z variable, as if it could pass freely through the scattering region without any reflection.

Consider then a total energy E just below the first excited level, i.e., $E_0 = \hbar\omega < E < E_1 = 3\hbar\omega$, such that $n_e = 0$. In this single mode regime, only the

ground state is open with a longitudinal scattering energy $E_{||} = \hbar^2 k_0^2/2\mu$ and momentum k_0 along the z-axis such that $E = E_0 + E_{||}$ and the incident state should be restricted to $b_n = \delta_{n0}$. Supposing additionally that only the phase shifts δ_l for $l = 0$ and $l = 1$ are large, e.g., due to shape resonances of $v(r)$, by neglecting the contribution of all terms with $l > 1$ one obtains [55]

$$f_0^g = -\frac{1}{1 - i\left[a_\perp/a_s - (C^2 - a_\perp^2 k_0^2)^{1/2}\right]\frac{a_\perp k_0}{2}}$$
$$f_0^u = -\frac{1}{1 - i\left[a_\perp^3/a_p^3 - (C^2 - a_\perp^2 k_0^2)^{3/2}\right]\frac{1}{6a_\perp k_0}} \tag{4.108}$$

where $C = 2$. The quasi-1D scattering cross section can be obtained from the reflection coefficient R, which in the present situation can be written as

$$R = |f_0^g - f_0^u|^2 \tag{4.109}$$

In the absence of any confinement, the equivalent 3D quantity describing the scattering by the *same* potential is the standard total cross section

$$\sigma = \sigma_s + \sigma_p = 4\pi\frac{a_s^2}{1 + (ka_s)^2} + 12\pi\frac{(ka_p)^4}{1 + (ka_p)^6}a_p^2 \tag{4.110}$$

Evidently, σ can only increase as a_p is no longer negligible, particularly if $ka_p \sim 1$ as a_p becomes comparable to the confining length scale $R_U \sim a_\perp$ due, e.g., to a shape resonance in $v(r)$. Under confinement, however, the reflection coefficient R could be sharply decreased if the s and p waves interfere destructively. This can results in an almost complete transmission in spite of the strong interatomic interaction in free space. This has been shown [36, 38] for spherical square well (i.e., $V(r) = V_0$, if $0 < r < r_0$, and zero otherwise), for which the zero energy scattering lengths a_s and a_p can be found straightforwardly as functions of the well depth V_0, as well as for a more realistic interaction, namely, an attractive ($V_0 < 0$) screened Coulomb interaction with a screening length r_0

$$V(r) = V_0\frac{r_0}{r}e^{-r/r_0} \tag{4.111}$$

(see Fig. 4.4).

5. NUMERICAL DESCRIPTION OF ATOMIC SCATTERING AND CONFINEMENT-INDUCED RESONANCES IN WAVEGUIDES

In the present work we develop a general grid method for multichannel scattering of identical as well as distinguishable atoms confined by a transverse harmonic trap. The method applies to arbitrary atomic interactions, permitting a rich spectral structure where several different partial waves are participating in the scattering process, or even the case of an anisotropy of the interaction. The only limitation is that we consider harmonic traps with a single frequency for every atom causing a separation of the c.m. and relative motion. With our approach we analyze transverse excitations and deexcitations in the course of the collisional process (distinguishable or identical atoms) including all important partial waves and their couplings due to the broken spherical symmetry. Special attention is paid to the analysis of the CIRs in the multimode regimes for non-zero collision energies, i.e., to suggest a non-trivial extension of the CIRs theory developed so far only for the single-mode regime and zero-energy limit.

5.1 Hamiltonian and Two-body Scattering Problem in a Waveguide

Let us consider collisions of two atoms under the action of the transverse harmonic confinement. We address both cases, distinguishable and indistinguishable atoms under the action of the same confining potential, i.e., the trap is characterized by a single frequency ω for every atom. The corresponding Hamiltonian is given by

$$H = -\frac{\hbar^2}{2m_1}\nabla_1^2 - \frac{\hbar^2}{2m_2}\nabla_2^2 + \frac{1}{2}m_1\omega^2\rho_1^2 + \frac{1}{2}m_2\omega^2\rho_2^2 + V(\mathbf{x}_1 - \mathbf{x}_2) \tag{5.1}$$

where m_i is the mass of the ith atom, $V(\mathbf{x}_1 - \mathbf{x}_2)$ is the two-body potential describing the interaction between two colliding atoms in free space, and $\mathbf{x}_i = (\rho_i, z_i) = (r_i, \theta_i, \phi_i)$ is the coordinate of the ith atom. As we have seen in chapter 4 the Hamiltonian is separable with respect to the relative/CM variables, the problem, thus, reduces to scattering of a single effective particle with the reduced mass μ and collision energy $E > \hbar\omega$, off a scatterer $V(r)$ at the origin, under transverse harmonic confinement with frequency ω

$$\left[-\frac{\hbar^2}{2\mu}\nabla_{\mathbf{x}}^2 + \frac{1}{2}\mu\omega^2\rho^2 + V(r)\right]\psi(\mathbf{x}) = E\psi(\mathbf{x}) \tag{5.2}$$

For the two-body interaction we choose a screened Coulomb potential

$$V(r) = V_0 \frac{r_0}{r} e^{-r/r_0} \tag{5.3}$$

already employed in Ref. [38, 39, 40] for analyzing the ultracold scattering in cylindrical waveguides in the single-mode regime as $E_\perp = E - E_\parallel$. The chosen potential (5.3) depends on two parameters - the depth $V_0 < 0$ and the screening length $r_0 > 0$. Following the computational scheme already developed in Ref. [40], we implement different spectral structures of the atomic interaction by varying the single parameter V_0 for a fixed length scale r_0. Obvious advantages of the screened Coulomb potential (5.3) compared to the s-wave pseudopotential used in ref. [43] that is devoted to the multi-channel scattering of bosons are the following. First, by varying V_0 one can vary the number of bound states of s-wave character in the interaction potential, and second, one can create new bound and resonant states of higher partial wave character. As a consequence we can consider not only bosonic but also fermionic as well as mixed collisions in a trap and including the case of higher energies. This will, as we shall see below, permit us to investigate new regimes and effects of multi-channel confined scattering.

Performing the scale transformation

$$r \to \frac{r}{a_0} \quad , \quad E \to \frac{E}{E_0} \quad , \quad V_0 \to \frac{V_0}{E_0} \quad \text{and} \quad \omega \to \frac{\omega}{\omega_0} \tag{5.4}$$

with the units $a_0 = \hbar^2/\mu V_0 r_0$, $E_0 = \hbar^2/\mu a_0^2$, and $\omega_0 = E_0/\hbar$, it is convenient to rewrite the equation (5.2) in the rescaled form

$$\left[-\frac{1}{2}\nabla_{\mathbf{x}}^2 + \frac{1}{2}\omega^2\rho^2 + V(r) \right] \psi(\mathbf{x}) = E\psi(\mathbf{x}) \tag{5.5}$$

where V is now the correspondingly scaled potential and we fix $\mu = 1$ and $r_0 = 1$ in the subsequent consideration.

In the asymptotic region $|z| \to \infty$, where the transverse trapping potential dominates the interaction potential, the axial and transverse motions decouple and the asymptotic wavefunction can be written as a product of the longitudinal $e^{ik_n z}$ and transverse $\phi_{n,m}(\rho, \varphi)$ components with

$$\phi_{n,m}(\rho,\varphi) = [\frac{\pi a_\perp^2 (n+|m|)!}{n!}]^{-1/2} (\frac{\rho}{a_\perp})^{|m|} e^{-\rho^2/(2a_\perp^2)} L_n^{|m|}(\rho^2/a_\perp^2) e^{im\varphi} \tag{5.6}$$
$$(n = 0, 1, 2, \ldots \infty \quad \text{and} \quad m = 0, \pm 1, \pm 2, \ldots \pm \infty)$$

being the eigenfunctions of the transverse trapping Hamiltonian

$$H_\perp = -\frac{1}{2}(\frac{\partial^2}{\partial\rho^2} + \frac{1}{\rho}\frac{\partial}{\partial\rho} + \frac{1}{\rho^2}\frac{\partial^2}{\partial\varphi^2}) + \frac{1}{2}\omega^2\rho^2, \tag{5.7}$$

with the corresponding eigenvalues $E_\perp = \omega(2n + |m| + 1)$ and the angular momentum projection m onto the z axis. Here $L_n^m(x)$ are the generalized Laguerre polynomials and $a_\perp = 1/\sqrt{\omega}$, is the transverse oscillator length.

Due to the axial symmetry of the transverse confinement and the spherical symmetry of the interatomic interaction (5.3) the angular momentum component along the z axis is conserved. Therefore, the problem (5.5) is reducible to a 2D one by separating the φ-variable and can be solved for every m independently. The quantum number n is a good one only in the asymptotic region $|z| \to \infty$ and used for the definition of the initial (incident) asymptotic state, i.e., channel

$$\psi^{in}_{n,m}(\mathbf{x}) = e^{ik_n z}\phi_{n,m}(\rho,\varphi) \tag{5.8}$$

of two infinitely separated atoms confined in a transverse state $< \rho\varphi|nm >$. In addition to the quantum numbers n and m the asymptotic scattering state is defined also by the momentum k_n of the channel

$$k_n = \frac{2}{a_\perp}\sqrt{\varepsilon - n - \frac{|m|}{2}} \tag{5.9}$$

which we express through the dimensionless energy $\varepsilon = E/(2\omega) - 1/2$. It is clear that the integer part of the dimensionless energy ε coincides with the number n_e of open excited transverse channels. For $n \le n_e$ we have $(\varepsilon - n - \frac{|m|}{2}) > 0$. The spherically symmetric interatomic interaction (5.3) mixes different transversal channels and leads to transitions $n \to n'$ between the open channels $n, n' \le n_e$, i.e. to transverse excitation and deexcitation processes during the collisions.

Assuming the system to be initially in the channel n, the asymptotic wavefunction takes at $\mid z \mid \to +\infty$ the form [43]

$$\psi_{n,m}(\mathbf{x}) = e^{ik_n z}\phi_{n,m}(\rho,\varphi) + \sum_{n'=0}^{n_e}\left[f^e_{nn'} + sgn(z) f^o_{nn'}\right] e^{ik_{n'}|z|}\phi_{n',m}(\rho,\varphi) \tag{5.10}$$

where $f^e_{nn'}$ and $f^o_{nn'}$ are the matrix elements of the inelastic scattering amplitudes for the even and odd partial waves, respectively, which describe transitions between the channels n and n'. For a bosonic (fermionic) collision just the symmetric (antisymmetric) part of (5.10) should be considered.

It is clear that the scattering amplitude depends also on the index m which, however, remains unchanged during the collision due to the axial symmetry of the problem. Hereafter we consider only the case $m = 0$ and the index is omitted in the following.

Using the asymptotic wavefunction (5.10) and the total current conservation one obtains

$$\sum_{n'=0}^{n_e}\left(T_{nn'} + R_{nn'} - \delta_{nn'}\right) = 0 \tag{5.11}$$

for the inelastic transmission (reflection) coefficients $T_{nn'}$ ($R_{nn'}$). k_n ($k_{n'}$) is the initial (final) relative wave vector and n (n') the transverse excitation numbers according to (5.9). We have

$$T_{nn'} = \Theta[\varepsilon - n']\frac{k_{n'}}{k_n}|\delta_{n,n'} + f^e_{nn'} + f^o_{nn'}|^2 \tag{5.12}$$

$$R_{nn'} = \Theta[\varepsilon - n'] \frac{k_{n'}}{k_n} |f^e_{nn'} + f^o_{nn'}|^2 \tag{5.13}$$

where $\Theta(x)$ is the Heavyside step function. The transition probability $W_{nn'}$, characterizing the transverse excitation/deexcitation, into a particular channel n' from the initial state n is given by the sum of the corresponding transmission and reflection coefficients

$$W_{nn'} = T_{nn'} + R_{nn'} \tag{5.14}$$

Due to the time reversal symmetry of the Hamiltonian we have $T_{nn'} = T_{n'n}$, $R_{nn'} = R_{n'n}$, and $W_{nn'} = W_{n'n}$. The total transmission (reflection) coefficient $T = \sum_{n'} T_{nn'}$ ($R = \sum_{n'} R_{nn'}$) is given by the sum of the transmission (reflection) coefficients of all the open channels. (5.11) leads to $T + R = 1$.

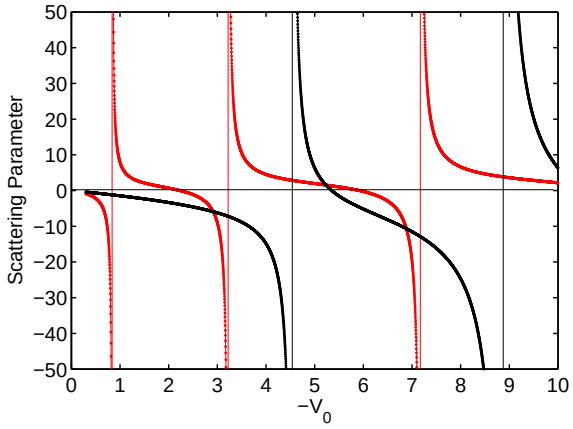

Fig. 5.1: s- and p-wave scattering parameters a_s (red) and V_p (black) as a function of the potential depth V_0 for the free-space effective potential $V(r) + l(l+1)/(2r^2)$. Divergences correspond to the appearance of new bound (s-wave scattering) or shape resonant (p-wave scattering) states in the effective potential. All quantities are given in the units (5.4).

5.2 Numerical approach

To obtain the observable quantities $T_{nn'}$, $R_{nn'}$, and $W_{nn'}$ of the scattering process, we have to calculate the matrix elements $f_{nn'}$ of the scattering amplitude $\hat{f}$ by matching the numerical solution of the Schrödinger equation (5.5) with the scattering asymptotics (5.10). To integrate this multi-channel scattering problem in two dimensions r and θ (z and ρ) we adopt the discrete-variable method suggested in Ref. [58] for solving the nonseparable 2D scattering problems. This approach was applied in Ref. [59] to the case of a 3D anisotropic scattering problem of ultracold atoms in external laser fields.

First, we discretize the 2D Schrödinger equation (5.5) on a 2D grid of angular $\{\theta_j\}_{j=1}^{N_\theta}$ and radial $\{r_j\}_{j=1}^{N}$ variables. The angular grid points θ_j are defined as the zeroes of the Legendre polynomial $P_{N_\theta}(\cos\theta)$ of the order N_θ. Using the completeness property of the normalized Legendre polynomials which remains valid also on the chosen angular grid

$$\sum_{l=0}^{N_\theta-1} P_l(\cos\theta_j)P_l(\cos\theta_{j'})\sqrt{\lambda_j\lambda_{j'}} = \delta_{jj'} \tag{5.15}$$

where λ_j are the weights of the Gauss quadrature, we expand the solution of equation (5.5) in the basis $f_j(\theta) = \sum_{l=0}^{N_\theta-1} P_l(\cos\theta)(\mathbf{P}^{-1})_{lj}$ according to

$$\psi(r,\theta) = \frac{1}{r}\sum_{j=1}^{N_\theta} f_j(\theta)u_j(r) \tag{5.16}$$

Here $\mathbf{P}^{-1}$ is the inverse of the $N_\theta \times N_\theta$ matrix $\mathbf{P}$ with the matrix elements defined as $\mathbf{P}_{jl} = \sqrt{\lambda_j}P_l(\cos\theta_j)$. Due to this definition one can use the completeness relation (5.15) in order to determine the matrix elements $(\mathbf{P^{-1}})_{lj}$ as $(\mathbf{P^{-1}})_{lj} = \sqrt{\lambda_j}P_l(\cos\theta_j)$. It is clear from (5.16) that the unknown coefficients $u_j(r)$ in the expansion are the values $\psi(r,\theta_j)$ of the two-dimensional wave function $\psi(r,\theta)$ at the grid points θ_j multiplied by $\sqrt{\lambda_j}r$. Near the origin $r \to 0$ we have $u_j(r) \simeq r \to 0$ due to the definition (5.16) and the demand for the probability distribution $\mid \psi(r,\theta_j) \mid^2$ to be bounded. Substituting (5.16) into (5.5) results a system of N_θ Schrödinger-like coupled equations with respect to the N_θ-dimensional unknown vector $\mathbf{u}(r) = \{\lambda_j^{1/2}u_j(r)\}_1^{N_\theta}$

$$[\mathbf{H}^{(0)}(r) + 2(E\mathbf{I} - \mathbf{V}(r))]\mathbf{u}(r) = 0 \tag{5.17}$$

where

$$\mathbf{H}^{(0)}_{jj'}(r) = \frac{d^2}{dr^2}\delta_{jj'} - \frac{1}{r^2}\sum_{l=0}^{N_\theta-1} \mathbf{P}_{jl}l(l+1)(\mathbf{P}^{-1})_{lj'} \tag{5.18}$$

$$\mathbf{V}_{jj'}(r) = V(r,\theta_j)\delta_{jj'} = \{V(r) + \frac{1}{2}\omega^2\rho_j^2\}\delta_{jj'}, \quad \rho_j = r\sin\theta_j \tag{5.19}$$

and $\mathbf{I}$ is the unit matrix. We solve the system of equations (5.17) on the quasi-uniform radial grid [60]

$$r_j = R\frac{e^{\gamma x_j} - 1}{e^\gamma - 1}\ ,\ j = 1, 2, ..., N \tag{5.20}$$

of N grid points $\{r_j\}$ defined by mapping $r_j \in (0, R \to +\infty]$ onto the uniform grid $x_j \in (0, 1]$ with the equidistant distribution $x_j - x_{j-1} = 1/N$. By varying N and the parameter $\gamma > 0$ one can choose more adequate distributions of the grid points for specific interatomic and confining potentials.

By mapping the initial variable r in (5.17) onto x we obtain

$$[H^{(0)}(x) + 2\{E\mathbf{I} - \mathbf{V}(r(x))\}]\mathbf{u}(r(x)) = 0 \tag{5.21}$$

with

$$\mathbf{H}^{(0)}_{jj'}(x) = f^2(x)\delta_{jj'}\left(\frac{d^2}{dx^2} - \gamma\frac{d}{dx}\right) - \frac{1}{r^2(x)}\sum_{l=0}^{N_\theta-1}\mathbf{P}_{jl}l(l+1)(\mathbf{P}^{-1})_{lj'} \quad (5.22)$$

where

$$f(x) = \frac{e^\gamma - 1}{Re^{\gamma x}\gamma} \quad (5.23)$$

The uniform grid with respect to x gives six-order accuracy for applying a seven-point finite-difference approximation of the derivatives in the equation (5.21). Thus, after the finite-difference approximation the initial 2D Schrödinger equation (5.5) is reduced to the system of N algebraic matrix equations

$$\begin{aligned}\sum_{p=1}^{3}\mathbf{A}^j_{j-p}\mathbf{u}_{j-p} + [\mathbf{A}^j_j + 2\{E\mathbf{I} - \mathbf{V}_j\}]\mathbf{u}_j + \sum_{p=1}^{3}\mathbf{A}^j_{j+p}\mathbf{u}_{j+p} = 0 \\ \text{for} \quad j = 1, 2, ..., N-3 \\ \mathbf{u}_j + \alpha^{(1)}_j\mathbf{u}_{j-1} + \alpha^{(2)}_j\mathbf{u}_{j-2} + \alpha^{(3)}_j\mathbf{u}_{j-3} + \alpha^{(4)}_j\mathbf{u}_{j-4} = \mathbf{g}_j \\ \text{for} \quad j = N-2, N-1, N\end{aligned} \quad (5.24)$$

where each coefficient $\mathbf{A}^j_{j'}$ is a $N_\theta \times N_\theta$ matrix, each α_j is a diagonal $N_\theta \times N_\theta$ matrix, and each $\mathbf{g}_j$ is a N_θ-dimensional vector. Here the functions $\mathbf{u}_{-3}$, $\mathbf{u}_{-2}$, $\mathbf{u}_{-1}$, and $\mathbf{u}_0$ in the first three equations of the system (for $j = 1, 2$, and 3) are eliminated by using the "left-side" boundary conditions: $\mathbf{u}_0 = 0$ and $\mathbf{u}_{-j} = \mathbf{u}_j$ ($j = 1, 2, 3$). The last three equations in this system for $j = N, N-1$, and $N-2$ are the "right-side" boundary conditions approximating at the edge points r_{N-2}, r_{N-1}, and $r_N = R$ of the radial grid, the scattering asymptotics (5.10) for the desired wave function $\mathbf{u}(r_j)$. In order to construct the "right-side" boundary conditions (5.24) at $j = N-2, N-1$, and N we used an idea of Ref. [59], i.e., the asymptotic behavior (5.10) at the edge points r_{N-2}, r_{N-1}, and $r_N = R$ are considered as a system of vector equations with respect to the unknown vector $f_{nn'}$ of the scattering amplitude for a fixed n. By eliminating the unknowns $f_{nn'}$ from this system we implement the "right-side" boundary conditions defined by (5.24) at $j = N-2, N-1$, and N (see Appendix E).

The reduction of the 2D multi-channel scattering problem to the finite-difference boundary value problem (5.24) permits one to apply efficient computational methods. Here we use, in the spirit of the *LU* decomposition [61], and the sweep method [62] (or the Thomas algorithm [63]), a fast implicit matrix algorithm which is briefly described in Appendix B. The block-diagonal structure of the matrix of the coefficients in the system of equations (5.24) with the width of the diagonal band equal to $7 \times N_\theta$ makes this computational scheme an efficient one.

Solving the problem (5.24) for the defined initial vector k_n and a fixed n from the possible set $0 \le n \le n_e$ we first calculate the vector function $\psi(k_n, r, \theta_j)$.

Then, by matching the calculated vector $\psi(k_n, R, \theta_j)$ with the asymptotic behavior (5.10) at $r = R$, we calculate the nth row of the scattering amplitude matrix $f_{nn'}$ describing all possible transitions $n \to n' = 0, 1, ..., n_e$. This procedure is repeated for the next n from $0 \leq n \leq n_e$. After calculating all the elements $f_{nn'}$ of the scattering amplitude we obtain any desired scattering parameter T, R, or W .

5.3 Results and Discussion

With the above-described method being implemented we have analyzed the two-body scattering under the transverse harmonic confinement for both cases of identical and distinguishable colliding atoms. For confined scattering of identical atoms one has to distinguish the bosonic and fermionic cases. In the case of two colliding bosons the two-body wave function must be symmetric and only even scattering amplitude provides us with a nonzero contribution. First, we show that our result for the special case $\varepsilon < 1$ of a single-channel scattering is in agreement at $\varepsilon \to 0$ with the s-wave pseudopotential approach [27], and, particularly, reproduces s-wave CIR predicted and analyzed in Refs. [27, 28, 43, 38, 40] for bosons. Then we extend our consideration to the multi-channel scattering $\varepsilon > 1$. We demonstrate that our results are in a good agreement in the limit of a long-wavelength trap $\omega = 2\pi c/\lambda \to 0$ with the analytical expression given in [43] which has been obtained in the s-wave pseudopotential approach for the zero-energy limit. The range of validity of the analytical investigation in Ref. [43] is explored. Next we present results for multi-channel scattering of two fermions under transverse harmonic confinement. For a fermionic collision the two-body wave function is antisymmetric, i.e. only the odd scattering amplitude is nonzero. In the special case of single-channel scattering we reproduce the p-wave CIR for fermions [32]. These results are also in agreement with our previous investigations in Refs. [38, 39, 40] performed within a wave-packet propagation method [40]. Finally we consider the confined multi-channel scattering of two distinguishable atoms. In this case both even and odd amplitudes contribute to the scattering process.

For modelling different interatomic interactions in the subsequent sections we vary the depth V_0 of the potential (5.3) in the wide range $-10 < V_0 < 0$ for a fixed width $r_0 = 1$. In free space, this potential being superimposed with the centrifugal term $l(l+1)/(2r^2)$ makes an effective potential which may support some *even* or *odd* bound states depending on the value of the quantum number l and the parameter V_0. For $l \neq 0$ there might be also some *shape resonances* for certain relative energies. These *shape resonances* may enhance strongly the contribution of $l \neq 0$ partial waves in the energy domain where one would have expected a pure $l = 0$ scattering.

It is known that in the zero-energy limit, when the scattering process does not depend on the details of the potential, the collision can be described by a single parameter: the s-wave scattering length $a_s = -\lim_{k\to 0} \tan\delta_s(k)/k$ for $l = 0$ (bosonic collision) and the p-wave scattering volume $V_p = -\lim_{k\to 0} \tan\delta_p(k)/k^3$

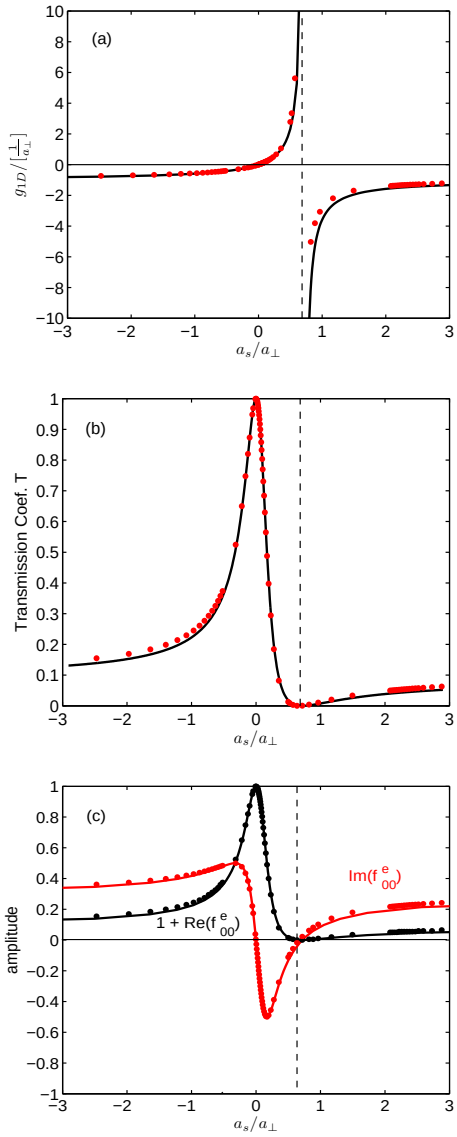

Fig. 5.2: (a) The effective quasi-1D coupling constant g_{1D}, (b) the transmission coefficient T, and (c) the scattering amplitude f^e_{00} as a function of the scattering length a_s for one-channel scattering of two bosons under a harmonic confining potential with $\omega = 0.002$ for a longitudinal relative energy $E_{\|} = 0.0002$ together with the analytical results obtained for the s-wave pseudo-potential zero-energy limit (solid curves) [27, 28, 43]. The constant V_0 is varied in the region $-2.30 < V_0 < -0.32$.

for $l = 1$ (fermionic collision). For sufficiently low collision energy the contribution of the partial waves with larger l can be neglected. In Fig. 5.1 we have plotted a_s and V_p in the region $-10 < V_0 < 0$. Fig. 5.1 demonstrates the rich spectral structure of the chosen form of the interatomic interaction: the scattering parameters a_s and V_p can be positive or negative and they diverge for the values of V_0 corresponding to the appearance of new bound states. In the case of p-wave scattering the increase of the depth V_0 of the potential first leads to a shape resonance which approaches zero energy and finally transforms to a p-wave bound state.

5.3.1 Multichannel scattering of bosons

For two bosons colliding in a transverse harmonic confinement the scattering wave function is symmetric with respect to the exchange $z \to -z$, i.e. $f^o_{nn'} = 0$ in (5.10). We consider multichannel scattering with the dimensionless energy $\varepsilon = E/(2\omega) - 1/2 < 4$ (5.9) permitting the collisional transverse excitations and deexcitations $n \to n' < 4$ up to four open channels (four-mode regime). For comparison with analytical results [28, 43] obtained in the s-wave pseudopotential approach, we have extracted the effective quasi-1D coupling constant $g_{1D} = \lim_{k\to 0} Re\{f^e_{00}(k)\}/Im\{f^e_{00}(k)\}k/\mu$ as well as the transmission coefficient $T = T_{00}$ (5.12) and the scattering amplitude f^e_{00} (5.10), as a function of the scattering length a_s in the single-mode regime ($0 < \varepsilon < 1$). The calculated parameters are presented along with the analytical results in Fig. 5.2 for $\omega = 0.002$ and the longitudinal relative energy $E_\parallel = E - E_\perp = 0.0002$. Fig. 5.2(a) shows the coupling constant g_{1D} as a function of the scattering length a_s. Our numerical result clearly exhibit a singularity at $a_s/a_\perp \approx 1/C$ with $C = -\zeta(1/2) = 1.4603..$, which corresponds to the well-known s-wave CIR [27, 28]. In Fig. 5.2(b) we present the transmission coefficient T versus a_s. The transmission coefficient T goes to unity (total transmission) when a_s tends to zero (i.e. no interaction between the atoms), while at the CIR position, it exhibits the well-known minimum (blocking of the atomic current by the CIR). Fig. 5.2(c) shows the scattering amplitude f^e_{00} as a function of a_s. The amplitude approaches zero at $a_s/a_\perp = 0$ and -1 at the CIR position , which results in total transmission and total reflection, respectively. In general the presented values of f^e_{00} are in very good agreement with the analytical results.

In the multimode regime our results are in good agreement with the analytical ones obtained within the s-wave pseudopotential approach in the zero-energy limit [43] for long-wavelength traps (tight confinement: $\omega = 2\pi c/\lambda \to 0$). In Fig. 5.3 we present our scattering amplitude f^e_{00} along with the analytical results as a function of the dimensionless energy ε for $\omega = 0.0002$ and $V_0 = -3.0$. Apart from energies close to the channel thresholds, the real and imaginary part of the scattering amplitude f^e_{00} show a monotonous behavior: $Re(f^e_{00})$ is monotonically increasing and approaching zero asymptotically whereas $Im(f^e_{00})$ decays monotonically and also approaches zero for large values of ε. The peak structure located at integer values of ε is due to the resonant scattering once a new previously closed channel opens with increasing energy. There is a good

agreement between our results and the analytical ones given by (6.9) in Ref. [43] for the complete range $0 < \varepsilon < 4$. However, we encounter major deviations with increasing ω except for narrow regions close to the channel thresholds (as ε approaches integer values) for the real parts of the scattering amplitudes (see Fig. 5.4). These deviations are most presumably due to the energy dependence of the s-wave scattering length which is neglected in Ref. [43].

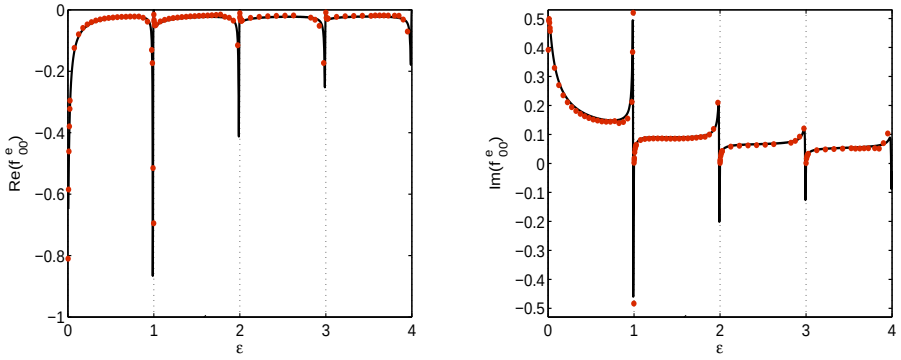

Fig. 5.3: The scattering amplitude f^e_{00} (dots) as a function of the dimensionless energy ε along with the analytical results -solid curves- for $\omega = 0.0002$ and $V_0 = -3.0$ (i.e., $a_s = -8.95$).

For the multichannel regime ($\varepsilon > 1$) we find a strong dependence of the total transmission coefficient T on the population of the initial state n, except for the case $a_s/a_\perp \to 0$ of noninteracting bosons in free space. Fig. 5.5 shows the calculated transmission coefficients (5.12) as a function of $a_s/a_\perp$ for $\omega = 0.002$ for the (a) two-mode regime with $\varepsilon = 1.05$ and (b) the three-mode regime with $\varepsilon = 2.05$. Note, that all these cases correspond to near-threshold collision energies if the maximal integer is subtracted from ε. Similar to the single-mode regime, T goes to unity (total transmission) when a_s tends to zero. We also encounter a minimum. However, the value of the transmission at the minimum is not zero anymore in the multi-mode regime, the larger the number of open channels, the position of the minima will be more shifted to the left. For a fixed value of the ratio $a_s/a_\perp \neq 0$, a lower initially populated transverse level n, leads to a larger total transmission.

In Fig. 5.6 we present the transmission as a function of the dimensionless energy ε for the two cases of the system being initially in the ground $n = 0$ (a) or first excited $n = 1$ (b) transverse states, for different values of the ratio $a_s/a_\perp$. With increasing collision energy the transmission coefficient exhibits a nonmonotonic behavior: we observe a sequence of minima and peaks. For $0 < \varepsilon < 1$ the value of T at the minimum is zero. As the number of open channels increases with increasing collision energy E, the transmission values at the corresponding minima increase strongly. The corresponding transmission peaks $T = 1$ are located at the channel thresholds. The shape of the transmis-

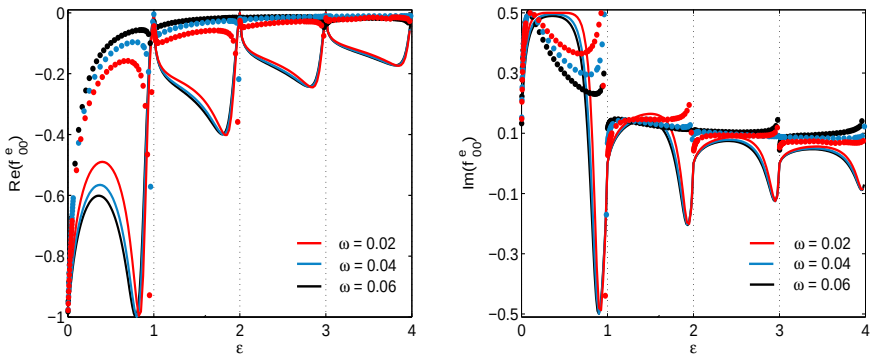

Fig. 5.4: The scattering amplitude f^e_{00} (dots) as a function of the dimensionless energy ε along with the analytical results (solid curves) for $\omega = 0.02$ (red), $\omega = 0.04$ (blue) and $\omega = 0.06$ (black). The amplitudes have been calculated for $V_0 = -3.0$ ($a_s = -8.95$).

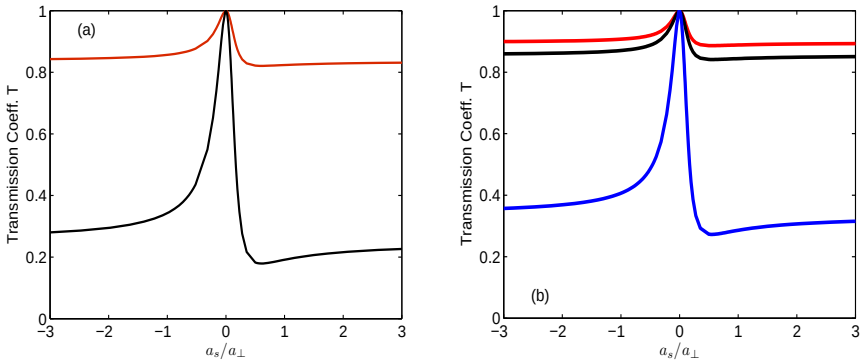

Fig. 5.5: The total transmission coefficient T for a bosonic collision in a harmonic confinement $\omega = 0.002$ as a function of $a_s/a_\perp$ for (a) two-open channels with $\varepsilon = 1.05$ being initially in the transverse ground state $n = 0$ (red) and first excited state $n = 1$ (black), and (b) three-open channels with $\varepsilon = 2.05$ being initially in the ground state $n = 0$ (red), first excited state $n = 1$ (black) and second excited state $n = 2$ (blue).

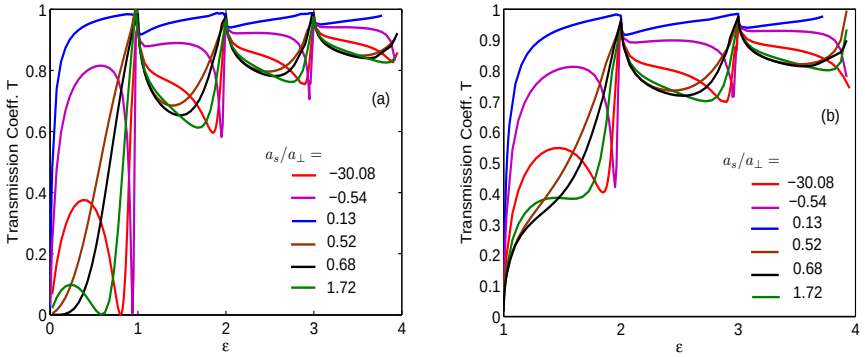

Fig. 5.6: The total transmission coefficients T for bosonic collisions as a function of the dimensionless energy ε for the two cases of the system being initially in the ground $n = 0$ (a) and first excited $n = 1$ (b) transverse states, for several ratios of $a_s/a_\perp$ and $\omega = 0.002$. The black curve corresponds to $a_s/a_\perp = 1/C$ for which the zero-energy CIR in the single-mode regime is encountered.

sion "valleys" in between two integer values of ε as well as the positions of the minima strongly depend on the ratio $a_s/a_\perp$ which can be changed by varying the strength of the interatomic interaction V_0 or the trap frequency ω. Both, changing V_0 and/or ω leads to energetic shifts of the bound states (in particular for the excited transversal channels) of the atoms in the presence of the confinement. If the collision energy coincides with a bound state of the corresponding closed channel we encounter an occupation of the closed channel in the course of the scattering process, i.e. a Feshbach resonance occurs. The interpretation of the minimum of the transmission T in terms of a Feshbach resonance at the point $a_s/a_\perp = 1/C$ for the zero-energy limit was provided in Refs. [27, 28], where it was shown that the origin of the CIR is an intermediate occupation of a bound state belonging to an excited transverse (closed) channel.

To demonstrate that the above-discussed behavior (minima) of the transmission coefficient $T(\varepsilon)$ in certain regions of ε is due to Feshbach resonances we have analyzed the probability density of the scattering wave function of the atoms in the trap. In the single-mode regime and in the zero-energy limit we encounter the well-known CIR: Fig. 5.7 shows the corresponding probability density $|\psi(x,z)|^2$ for an initial transverse ground state $n = 0$ and $\varepsilon = 0.05$ as well as $a_s/a_\perp = 0.68$. For small $|z|$ one observes additional two pronounced peaks along the transverse (x-) direction corresponding to the occupation of the bound state (with the binding energy $\varepsilon^B_{n=1} \sim 0$) in the first excited closed channel of the transverse potential. The probability density tends to zero as $z \to +\infty$. This leads to a zero of the transmission $T(\varepsilon)$ for $\varepsilon \to 0$ [see Fig. 5.6(a)] corresponding to the zero-energy CIR.

In Fig. 5.8 we show the probability densities $|\psi(x,z)|^2$ at $a_s/a_\perp = +4.39$ for several values of the dimensionless energy ε for (a) the single- and (b) two-

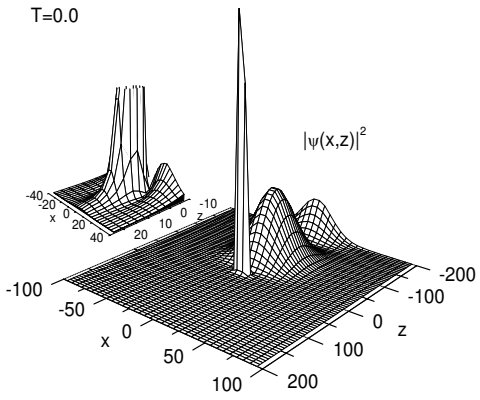

Fig. 5.7: The probability density $|\psi(x,z)|^2$ for bosonic collisions as a function of x and z at $a_s/a_\perp = 0.68$ for $\varepsilon = 0.05$ - zero-energy CIR . The corresponding transmission values are also indicated. The result has been obtained for $\omega = 0.002$.

mode regimes for collisions with initial transverse state $n = 0$. The corresponding probability density exhibits for small values of $|z|$ additional two (for the single-mode regime) and four (for the two-mode regime) pronounced peaks with respect to the transverse (x) direction as ε approaches the CIR position. This demonstrates the occupation of bound states of higher, namely first excited (with binding energy $\varepsilon^B_{n=1}$) and second excited (with binding energy $\varepsilon^B_{n=2}$) channels in the course of the scattering process. The corresponding transmission values are also indicated in Fig. 5.8 . Zero transmission is observed also for $a_s/a_\perp = +4.39$ and $\varepsilon = 0.75$ with no probability density being present for large positive values of z, see Fig. 5.8(a).

The energy of the bound state $\varepsilon^B_{n=1}$, that leads to a minimal transmission due to a resonant scattering process, changes with varying $a_s/a_\perp$ as follows. It is below $\varepsilon = 0$ for $0 < a_s/a_\perp < 0.68$ and consequently no minimum is encountered for $T(\varepsilon)$ in the range $0 < \varepsilon < 1$ (see Fig. 5.6). At the position of the zero-energy CIR it is located just above the threshold $\varepsilon = 0$ leading to a zero transmission for $\varepsilon \to 0$. For $a_s/a_\perp > 0.68$ the bound state energy is somewhere in between the channel thresholds $\varepsilon = 0$ and $\varepsilon = 1$ whereas for $a_s/a_\perp < 0$ it is below but close to $\varepsilon = 1$ leading again to a corresponding minimum of T. For both cases, $a_s/a_\perp < 0$ and $a_s/a_\perp > 0.68$, an increase of $a_s/a_\perp$ leads to a narrow transmission well and the corresponding transmission minimum is shifted towards the next higher channel threshold. The dependence of $\varepsilon^B_{n=1}$ on the parameter $a_s/a_\perp$ is in agreement with the pseudopotential analysis given in ref.[28] (see Fig. 2 of this reference).

In Fig. 5.9(a) we show the transition probabilities $W_{nn'}$ as a function of $a_s/a_\perp$ for $\omega = 0.002$ and $\varepsilon = 3.05$ corresponding to four open channels. We

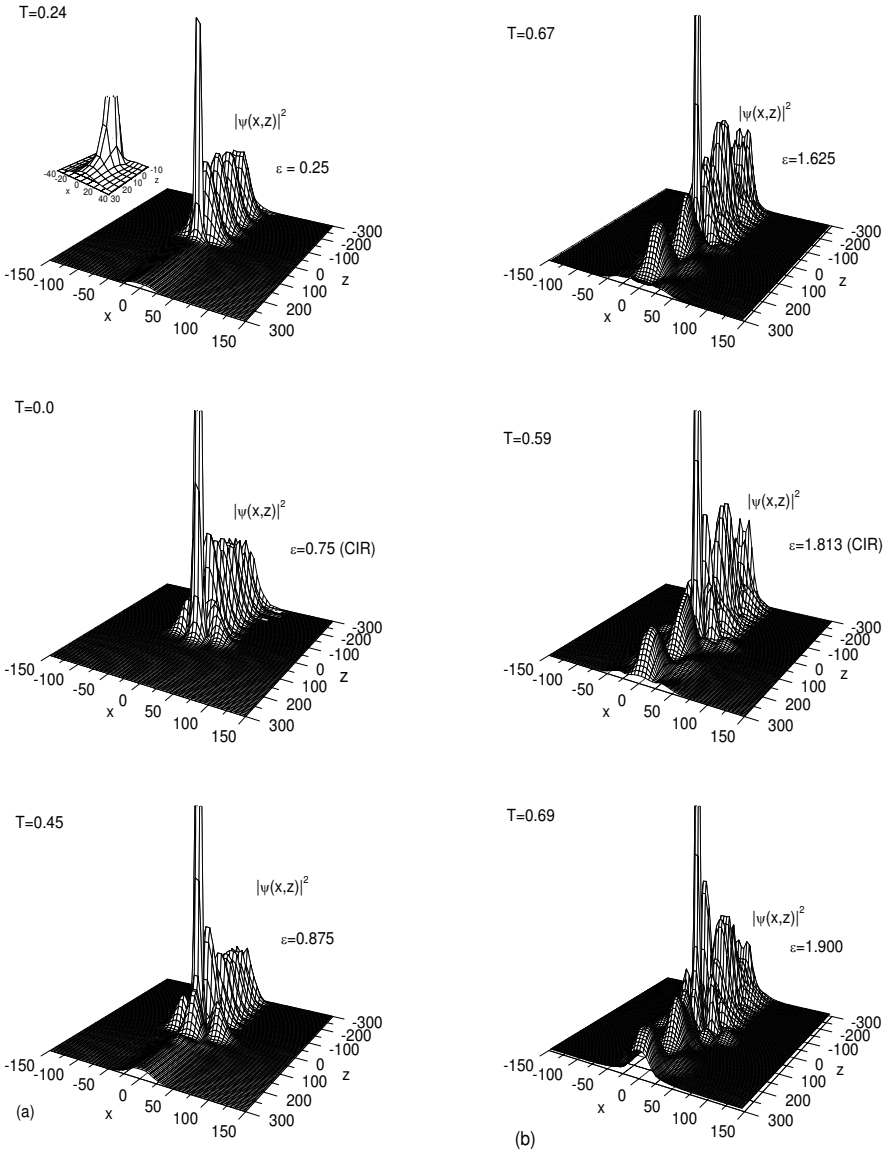

Fig. 5.8: The probability density $|\psi(x,z)|^2$ for bosonic collisions as a function of x and z at $a_s/a_\perp = +4.39$ for two cases of the single-mode regime (a) and two-mode regime (b) with different values of ε. The corresponding transmission values are also indicated. All subfigures are for $\omega = 0.002$ and $n = 0$.

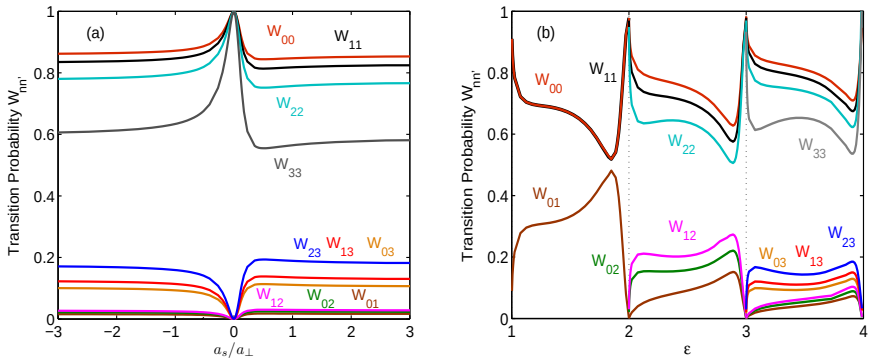

Fig. 5.9: (a) The transition probabilities $W_{nn'}$ as a function of $a_s/a_\perp$ in the four mode regime for $\varepsilon = 3.05$. (b) The calculated transition probabilities $W_{nn'}$ as a function of ε up to four open channels for $a_s/a_\perp = -30.08$. $\omega = 0.002$ for both subfigures.

observe that the probability of remaining at the same initial state W_{nn} (i.e. elastic scattering) is in the complete range of the ratio $a_s/a_\perp$ much larger than the probability of a transition into a different state $W_{nn'}$ (i.e. inelastic scattering). With increasing n or n' the inelastic transition probabilities $W_{nn'}$ increase but the elastic probabilities W_{nn} decrease. In an inelastic (elastic) collision $W_{nn'}$ (W_{nn}) goes to zero (unity) as a_s tends to zero. $W_{nn'}$ (W_{nn}) possess a maximum (minimum) at the resonance position $a_s/a_\perp \approx 0.35$ consistent with the minimum of $T(\varepsilon)$ at $\varepsilon = 3.05$. It is instructive to see how the distribution of the initial flux among the open channels changes due to pair collisions as a function of the collision energy. Fig. 5.9(b) shows the transition probabilities $W_{nn'}$ as a function of the dimensionless energy up to four open channels. The probability of elastic scattering remains larger than that of inelastic scattering in the complete range of the energy. For two open channels the elastic collision probability W_{nn} is independent of the initial state ($W_{00} = W_{11}$). For a higher number of open channels W_{nn} is decreasing with increasing initial value of n. Near the thresholds, the probabilities of the inelastic (elastic) transitions $W_{nn'}$ (W_{nn}) go to zero (unity).

5.3.2 Multichannel scattering of fermions

In this section we focus on fermionic collisions in harmonic traps. In this case the interatomic wave function is antisymmetric with respect to the interchange of the two fermions and the even amplitude $f^e_{nn'}$ in (5.10) is zero. We have analyzed the multichannel scattering of fermions up to four open transverse channels for different interatomic interactions, by varying the potential strength V_0 in the vicinity of the value $V_0 = -4.54$ (see Fig. 5.1) generating a resonant p-wave state in free space. Fig. 5.10 shows corresponding results for the single-mode regime. Fig. 5.10(a) shows the *mapped coupling constant*

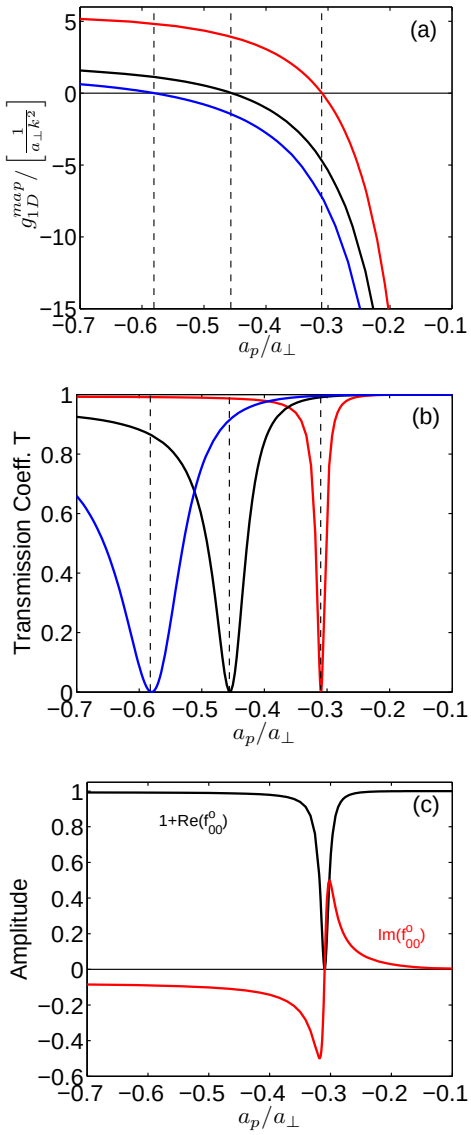

Fig. 5.10: (a),(b) The *mapped coupling constant* g_{1D}^{map} and the transmission coefficient T as a function of the scattering length a_p for single-channel scattering of two fermions under a harmonic confinement $\omega = 0.002$ and for the longitudinal energy $E_\parallel = 0.0002$ (red), $\omega = 0.02$, $E_\parallel = 0.002$ (black), and $\omega = 0.06$, $E_\parallel = 0.002$ (blue). (c) The scattering amplitude f_{00}^o as a function of the scattering length a_p for $\omega = 0.002$ and $E_\parallel = 0.0002$. The corresponding constant V_0 is varied in the region $-4.54 < V_0 < -4.47$.

$g_{1D}^{map} = \lim_{k\to 0} Im\{f^o(k)\}/Re\{f^o(k)\}\mu k$ [32, 40] as a function of the p-wave scattering length $a_p = \sqrt[3]{V_p}$. The *mapped coupling constant* g_{1D}^{map} goes to zero at the position of the mapped CIR [32], which for $\omega = 0.002$ and $E_{\|} = 0.0002$ is equal to $a_p/a_\perp = -0.31$. The position of the mapped CIR obviously depends on the values of ω and ε. In Fig. 5.10(b) we have plotted the transmission coefficient T as a function of a_p. The transmission coefficient exhibits a minimum and an accompanying well (i.e. the blocking due to the resonance) at the position of the CIR, and tends to unity (i.e. total transmission) for a_p far from the CIR position. For larger ω the well becomes wider, and its minimum is shifted to the left, see also Ref. [38]. Fig. 5.10(c) shows the scattering amplitude f_{00}^o as a function of a_p for $\omega = 0.002$ and $E_{\|} = 0.0002$. The amplitude approaches zero far from the CIR position and -1 at the CIR position , which results in total transmission $T = |1 + f_{00}^o|^2 \to 1$ (i.e. the fermions do not scatter each other) and total reflection $T = |1 + f_{00}^o|^2 \to 0$ (i.e. strongly interacting and impenetrable fermions), respectively.

In Fig. 5.11 we present the total transmission coefficient as a function of a_p for $\omega = 0.002$ in (a) two-mode regime for $\varepsilon = 1.05$ and (b) three-mode regime for $\varepsilon = 2.05$. Similar to the single-mode regime, T exhibits a minimum and accompanying well, however, the position of the minimum is shifted to the right and the value at the minimum is nonzero. For the lower degree of transversal excitation, we observe a deeper and narrower transmission well. With increasing energy the transmission well becomes wider and more shallow and its position is shifted to larger values of $a_p/a_\perp$. This is also demonstrated in Fig. 5.12, where the transmission coefficient is plotted as a function of ε for several values of $a_p/a_\perp$ for the two cases of being initially in the ground $n = 0$ (a) and the first excited $n = 1$ (b) transverse states for $\omega = 0.002$. We observe that for any number of open channels, T exhibits a minimum for some value of $a_p/a_\perp$. With increasing $a_p/a_\perp$ the transmission well becomes more shallow (except for the single-mode regime) and wider. In contrast to the bosonic case, there is no specific threshold behavior. This is a consequence of the fact that the relative motion does not feel the interatomic interaction in the closed channels which are strongly screened by the centrifugal repulsion playing a dominant role for near-threshold collision energies or in other words, we encounter a weak coupling of the different scattering channels.

In Fig. 5.13 we show the transition probabilities $W_{nn'}$ as a function of $a_p/a_\perp$ for four open channels. We see that the probability of an elastic scattering process (i.e. to remain in the same transversal state) is much larger than that of an inelastic collision (i.e. the transition to a different transversal state). For an elastic collision the probability W_{nn} shows a minimum and corresponding well which becomes wider and more shallow with increasing initial quantum number n (i.e., with the population of a higher excited initial transversal state). For an inelastic collision $W_{nn'}$ $(n \neq n')$ exhibits a peak which becomes less pronounced as the quantum numbers n or n' increase.

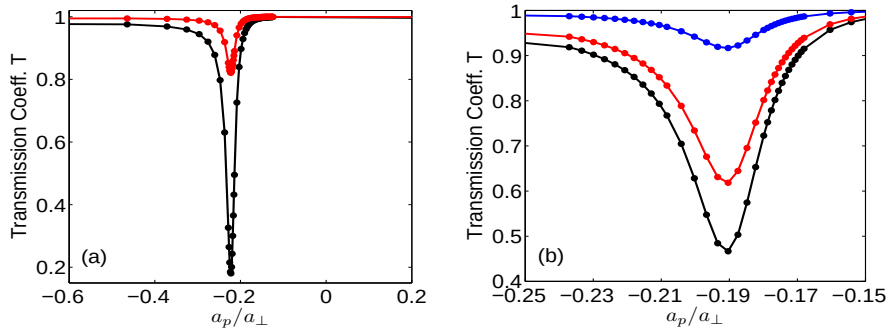

Fig. 5.11: Total transmission coefficient T in a fermionic collision as a function of a_p for $\omega = 0.002$ for (a) two-open channels with $\varepsilon = 1.05$ being initially in the ground state $n = 0$ (black) and first excited state $n = 1$ (red), and (b) three-open channel with $\varepsilon = 2.05$ being initially in the ground state $n = 0$ (black), first excited state $n = 1$ (red) and second excited state $n = 2$ (blue).

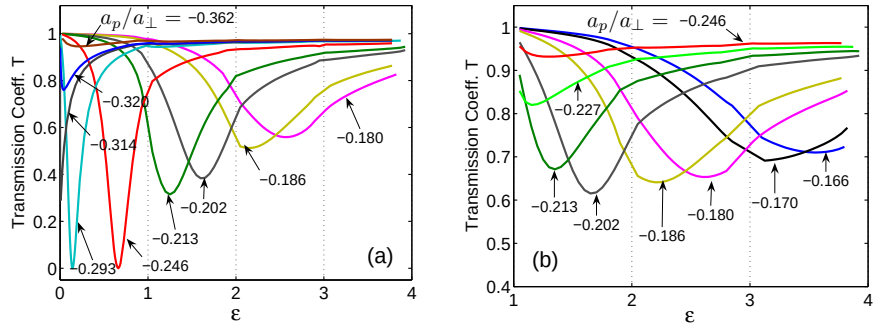

Fig. 5.12: Total transmission coefficient T for a fermionic collision as a function of the dimensionless energy ε for the two cases of the system being initially in the ground $n = 0$ (a) and first excited $n = 1$ (b) transverse states, for several ratios of $a_p/a_\perp$. We have used $\omega = 0.002$.

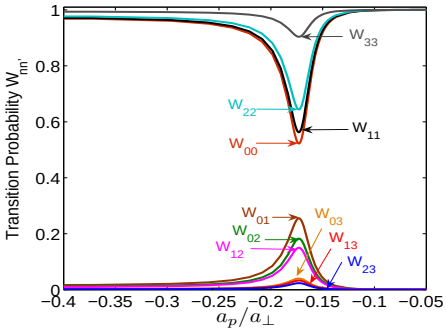

Fig. 5.13: Transition probabilities $W_{nn'}$ in fermionic collisions as a function of $a_p/a_\perp$ for four open channels. $\omega = 0.002$ and $E = 0.0142$ are employed.

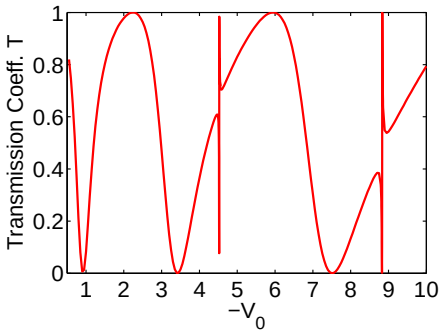

Fig. 5.14: Transmission T as a function of the depth $-V_0$ of the potential (5.3) for two distinguishable atomic species for $\omega = 0.002$ for $E_\parallel = 0.0002$. Units according to (5.4).

5.3.3 Multichannel scattering of distinguishable particles

In this section we analyze the multichannel scattering of two distinguishable particles in a harmonic trap with the same trap frequency $\omega_1 = \omega_2 = \omega$ allowing the separation of the CM motion. Such a case corresponds to the different atomic species confined by the same potential as it is the case, e.g., for two different isotopes in the same optical dipole trap. The two-body scattering wave function of the distinguishable atoms does not possess a well-defined symmetry with respect to the reflection $z \to -z$, i.e. both s- and p-state contributions (f^e and f^o) must be taken into account for the scattering amplitude. Fig. 5.14 shows our results for the transmission coefficient T in the single-mode regime ($0 < \varepsilon < 1$), which is plotted as a function of the tuning parameter $-V_0$ of the interparticle interaction. In general the scattering process can not be described by a single scattering length a_s or a_p for this case. In regions with a negligible p-wave contribution (see the regions in Fig. 5.1 with $V_p \to 0$), T exhibits a

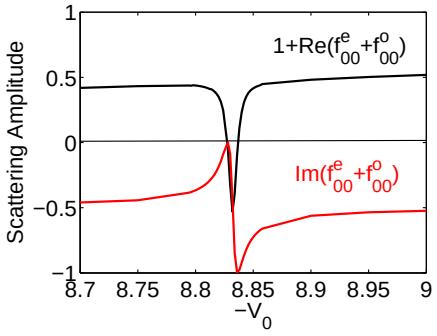

Fig. 5.15: Scattering amplitude as a function of the depth $-V_0$ of the potential (5.3) for two distinguishable atomic species for $\omega = 0.002$ and $E_{\|} = 0.0002$. Units according to (5.4).

behavior similar to bosonic scattering. We observe the well-known s-wave CIRs which lead to zeros of the transmission T at the positions $a_s/a_\perp = 1/C$ and tend to unity when a_s goes to zero (together with a_p). In regions, where a_s and a_p are comparable we observe the effect reported in Ref. [38]: remarkable peaks of the transmission $T = |1 + f^e_{00} + f^o_{00}|^2 \to 1$, i.e., almost complete transmission in spite of the strong interatomic interaction in free space. This is the so-called dual CIR: Quantum suppression of scattering in the presence of confinement due to destructive interference of odd and even scattering amplitudes. Equally minima of $T = |1 + f^e_{00} + f^o_{00}|^2 \to 0$ due to the interference of even and odd scattering amplitudes under the action of the transverse confinement can occur (see Fig. 5.14). Complete transmission corresponds to $f^e_{00} + f^o_{00} = -1 - i$ while total reflection corresponds to $f^e_{00} + f^o_{00} = -1$. Fig. 5.15 shows the corresponding amplitudes $f^e_{00} + f^o_{00}$ as a function of $-V_0$.

Fig. 5.16 shows the total transmission coefficient versus $-V_0$ in the three-mode regime for $\omega = 0.002$ and $\varepsilon = 2.05$. Similar to the single-mode regime, when a_p is negligible compared to a_s, T behaves analogously to the case of a bosonic collision, and tends to unity (complete transmission) when a_s tends to zero, while at the s-wave CIR position, it exhibits a minimum with a nonzero value. For a lower degree of transversal excitation of the initial state, we encounter a larger transmission coefficient. For the same reasons as in the single-mode regime, we observe in the regions of V_0 where the p-wave scattering length a_p is comparable to a_s, sharp peaks of T. However, in contrast to the single-mode regime we do not observe complete transmission, i.e., $T \neq 1$ (see, e.g., T at $V_0 = -8.85$ in Fig. 5.16).

Figure 5.17 presents the transmission coefficients as a function of the dimensionless energy ε for $\omega = 0.002$. Figure 5.17(a) shows the results for several ratios of $a_s/a_\perp$ if $|a_p|$ is small compare to $|a_s|$. Here the system is initially in the transversal ground state. The behavior of the transmission coefficient is similar to the case of two-boson scattering [see Fig. 5.6(a)]. Figure 5.17(b)

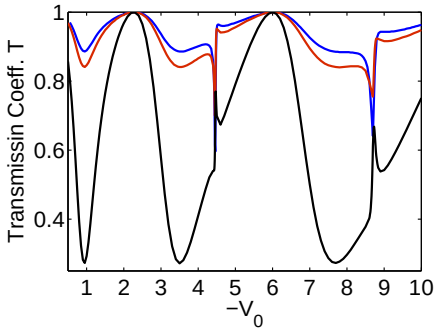

Fig. 5.16: Transmission coefficient T as a function of the depth $-V_0$ of the potential (5.3) for two distinguishable atomic species for $\omega = 0.002$ and $\varepsilon = 2.05$ in the three-mode regime, being initially in transverse ground state (blue), first excited state (red) and second excited state (black). Units according to (5.4).

shows the transmission for the scattering of two distinguishable atoms together with the results for bosonic-collision (blue) and fermionic-collisions (black), for $-V_0 = -4.505$ when both scattering length a_s and a_p are large. In the limit $\varepsilon \to 0$ the behavior of the transmission for the distinguishable and the bosonic case are very similar while in the vicinity of the energy of the p-wave shape resonance $\varepsilon \sim 0.7$, apart from a small shift to larger energies, we can find a complete coincidence of the transmission behavior for the case of distinguishable and fermionic scattering. At the threshold energy $\varepsilon = 1$ the latter two transmission curves cross. Figure 5.17(c) shows the transmission coefficient versus ε for $-V_0 = -4.505$ initially occupying the ground state $n = 0$ (blue), the first excited state $n = 1$ (black), the second excited state $n = 2$ (red), and the third excited state $n = 3$ (green). In the limit $\varepsilon_{\|} \to 0$, T drops rapidly to zero. Apart from the single mode regime, it is for $\varepsilon_{\|} >> 0$ approximately constant with $T \approx 1$.

In Fig. 5.18 we present the transition probabilities $W_{nn'}$ as a function of $-V_0$ for four open channels. For the regions of V_0 where a_p is negligible compared to a_s, a very good agreement of the transmission behavior for distinguishable and bosonic atoms is observed. In regions where a_s and a_p are comparable, similar to the fermionic case, we observe narrow and deep wells (for elastic collision) and narrow as well as strongly pronounced peaks (for inelastic collision).

5.4 Summary and conclusions

We have analyzed atomic multichannel scattering in a 2D harmonic confinement. Identical bosonic and fermionic scattering as well as scattering of distinguishable atoms in traps with the same frequency for the different species have been explored. Equal frequencies allows us to separate the c.m. and relative motion.

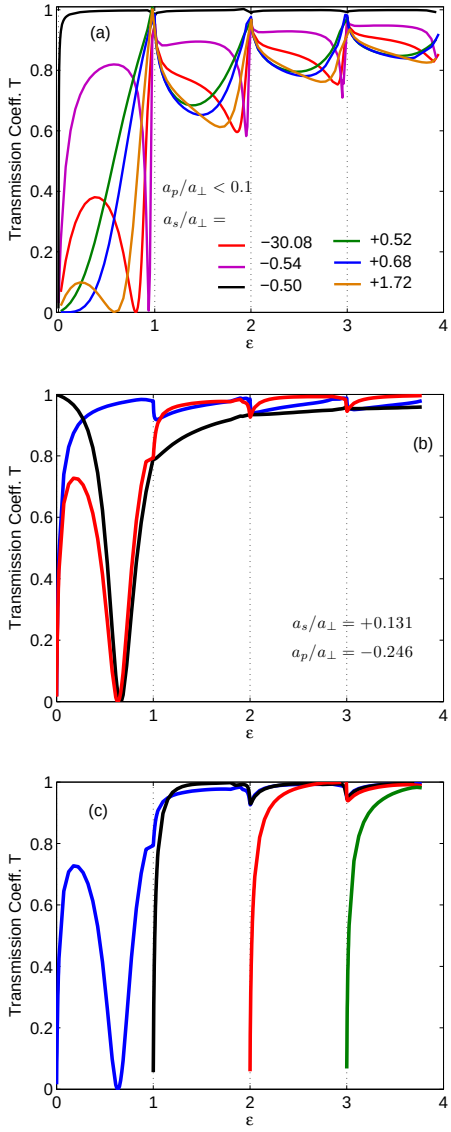

Fig. 5.17: Transmission coefficient T as a function of the dimensionless energy ε for scattering of two distinguishable particles in a harmonic confinement $\omega = 0.002$ (a) for several ratios $a_s/a_\perp$ in the case where a_p is negligible compared to a_s, (b) for $-V_0 = -4.505$ when both scattering lengths a_s and a_p are comparable [here the transmission coefficients for bosonic-collision (blue) and fermionic-collision (black) are also provided], and (c) for $-V_0 = -4.505$ when the system is initially in the ground transversal state (blue), in the first excited state (black), in the second excited state (red), and in the third excited state (green).

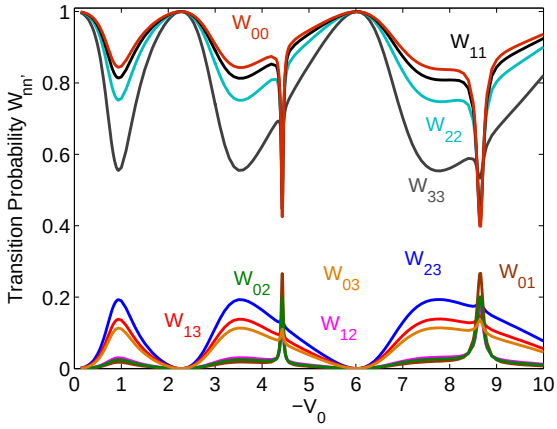

Fig. 5.18: Transition probabilities $W_{nn'}$ for quasi-1D scattering of distinguishable particles in a harmonic trap $\omega = 0.002$, as a function of $-V_0$ for four open channels and $\varepsilon = 3.05$. V_0 is given in units of (5.4).

First we reproduced the well-known s-wave CIR for bosonic collision in the single-mode regime [27, 28, 43, 38, 39, 40]. Next bosonic collisions in the multichannel regime including elastic and inelastic processes, i.e., transverse excitations and deexcitations have been investigated. Transmission coefficients as well as transition probabilities for energies covering up to four open channels are reported on. It is shown that the transmission coefficient as a function of the scattering length exhibits a minimum at the CIR position. Except for $0 < a_s/a_\perp < 1/C$ in the first channel, the transmission curves show, with varying energy, a minimum and accompanying well. For a single open channel the value of the minimum of the transmission is zero. Increasing the degree of transverse excitation leads to an increase of the transmission minima. A distinct threshold behavior is observed at every $\varepsilon = n$.

For $a_s/a_\perp < 0$ the accompanying transmission well is more pronounced compared to the case $a_s/a_\perp > 0$ and it is also deeper in the case of several open channels. The position of the minimum is closer to the upper threshold again when compared to the case $a_s/a_\perp > 0$. With increasing ratio $a_s/a_\perp$ for either $a_s/a_\perp > 0$ or $a_s/a_\perp < 0$, the corresponding transmission well becomes also more pronounced, i.e., we encounter a deeper and narrower well for more open channels and the energetic position of the minimum moves to the neighboring upper threshold. Our results for the transition probabilities $W_{nn'}$ show that the probability of remaining in the same state (elastic collision) is larger than transitions into a different transversal state (inelastic collision). In the case of elastic collisions (inelastic collisions) it has to go to unity (zero) as a_s tends to zero. The inelastic transition probability $W_{nn'}$ increases as the numbers n or n' increase while the elastic transition probability $W_{nn'}$ decreases.

Our next focus has been the multichannel scattering of fermions address-

ing up to four open channels in the waveguide. In the regime of a single open channel we reproduced the well-known p-wave mapped CIR in the zero-energy limit [32, 40]. We have analyzed the p-wave CIR dependence on the collision energy ϵ and the trapping frequency ω. Consequently the multimode regime has been explored by determining the behavior of the transmission as well as the transition probabilities. The dependence of the transmission on the p-wave scattering length exhibits a minimum with zero transmission and an accompanying well for the single-mode regime. Increasing the energy, this well becomes more shallow (except for the single-mode regime),wider and its position is shifted to the region of higher energies. In the multimode regime the transmission well depends also on the degree of the initial transverse excitation. Increasing the degree of initial transverse excitation the transmission well becomes shallower and wider and the transmission is overall increased. For a fixed number of open channels the transmission exhibits as a function of the energy a minimum for some value of the p-wave scattering length. Increasing $a_p/a_\perp$ leads to a shift of the transmission minimum to higher energies and an increasingly shallower well. This holds except for the single mode regime in which the minimal value is zero.

In contrast to the bosonic case, we do not observe a distinct threshold behavior. The transition probabilities $W_{nn'}$ for fermionic collisions show that elastic collisions are more probable than inelastic ones. The probability W_{nn} for an elastic process shows a well which becomes wider and shallower as the initial population of the excited states n increases, while for an inelastic collision it exhibits a peak which becomes smaller as the channel numbers n or n' increase. By varying the potential parameter V_0 in the vicinity of the value $V_0 = -4.54$, we found a set of shape-resonances.

Finally we analyzed the multichannel-1D scattering of distinguishable atoms in the trap. Here both s- and p-wave contributions have been taken into account. We have studied the transmission coefficient in the single-mode regime and reproduced the CIR [27, 28, 43, 32] as well as the dual-CIR [38, 39, 40] corresponding to total reflection and transmission, respectively. In the multimode regime the transmission versus $-V_0$ shows except for the regions where a_p is comparable with a_s a behavior analogous to the situation of bosonic scattering. We encounter $T \to 0$ for $a_s \to 0$. At the position of the CIR, T exhibits a minimum with a nonzero value. The lower is the transverse excitation of the initial state, the larger is the transmission coefficient. In regions of V_0 where the p-wave scattering length a_p is comparable to a_s, T exhibits sharp peaks or dips near the dual-CIRs due to comparable contributions of both s and p waves. In contrast to the single-mode regime there is not a complete transmission at the dual CIR points. Our results for the transmission coefficient versus energy show that in the limit of zero longitudinal relative energy the distinguishable atoms behave similar to bosons, while in the vicinity of the position of a shape resonance, they behave similar to fermions. For larger energies $\varepsilon >> 1$ T is close to unity. Finally we have analyzed the transition probability as a function of $-V_0$. For values of V_0 where a_p is negligible compared to a_s we find an excellent agreement with the results for bosonic collisions. In regions where these

two scattering parameters are comparable, we observe, similar to the fermionic case, sharp downward (for elastic collision) and upward (for inelastic collision) peaks but with different values. We conclude with the general statement that our multichannel scattering results in waveguides are of immediate relevance to cold or ultracold atomic collisions in atomic waveguides or impurity scattering in quantum wires.

Part III

ATOMIC RESONANCES IN A QUADRUPOLE MAGNETIC TRAP

6. ATOMIC RESONANCES IN MAGNETIC QUADRUPOLE FIELDS: AN OVERVIEW

Ultracold atomic gases offer a wealth of opportunities for studying quantum phenomena at mesoscopic and macroscopic scales [64, 65, 66, 67, 68]. The interaction among the atoms as well as their behavior in external fields depends crucially on their electronic and to some extent also on their nuclear properties. The majority of experiments in the ultra-low temperature regime have been performed with alkali atoms. Their ground-state electronic structure is characterized by the fact that all electrons but one occupy closed shells. The latter, the so-called valence electron, is situated in the s-orbital of the outermost shell. The coupling of the nuclear spin $\mathbf{I}$ to the total angular momentum of the active electron via the hyperfine interaction causes a splitting of the electronic energy levels into several branches which can be characterized by the quantum number of the total spin $\mathbf{F}$. Due to a vanishing orbital angular momentum this hyperfine interaction consist exclusively of the coupling of the electronic spin $S = \frac{1}{2}$, to the nuclear spin I. This leads to the two possibilities $F = I \pm S$.

Inhomogeneous magnetic fields represent a very powerful and versatile tool for trapping and confining of ultracold atoms. They allow to influence and control the dynamical properties of atoms and molecules, which result in a wealth of new and often surprising phenomenon. In particular they are very well suited for miniaturization via, e.g., so-called atom-chips [69, 70, 71]. Atom-chips are surface mounted wires with a typical width of about a few micrometers, which create a miniaturized landscape of inhomogeneous magnetic field. Depending on the particular structure setup a wide variety of magnetic field landscape can be created, enabling to trap ensemble of atoms very close to the chip surface ($\sim 10\mu m$) where the magnetic field gradient is extremely large.

The basic idea behind the control of ultracold atoms via inhomogeneous magnetic fields is very simple. The neutral atoms couple to the magnetic field via their magnetic moment. In the case of enough weak gradient field, when the spatial variations of the field is small enough, it can be considered homogeneous over the size of an atom, therefore the atom can be assumed as a point-like particle. For ground state atoms, this assumption is in general justified.

Assuming strong hyperfine interactions (compared to the magnetic interactions) the atomic magnetic moment is due to the total angular momentum being composed of the electronic and nuclear angular momentum. Traditionally an adiabatic approximation, which reduces the vector coupling of the magnetic moment to the field to a potential term proportional to the magnitude of the field, is then employed. However, in order to understand the basic physics of

(individual) atoms in magnetic traps it is likewise necessary to study the quantum dynamics of the Hamiltonian for the case of the vector coupling. A number of investigations in this direction have been performed in the past.

Firstly fundamental configurations of static fields for the trapping of ground state atoms have been explored in the late eighties and early nineties [72, 73]. Because of their pioneering work in trapping of ultracold atoms by magnetic traps, S. Chu, C.N. Cohen-Tannoudji and W.D. Phillips were awarded the Nobel prize of physics in 1997. Planar current geometries for microscopic magnetic traps were investigated in Ref. [74]. Specifically the quadrupole field [75, 76], the wire trap [77, 78, 79, 80] and the magnetic guide and Ioffe trap [81, 82, 83, 84, 85] have been addressed. In these traps we typically encounter quantum resonances with a certain lifetime instead of stationary *stable* quantum states. For example, in Refs. [81, 82] the resonances of particles with spin $\frac{1}{2}$ and 1 in a magnetic guide have been determined via the phase shift of scattered waves. Alternatively the complex scaling method can be used to study the widths and positions of the resonances [83]. More recently [76] an extensive study of the quantum dynamics of neutral spin $\frac{1}{2}$ and spin 1 particles in a 3D magnetic quadrupole field has been performed, including the derivation of an effective scalar Schrödinger equation to describe and understand long-lived states possessing large angular momenta.

Very recently [86] a new class of short-lived resonances possessing negative energies for the case of the 3d magnetic quadrupole field was found. These resonances, which have been overlooked in previous investigations [75, 76], originate from a fundamental symmetry of the underlying Hamiltonian. In contrast to the positive energy resonances, they are characterized by the fact that the atomic magnetic moment is aligned antiparallel to the local direction of the magnetic field, and their lifetimes decrease with increasing total magnetic quantum number. A mapping of the two branches of positive and negative energy states has been derived [86].

In the above works, the hyperfine interaction has been assumed to be much stronger than the interaction with the external inhomogeneous magnetic field and therefore the electronic and nuclear angular momenta firstly provide a total angular momentum which then interacts with the magnetic field. This physical picture truly holds for (alkali) atoms in their electronic ground state and macroscopic as well as microscopic (atom chip) gradient fields. The atom is consequently treated as a point particle with the total angular momentum $\mathbf{F}$. However in the case of small hyperfine interactions and/or strong gradient fields (e.g., for electronically excited atoms) this simplification fails and an admixture of different hyperfine states F due to the field interaction has to be expected. In Ref. [87], the resonance of alkali-atoms in a magnetic quadrupole field have been analyzed in the case for which both the hyperfine interaction and the field interaction, have to be taken into account on equal level for the description of the neutral atoms in the field.

In this part firstly we describe the magnetic quadrupole trap in details and then we study resonances of neutral particles in this kind of trap. Finally we study atomic hyperfine resonances of alkali atoms in a magnetic quadrupole field.

6.1 The Magnetic Quadrupole Field

In ultra-cold atom experiment, the Zeeman interaction between magnetic moment of the atom and magnetic field is used to confine atoms to certain spatial regions. Depending on the direction of the magnetic moment with respect to the magnetic field this gives rise to either confining or nonconfining potentials. Maxwell's equation do not permit the occurrence of magnetic field maxima but only minima in a source-free region. Therefore in order to ensure trapping one has to focus on such atomic states for which the underlying potentials grows with increasing magnetic field strength. Atoms in such states are referred to as low-field seeker [69]. Several magnetic field configuration exhibit a local field minimum, from which, the 3D quadrupole field is probably the most prominent. Such field finds its application in virtually any ultra-cold atom experiment as it is a main element of a magneto-optical trap MOT [88]. It is generated by a so-called anti-Helmholtz configuration, which consists of a pair of axially assembled coils of radius R, separated by a distance $2D$ (Fig. 6.1). The two coils are flown through by counter-propagating currents of equal magnitude I. According to Biot and Savart's law, the magnetic field $B(\mathbf{r})$ resulting from the infinitely thin coils is given by

$$\begin{aligned}\mathbf{B}(\mathbf{r}) &= \frac{\mu_0 I}{4\pi}\int \frac{d\mathbf{r}'\times(\mathbf{r}-\mathbf{r}')}{|\mathbf{r}-\mathbf{r}'|^3} \\ &= \frac{\mu_0 I}{4\pi}\int_{\mathbf{r}_1'(s)} ds \frac{\frac{\partial \mathbf{r}_1'(s)}{\partial s}\times(\mathbf{r}-\mathbf{r}_1'(s))}{|\mathbf{r}-\mathbf{r}_1'(s)|^3} + \frac{\mu_0 I}{4\pi}\int_{\mathbf{r}_2'(s)} ds \frac{\frac{\partial \mathbf{r}_2'(s)}{\partial s}\times(\mathbf{r}-\mathbf{r}_2'(s))}{|\mathbf{r}-\mathbf{r}_2'(s)|^3}\end{aligned} \tag{6.1}$$

In the second step, the current loops have been parameterized by the curves $\mathbf{r}_1'(s)$ and $\mathbf{r}_2'(s)$. A suitable parametrization is given by

$$\mathbf{r}_1'(s) = \begin{pmatrix} R\cos(s) \\ -R\sin(s) \\ D \end{pmatrix} \quad \text{and} \quad \mathbf{r}_2'(s) = \begin{pmatrix} R\cos(s) \\ R\sin(s) \\ -D \end{pmatrix} \tag{6.2}$$

with $0 \le s \le 2\pi$. The $z-$axis has been chosen to point along the symmetry axis of the setup. In the vicinity of the origin we can expand the integrand in equation (6.1) in terms of the small dimensionless vector $\widetilde{\mathbf{r}} = \mathbf{r}/\sqrt{D^2+R^2}$ around $\mathbf{r} = \mathbf{0}$. Carrying out the integration one obtains

$$\mathbf{B}(\widetilde{\mathbf{r}}) = \frac{3\mu_0 I D R^2}{2(D^2+R^2)^2}\begin{pmatrix} \widetilde{x} \\ \widetilde{y} \\ -2\widetilde{z} \end{pmatrix} + o(|\widetilde{\mathbf{r}}^2|). \tag{6.3}$$

or

$$\mathbf{B}(\mathbf{r}) = b\begin{pmatrix} x \\ y \\ -2z \end{pmatrix} \quad \text{with} \quad b = \frac{3\mu_0 I D R^2}{2(D^2+R^2)^{5/2}} \tag{6.4}$$

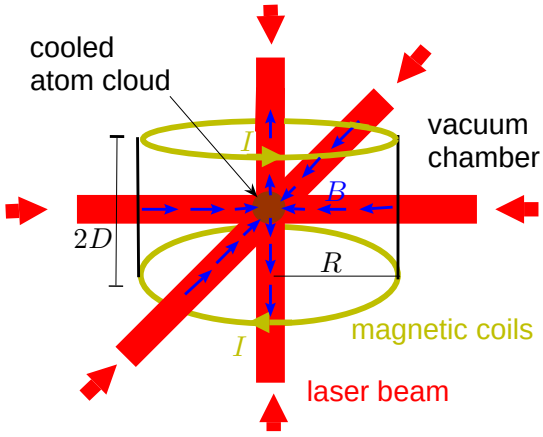

Fig. 6.1: Experimental setup of the MOT.

The magnetic field gradient b is the only variable parameter characterizing the quadrupole field.

Since $\sqrt{D^2+R^2}$ is of macroscopic size (typically $\sim 10^{-1}m$), it should be clear from (6.3) that for regions of atomic or mesoscopic size ($|\mathbf{r}| \leq 10^{-5}m$) around the trap center, Eq. (6.4) will be a fairly accurate description of the actual geometry of the magnetic field $\mathbf{B}$ created by a pair of anti-Helmholtz coils.

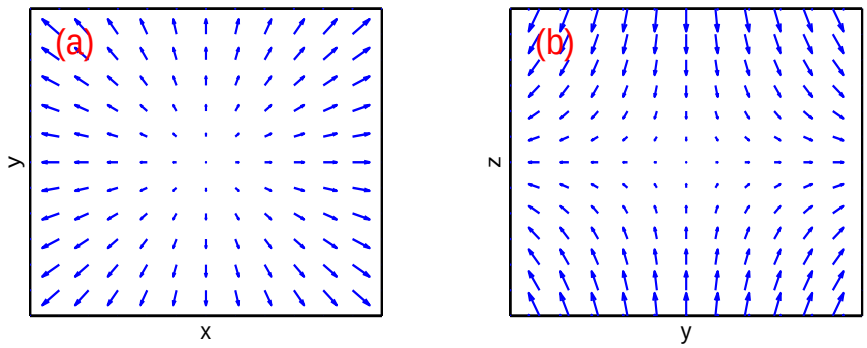

Fig. 6.2: The intersection of the magnetic field given in (6.4) along the (a) $x-y$- and (b) $y-z$-plane.

The macroscopic setup which has been considered here is bulky and therefore inflexible. As a result of the growing efforts for miniaturization and integration the so-called atom chips have been developed. Atom chips are surface mounted wires with a typical width of about a few micrometers, which create a miniatur-

ized landscape of inhomogeneous magnetic field. Depending on the particular structure setup a wide variety of magnetic field landscape can be created, enabling to trap ensemble of atoms very close to the chip surface ($\sim 10\mu m$) where the magnetic field gradient is extremely large. A 3D quadrupole field is achieved by using a U-shaped wire. An expression for magnetic field configurations and atom chips in more details can be found in Ref. [89].

6.1.1 Symmetry properties of the quadrupole magnetic field

The quadrupole magnetic field given in (6.4) in cylindrical polar coordinates ρ, φ, and z reads

$$\mathbf{B}(\rho, \varphi, z) = b(\rho \widehat{e}_\rho - 2z\widehat{e}_z) \tag{6.5}$$

Since $\mathbf{B}$ does not depend on the azimuthal angle φ, it is symmetric with respect to continuous rotation around the z-axis. Apart from this, $\mathbf{B}$ exhibits a discrete mirror symmetry with respect to the $x-y$-plane. Figure 6.2 shows the intersection of the magnetic field given in (6.4) along the $x-y$- and $y-z$-plane.

7. SCATTERING RESONANCES OF SPIN-1 PARTICLES IN A MAGNETIC QUADRUPOLE FIELD

In this chapter, we investigate resonances of spin 1 bosons in a three-dimensional magnetic quadrupole field. Complementary to the well-known positive energy resonances it is shown that there exist short-lived, i.e., broad, negative energy resonances. The latter originate from a fundamental symmetry of the underlying Hamiltonian and are characterized by an atomic spin that is aligned antiparallel to the local magnetic field direction. In contrast to the positive energy resonances the lifetimes of the negative energy resonances decreases with increasing total magnetic quantum number. We derive a mapping of the two branches of the spectrum.

7.1 The Hamiltonian

The Hamiltonian describing the motion of a point-like particle of mass M and magnetic moment μ in a 3D magnetic quadrupole field $\mathbf{B} = b(x, y, -2z)$ reads

$$H = \frac{\mathbf{p^2}}{2M} - \mu \cdot \mathbf{B} \tag{7.1}$$

For a spin-S-particle with magnetic moment $\mu = -\frac{g}{2}\mathbf{S}$, one obtains in atomic units

$$H = \frac{1}{2M}[\mathbf{p}^2 + bgM(xS_x + yS_y - 2zS_z)] \tag{7.2}$$

Here g is the g-factor of the particle. Performing the scale transformation

$$\bar{p}_i = (2Mb\mu_B g_s)^{-1/3} p_i \quad \text{and} \quad \bar{x}_i = (2Mb\mu_B g_s)^{1/3} x_i$$

and thereupon omitting the bars one obtains

$$M(bgM)^{-2/3} H \to H = \frac{1}{2}(\mathbf{p}^2 + xS_x + yS_y - 2zS_z) \tag{7.3}$$

Therefore the energy level spacing scales according to $\frac{1}{M}(bgM)^{2/3}$. The scaled Hamiltonian ($\hbar = 1$) in spherical coordinates reads

$$H = \frac{1}{2}(-\frac{\partial^2}{\partial r^2} - \frac{2}{r}\frac{\partial}{\partial r} + \frac{L^2}{r^2} + r\sin\theta K - 2r\cos\theta S_z) \tag{7.4}$$

$\Sigma_x = U_1 P_y P_z$	$\Sigma_y = P_x U_2 P_z$	$\Sigma_z = P_x P_y U_3$	1
$P_x P_y P_z I_{xy} U_4$	$P_z I_{xy} U_4^*$	$P_y I_{xy} U_5$	$P_x I_{xy} U_5^*$
$T U_1 P_z$	$T P_x P_y U_2 P_z$	$T P_x U_3$	$T P_y$
$T P_x P_z I_{xy} U_4$	$T P_y P_z I_{xy} U_4^*$	$T I_{xy} U_5$	$T P_x P_y I_{xy} U_5^*$

Tab. 7.1: Discrete symmetries of the Hamiltonian (7.3). Each symmetry is composed of a number of elementary symmetries which are listed in table II

Operator	Operation
T	$A \to A^*$
P_{x_i}	$x_i \to -x_i$
I_{xy}	$x \to y \quad y \to x \quad z \to z$
$U_1 = e^{\frac{i}{\hbar}\pi S_x}$	$S_x \to S_x \quad S_y \to -S_y \quad S_z \to -S_z$
$U_2 = e^{\frac{i}{\hbar}\pi S_y}$	$S_x \to -S_x \quad S_y \to S_y \quad S_z \to -S_z$
$U_3 = e^{\frac{i}{\hbar}\pi S_z}$	$S_x \to -S_x \quad S_y \to -S_y \quad S_z \to S_z$
$U_4 = U_1 e^{-\frac{i}{\hbar}\frac{\pi}{2} S_z}$	$S_x \to -S_y \quad S_y \to -S_x \quad S_z \to -S_z$
$U_5 = e^{\frac{i}{\hbar}\frac{\pi}{2} S_z}$	$S_x \to -S_y \quad S_y \to S_x \quad S_z \to S_z$

Tab. 7.2: Set of discrete operations out of which all discrete operations of the Hamiltonian (7.3) can be composed.

Here $K = \cos\varphi S_x + \sin\varphi S_y$. For a spin-1-particle, which is the case we focus on in the following except explicitly stated otherwise, we have

$$K = \frac{1}{\sqrt{2}} \begin{pmatrix} 0 & e^{-i\varphi} & 0 \\ e^{i\varphi} & 0 & e^{-i\varphi} \\ 0 & e^{i\varphi} & 0 \end{pmatrix} \quad \text{and} \quad S_z = \begin{pmatrix} 1 & 0 & 0 \\ 0 & 0 & 0 \\ 0 & 0 & -1 \end{pmatrix}$$

7.2 Symmetries and Degeneracies

By analyzing the symmetry properties of the resulting Hamiltonian one obtains 16 discrete symmetries, which are listed in table 7.1. Each symmetry operation is composed of a number of elementary operations given in table 7.2.

The discrete operation U_i, acts on the spin space only and their appearance depends on the choice of the representation of the spin operators. General representations of U_i operations are given in table 7.2. The operations P_{x_i} and I_{xy} act on coordinate space only. These operations are unitary. The operation T acts on both, the coordinate and the spin space, and is an antiunitary operation. It is the conventional time reversal operation for spinless particles, and corresponds to complex conjugation. Its action on the coordinate x_i, the momentum P_i, the angular momentum L_i, and the spin operators S_i is given by

$$\begin{aligned} T X_i T^{-1} &: X_i \to X_i \\ T P_i T^{-1} &: P_i \to -P_i \\ T L_i T^{-1} &: L_i \to -L_i \end{aligned}$$

$$TS_iT^{-1} : S_x \to S_x \quad S_y \to -S_y \quad S_z \to S_z \tag{7.5}$$

The operations discussed above satisfy the relations

$$[P_{x_i}, T] = [T, U_i] = [U_i, P_{x_i}] = [P_{x_i}, P_{x_j}] = [U_i, U_j] = 0 \tag{7.6}$$

and

$$U_i^2 = P_{x_i}^2 = T^2 = 1 \tag{7.7}$$

The symmetry operations listed in table 1 are either unitary or anti-unitary. The anti-unitary operations, involve the conventional time reversal operator T. The symmetry operations shown in the table 7.1, formally possess the same decomposition in terms of elementary operations for both fermions and bosons, but however their algebraic structure are different. For instance for bosons we have $[\Sigma_i, \Sigma_j] = 0$, while in the case of fermions one finds $\{\Sigma_i, \Sigma_j\} = 0$

Apart from the discrete symmetries there is a continuous symmetry generated by $J_z = L_z + S_z$ which is the z-component of the total angular momentum. This is a consequence of the rotational invariance of the system around the z-axis of the coordinate system. Due to $[J_z, H] = 0$ one can find energy eigenfunctions which are simultaneously eigenfunctions of J_z. For a spin-S-particle they read in the spatial representation

$$|m\rangle^{(S)} = \sum_{m_S=-S}^{S} C_{m_S} e^{i(m-m_S)\varphi} |m_S\rangle \tag{7.8}$$

with $\sum_{m_S} |C_{m_S}|^2 = 1$ where $|m_S\rangle$ are the spin eigenfunctions with respect to S_z. Exploiting the discrete and continuous symmetries of the system one can show that there exists a twofold degeneracy in the energy spectrum of the Hamiltonian (7.3) for $m \neq 0$. Let us consider $\mid E, m\rangle$ to be an energy eigenstate which is simultaneously an eigenstate of J_z. Using the anti-commutator $\{J_z, \Sigma_x\} = 0$ we have

$$J_z\Sigma_x \mid E, m\rangle = -\Sigma_x J_z \mid E, m\rangle = -m\Sigma_x \mid E, m\rangle \tag{7.9}$$

Therefore the state $\Sigma_x \mid E, m\rangle$ is an eigenstate of J_z with eigenvalue $-m$. On the other hand, because of the symmetry of the Hamiltonian $\Sigma_x \mid E, m\rangle$ is an energy eigenstate with energy E and thus it can be identified with $\mid E, -m\rangle$. For $m = 0$ the states $\mid E, m\rangle$ and $\Sigma_x \mid E, m\rangle$ form no degenerate pair.

7.3 Numerical Approach

We are interested in the resonances of the Hamiltonian (7.4). In order to investigate the resonances we employ the method of complex scaling theory together with linear variational method. To this end we employ a so-called Sturmian basis set of the form

$$\mid n, l, m_S\rangle_m = R_n^{(\zeta)}(r) Y_l^{m-m_S}(\theta, \varphi) \chi^S(m_S), \tag{7.10}$$

here the functions Y_l^m are the spherical harmonics. For fixed m the linear variational combination of the basis functions ψ^m_{n,l,m_S}, yields, per construction, eigenstates of the Hamiltonian and J_z simultaneously. For expanding the radial part we take the non-orthogonal set of functions

$$R_n^{(\zeta)}(r) = e^{-\frac{\zeta r}{2}} L_n(\zeta r) \tag{7.11}$$

where $L_n(x)$ are the Laguerre polynomials. The free parameter, ζ, has the dimension of an inverse length and can be tuned to improve the convergence behavior in different regions of the energy spectrum. It should be chosen such that $1/\zeta$ corresponds to the typical length scale of the states to be approximated.

7.4 Results

We shall see below that the spectrum consists of two well-separated parts: One set of resonances localized in the negative energy region with short lifetimes and a second set localized in the positive energy domain where the lifetimes are much larger and can, at least in principle, become arbitrarily long. The positive energy resonances have already been investigated in several works (see Refs. [75, 76] and references therein) whereas, to our knowledge, no negative energy resonances have been reported up to date.

7.4.1 Positive-energy resonances

In Fig. 7.1 we present the energies and decay widths for positive energy resonances for a spin-1-particle. For low total angular momentum [see figure 7.1(a)-(b)] one observes the resonances to cover the area of a right triangle in the $\epsilon - \Gamma$ plane. They are located on lines with similar negative slopes. This pattern becomes increasingly disturbed when considering resonances with higher energies and small decay widths. For sufficiently large values of the angular momentum m we observe a very regular pattern for their distribution in the $\epsilon - \Gamma$ plane, still with a triangular boundary, but now the resonances are located on lines possessing a positive slope [see figure 7.1(c)-(d)].

The decay width decreases exponentially with increasing value m for the angular momentum. The larger the angular momentum of a state the farther away it is located from the center of the trap which is the zero of the magnetic field. In the vicinity of the center spin-flip transition from, e.g., bound to unbound states take place. With increasing angular momentum the resonances probe less and less of this central region and become therefore increasingly stable.

For sufficiently large values of the angular momentum the wave functions become localized far away from the center of the trap. They form concentric circles around the z-axis. Since transitions to continuum states mainly occur in the center this results in a significant increase of the lifetimes of the states. Thus one could expect such states to be approximately describable as bound states of a certain effective Schrödinger equation. Such an equation has been

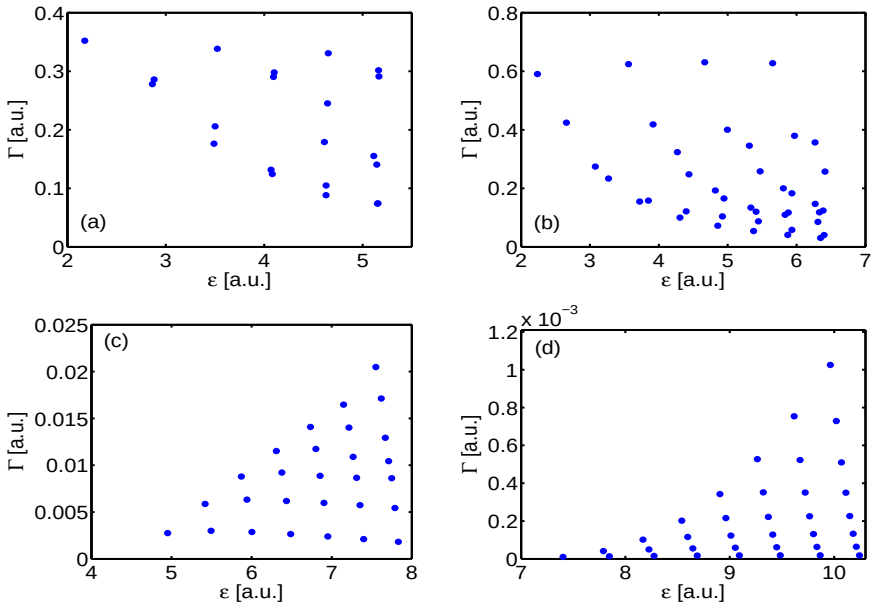

Fig. 7.1: Decay width and energies of the resonances possessing positive energies for $m = 0$ (a), $m = 1$ (b), $m = 10$ (c) and $m = 20$ (d).

obtained in [76] by applying the unitary transformation

$$U_1 = e^{-iS_z\varphi} \tag{7.12}$$

to the Hamiltonian (7.3) which in cylindrical coordinates yields

$$\begin{aligned}\widetilde{H} &= U_1^\dagger H U_1 \\ &= \frac{1}{2}\left[-\frac{\partial^2}{\partial\rho^2} - \frac{1}{\rho}\frac{\partial}{\partial\rho} + \frac{1}{\rho^2}(L_z - S_z)^2 - \frac{\partial^2}{\partial z^2} + \rho S_x - 2zS_z\right]\end{aligned} \tag{7.13}$$

In this frame any explicit dependence on the azimuthal angle φ is removed. Hence now L_z instead of J_z is conserved which is because of

$$U_1^\dagger J_z U_1 = L_z \tag{7.14}$$

Therefore we can replace L_z by its quantum number m and consider each L_z subspace separately. The spatially dependent unitary transformation

$$U_2 = e^{-iS_y\beta} \tag{7.15}$$

with $\sin\beta = \frac{\rho}{\sqrt{\rho^2+4z^2}}$ and $\cos\beta = \frac{-2z}{\sqrt{\rho^2+4z^2}}$ diagonalizes the spin-field interaction term of (7.13), i.e.,

$$U_2^\dagger(\rho S_x - 2zS_z)U_2 = \sqrt{\rho^2+4z^2}\,S_z \tag{7.16}$$

The derivatives result in additional terms, which gives rise to additional off-diagonal couplings. However, these terms are proportional to powers of z^{-1} as $\rho \to 0$ and ρ^{-1} as $z \to 0$. Therefore they can be neglected far from the center of the trap. Considering only the component of $U_2^\dagger \widetilde{H} U_2$ which allows for bound solutions that we denote as $|\psi_{qb}\rangle$ we obtain the Schrödinger equation

$$\frac{1}{2}\left[-\frac{\partial^2}{\partial\rho^2} - \frac{\partial^2}{\partial z^2} + \frac{m^2}{\rho^2} + \frac{2mz}{\rho^2\sqrt{\rho^2+4z^2}} + \frac{\rho^2+z^2}{(\rho^2+4z^2)^2} + \frac{1}{2}\sqrt{\rho^2+4z^2}\right]|\phi_{qb}\rangle = E_{qb}|\phi_{qb}\rangle \quad (7.17)$$

Here we have introduced the wavefunction $|\phi_{qb}\rangle = \rho^{\frac{1}{2}}|\psi_{qb}\rangle$. For all m there is a remarkably good agreement between the exact resonance energies E and the energies of the quasi-bound states E_{qb} [76]. The approaching performs better and better with increasing values of the quantum number m. The angular momentum term m^2/ρ^2 together with the two consecutive terms in equation (7.17) constitute a potential barrier which prevents a particle from entering the vicinity around the center of the trap. We have already stated the off-diagonal elements of $U_2^\dagger \widetilde{H} U_2$ involve inverse powers of the spatial coordinates. Thus the matrix element for transition between bound and unbound solutions becomes only significant if there is a sufficiently large overlap of the wave function with the central region of the trap. This explain why the approximation performs better for larger values of m.

We can now discuss the origin of the regular pattern formed by the resonance positions which emerges for high values of the quantum number m. For larger m the minimum and the associate well of the effective potential in the Schrödinger equation (7.17) becomes more and more pronounced. The minimum is approximately located at the position $(z_0 = 0, \rho_0 = (2m)^{2/3})$. The system now becomes almost integrable, and consequently the states can be characterized by their number of nodes in ρ- and z-direction which we designate by n_ρ and n_z, respectively. States with higher number of nodes in ρ-direction posses larger widths (figure 7.2). This is easily understood considering that such states are elongated in the ρ-direction and the particles therefore posses higher oscillation frequencies in that direction. Hence these states posses a higher probability to penetrate the angular momentum barrier and undergo a transition to unbound solutions (which takes place in the vicinity of the center of the trap). Unlike that, states with small n_ρ are mainly elongated along the z-direction and thus avoid contact with the trap center [76].

7.4.2 Negative-energy resonances

Figure 7.3 shows the energies and decay widths for the negative energy resonances. One immediately notices that they are arranged somewhat similarly to the ones with positive energy but on lines with a *negative slope*. The pattern of their distribution becomes more regular for higher m values. Unlike the positive energy resonances their decay width increases with increasing angular momentum. States with a larger angular momentum experience a stronger

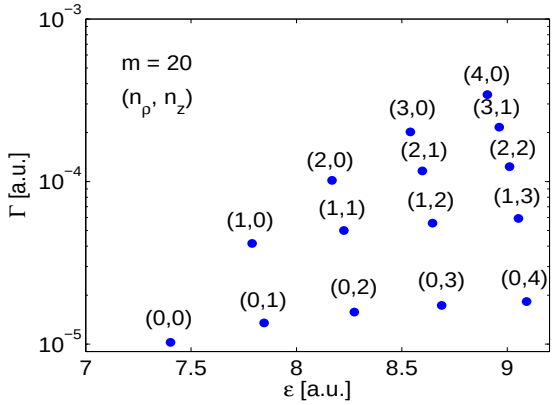

Fig. 7.2: Resonances in the $m = 20$ subspace. The resonance states can be characterized by the two quantum numbers (n_ρ, n_z) which denote the number of nodes in the ρ- and z-direction, respectively.

magnetic field and, as we shall show below, the magnetic moment of the atom is parallel to the local direction of the field in case of a negative energy resonance. Consequently the atom feels an increasingly repelling force with respect to the trap center if the total angular momentum increases. The latter leads to correspondingly broader resonances.

7.4.3 Comparing the two classes of resonances

In Fig. 7.4 we present the expectation value $Re(\langle \mathbf{S} \cdot \mathbf{B}/|\mathbf{B}| \rangle)$ of the spin component which points along the local direction of the field as a function of the energy for the two cases $m = 0$ and $m = 10$. For the negative energy resonances this value is approximately -1 indicating that the spin is aligned opposite to the local direction of the magnetic field and the magnetic moment is in the same direction as the field (we have assumed $g > 0$). For positive energy resonances the spin is parallel to the local field and the magnetic moment is antiparallel.

It is instructive to consider the average value of the radial coordinate r as a function of the energy (see Fig. 7.5) . The resonances are distributed in an area possessing the shape of a triangle. Again this pattern becomes increasingly regular, when considering higher angular momenta [see Fig. 7.5(b)]. $Re(\langle r \rangle)$ increases with increasing absolute value of the energy which is in agreement with our above argumentation with respect to the localization of the resonances.

7.4.4 Mapping among the two classes of resonances

The results on the negative and positive energy resonances suggest an intimate relationship among the two. Indeed due to a complex symmetry, which we shall derive in the following, there exists a mapping of the two classes of resonances. The Schrödinger equation belonging to the Hamiltonian which results when

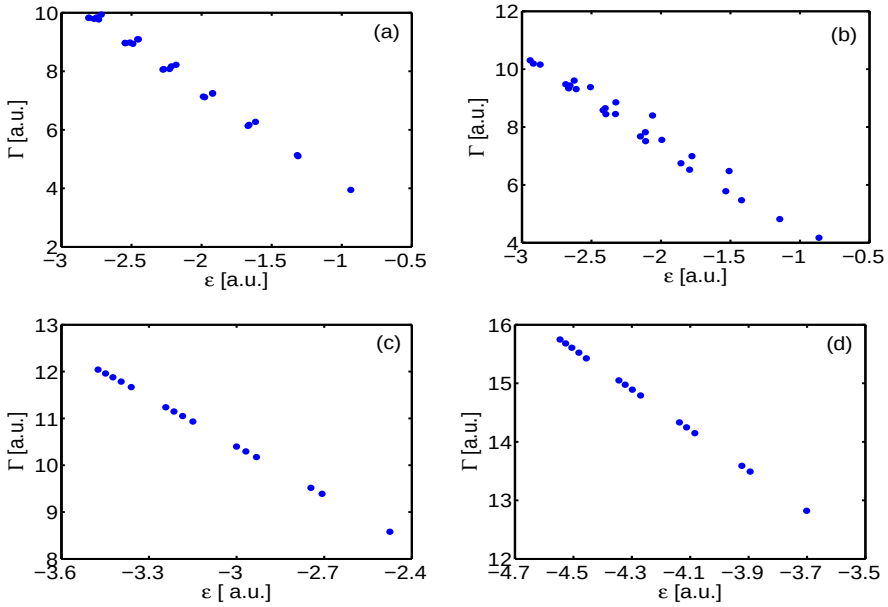

Fig. 7.3: Decay width and energies of the resonances possessing negative energies for $m = 0$ (a), $m = 1$ (b), $m = 10$ (c), and $m = 20$ (d).

applying the complex scaling to the Hamiltonian (7.4) reads

$$\frac{1}{2}(-e^{-i2\eta}\frac{\partial^2}{\partial r^2} - e^{-i2\eta}\frac{2}{r}\frac{\partial}{\partial r} + e^{-i2\eta}\frac{m^2}{r^2} + e^{i\eta}r\sin\theta K - 2e^{i\eta}r\cos\theta S_z)\psi_{E,m} = E\psi_{E,m} \qquad (7.18)$$

Taking the complex conjugate and multiplying by $e^{-i\frac{2\pi}{3}}$ one obtains

$$\frac{1}{2}(-e^{-i2(\frac{\pi}{3}-\eta)}\frac{\partial^2}{\partial r^2} - e^{-i2(\frac{\pi}{3}-\eta)}\frac{2}{r}\frac{\partial}{\partial r} + e^{-i2(\frac{\pi}{3}-\eta)}\frac{m^2}{r^2} + e^{i(\frac{\pi}{3}-\eta)}e^{-i\pi}r\sin\theta K^* - 2e^{i(\frac{\pi}{3}-\eta)}e^{-i\pi}r\cos\theta S_z^*)\psi^*_{E,m} = e^{-i\frac{2\pi}{3}}E^*\psi^*_{E,m} \qquad (7.19)$$

By transforming

$$S_i \to \bar{S}_i = e^{-i\pi}S_i^* = -S_i^*$$
$$\eta \to \bar{\eta} = \frac{\pi}{3} - \eta \qquad (7.20)$$

one can show that

$$\frac{1}{2}(-e^{-i2\bar{\eta}}\frac{\partial^2}{\partial r^2} - e^{-i2\bar{\eta}}\frac{2}{r}\frac{\partial}{\partial r} + e^{-i2\bar{\eta}}\frac{m^2}{r^2} + e^{i\bar{\eta}}r\sin\theta\bar{K} - 2e^{i\bar{\eta}}r\cos\theta\bar{S}_z)\bar{\psi}_{\bar{E},m} = \bar{E}\bar{\psi}_{\bar{E},m} \qquad (7.21)$$

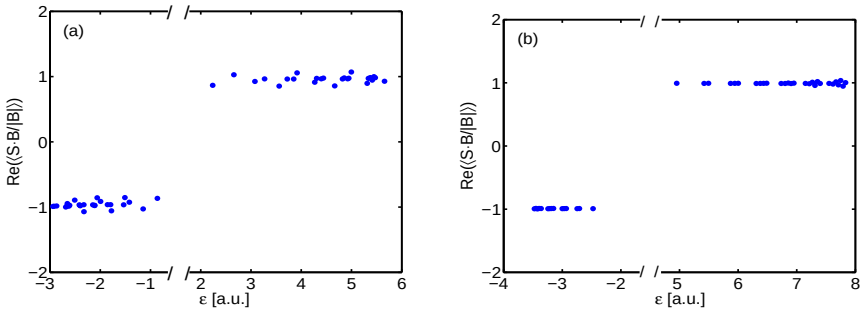

Fig. 7.4: Expectation values of the spin component along the local direction of the magnetic field for the positive and negative energy resonances for $m = 0$ (a) and $m = 10$ (b).

which is unitarily equivalent to (7.18) with the transformed energies and resonance wave functions

$$E \to \bar{E} = e^{-i\frac{2\pi}{3}} E^*$$
$$\psi_{E,m} \to \bar{\psi}_{\bar{E},m}(e^{i\bar{\eta}} r, \theta, \varphi, m_s) = \psi^*_{E,m}(e^{i\eta} r, \theta, \varphi, -m_s) \tag{7.22}$$

Therefore each resonance belonging to (7.18) with eigenvalue E possesses a counterpart, i.e., a *partner resonance* with the eigenvalue $\bar{E} = e^{-i2\pi/3}E^*$. We therefore have a mirror symmetry of the underlying Hamiltonian the corresponding mirror line being placed at $-\pi/3$. While the positive energy continuum rotates clockwise around its zero energy threshold by 2η its image rotates anticlockwise by 2η starting from the line defined by the polar angle $-\frac{2\pi}{3}$. When a resonance is revealed at the angle $-2\eta_0$ in the positive energy domain, its image resonance for negative energies is revealed at the polar angle position $-2\pi/3 + 2\eta_0$ (figure 7.6).

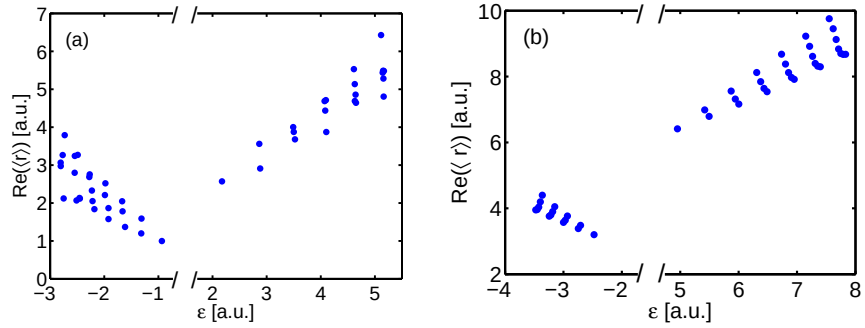

Fig. 7.5: Average of the radial coordinate r as a function of the energy for both positive and negative energy resonances for $m = 0$ (a) and $m = 10$ (b).

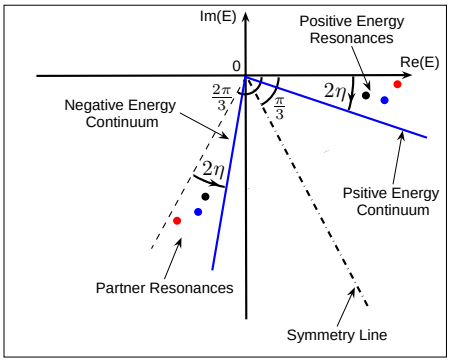

Fig. 7.6: Mapping among the two classes of resonances. Each resonance possesses a partner with the eigenvalue given by (7.22)

Employing the transformation (7.20), the expectation values of r and of the spin-component along the local direction of the magnetic field $\frac{\mathbf{S}\cdot\mathbf{B}}{|\mathbf{B}|}$ transforms as follows

$$\langle r\rangle \rightarrow e^{i\pi/3}\langle r\rangle^* \tag{7.23}$$

$$\left\langle \frac{\mathbf{S}\cdot\mathbf{B}}{|\mathbf{B}|}\right\rangle \rightarrow e^{i\pi}\left\langle \frac{\mathbf{S}\cdot\mathbf{B}}{|\mathbf{B}|}\right\rangle^* = -\left\langle \frac{\mathbf{S}\cdot\mathbf{B}}{|\mathbf{B}|}\right\rangle^* \tag{7.24}$$

which are in good agreement with the results of our numerical calculations. Finally we remark that although our study was performed for the specific case of a spin-1-particle our conclusions hold for any boson with non-zero spin and also for fermions.

7.5 Summary and Concludes

In summary we observe, to our knowledge, for the first time negative energy resonances of spin-1-bosons in a 3D quadrupole magnetic trap. The overall spectrum is arranged in two disconnected parts each of which contains exclusively resonances with positive and negative energies. The latter are exclusively of short-lived character and the spin is antiparallel to the local direction of the magnetic field while for the former the spin is parallel to the field. As the total angular momentum of the boson increases, the decay width of a negative energy resonance state increases while for a positive energy resonance it decreases (assuming a typical laboratory gradient field $5T/m$ and the species ^{87}Rb the order of magnitude for the lifetimes of the negative energy resonances is microseconds). A property of the complex scaled Hamiltonian has been established which allows to map the two branches of the spectrum.

8. ATOMIC HYPERFINE RESONANCES IN A MAGNETIC QUADRUPOLE FIELD

In the previous chapter we assumed that the hyperfine interaction is much stronger than the interaction with the external inhomogeneous magnetic field and therefore the electronic and nuclear angular momenta firstly provide a total angular momentum which then interacts with the magnetic field. This physical picture truly holds for (alkali) atoms in their electronic ground state and macroscopic as well as microscopic (atom chip) gradient fields. The atom is consequently treated as a point particle with the total angular momentum **F**. In the present work we study the case for which both interactions, the hyperfine and the field interaction, have to be taken into account on equal level for the description of the neutral atoms in the field. This case is primarily of principal interest but is expected to describe the magnetized hyperfine properties of systems with very small hyperfine interactions and/or strong gradient fields, such as electronically excited atoms. In the latter case an admixture of different hyperfine states F due to the field interaction has to be expected. In Ref. [90] the possibility to tune the hyperfine splitting by dressing the electronic energy levels by a microwave has been demonstrated. Hence, by this method it is thinkable to achieve a scenario in which the magnetic and the hyperfine-interaction become comparable even for ground state atoms.

We focus on atoms possessing a single active valence electron with spin $S = \frac{1}{2}$ and a nucleus with spin $I = \frac{3}{2}$ in a three dimensional magnetic quadrupole field and describe, as indicated, the combined influence of the hyperfine interaction and the Zeeman effect on the quantum resonances.

8.1 Hamiltonian

Taking into account the hyperfine interaction, the Hamiltonian describing the motion of an atom with mass M and electronic and nuclear spin **S** and **I**,

$\Sigma_x = U_1 P_y P_z$	$\Sigma_y = P_x U_2 P_z$	$\Sigma_z = P_x P_y U_3$	1
$P_x P_y P_z I_{xy} U_4$	$P_z I_{xy} U_4^*$	$P_y I_{xy} U_5$	$P_x I_{xy} U_5^*$
$T U_1 P_z$	$T P_x P_y U_2 P_z$	$T P_x U_3$	$T P_y$
$T P_x P_z I_{xy} U_4$	$T P_y P_z I_{xy} U_4^*$	$T I_{xy} U_5$	$T P_x P_y I_{xy} U_5^*$

Tab. 8.1: Discrete symmetries of the Hamiltonian (8.9). Each symmetry is composed of a number of elementary operations which are listed in table 8.2.

Operator	Operation
T	$A \to A^*$
P_{x_i}	$x_i \to -x_i$
I_{xy}	$x \to y \quad y \to x \quad z \to z$
$U_1 = e^{\frac{i}{\hbar}\pi(S_x+I_x)}$	$S_x \to S_x \quad S_y \to -S_y \quad S_z \to -S_z$ $I_x \to I_x \quad I_y \to -I_y \quad I_z \to -I_z$
$U_2 = e^{\frac{i}{\hbar}\pi(S_y+I_y)}$	$S_x \to -S_x \quad S_y \to S_y \quad S_z \to -S_z$ $I_x \to -I_x \quad I_y \to I_y \quad I_z \to -I_z$
$U_3 = e^{\frac{i}{\hbar}\pi(S_z+I_z)}$	$S_x \to -S_x \quad S_y \to -S_y \quad S_z \to S_z$ $I_x \to -I_x \quad I_y \to -I_y \quad I_z \to I_z$
$U_4 = U_1 e^{-\frac{i}{\hbar}\frac{\pi}{2}(S_z+I_z)}$	$S_x \to -S_y \quad S_y \to -S_x \quad S_z \to -S_z$ $I_x \to -I_y \quad I_y \to -I_x \quad I_z \to -I_z$
$U_5 = e^{\frac{i}{\hbar}\frac{\pi}{2}(S_z+I_z)}$	$S_x \to -S_y \quad S_y \to S_x \quad S_z \to S_z$ $I_x \to -I_y \quad I_y \to I_x \quad I_z \to I_z$

Tab. 8.2: Set of discrete operations out of which all discrete symmetry operations of the Hamiltonian (8.9) can be composed.

respectively, reads in a magnetic quadrupole field

$$H = \frac{\mathbf{p}^2}{2M} + H_{HF} + H_B \tag{8.1}$$

where H_{HF} describes the hyperfine interaction between the outermost single valence electron and the nucleus

$$H_{HF} = A\mathbf{I} \cdot \mathbf{S} \tag{8.2}$$

Here A is a constant which for an s-electron is given by [93]

$$A = \frac{2}{3}\frac{\mu_0}{\hbar^2} g_S g_I \mu_B \mu_N |\psi_s(0)|^2 \tag{8.3}$$

g_S and g_I are the g-factors of the electron and the nucleus, respectively, and $\psi_s(0)$ is the value of the valence s-electron wave function at the nucleus. $\mu_B = \frac{e\hbar}{2m_e}$ and $\mu_N = \frac{e\hbar}{2m_p}$ are the Bohr magneton for the electron and the proton, respectively. H_B accounts for the interaction of the magnetic moment of the electron and the nucleus with the magnetic field

$$H_B = -\mu_e \cdot \mathbf{B} - \mu_n \cdot \mathbf{B} \tag{8.4}$$

where $\mu_e = -\mu_B g_S \mathbf{S}$ and $\mu_n = \mu_N g_I \mathbf{I}$. Conventionally one introduces the ratio

$$\alpha = -\frac{\mu_N g_I}{\mu_B g_S} \approx -\frac{m_e}{m_p} \tag{8.5}$$

and writes

$$H_B = \mu_B g_S (\mathbf{S} + \alpha \mathbf{I}) \cdot \mathbf{B} \tag{8.6}$$

The vector of the three-dimensional quadrupole magnetic field is given by

$$\mathbf{B}(\mathbf{r}) = b(x, y, -2z) \tag{8.7}$$

Consequently the total Hamiltonian becomes

$$H = \frac{1}{2M}[\mathbf{p}^2 + 2Mb\mu_B g_S(x(S_x + \alpha I_x) + y(S_y + \alpha I_y) - 2z(S_z + \alpha I_z)) \\ +2MA\mathbf{I}\cdot\mathbf{S}] \tag{8.8}$$

Performing the scale transformation

$$\bar{p}_i = (2Mb\mu_B g_S)^{-1/3} p_i \quad \text{and} \quad \bar{x}_i = (2Mb\mu_B g_S)^{1/3} x_i$$

and thereupon omitting the bars one obtains

$$H = \frac{1}{2}[\mathbf{p}^2 + x(S_x + \alpha I_x) + y(S_y + \alpha I_y) - 2z(S_z + \alpha I_z) + \beta\mathbf{I}\cdot\mathbf{S}] \tag{8.9}$$

with $\beta = \frac{A}{b\mu_B g_S}$. The energy is now measured in units of $\frac{1}{M}(2Mb\mu_B g_S)^{2/3}$. For convenience and in anticipation of the forthcoming discussion we transform the Hamiltonian to a spherical coordinate system, i.e., $(x, y, z) \to (r, \theta, \phi)$. Writing the momentum operator explicitly and using atomic units we obtain

$$\begin{aligned} H \quad = \quad & \frac{1}{2}[-\frac{\partial^2}{\partial r^2} - \frac{2}{r}\frac{\partial}{\partial r} + \frac{L^2}{r^2} + r\sin\theta\cos\varphi(S_x + \alpha I x) + r\sin\theta\sin\varphi(S_y + \alpha I_y) \\ & - 2r\cos\theta(S_z + \alpha I_z) + \beta\mathbf{I}\cdot\mathbf{S}] \end{aligned} \tag{8.10}$$

8.2 Symmetries and Degeneracies

Let us now study the symmetry properties of the Hamiltonian (8.9) in order to gain first insights into the resonance spectrum of the system. We obtain 16 discrete symmetry operations which are listed in table 8.1. Each symmetry operation is composed of a number of elementary operations given in table 8.2 along with the general representation of U_i operations.

Apart from the discrete symmetries given in table 8.1 there is a continuous symmetry group generated by $J_z = L_z + F_z$ which is the $z-$component of the total angular momentum of the atom. Here L_z and F_z are the $z-$component of the orbital angular momentum and the total spin, respectively. With the same argument as the previous chapter one can find a two degeneracy in the energy spectrum of the Hamiltonian (8.9) for $m \neq 0$. The general result for an atom with electron spin S and nuclear spin I reads

$$\mid m\rangle^{(I,S)} = \sum_{\substack{m_S=-S \\ m_I=-I}}^{S,I} C^m_{m_I,m_S} e^{i(m-m_I-m_S)\varphi} \mid m_I\rangle \otimes \mid m_S\rangle \tag{8.11}$$

with $\sum_{m_I,m_S} \mid C^m_{m_I,m_S}|^2 = 1$.

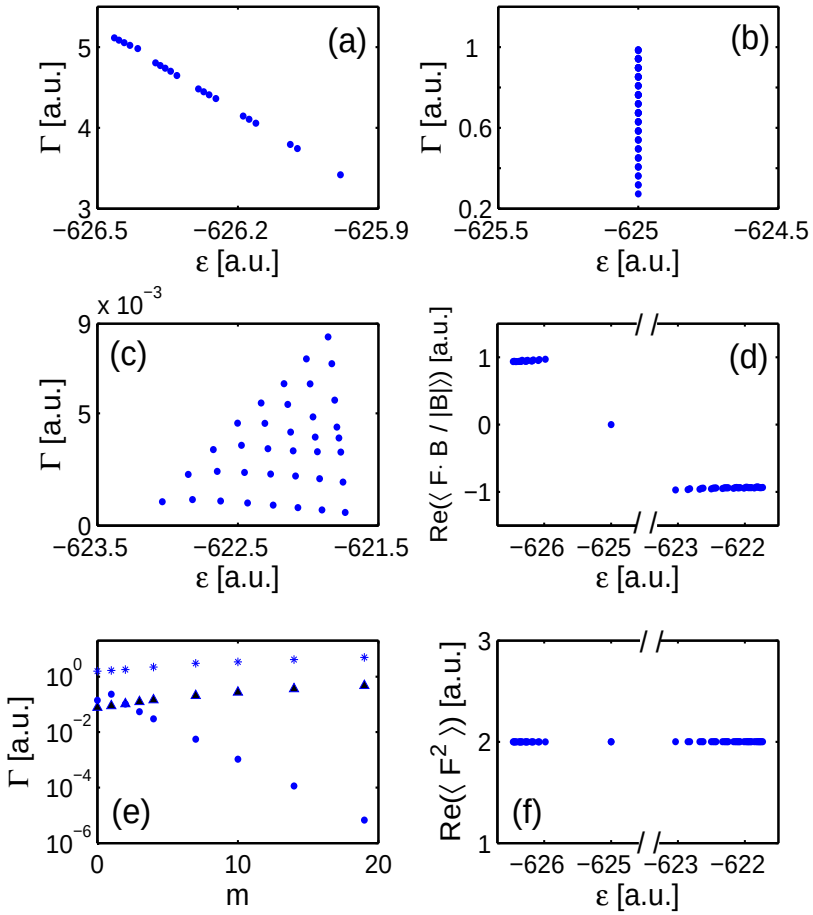

Fig. 8.1: Decay width and energies of the resonances for $\beta = 1000$, $m = 10$ for $m_F = 1$ (a), $m_F = 0$ (b) and $m_F = -1$ (c). (d) Expectation values of the total spin component along the local direction of the magnetic field for the three sets of resonances. (e) Decay width as a function of the quantum number m for the energetically lowest state with $m_F = -1$ (square), the energetically highest state with $m_F = 0$ (triangle) and the energetically highest state with $m_F = +1$ (star). (f) Expectation value of the total spin squared as a function of the energy.

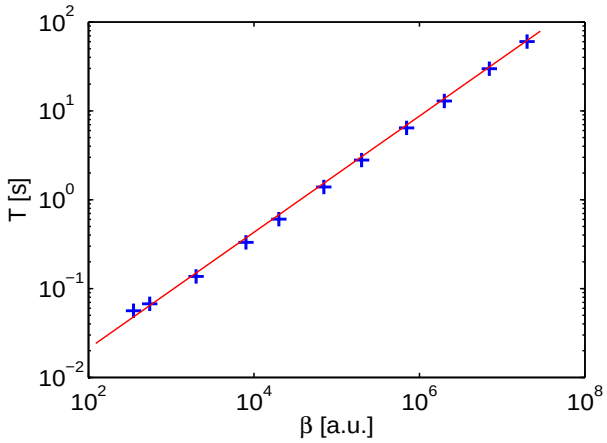

Fig. 8.2: The lifetime of the energetically lowest long-lived resonance state for $m = 25$ as a function of the parameter β (Zeeman regime).

8.3 Numerical Approach

The Hamiltonian (8.9) does not support bound states. In order to calculate the energies and decay widths of the scattering wave functions we employ the complex scaling method in conjunction with the linear variational method. To this end we employ a so-called Sturmian basis set of the form

$$\mid n, l, m_I, m_S\rangle_m = R_n^{(\zeta)}(r) Y_l^{m-m_I-m_S}(\theta,\varphi)\chi^I(m_I)\chi^S(m_S), \tag{8.12}$$

here the functions Y_l^m are the spherical harmonics. For fixed m the linear variational combination of the basis functions ψ^m_{n,l,m_I,m_S}, yields, per construction, eigenstates of the Hamiltonian and J_z simultaneously. For expanding the radial part we take the non-orthogonal set of functions $R_n^\zeta(r)$ which has been introduced in the previous chapter. Using the basis set (8.12) all matrix elements of the Hamiltonian (8.10) can be calculated analytically.

8.4 Results

Let us now discuss the results we obtained while studying an atom with hyperfine interaction in a magnetic quadrupole field. We present the resonance energies and decay widths for different values of the field gradient. The resulting spectrum consist of several well-separated parts. Concerning the resonance positions one can distinguish three regimes, each of which reveals individual characteristics: the weak, the intermediate, and the strong gradient regimes. In the weak gradient regime, the Zeeman term H_B is very small compared with the hyperfine interaction H_{HF} and only slightly perturbs the zero-field eigenstates of H. In this case the atom, being primarily in its hyperfine ground state

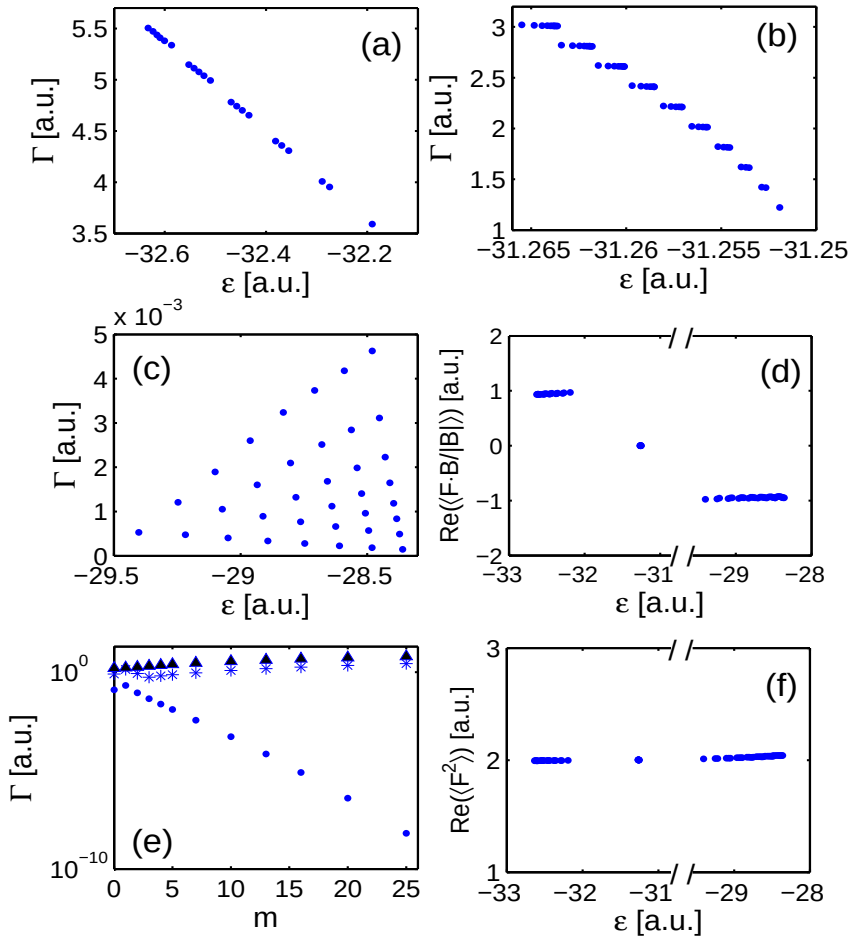

Fig. 8.3: Decay width and energies of the resonances for $\beta = 50$, $m = 10$ for $m_F = 1$ (a), $m_F = 0$ (b) and $m_F = -1$ (c). (d) Expectation values of the total spin component along the local direction of the magnetic field for the three sets of resonances. (e) The decay width of the energetically lowest state with $m_F = -1$ (square), the decay width of the energetically highest state with $m_F = 0$ (triangle), the decay width of the energetically highest state with $m_F = +1$ (star), as a function of the quantum number m. (f) The expectation value of the total spin squared as a function of the energy.

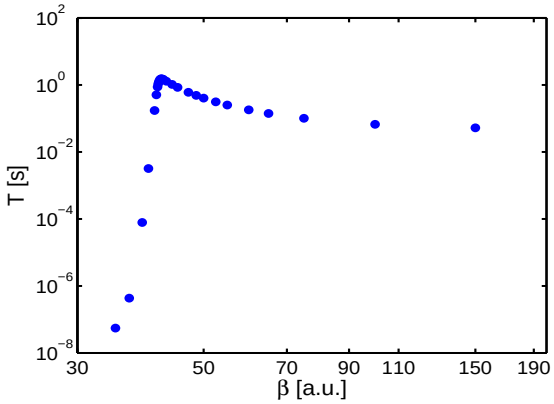

Fig. 8.4: The lifetime of the energetically lowest long-lived resonance state for $m = 25$ as a function of the parameter β (intermediate regime).

$F = I - \frac{1}{2}$, remains in this manifold and behaves approximately like a neutral particle of spin F with the g-factor

$$g_F \simeq g_S \frac{F(F+1) - I(I+1) + S(S+1)}{2F(F+1)} \tag{8.13}$$

This regime is also called the Zeeman regime. In the intermediate gradient regime the Zeeman and the hyperfine interactions are of the same order of magnitude, and the atom in the ground state may represent a significant admixture of different hyperfine states F. Finally in the strong gradient regime the Zeeman term dominates the hyperfine energies at least for sufficiently large distances from the coordinate origin. In this case the spin component of the electron along the local direction of the magnetic field is almost conserved and as we will see, the resonance positions in the complex energy plane are grouped according to different values of its quantum number m_S. This regime is also called the Paschen-Back Regime.

We will analyze the average values of the components of the spins which point along the local direction of the field as a function of the energy. This enable us to explain different sets of resonances in each regime. We also discuss in this section the dependence of the decay width of a resonance state on its angular momentum as well as on the field gradient.

8.4.1 Resonance positions in the Zeeman regime

For large values of β ($\beta > 200$) we are in the Zeeman regime. In Fig. 8.1(a)-(c) we present the energies and decay widths for $\beta = 1000$ and $m = 10$, for an atom with nuclear spin $I = \frac{3}{2}$ being in its hyperfine ground state. The resonances are localized in the negative energy region and their distribution consists of three well-separated parts. They can be classified according to the expectation value

$m_F = Re(\langle \mathbf{F} \cdot \mathbf{B}/|\mathbf{B}| \rangle)$ which is the projection of the total spin onto the local direction of the magnetic field. There are long-lived resonances which can be identified with $m_F = -1$, and two sets of resonances with shorter lifetimes whose spin projections are $m_F = 0, +1$. The values of m_F are shown in the panel d. For $m_F = -1$ one observes the resonances to be located on lines with similar slopes covering the area of a right triangle in the $\epsilon - \Gamma$ plane. For $m_F = 0$ and $m_F = +1$ one immediately notices that both sets are arranged on lines with an infinity and a negative slope respectively. In Fig. 8.1(e) we present decay width of the energetically lowest state of the long-lived resonances (the resonances with $m_F = -1$) as a function of the angular momentum m. The decay width decreases exponentially with increasing value of m. We also present the decay width of the energetically highest state of the two sets of short-lived resonances as a function of the quantum number m. Unlike the case $m_F = -1$, the decay width of resonances with $m_F = +1$ and $m_F = 0$ increases with increasing angular momentum (for an explanation of this behavior see [76]). Fig. 8.1(f) shows the expectation value of the total spin squared, $Re(\langle \mathbf{F}^2 \rangle)$ as a function of the energy for the same parameter values. For all resonance states, the value is approximately $+2$ which corresponds to $F = 1$, i.e., the atom behaves like a spin-1 particle.

In Fig. 8.2 we present the lifetime of the energetically lowest long-lived resonance state ($m_F = -1$) for $m = 25$ as a function of the parameter β. The lifetime decreases as the hyperfine parameter β decreases, i.e., the gradient field b increases. Performing a line fit we find the dependence $T(s) \approx 8.3 \times 10^{-4} \beta^{2/3} [a.u.]$.

8.4.2 Resonance positions in the intermediate regime

Let us now focus on the intermediate regime covering the values $0.2 < \beta < 200$, where the Zeeman and hyperfine interactions become comparable. We observe three different types of behavior. For $40 < \beta < 200$, the resonance spectrum for an atom being in the hyperfine ground state, is localized in the negative energy domain and consists of three well-separated parts to which we can assign the values $m_F = -1, 0, +1$. (see Fig. 8.3 for $m = 10$ and $\beta = 50$). In Fig. 8.3(c) we present the decay width of the lowest energy state of the long lived resonances as well as the decay width of the highest energy state of the two sets of short-lived resonances as a function of the quantum number m. For the two short-lived states, following the same reasoning as above, the width increases when m increases, while for the long-lived states it decreases. Fig. 8.3(f) shows the expectation value of the total spin squared, $Re(\langle \mathbf{F}^2 \rangle)$ of the three sets of resonances as a function of energy. Note that the atom still behaves approximately like a spin-1 particle. However, in contrast to the Zeeman regime (see Fig. 8.2), the lifetime of the long-lived states ($m_F = -1$) increases when the hyperfine parameter β decreases, i.e., the field gradient b increases (see Fig. 8.4).

For $\beta < 40$ this value decreases very rapidly when β decreases. In this case the resonance states which correspond to higher hyperfine levels $F = 2$

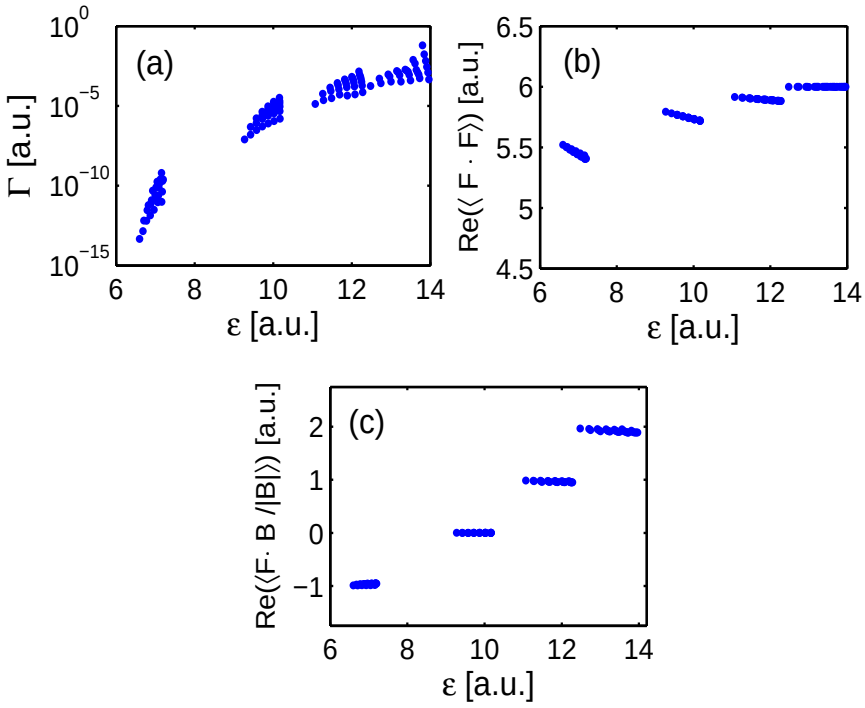

Fig. 8.5: (a) Decay width and energies of the long-lived resonances with higher hyperfine quantum number $F = 2$ for $\beta = 19$ and $m = 25$. (b) The expectation value of the total spin squared as a function of the energy. (c) Expectation values of the total spin component along the local direction of the magnetic field as a function of the energy.

are more stable, and are localized in the positive region of the spectrum. Fig. 8.5(a) shows the decay widths and energies of the resonances possessing positive energies for $\beta = 19$. We observe four different curved and triangular shaped regions with distinct classes of resonances. In Fig. 8.5(b) we present the expectation values of the total spin squared, $Re(\langle \mathbf{F}^2 \rangle)$, of these resonances as a function of the energy. The values range from approximately 5.5 to 6.0 indicating a substantial conservation of F. Fig. 8.5(c) shows the expectation values of the total spin component along the local direction of the field for the resonances of Fig. 8.5(a). The resonances are divided into four well-separated parts corresponding to $m_F = +2, +1, 0, -1$. Resonances with $m_F = -2$ have very short lifetime and are not shown. For $\beta < 3$ the non-conservation of F becomes even more explicit [see Fig. 8.6(a) for $\beta = 1$]. In Fig. 8.6(b)-(c) we present the respective decay widths and energies. The resonances which are localized in the negative energy region have short lifetimes and are divided into four subgroups. Each group lies on a line with negative slope, the four slopes

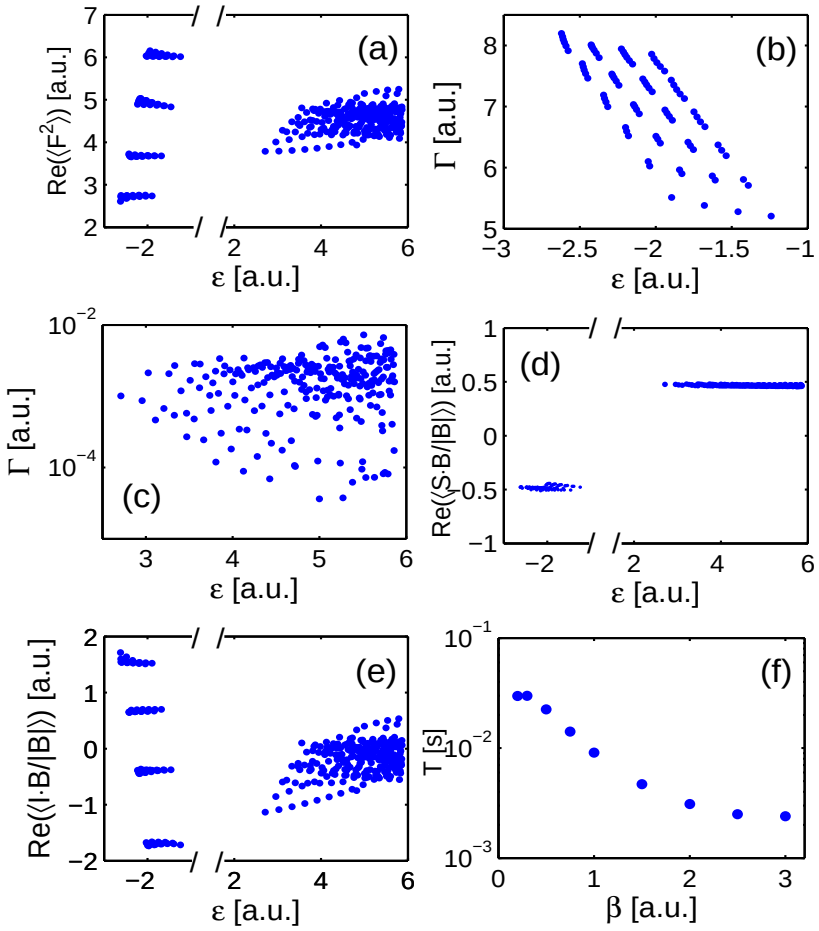

Fig. 8.6: (a) Expectation value of the total spin squared as a function of the energy. Decay width and energies of the resonances with $m_S = -\frac{1}{2}$ (b), and $m_S = +\frac{1}{2}$ (c). (d) Expectation values of the electronic spin component along the local direction of the magnetic field. (e) Expectation values of the nuclear spin component along the local direction of the magnetic field. (f) Lifetime of the energetically lowest resonance state of the positive energy domain of the spectrum as a function of β. The data have been calculated for $m = 10$ and $\beta = 1.0$.

being very similar. Moreover, the resonances investigated form subgroups on these lines. The positive energy resonances have much longer lifetimes and cover an area of approximately triangular shape in an irregular manner, i.e., no pattern is visible. In Fig. 8.6(d) the corresponding expectation values of the electronic spin component along the local direction of the magnetic field, $Re(\langle \mathbf{S}\cdot\mathbf{B}/|\mathbf{B}|\rangle)$ is shown. For the negative energy resonances this value is approximately -0.5 indicating that the spin is aligned opposite to the local direction of the magnetic field, while for positive energies the spin is parallel to the magnetic field. Fig. 8.6(e) shows the expectation values of the nuclear spin component along the local direction of the field. In the negative energy domain of the spectrum the pattern divides into four parts with values $m_I = -\frac{3}{2}, -\frac{1}{2}, +\frac{1}{2}, +\frac{3}{2}$, while in the positive energy region, the pattern is strongly disturbed and m_I is not conserved. Fig. 8.6(f) presents the lifetime of the energetically lowest long-lived state as a function of β. This value increases when β decreases, i.e., the gradient field b increases. Our results show that for the short-lived state, i.e., the negative energy resonance state, the width increases when m increases, while for the long-lived state, i.e., the positive energy resonance state it decreases.

8.4.3 Resonance positions in the hyperfine Paschen-Back regime

The hyperfine Paschen-Back regime includes $\beta < 0.2$. In case the Zeeman term dominates the hyperfine energy, it is natural to decompose the Hamiltonian according to $H = H_0 + H_1$ where $H_0 = \frac{1}{2}(p^2 + xS_x + yS_y - 2zS_z)$ describes the motion of a spin $\frac{1}{2}$ particle in the magnetic field, and $H_1 = \alpha(xI_x + yI_y - 2zI_z) + \beta\mathbf{I}\cdot\mathbf{S}$ perturbs the eigenstates of H_0. The spectrum consists of two parts: again we have one set of resonances localized in the negative energy region with short lifetimes and a second set localized in the positive energy domain possesses much larger lifetimes. In Fig. 8.7(a)-(b) we present the energies and decay widths of resonances for $\beta = 0.1$ and $m = 10$. The negative energy resonances are arranged on lines with a negative slope. The positive energy resonances cover an area of triangular shape, some of them being located on straight lines. Fig. 8.7(c) shows the expectation value $Re(\langle \mathbf{F}^2\rangle)$ of the square of the total spin for $m = 10$ and $\beta = 0.1$. This value is almost 4.5 which again indicates that the total spin quantum number F is not conserved. In Fig. 8.7(d) the respective expectation value $Re(\langle \mathbf{S}\cdot\mathbf{B}/|\mathbf{B}|\rangle)$ of the electronic spin component which points along the local direction of the magnetic field is presented. For the positive energy resonances this value is approximately +0.5 indicating that the spin is aligned parallel to the local direction of the magnetic field while for negative energy resonances it is antiparallel. The nuclear spin component along the local field is not conserved, however it is instructive to consider its average value, $Re(\langle \mathbf{I}\cdot\mathbf{B}/|\mathbf{B}|\rangle)$, as a function of the energy. For large values of m [see Fig. 8.7(e) for $m = 10$] the resonances are grouped into four regular subparts for both the positive and negative energy domain.

We remark that the decay widths of the energetically lowest states of the positive energy resonances [see Fig. 8.7(b)] show again an exponential decaying behavior as a function of the quantum number m whereas the decay widths of the

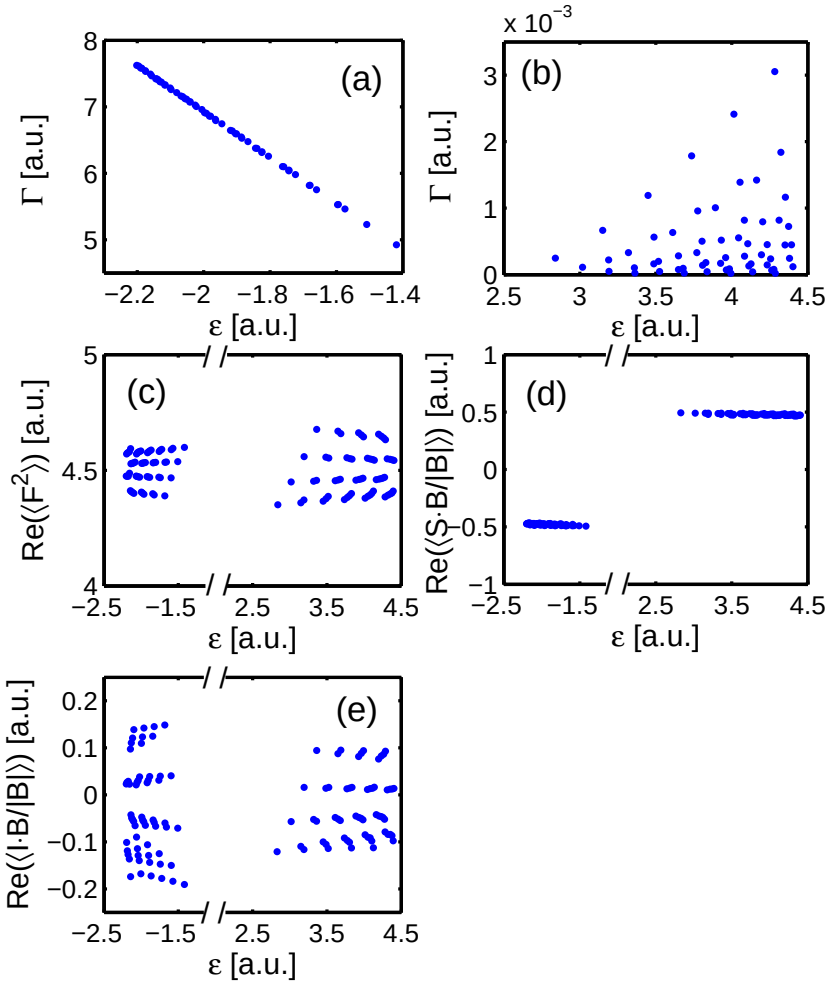

Fig. 8.7: Decay width and energies of the resonances for $\beta = 0.1$, $m = 10$ with $m_S = -\frac{1}{2}$ (a) and $m_S = +\frac{1}{2}$ (b). (c) The corresponding expectation value of the total spin squared as a function of the energy. (d) Expectation values of the electronic spin component along the local direction of the magnetic field for the two sets of resonances. (e) Expectation values of the nuclear spin component along the local direction of the magnetic field.

energetically highest negative energy resonance states increases with increasing m. The lifetime of the energetically lowest long-lived resonances for $m = 25$ as a function of β can be fitted according to $T(s) \approx 1.1 \times 10^{-1}\beta^{2/3}[a.u.]$.

8.5 Summary

We have investigated the resonant quantum properties of an atom with a single active valence electron taking into account its hyperfine structure ($I = \frac{3}{2}$) in a 3D magnetic quadrupole field. The underlying Hamiltonian possesses 16 discrete symmetry operations as well as a continuous unitary symmetry generated by the conserved quantity $J_z = L_z + F_z$. Exploiting these symmetries we have found a twofold degeneracy of any energy level with $m \neq 0$.

We have calculated and analyzed the energies and decay widths of the resonance states of the Hamiltonian employing the complex scaling approach and a Sturmian basis set. With respect to the resonance position one can distinguish essentially three regimes. In the weak gradient regime, the Zeeman term is very small compared with the hyperfine interaction and only slightly perturbs the zero-field eigenstates of the Hamiltonian. In this case the atom in the hyperfine ground state behaves approximately like a particle of spin 1, and the resonance states are grouped into three well-separated parts, corresponding to three different directions of the total spin with respect to the local direction of the field. The resonance states with the total spin being perpendicular ($m_F = 0$) or parallel ($m_F = 1$) to the local field possess short lifetimes, while the resonances for which the total spin is antiparallel to the field ($m_F = -1$) possess much more longer lifetimes. As the total angular momentum of the atom increases, the decay width of a short-lived resonance state increases while for a long-lived resonance state it decreases. We have calculated the lifetimes of some low energy state belonging to the class of long-lived resonances as a function of the scaled hyperfine parameter β, showing that if β increases so does the lifetime.

In the intermediate regime the Zeeman and hyperfine interactions are comparable. For a sufficiently weak field gradient the atom in the hyperfine ground state behaves approximately like a spin-1 particle, and the resonances are arranged somehow similar to the Zeeman regime but in contrast to the Zeeman regime its long-lived resonance states become more stable when the gradient field increases and/or β decreases. For stronger field gradients and/or smaller values of the parameter β the lifetime decreases rapidly. In this case resonances which correspond to the higher hyperfine level, $F = 2$, are more stable. For even smaller values of β, the non-conservation of F becomes remarkable. In this case the electronic spin component along the local direction of the magnetic field is almost conserved. A resonance which is localized in the negative energy region of the spectrum possesses a short lifetime. In such a state the electronic spin is aligned opposite to the local direction of the magnetic field. The positive energy resonances possess a much longer lifetime with their electronic spin being parallel to the magnetic field. We have studied the dependence of the resonances on the total angular momentum of the atom. For a short-lived state the width

increases with increasing m, while for a long-lived state it decreases. For the latter we also investigated the dependence on the parameter β. Our results show that the lifetime of this state increases with decreasing values of β.

In the strong gradient regime, the Zeeman term dominates the hyperfine energy. Here the component of the electronic spin along the local direction of the field is almost conserved. The energy spectrum is arranged into two disconnected parts each of which contains exclusively resonance states with negative and positive energies. The former are of short-lived character and the electronic spin is antiparallel to the local direction of the magnetic field. The latter possess much longer lifetimes and the spin of the electron is parallel to the field. As the total angular momentum of the atom increases, the decay width of a negative energy resonance state increases while for a positive energy resonance state it decreases. We have calculated the lifetimes of the energetically lowest resonance states possessing a positive energy as a function of the parameter β. Similar to the weak gradient regime, it decreases with decreasing β.

APPENDIX

A. SCATTERING THEORY IN FREE SPACE: SINGLE-MODE REGIME

Let's consider a single spinless particle in a fixed potential. Thus $\mathcal{H}$ is the space $\mathcal{L}^2(\mathcal{R}^3)$, with wave functions $\psi(\mathbf{x}) \equiv \langle \mathbf{x}|\psi\rangle$ depending on a single variable $\mathbf{x}$; and the Hamiltonian has the form $H = H^0 + V$, where $H^0 = p^2/2m$, is the Hamiltonian of a free particle, and V is the potential. We shall suppose that the potential is local; that is, that V is a function of the particle's position only.

Let us suppose that the orbit $U(t)|\psi\rangle$ describes the evolution of some scattering experiment. This means that when followed back to a time well before the collision, $U(t)|\psi\rangle$ represents a wave packet that is localized far away from the scattering center and, therefore, behaves like a free wave packet. Now, the motion of a free particle is given by the free evolution operator $U^0(t) \equiv e^{-iH^0t}$, and we therefore expect that as $t \to -\infty$,

$$U(t)|\psi\rangle \xrightarrow[t \to -\infty]{} U^0(t)|\psi_{in}\rangle \tag{A.1}$$

for some vector $|\psi_{in}\rangle$. Similarly, after the collision the particle moves away again and we expect that

$$U(t)|\psi\rangle \xrightarrow[t \to +\infty]{} U^0(t)|\psi_{out}\rangle \tag{A.2}$$

for some vector $|\psi_{out}\rangle$. This two limits are analogous to the classical limits (2.1) and in analogy with the classical terminology we shall call the asymptotic free orbits of (A.1) and (A.2) the *in* and *out* asymptotes of the actual orbit $U(t)|\psi\rangle$.

The results of scattering theory will certainly not hold for all possible potentials. For example, if $V(\mathbf{r})$ does not fall off sufficiently fast as $\mathbf{r} \to \infty$, the particle will not behave like a free particle as it moves far away.

Unfortunately, the conditions under which some of the principal results have been proved are quite complicated; different proofs use different conditions. Further, a set of conditions that is both sufficient and necessary for all results is not known. However, the principal results of scattering theory hold for a wide class of "reasonable" potentials, but definitely excluding the Coulomb and any attractive potentials more singular than r^{-2} at the origin. In the continue we assume that the potential satisfies all the conditions which are necessary for the results which we discuss.

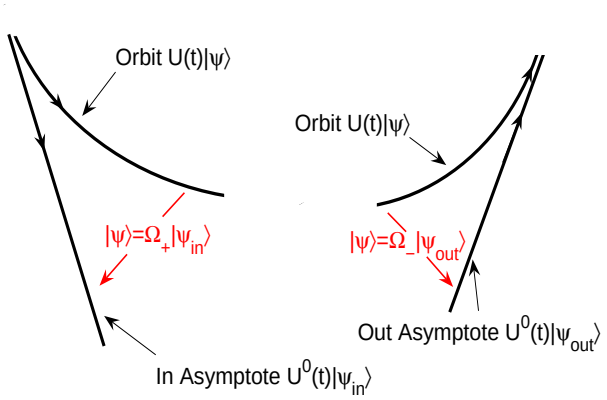

Fig. A.1: Classical representation of roles of the Møller operators.

A.1 The Asymptotic Condition

Every vector in $\mathcal{H}$ (labelled by $|\psi_{in}\rangle$ or $|\psi_{out}\rangle$ as appropriate) does represent the asymptote of some actual orbit; that is , for every $|\psi_{in}\rangle$ in $\mathcal{H}$ there is a $|\psi\rangle$ such that

$$\lim_{t\to-\infty} U(t)|\psi\rangle - U^0(t)|\psi_{in}\rangle = 0$$

and likewise for every $|\psi_{out}\rangle$ in $\mathcal{H}$ as $t \to +\infty$.

The asymptotic condition guaranties that any $|\psi_{in}\rangle$ in $\mathcal{H}$ is in fact the *in* asymptote of some actual orbit $U(t)|\psi\rangle$. The actual state $|\psi\rangle$ of the system at $t = 0$ is linearly related to the *in* asymptote $|\psi_{in}\rangle$, specifically,

$$|\psi\rangle = \lim_{t\to-\infty} U(t)^\dagger U^0(t)|\psi_{in}\rangle \equiv \Omega_+|\psi_{in}\rangle \tag{A.3}$$

Similarly the actual state $|\psi\rangle$ at $t = 0$ that will evolve into the *out* asymptote labelled by $|\psi_{out}\rangle$ is

$$|\psi\rangle = \lim_{t\to+\infty} U(t)^\dagger U^0(t)|\psi_{out}\rangle \equiv \Omega_-|\psi_{out}\rangle \tag{A.4}$$

The two operators $\Omega_\pm$, defined as the limits

$$\Omega_\pm = \lim_{t\to\mp\infty} U(t)^\dagger U^0(t) \tag{A.5}$$

are called the Møller wave operators. They are the limits of a unitary operator and so, are isometric. Their significance should be clear: Acting on $|\psi_{in}\rangle$ (or $|\psi_{out}\rangle$) in $\mathcal{H}$, they give the actual state at $t = 0$ that would evolve from (or to) the asymptote represented by this vector. This is illustrated symbolically in Fig. A.1.

A.2 Orthogonality and Asymptotic Completeness

We have seen that every vector in $\mathcal{H}$ labels the *in* or *out* asymptote of some actual orbit $U(t)|\psi\rangle$. We must now consider the converse question: **Does every $|\psi\rangle$ in $\mathcal{H}$ define an orbit $U(t)|\psi\rangle$ that has *in* and *out* asymptote?** Just as in the classical case the answer to this question is, in general, no. The Hamiltonian $H = H^0 + V$ will usually have some bound states; and if $|\phi\rangle$ is a bound state, then the orbit $U(t)|\phi\rangle$ describes a stationary state in which the particle remains localized close to the potential and, hence, never behaves freely.

The situation is analogous to that of the classical problem. We do not expect that every orbit $U(t)|\psi\rangle$ will have asymptotes. We expect rather that there will be certain scattering orbits that do have asymptotes, and that there may be some bound states. Under some special conditions, there might be also some resonances. The scattering states together with the bound states will span the space $\mathcal{H}$ of all normalizable states. The resonance states however are not normalizable and thus, they are not in the Hilbert space $\mathcal{H}$.

Let us denote by $\mathcal{B}$ the subspace spanned by the bound states. We next note that any state with an *in* asymptote is given by $|\psi\rangle = \Omega_+|\psi_{in}\rangle$. These vectors make up the *range* of Ω_+. We denote this range by $\mathcal{R}_+$. Similarly, $\mathcal{R}_-$ will denote the range of Ω_- which is the set of all states with out asymptote.

The following theorems hold for a wide class of potentials

1. Orthogonality Theorem. The subspaces $\mathcal{R}_\pm$ are orthogonal to the subspace $\mathcal{B}$:

$$\mathcal{R}_+ \perp \mathcal{B}$$
$$\mathcal{R}_- \perp \mathcal{B}$$

2.Asymptotic Completeness. The subspaces $\mathcal{R}_+$ and $\mathcal{R}_-$ are the same:

$$\mathcal{R}_+ = \mathcal{R}_- = \mathcal{R}$$

If the scattering theory holds the asymptotic completeness, it is called asymptotically complete.

Due to above theorems, the space $\mathcal{H}$ can be written as *direct sum* of $\mathcal{R}$ and $\mathcal{B}$:

$$\mathcal{H} = \mathcal{R} \oplus \mathcal{B} \tag{A.6}$$

Our description of the scattering process can be summarized as follows: As far as the actual orbits of the system are concerned, the Hilbert space $\mathcal{H}$ is divided into two orthogonal parts; the subspace $\mathcal{B}$ spanned by the bound states, and the subspace $\mathcal{R}$ of scattering states. For every $|\psi\rangle$ in $\mathcal{R}$, the orbit $U(t)|\psi\rangle$ describes a scattering process with *in* and *out* asymptote,

$$\begin{aligned} U(t)|\psi\rangle &\xrightarrow[t \to -\infty]{} U^0(t)|\psi_{in}\rangle \\ &\xrightarrow[t \to +\infty]{} U^0(t)|\psi_{out}\rangle \end{aligned} \tag{A.7}$$

Every $|\psi_{in}\rangle$ (or $|\psi_{out}\rangle$) in $\mathcal{H}$ labels the *in* (or *out*) asymptote of a unique actual orbit $U(t)|\psi\rangle$ and the Møller operators $\Omega_{\pm}$ map each $|\psi_{in}\rangle$ (or $|\psi_{out}\rangle$) in $\mathcal{H}$ onto the corresponding scattering state $|\psi\rangle$ in $\mathcal{R}$,

$$|\psi\rangle = \Omega_{+}|\psi_{in}\rangle = \Omega_{-}|\psi_{out}\rangle \tag{A.8}$$

As we have already noted, the Møller operators are isometric. This means that for each normalized $|\psi_{in}\rangle$ or $|\psi_{out}\rangle$ in $\mathcal{H}$, there is a unique corresponding normalized $|\psi\rangle$ in $\mathcal{R}$, and conversely, for each normalized $|\psi\rangle$ in $\mathcal{R}$ there are unique normalized asymptotes $|\psi_{in}\rangle$ and $|\psi_{out}\rangle$. This situation is summarized schematically in Fig. A.2

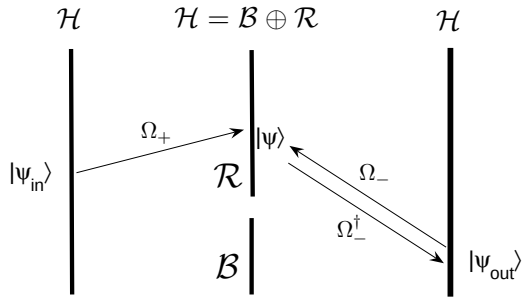

Fig. A.2: The Møller operators $\Omega_{\pm}$ map the *in* and *out* asymptotes, represented by $|\psi_{in}\rangle$ and $|\psi_{out}\rangle$, onto the actual orbit labelled by $|\psi\rangle$.

One question which may arises here, is that how a bound state vector $|\phi\rangle$ can possibly represent a free asymptote? To answer this, one has only to recall the *significance* of the asymptotes. The statement that $|\phi\rangle$ represents a possible *in* asymptote (for example) means that if we multiply $|\phi\rangle$ by the *free* evolution operator $U^0(t)$ and take t large and negative, then $U^0(t)|\phi\rangle$ will look very like some actual scattering orbit. Now, the free evolution operator spreads *all* states; in particular, it will take no notice of the fact that $|\phi\rangle$ is an eigenstate of the full Hamiltonian $H^0 + V$. Thus, at the times in question (t large and negative) $U^0(t)|\phi\rangle$ does indeed represent the free motion of a particle far from the potential; and as such is a legitimate in asymptote. It is for this reason that all vectors in $\mathcal{H}$ can represent *in* or *out* asymptote.

A.3 The Scattering Operator

So far we have expressed the actual scattering state at $t = 0$ in terms of either of its two asymptotes. Our ultimate goal is to express the *out* asymptote in terms

of the *in* asymptote without reference to the experimentally uninteresting actual orbit. Since Ω_- is isometric, the relation $|\psi\rangle = \Omega_-|\psi_{out}\rangle$ can be inverted. In fact, since $\Omega_-^\dagger \Omega_- = 1$, we simply multiply on the left by $\Omega_-^\dagger$ to give

$$|\psi_{out}\rangle = \Omega_-^\dagger|\psi\rangle = \Omega_-^\dagger \Omega_+|\psi_{in}\rangle \tag{A.9}$$

If we define the scattering operator as

$$S = \Omega_-^\dagger \Omega_+ \tag{A.10}$$

this equation becomes

$$|\psi_{out}\rangle = S|\psi_{in}\rangle \tag{A.11}$$

which is the desired result. The scattering operator S gives $|\psi_{out}\rangle$ directly in terms of $|\psi_{in}\rangle$. Since only the asymptotic free motion is observed in practice, the single operator S contains all information of experimental interest. The probability that a particle that entered the collision with *in* asymptote $|\psi_{in}\rangle = |\phi\rangle$ will be observed to emerge with *out* asymptote $|\psi_{out}\rangle = |\chi\rangle$ is given by

$$w(\chi \leftarrow \phi) = |\langle\chi|\Omega_-^\dagger \Omega_+|\phi\rangle|^2 = |\langle\chi|S|\phi\rangle|^2 \tag{A.12}$$

The probability amplitude for the process $(\chi \leftarrow \phi)$ is just the $S-$matrix element $\langle\chi|S|\phi\rangle$.

In practice even the quantity $w(\chi \leftarrow \phi)$ is not directly observable; this is because one can not actually produce or identify uniquely defined wave packets $|\phi\rangle$ and $|\chi\rangle$ (even tough in principle they can). However, the quantity that is experimentally observable, the differential cross-section, can be expressed directly in terms of the matrix elements of S. In practice, concerning the initial state $|\phi\rangle$ we know only that it is a wave packet whose position and momentum are both reasonably well defined. Concerning the final state, we measure only wether or not the outgoing direction of motion lies in some element of solid angle $d\Omega$. The nature of the measurement on the outgoing particle is easily allowed for, instead of $w(\chi \leftarrow \phi)$ we have only to calculate the probability $w(d\Omega \leftarrow \phi)$ that the direction of motion of the *out* state lie inside the element of solid angle $d\Omega$. Our ignorance of the precise *in* asymptote $|\phi\rangle$ means that we must then average this probability over all relevant states $|\phi\rangle$. It is this averaging process that leads to the notion of the differential cross section.

Before we calculate the cross section, it is convenient to establish two important properties of the S operator, conservation of energy and the decomposition of S in terms of the scattering amplitude.

A.4 Conservation of Energy

One of the most important properties of the S operator is that it conserves the energy. Because the Hamiltonian H is independent of time, energy is, of course, conserved, and the expectation value of H for any actual orbit is constant. However, the S operator is mapping of the asymptotic free orbits, which label

the particle's state only when it is far away from the scatterer and does not feel the potential. As far as the asymptotic states are concerned, the actual energy is simply the kinetic energy and we need therefore to prove that S commutes with the kinetic energy operator H^0. The essential step in the proof is the so-called intertwining relation for the Møller operators

$$H\Omega_{\pm} = \Omega_{\pm} H^0 \tag{A.13}$$

Which can be proved by the following manipulation ($\hbar = 1$)

$$\begin{aligned} e^{iH\tau}\Omega_{\pm} &= e^{iH\tau}[\lim_{t\to\mp\infty} e^{iHt}e^{-iH^0t}] \\ &= \lim_{t\to\mp\infty}[e^{iH(\tau+t)}e^{-iH^0t}] \\ &= \lim_{t\to\mp\infty}[e^{iH(\tau+t)}e^{-iH^0(\tau+t)}]e^{iH^0\tau} \\ &= \Omega_{\pm}e^{iH^0\tau} \end{aligned} \tag{A.14}$$

Differentiating with respect to τ and setting $\tau = 0$, we obtain the desired result. Now we have

$$SH^0 = \Omega_-^{\dagger}\Omega_+ H^0 = \Omega_-^{\dagger} H\Omega_+ = H^0\Omega_-^{\dagger}\Omega_+ = H^0 S \tag{A.15}$$

It is convenient to write the matrix elements of S in the momentum representation. We often refer to $\{\langle \mathbf{p}'|S|\mathbf{p}\rangle\}$ as the S matrix. The physical significance of the improper matrix elements $\langle \mathbf{p}'|S|\mathbf{p}\rangle$ is in the corresponding expansion of the *out* wave function $\psi_{out}(\mathbf{p})$ in terms of $\psi_{in}(\mathbf{p})$,

$$\psi_{out}(\mathbf{p}) = \int d^3p' \langle \mathbf{p}|S|\mathbf{p}'\rangle \psi_{in}(\mathbf{p}') \tag{A.16}$$

So it is convenient to visualize $\langle \mathbf{p}'|S|\mathbf{p}\rangle$ as the probability amplitude that an *in* state of momentum $\mathbf{p}$ lead to an *out* state of momentum $\mathbf{p}'$.

Since S commutes with H^0, its momentum-space matrix elements satisfy

$$0 = \langle \mathbf{p}'|[H^0, S]|\mathbf{p}\rangle = (E_{p'} - E_p)\langle \mathbf{p}'|S|\mathbf{p}\rangle \tag{A.17}$$

This implies that $\langle \mathbf{p}'|S|\mathbf{p}\rangle$ is zero except when $E_{p'} = E_p$ and hence it has the form

$$\langle \mathbf{p}'|S|\mathbf{p}\rangle = \delta(E_{p'} - E_p) \times \text{remainder} \tag{A.18}$$

To explore further the structure of the momentum-space S matrix it is convenient to write it as

$$\langle \mathbf{p}'|S|\mathbf{p}\rangle = \delta_3(\mathbf{p}' - \mathbf{p}) + \frac{i}{2\pi\mu}\delta(E_{p'} - E_p) f(\mathbf{p}' \leftarrow \mathbf{p}) \tag{A.19}$$

here $f(\mathbf{p}' \leftarrow \mathbf{p})$ is called the scattering amplitude. The significance of the two terms in this decomposition of the S matrix is easily understood. The first term, $\delta_3(\mathbf{p}' - \mathbf{p})$ is obviously the amplitude for the particle to pass the force center

without being scattered. The second is therefore the amplitude that it actually is scattered. When the particle is scattered its momentum changes, while its energy stays the same. Thus the second term should conserve energy, but not the individual components of momenta.

Replacing $\langle p|S|p'\rangle$ in (A.16) by its decomposition (A.19) one obtains

$$\psi_{out}(\mathbf{p}) = \psi_{in}(\mathbf{p}) + \frac{i}{2\pi\mu}\int d^3p'\delta(E_p - E_{p'})f(\mathbf{p} \leftarrow \mathbf{p}')\psi_{in}(\mathbf{p}') \tag{A.20}$$

Here the first term is the unscattered wave and second the scattered wave.

A.5 Scattering of two spinless particles

The quantum scattering of two distinct spinless particles, can be reduced to the scattering of a single spinless particle with a fixed target.

The states of the two particles system are represented by function $\psi(\mathbf{x}_1, \mathbf{x}_2)$ depending on the positions $\mathbf{x}_1$ and $\mathbf{x}_2$ of the two particles. The vector $|\psi\rangle$ belongs to the two-particle Hilbert space $\mathcal{H}$, which can be written as

$$\mathcal{H} = \mathcal{H}_1 \otimes \mathcal{H}_2 \tag{A.21}$$

where $\mathcal{H}_1$ and $\mathcal{H}_2$ are the one-particle space of the first particle and the second, respectively. The space $\mathcal{H}$ can be spanned by product vectors; that is, every vector can be expressed as a sum of product vectors like $|\phi_1\rangle \otimes |\phi_2\rangle$. Here $|\phi_1\rangle$ is in the one-particle space $\mathcal{H}_1$ and $|\phi_2\rangle$ is in space $\mathcal{H}_2$. Two important properties of product vectors are: first, if $\{|n_1\rangle\}$ and $\{|n_2\rangle\}$ are orthonormal bases of the one-particle spaces $\mathcal{H}_1$ and $\mathcal{H}_2$, then the products, $|n_1\rangle \otimes |n_2\rangle$ form an orthonormal basis of the two-particle space $\mathcal{H}$. Second, the scaler products satisfy

$$(\langle\phi_1'| \otimes \langle\phi_2'|)(|\phi_1\rangle \otimes |\phi_2\rangle) = \langle\phi_1'|\phi_1\rangle\langle\phi_2'|\phi_2\rangle \tag{A.22}$$

Similar to vectors, for any operators A_1 and A_2, acting on $\mathcal{H}_1$ and $\mathcal{H}_2$ respectively, we can define an operator $(A_1 \otimes A_2)$ acting on $\mathcal{H}$ by the relation

$$(A_1 \otimes A_2)(|\phi_1\rangle \otimes |\phi_2\rangle) = (A_1|\phi_1\rangle) \otimes (A_2|\phi_2\rangle) \tag{A.23}$$

In particular, the basic dynamical variables of a two particles system are all operators of the form $A_1 \otimes 1$ or $1 \otimes A_2$.

It is usually unnecessary to distinguish $A_1 \otimes 1$ from A_1 and we shall write just A_1 for either, similarly $1 \otimes A_2$ will be abbreviated to A_2, and hence $A_1 \otimes A_2$ which is the same as $(A_1 \otimes 1)(1 \otimes A_2)$, to A_1A_2.

The two particle Hamiltonian will be of the form

$$H = \frac{\mathbf{p}_1^2}{2m_1} + \frac{\mathbf{p}_2^2}{2m_2} + V(\mathbf{x}) \tag{A.24}$$

where V is a function of the relative coordinate $\mathbf{x}_1 - \mathbf{x}_2 = \mathbf{x}$ only (we have assumed a local and translationally invariant interaction), and the momentum

operators defined as follows

$$\begin{aligned} \mathbf{p}_1 &= \mathbf{p}_1(\text{on} \quad \mathcal{H}_1) \otimes 1(\text{on} \quad \mathcal{H}_2) \\ \mathbf{p}_2 &= 1(\text{on} \quad \mathcal{H}_1) \otimes \mathbf{p}_2(\text{on} \quad \mathcal{H}_2) \end{aligned} \tag{A.25}$$

For any purposes, it is convenient to use center of mass and relative coordinates, defined by

$$\begin{aligned} \mathbf{X} &= \frac{m_1\mathbf{x}_1 + m_2\mathbf{x}_2}{m_1 + m_2} \quad (\text{on} \quad \mathcal{H}_{CM}) \\ \mathbf{x} &= \mathbf{x}_1 - \mathbf{x}_1 \quad (\text{on} \quad \mathcal{H}_{rel}) \end{aligned} \tag{A.26}$$

The two-particles Hilbert space $\mathcal{H}$ can be defined as

$$\mathcal{H} = \mathcal{H}_{CM} \otimes \mathcal{H}_{rel}. \tag{A.27}$$

By defining the total and relative momenta as

$$\begin{aligned} \mathbf{P} &= \mathbf{p}_1 + \mathbf{p}_2 \quad (\text{on} \quad \mathcal{H}_{CM}) \\ \mathbf{p} &= \frac{m_1\mathbf{p}_1 + m_2\mathbf{p}_2}{m_1 + m_2} \quad (\text{on} \quad \mathcal{H}_{rel}) \end{aligned} \tag{A.28}$$

(which are, of course, the momenta conjugate to the CM and relative position operators), the Hamiltonian reads

$$\begin{aligned} H &= \frac{\mathbf{P}^2}{2M} + \left[\frac{\mathbf{p}^2}{2\mu} + V(\mathbf{x})\right] \\ &\equiv H_{CM} + H_{rel} \end{aligned} \tag{A.29}$$

Where $M = m_1 + m_2$ and $\mu = m_1 m_2 / m_1 + m_2$ are the total and reduced masses respectively. Since H_{CM} and H_{rel} act on different spaces, they commute, and so the evolution operator can be factored as follows

$$\begin{aligned} U(t) = e^{-iHt} &= e^{-i(H_{CM}+H_{rel})t} \\ &= e^{-iH_{CM}t} e^{-iH_{rel}} \\ &= e^{-iH_{CM}t} \otimes e^{-iH_{rel}t} \end{aligned} \tag{A.30}$$

Here the last expression serves to emphasize that $U(t)$ is a product of two evolution operators, one for H_{CM} and the other for H_{rel}. This result means that the motion of the center of mass and the relative coordinates are independent, and the two-particle scattering problem, reduces to two single-particle scattering problems. In particular, since H_{CM} is just $\mathbf{P}^2/2M$, the center of mass moves like a free particle of mass M. H_{rel} describes the scattering of a single-particle of mass μ, off a fixed potential V.

The free evolution operator can also be factored in the same way,

$$U^0(t) \equiv e^{-iH^0 t} = e^{-iH_{CM}t} \otimes e^{-iH^0_{rel}t} \tag{A.31}$$

of course $U^0(t)$ can also be factored as

$$U^0(t) = exp(-i\frac{\mathbf{p}_1^2}{2m_1}t) \otimes exp(-i\frac{\mathbf{p}_2^2}{2m_2}t) \tag{A.32}$$

corresponding to the factoring of H as $H_1 \otimes H_2$. This second result expresses the obvious fact that two noninteracting particles move independently. The same result obviously does not hold for the full evolution operator $U(t)$.

The general orbit of our two-particle system is $U(t)|\psi\rangle$ where $|\psi\rangle$ is any vector in the two-particle space $\mathcal{H}$. Just as in the one-particle case we expect there to be certain scattering orbits for which the two particles move far apart as $t \to \mp\infty$ and $U(t)|\psi\rangle$ behaves like some freely moving $U^0(t)|\psi_{in/out}\rangle$. The actual orbit is given by

$$|\psi\rangle = \mathbf{\Omega}_+|\psi_{in}\rangle = \mathbf{\Omega}_-|\psi_{out}\rangle \tag{A.33}$$

where

$$\mathbf{\Omega}_\pm \equiv \lim_{t\to\mp\infty} U(t)^\dagger U^0(t) = (1 \otimes \Omega_\pm) \tag{A.34}$$

The single-particle Møller operators $\Omega_\pm$ act on $\mathcal{H}_{rel} = \mathcal{L}^2(\mathcal{R}^3)$ and are given by

$$\Omega_\pm = \lim_{t\to\mp\infty} e^{iH_{rel}t}e^{-iH^0_{rel}t} \tag{A.35}$$

The factor 1_{CM} in $\mathbf{\Omega}_\pm$ reflects the fact that the center of mass moves like a free particle and is not scattered.

The two-particle operator $\mathbf{S}$ which maps any $|\psi_{in}\rangle$ in $\mathcal{H}$ onto the corresponding $|\psi_{out}\rangle = \mathbf{S}|\psi_{in}\rangle$, simply is given by

$$\mathbf{S} = \mathbf{\Omega}_-^\dagger \mathbf{\Omega}_+ = 1_{CM} \otimes S \tag{A.36}$$

the single-particle operator, $S = \Omega_-^\dagger \Omega_+$, acts on $\mathcal{H}_{rel}$ and can be computed from the Hamiltonian H_{rel}.

A.5.1 Conservation of energy-momentum and the scattering amplitudes

From the expression $\mathbf{S} = 1_{CM} \otimes S$ it is immediately clear that $\mathbf{S}$ commutes with $\mathbf{P}$ (which acts only on $\mathcal{H}_{CM}$), and hence, the total momentum is conserved. Just as in the one-particle case, $\mathbf{S}$ commutes with H^0 and energy is conserved. From conservation of energy and momentum it follows that the matrix elements,

$$\langle \mathbf{p}_1', \mathbf{p}_2'|\mathbf{S}|\mathbf{p}_1, \mathbf{p}_2\rangle$$

contain the factors

$$\delta(E_1' + E_2' - E_1 - E_2)\delta_3(\mathbf{p}_1' + \mathbf{p}_2' - \mathbf{p}_1 - \mathbf{p}_2)$$

where $E_1 = \mathbf{p}_1^2/2m_1$ and so on. As before it is convenient to decompose this matrix element in terms of scattering amplitudes f

$$\langle \mathbf{p}_1', \mathbf{p}_2' | \mathbf{S} | \mathbf{p}_1, \mathbf{p}_2 \rangle = \delta_3(\mathbf{p}_1' - \mathbf{p}_1)\delta_3(\mathbf{p}_2' - \mathbf{p}_2) + \frac{i}{2\pi\mu}\delta(\sum E_i' - \sum E_i)\delta_3(\sum \mathbf{p}_i' - \sum \mathbf{p}_i) f(\mathbf{p}' \leftarrow \mathbf{p}) \quad \text{(A.37)}$$

The first term is the amplitude that each particle passes through unscattered; the second is the amplitude that the two particles actually scatter. The later conserves total energy and total momentum but not, of course the individual components of the relative momentum.

A.6 Invariance Principles and Conservation Laws

In this section we shall discuss the application of invariance principles to the scattering theory. We shall find that invariance of the system under any of the possible symmetry operations (rotation, parity, time reversal, etc.) implies sever restrictions on the possible form of the scattering amplitude.

A.6.1 Translational invariance and conservation of momentum

The effect of a rigid translation through a vector $\mathbf{a}$ on any system is given by the unitary translation operator

$$D(\mathbf{a}) = e^{-i\mathbf{a}\cdot\mathbf{P}} \quad \text{(A.38)}$$

where $\mathbf{P}$ is the total momentum operator of the system. This means simply that if the system occupies any state $|\psi\rangle$ and is then rigidly displaced through $\mathbf{a}$, then the resulting state is $D(\mathbf{a})|\psi\rangle$.

Coming back to our two-particle system with Hamiltonian $H = H^0 + V$, we know that H^0 automatically commutes with $D(\mathbf{a})$. Thus, if the system is translationally invariant, the translation operators $D(\mathbf{a})$ commutes with both H and H^0, and from this it follows that they commute with the Møller operators $\mathbf{\Omega}_\pm$, as well as with the scattering operator $\mathbf{S}$. Since $\mathbf{S}$ commutes with $D(\mathbf{a})$ for any $\mathbf{a}$, it must commute with $\mathbf{P}$, the total momentum, $[\mathbf{P}, \mathbf{S}] = 0$. In particular if we take momentum-space matrix elements of this equation we find that the momentum-space matrix element of $\mathbf{S}$ is zero unless the initial and final total momenta are equal, that is the total momentum is conserved.

A.6.2 Rotational invariance and the conservation of the angular momentum

The effect of any rotation on a quantum mechanic system through an angle α clockwise about the direction $\widehat{u}$ is given by the unitary rotation operator

$$R(\alpha, \widehat{\mathbf{u}}) = e^{-i\alpha\widehat{\mathbf{u}}\cdot\mathbf{J}} \quad \text{(A.39)}$$

where $\mathbf{J}$ is the total angular momentum operator.

Using the same arguments as above for our two-particle system and assume rotational invariance, we can show that $R(\alpha, \widehat{\mathbf{u}})$ commutes with $\mathbf{\Omega}_{\pm}$ and $\mathbf{S}$ which results in the conservation of total angular momentum $\mathbf{J}$. For two particles total angular momentum is

$$\begin{aligned}\mathbf{J} &= \mathbf{J}_1 + \mathbf{J}_2 \\ &= \mathbf{X} \times \mathbf{P} + \mathbf{J}_{int}\end{aligned} \tag{A.40}$$

Here the operator $\mathbf{X} \times \mathbf{P}$ is the angular momentum of the center of mass and acts only on the space $\mathcal{H}_{CM}$ of CM motion; while $\mathbf{J}_{int}$ is the internal angular momentum and acts only on the relative space $\mathcal{H}_{rel}$. Clearly $\mathbf{S} = 1 \otimes S$ commutes with the total angular momentum $\mathbf{J}$ if and only if S commutes with the internal angular momentum $\mathbf{J}_{int}$.

In the special case where both particles are spinless, the angular momentum $\mathbf{J}_{int}$ is simply $\mathbf{L}$ (the relative orbital angular momentum of the two particles). In this case the rotationally invariance requires simply that V be spherically symmetric; that is, a function of r only, $V(\mathbf{x}) = V(r)$. If V is spherically symmetric, then S commutes with all rotations R and we have

$$S = R^{\dagger} S R \tag{A.41}$$

Taking momentum-space matrix elements of this equation we find

$$\langle \mathbf{p}' | S | \mathbf{p} \rangle = \langle \mathbf{p}'_R | S | \mathbf{p}_R \rangle \tag{A.42}$$

where $\mathbf{p}_R$ denotes the momentum obtained from $\mathbf{p}$ by the rotation R. From this we fined the same result for the scattering amplitude f

$$f(\mathbf{p}' \leftarrow \mathbf{p}) = f(\mathbf{p}'_R \leftarrow \mathbf{p}_R) \tag{A.43}$$

This result means that the amplitude $f(\mathbf{p}' \leftarrow \mathbf{p})$, which is *a priori* a function of five variables, $\mathbf{p}$ and the direction of $\mathbf{p}'$ (recall that $|\mathbf{p}'| = |\mathbf{p}|$), is in fact only a function of two variables, which we take to be the energy E_p and the scattering angle θ between $\mathbf{p}$ and $\mathbf{p}'$

$$f(\mathbf{p}' \leftarrow \mathbf{p}) = f(E_p, \theta) \tag{A.44}$$

For a single spinless particle (or equivalently for relative motion of two spinless particles), the three operators H^0, L^2, and L_z form a complete set of commuting observables. We will denote the *spherical wave* basis vectors of this representation by $|E, l, m\rangle$ where E, $l(l+1)$, and m are the eigenvalues of H^0, L^2, and L_z respectively. The corresponding spatial wave functions $\langle \mathbf{x} | E, l, m \rangle$ are products of the spherical harmonics $Y_l^m(\theta, \varphi)$ and functions of r. If we write these products in the form $(1/r)u(r)Y_l^m(\theta, \varphi)$, then the radial wave function $u(r)$ satisfies the free radial Schrödinger equation

$$\left[\frac{d^2}{dr^2} - \frac{l(l+1)}{r^2} + p^2 \right] u(r) = 0 \tag{A.45}$$

This is an ordinary, second-order, linear, differential equation and so has two linearly independent solutions, of which the physically relevant solution is that which vanishes at the origin. As $r \to 0$, the centrifugal term $l(l+1)/r^2$ dominates the energy term $\mathbf{p}^2$, and the solutions behave like combination of r^{l+1} and r^{-l}. The physically acceptable wave function is the Riccati-Bessel function

$$\widehat{j}_l(z) = z j_l(z)$$

where $j_l(z)$ is the Spherical Bessel function. A convenient choice for the second solution is the Riccati-Neumann function

$$\widehat{n}_l(z) = z n_l(z)$$

where $n_l(z)$ is the spherical Bessel function of the second kind. Now the spatial wave functions look like

$$\langle \mathbf{x}|E,l,m\rangle = i^l (\frac{2\mu}{\pi p})^{1/2} \frac{1}{r} \widehat{j}_l(pr) Y_l^m(\theta,\varphi) \qquad [p \equiv (2\mu E)^{1/2}] \tag{A.46}$$

The normalization is

$$\langle E',l',m'|E,l,m\rangle = \delta(E'-E)\delta_{l'l}\delta_{m'm}. \tag{A.47}$$

Because S commutes with H^0 and L, the S matrix in this representation is diagonal and has the form

$$\langle E',l',m'|S|E,l,m\rangle = \delta(E'-E)\delta_{l'l}\delta_{m'm} s_l(E). \tag{A.48}$$

Here the number $s_l(E)$ is the eigenvalue of S corresponding to the eigenvector $|E,l,m\rangle$, and is actually independent of m (for a prove see Ref. [1] section 6.c).

Since S is unitary, each of its eigenvalue has modulus 1 and can be written as the exponent of a purely imaging number

$$s_l(E) = e^{2i\delta_l(E)} \tag{A.49}$$

where $\delta_l(E)$ is just the conventional phase shift, up to addition of an arbitrary multiple of π.

Using the transformation matrix

$$\langle \mathbf{p}|E,l,m\rangle = (\mu p)^{-1/2} \delta(E_p - E) Y_l^m(\widehat{\mathbf{p}}) \quad \text{with} \quad E_p = \mathbf{p}^2/2\mu \tag{A.50}$$

one can pass from the angular-momentum to the momentum basis. In particular, from (A.19) we find

$$\begin{aligned} \frac{i}{2\pi\mu}\delta(E_{p'}-E_p) f(\mathbf{p}' \leftarrow \mathbf{p}) &= \langle \mathbf{p}'|(S-1)|\mathbf{p}\rangle \\ &= \int dE \sum_{l,m} \langle \mathbf{p}'|(S-1)|E,l,m\rangle\langle E,l,m|\mathbf{p}\rangle \end{aligned} \tag{A.51}$$

Now, $|E,l,m\rangle$ is an eigenvector of $(S-1)$, which can therefore be replaced by the corresponding eigenvalue (s_l-1)

$$= \int dE \sum_{l,m} [s_l(E_p)-1] \langle \mathbf{p}'|E,l,m\rangle\langle E,l,m|\mathbf{p}\rangle$$
$$= \frac{1}{\mu p}\delta(E_{p'}-E_p)\sum_{l,m}[s_l(E_p)-1]Y_l^m(\widehat{\mathbf{p}}')Y_l^m(\widehat{\mathbf{p}})^* \tag{A.52}$$

Now we find for the amplitude $f(\mathbf{p}' \leftarrow \mathbf{p})$ that

$$f(E_p,\theta) \equiv f(\mathbf{p}' \leftarrow \mathbf{p}) = \sum_{l=0}^{\infty}(2l+1)f_l(E)P_l(\cos\theta) \tag{A.53}$$

where $f_l(E)$ is the partial-wave amplitude,

$$f_l(E) = \frac{s_l(E)-1}{2ip} = \frac{e^{i\delta_l(E)}\sin\delta_l(E)}{p} \tag{A.54}$$

and

$$P_l(\cos\theta) = \left(\frac{4\pi}{2l+1}\right)^{1/2} Y_l^0(\theta,\varphi) \tag{A.55}$$

is the Legendre polynomial. The expansion (A.53) is the so-called partial-wave expansion for the *full* amplitude $f(E,\theta)$ in terms of the partial-wave amplitude $f_l(E)$. It can of course be inverted. Using the well-known orthogonality of the Legendre polynomials we find

$$f_l(E) = \frac{1}{2}\int_{-1}^{1} d(\cos\theta) f(E,\theta)P_l(\cos\theta) \tag{A.56}$$

A.6.3 Parity

In addition to rotational invariance, many systems satisfy invariance under parity. Parity is defined as a reversal of the three spatial axes. More precisely, the parity operator P changes the signs of all positions and momenta but leaves all angular momenta (and the nature of the system itself) unchanged. Here the system of interest contains two spinless particles, for which (as was the case with rotations) we need only consider the space of the relative motion. For the wave function we have

$$\langle \mathbf{x}|P|\psi\rangle = \psi_P(\mathbf{x}) = \eta\psi(-\mathbf{x}) \tag{A.57}$$

and likewise for the momentum-space wave function. Here η is an arbitrary number of modulus one.

The dynamics are invariant under parity if and only if P commutes with H; or equivalently , $V(\mathbf{x}) = V(-\mathbf{x})$. This condition is automatically satisfied if $V(\mathbf{x})$ is spherically symmetric. It follows exactly as in our discussion of rotations

that invariance under parity implies that P commutes with S, and hence, that $S = P^\dagger SP$. If $|\phi\rangle$ and $|\phi'\rangle$ are two states of definite parity,

$$P|\phi\rangle = p|\phi\rangle \quad \text{and} \quad P|\phi'\rangle = p'|\phi'\rangle \tag{A.58}$$

then $\langle\phi'|S|\phi\rangle = 0$ unless $p = p'$; that is, parity is conserved. More generally, for any initial and final states $\langle\phi'|S|\phi\rangle = \langle\phi'_p|S|\phi_p\rangle$. In particular $\langle \mathbf{p}'|S|\mathbf{p}\rangle = \langle$-$\mathbf{p}'|S|-\mathbf{p}\rangle$ and, hence, for the amplitude we have the very natural result

$$f(\mathbf{p}' \leftarrow \mathbf{p}) = f(-\mathbf{p}' \leftarrow -\mathbf{p}) \tag{A.59}$$

A.6.4 Time reversal

So far we have discussed three types of symmetry operations, all of which are represented by unitary operators. We now discuss a symmetry that is not given by a unitary operator: time reversal. The time reversal operator T, is defined to change the sign of the momenta and spins of all particles but to leave their position unchanged.

The time reversal operator, T, is anti-unitary, that is T is a one-to-one map of $\mathcal{H}$ onto $\mathcal{H}$ that is norm-preserving and anti-linear such that

$$T(a|\psi\rangle + b|\phi\rangle) = a^*T|\psi\rangle + b^*T|\phi\rangle. \tag{A.60}$$

This differs from the definition of a unitary operator only in that T is anti-linear. The adjoint of the anti-linear operator T is defined by the relation

$$\langle\phi|(T|\psi\rangle) = \langle T^\dagger\phi|\psi\rangle^* \tag{A.61}$$

Using this definition one can show that

$$T^\dagger T = TT^\dagger = 1 \tag{A.62}$$

For a single spinless particle after suitable adjustment of the arbitrary overall phase of T, we will have

$$\begin{aligned} T|\mathbf{x}\rangle &= T^\dagger|\mathbf{x}\rangle = |\mathbf{x}\rangle \\ T|\mathbf{p}\rangle &= T^\dagger|\mathbf{p}\rangle = |-\mathbf{p}\rangle \end{aligned} \tag{A.63}$$

If we expand any $|\psi\rangle$ as

$$|\psi\rangle = \int d^3x\psi(\mathbf{x})|\mathbf{x}\rangle \tag{A.64}$$

we find for $T|\psi\rangle$ that

$$\begin{aligned} \psi_T(\mathbf{x}) \equiv \langle\mathbf{x}|T|\psi\rangle &= \langle T^\dagger\mathbf{x}|\psi\rangle^* \\ &= \langle\mathbf{x}|\psi\rangle^* \\ &= \psi^*(\mathbf{x}) \end{aligned} \tag{A.65}$$

$$\begin{aligned}\psi_T(\mathbf{p}) \equiv \langle \mathbf{p}|T|\psi\rangle &= \langle T^\dagger \mathbf{p}|\psi\rangle^* \\ &= \langle -\mathbf{p}|\psi\rangle^* \\ &= \psi^*(-\mathbf{p})\end{aligned} \tag{A.66}$$

The effect of T on the spatial wave function is simply to replace it by its complex conjugate, while for the momentum-space wave function it should be replaced by its complex conjugate plus a simultaneously change in the sign of $\mathbf{p}$.

Invariance under time reversal means that T commutes with H (and automatically with H^0), $TH = HT$. (For a spinless particle in a local potential, or equivalently the relative motion of two spinless particles, this requires simply that V be real, which it has to be anyway in order that H be Hermitian.) Because T is anti-unitary, this means that

$$Te^{iHt} = e^{-iHt}T \tag{A.67}$$

(The change of sign, arises because $Ti = -iT$.) It follows that

$$\begin{aligned}T\Omega_\pm &= T[\lim_{t\to\mp\infty} e^{iHt}e^{-iH^0t}] \\ &= [\lim_{t\to\mp\infty} e^{-iHt}e^{iH^0t}]T \\ &= \Omega_\mp T\end{aligned} \tag{A.68}$$

or since $T^\dagger T = 1$,

$$\Omega_\pm = T^\dagger \Omega_\mp T \tag{A.69}$$

Thus, the effect of T on the Møller operators is to interchange Ω_+ and Ω_-.

From (A.68) it follows that

$$TS = T\Omega_-^\dagger \Omega_+ = \Omega_+^\dagger T\Omega_+ = \Omega_+^\dagger \Omega_- T = S^\dagger T \tag{A.70}$$

or

$$S = T^\dagger S^\dagger T \tag{A.71}$$

Taking matrix elements of this equation we find

$$\begin{aligned}\langle \chi|(S|\phi\rangle) &= \langle \chi|(T^\dagger S^\dagger T|\phi\rangle) \\ &= \big(\langle T\chi|(S^\dagger T|\phi\rangle)\big)^* \\ &= \big(\langle \chi_T|S^\dagger|\phi_T\rangle\big)^*\end{aligned} \tag{A.72}$$

or

$$\langle \chi|S|\phi\rangle = \langle \phi_T|S|\chi_T\rangle \tag{A.73}$$

This result shows that, as one would expect, time reversal invariance implies that the probability $W(\chi \leftarrow \phi)$ is the same as the probability $W(\phi_T \leftarrow \chi_T)$ for the process in which initial and final states are time reversed and their roles exchanged.

In particular, for one-particle scattering (or equivalently the relative motion of two-particle scattering), the result (A.73) - when written in the momentum representation - gives

$$\langle \mathbf{p}'|S|\mathbf{p}\rangle = \langle -\mathbf{p}|S|-\mathbf{p}'\rangle \tag{A.74}$$

or equivalently

$$f(\mathbf{p}' \leftarrow \mathbf{p}) = f(-\mathbf{p} \leftarrow -\mathbf{p}') \tag{A.75}$$

for the amplitude.

A.7 Scattering of the Two Particles With Spin

In this section we shall extend our scattering formalism to include particles with spin. In moving from spinless particles to particles with spin we must anticipate two obvious complications. First, the Hilbert space for particles with spin is more complicated, because it must describe spin as well as spatial degrees of freedom. Second, the Hamiltonian may be spin-dependent and contain terms such as the spin-orbit interaction of an electron with a nucleus or the tensor interaction between two nucleons.

The Hilbert space appropriate to single particle of spin s is the tensor product,

$$\mathcal{H} = \mathcal{H}_{space} \otimes \mathcal{H}_{spin} \tag{A.76}$$

where $\mathcal{H}_{space}$ is the space $\mathcal{L}^2(R^3)$ of ordering wave functions and $\mathcal{H}_{spin}$ is the $(2s+1)$-dimensional spin space. As a basis for H_{spin} it is usual to use the eigenvectors $|m\rangle$ of the third component of the spin operator,

$$S_z|m\rangle = m|m\rangle \tag{A.77}$$

A basis for the space $\mathcal{H}$ can be constructed from any bases of $\mathcal{H}_{space}$ and $\mathcal{H}_{spin}$. One convenient basis is given by the eigenvectors of $\mathbf{p}$ and S_z,

$$|\mathbf{p}, m\rangle = |\mathbf{p}\rangle \otimes |m\rangle \tag{A.78}$$

which are products of the momentum eigenvectors $|\mathbf{p}\rangle$ in $\mathcal{H}_{space}$ and the S_z eigenvectors $|m\rangle$ in $\mathcal{H}_{spin}$.

The Hilbert space for two distinct particles with spins s_1, and s_2 is of course the product $\mathcal{H} = \mathcal{H}_1 \otimes \mathcal{H}_2$ of the two one-particle spaces, each of which is itself a product of the type just described. The spatial wave functions have the form $\psi_{m_1 m_2}(\mathbf{x}_1, \mathbf{x}_2)$ and just as in the spinless case it is convenient to rewrite these as functions $\psi_{m_1 m_2}(\mathbf{X}, \mathbf{x})$ of the CM and relative positions, $\mathbf{X}$ and $\mathbf{x}$. Because these can clearly be spanned by products of the form $\phi(\mathbf{X})\chi_{m_1 m_2}(\mathbf{x})$, we can regard the space $\mathcal{H}$ as $\mathcal{H} = \mathcal{H}_{CM} \otimes \mathcal{H}_{rel}$ where $\mathcal{H}_{CM}$ describes the motion of the CM position only, while $\mathcal{H}_{rel}$ describes the relative motion, *including both spins*. The space $\mathcal{H}_{rel}$ can itself be regarded as a product of one space for the relative coordinate $\mathbf{x}$ and another for both spins.

As a basis for the spin space we can use either the eigenvectors $|m_1, m_2\rangle$ of the two z components, or the eigenvectors $|s, m\rangle$ of the total spin and its z component. The relation between these is

$$|s, m\rangle = \sum_{m_1, m_2} |m_1, m_2\rangle\langle s_1 s_2 m_1 m_2 | s m\rangle \tag{A.79}$$

where $\langle s_1 s_2 m_1 m_2 | s m\rangle$ is the usual Clebsh-Gordan coefficient. When we do not wish to commit ourselves to a particular basis we shall use the notation $|\xi\rangle$ to label any convenient choice. In practice, ξ usually stands for either (m_1, m_2) or (s, m), and in any case is a label taking on $(2s_1 + 1)(2s_2 + 1)$ distinct values. The general spin state of the two particles can be expanded as

$$|\chi\rangle = \sum_{\xi} \chi_\xi |\xi\rangle \tag{A.80}$$

and is completely identified by the numbers χ_ξ, which can be grouped into a column spinor χ of $(2s_1 + 1)(2s_2 + 1)$ components.

For any basis $\{|\xi\rangle\}$ of the spin space there are several corresponding bases of the complete space $\mathcal{H}$ and the space of the relative motion $\mathcal{H}_{rel}$. The most important basis of $\mathcal{H}$ consists of the momentum eigenvectors, which we write (without serious danger of confusion) in either of the forms

$$|\mathbf{p}_1, \mathbf{p}_2, \xi\rangle \equiv |\mathbf{P}, \mathbf{p}, \xi\rangle \tag{A.81}$$

where $\mathbf{P}$ and $\mathbf{p}$ are the total and relative momenta as usual. The corresponding basis vectors of $\mathcal{H}_{rel}$ are just $|\mathbf{p}, \xi\rangle$ in terms of which we can write $|\mathbf{P}, \mathbf{p}, \xi\rangle$ as $|\mathbf{P}\rangle \otimes |\mathbf{p}, \xi\rangle$.

A.7.1 The S operator for particles with spin

Apart from the fact that the Hilbert space is a little more complicated than before, we can now set up a scattering formalism exactly as for the spinless case. The orbits have the usual form $U(t)|\psi\rangle$ where $|\psi\rangle$ is any vector in the space $\mathcal{H}$ just described. The evolution operator $U(t)$ is determined by the Hamiltonian

$$H = H^0 + V \tag{A.82}$$

where H^0 is the same as for the spinless case,

$$H^0 = \frac{\mathbf{p}_1^2}{2m_1} + \frac{\mathbf{p}_2^2}{2m_2} = \frac{\mathbf{P}^2}{2M} + \frac{\mathbf{p}^2}{2\mu} \tag{A.83}$$

Typical examples of interaction V would be a nucleon-nucleon interaction of the form

$$V = V_1(r) + \mathbf{S}_1 \cdot \mathbf{S}_2 V_2(r) + \mathbf{S}_1 \cdot \mathbf{x} \mathbf{S}_2 \cdot \mathbf{x} V_3(r) \tag{A.84}$$

(Remember that $\mathbf{x} = \mathbf{x}_1 - \mathbf{x}_2$ and $r = |\mathbf{x}|$) or the spin-orbit interaction of an electron in an atom or nucleon in a nucleus,

$$V = V_1(r) + \mathbf{L} \cdot \mathbf{S} V_2(r) \tag{A.85}$$

In all cases, whether or not V depends on the spins, one expects that V will go to zero as the two particles move apart. Thus, with the potentials (A.84) and (A.85) we expect that the coefficients $V_i(r)$ will go to zero suitably rapidly as $r \to \infty$.

Using the same arguments as in the spinless case one can prove the asymptotic condition, which asserts that every $|\psi_{in}\rangle$ in $\mathcal{H}$ labels the *in* asymptote of some actual orbit $U(t)|\psi\rangle$,

$$U(t)|\psi\rangle \quad \xrightarrow[t \to -\infty]{} \quad U^0(t)|\psi_{in}\rangle \tag{A.86}$$

Exactly as in the spinless case, the asymptotic condition and asymptotic completeness both hold, for all "reasonable" potentials and shall confine attention to these from now on. (As usual this excludes the Coulomb potential.) Thus the Møller operators $\mathbf{\Omega}_{\pm}$ exist as the limits of $U^{\dagger}(t)U^0(t)$ and map each *in* or *out* asymptote $|\psi_{in}\rangle$ or $|\psi_{out}\rangle$ onto the corresponding actual state $|\psi\rangle$ at $t = 0$, here as before we have

$$\begin{aligned} U(t)|\psi\rangle \quad &\xrightarrow[t \to -\infty]{} \quad U^0(t)|\psi_{in}\rangle \\ U(t)|\psi\rangle \quad &\xrightarrow[t \to +\infty]{} \quad U^0(t)|\psi_{out}\rangle \end{aligned} \tag{A.87}$$

The operator $\mathbf{S} = \mathbf{\Omega}^{\dagger}_{-}\mathbf{\Omega}_{+}$ is unitary and maps each $|\psi_{in}\rangle$ directly onto corresponding $|\psi_{out}\rangle$.

Exactly as in the spinless case the S operator has the structure

$$\mathbf{S} = 1_{CM} \otimes S \tag{A.88}$$

where of course, 1_{CM} refers to the motion of the CM position only, while S acts on the space of the relative motion, including both spins. This result can be regarded as reducing the problem of two particles with spin to an equivalent *quasi-one-particle* problem, namely the scattering of a single particle with spin s_1, off a fixed target of spin s_2.

A.7.2 The amplitudes and amplitude matrix

For the same reasons as before $\mathbf{S}$ conserves energy and momentum and its matrix elements can be decomposed into two terms,

$$\begin{aligned} \langle \mathbf{p}_1', \mathbf{p}_2', \xi' | \mathbf{S} | \mathbf{p}_1, \mathbf{p}_2, \xi \rangle &= \delta_3(\mathbf{p}_1' - \mathbf{p}_1)\delta_3(\mathbf{p}_2' - \mathbf{p}_2)\delta_{\xi'\xi} \\ &\quad - \frac{i}{2\pi\mu}\delta(\sum E_i' - \sum E_i)\delta_3(\sum \mathbf{p}_i' - \sum \mathbf{p}_i) f(\mathbf{p}', \xi' \leftarrow \mathbf{p}, \xi) \end{aligned} \tag{A.89}$$

In (A.89) the first term is the amplitude for no scattering and leaves both momenta and spins unchanged. The second conserves energy and total momentum but can in general connect states of different relative momenta and different spins. Just as before, the scattering amplitude is related directly to the operator S of the relative motion; specifically, if we insert (A.88) into (A.89) and

factor out the total-momentum delta function, we find

$$\langle \mathbf{p}', \xi' | S | \mathbf{p}, \xi \rangle = \delta_3(\mathbf{p}' - \mathbf{p})\delta_{\xi'\xi} - \frac{i}{2\pi\mu}\delta(E_{p'} - E_p) f(\mathbf{p}', \xi' \leftarrow \mathbf{p}, \xi) \qquad \text{(A.90)}$$

Exactly as in the spinless case we can calculate the CM cross sections in terms of the amplitude. However, in place of the single differential cross section of the spinless case, we now find an infinite number of differential cross section because the particles can enter the collision in any spin state $|\chi\rangle$ and one can (in principle at least) measure the number of particles emerging into $d\Omega$ with any given spin $|\chi'\rangle$. We consider first the case where the particles enter in one of the basis spin states $|\xi\rangle$ and we count the number emerging into $d\Omega$ in the basis spin state $|\xi'\rangle$. For this case we obtain

$$\frac{d\sigma}{d\Omega}(\mathbf{p}', \xi' \leftarrow \mathbf{p}, \xi) = |f(\mathbf{p}', \xi' \leftarrow \mathbf{p}, \xi)|^2 \qquad \text{(A.91)}$$

which is the CM differential cross section for observation of the final particles in the direction of $\mathbf{p}'$ with spin given by $|\xi'\rangle$ if the initial particles had relative momentum $\mathbf{p}$ and spin $|\xi\rangle$.

The cross section for observing an arbitrary final spin state $|\chi'\rangle$ coming from any initial spin state $|\chi\rangle$ can be evaluated in the same way. If

$$|\chi\rangle = \sum_{\xi} \chi_\xi |\xi\rangle \qquad \text{(A.92)}$$

and similarly $|\chi'\rangle$, we can calculate the relevant S-matrix element from (A.89) and, hence, the corresponding CM cross section, which is easily seen to be

$$\frac{d\sigma}{d\Omega}(\mathbf{p}', \chi' \leftarrow \mathbf{p}, \chi) = |\sum_{\xi', \xi} {\chi'_{\xi'}}^* f(\mathbf{p}', \xi' \leftarrow \mathbf{p}, \xi)\chi_\xi|^2 \qquad \text{(A.93)}$$

This result expresses the cross section for arbitrary spins ($|\chi'\rangle \leftarrow |\chi\rangle$) in terms of the amplitude for the $[(2s_1 + 1)(2s_2 + 1)]^2$ basis processes ($|\xi'\rangle \leftarrow |\xi\rangle$). Its form suggests that we rewrite the basic amplitudes as

$$f(\mathbf{p}', \xi' \leftarrow \mathbf{p}, \xi) = f_{\xi'\xi}(\mathbf{p}' \leftarrow \mathbf{p}) \qquad \text{(A.94)}$$

and then regard them as the elements of an *amplitude matrix*

$$F(\mathbf{p}' \leftarrow \mathbf{p}) = \{f_{\xi'\xi}(\mathbf{p}' \leftarrow \mathbf{p})\} \qquad \text{(A.95)}$$

Our result can then be written in the compact form

$$\frac{d\sigma}{d\Omega}(\mathbf{p}', \chi' \leftarrow \mathbf{p}, \chi) = |\chi'^\dagger F(\mathbf{p}' \leftarrow \mathbf{p})\chi|^2 \qquad \text{(A.96)}$$

from this it is clear that all information relevant to the scattering of the two particles is contained in the matrix $F(\mathbf{p}' \leftarrow \mathbf{p})$, just as, in the spinless case, all information was contained in the single amplitude $f(\mathbf{p}' \leftarrow \mathbf{p})$.

As a simple example, let's consider a spin-half particle scattering off a spinless target. This example includes such important processes as the scattering of electrons off a spin-zero atom, of nucleons off a spinless nucleus, and a number of elementary particle processes, of which the most important is pion-nucleon scattering. Because one particle is spinless, the spin space of the whole system is just the two-dimensional spin space of the spin-half projectile. We use the usual S_z basis with basis vectors $|+\rangle$ and $|-\rangle$ corresponding to the eigenvalues $m = \pm 1/2$. According to (A.96), the scattering is determined by a (2×2) amplitude matrix

$$F(\mathbf{p}' \leftarrow \mathbf{p}) = \begin{pmatrix} f_{++}(\mathbf{p}' \leftarrow \mathbf{p}) & f_{+-}(\mathbf{p}' \leftarrow \mathbf{p}) \\ f_{-+}(\mathbf{p}' \leftarrow \mathbf{p}) & f_{--}(\mathbf{p}' \leftarrow \mathbf{p}) \end{pmatrix} \tag{A.97}$$

The element $f_{m'm}(\mathbf{p}' \leftarrow \mathbf{p})$ is the amplitude for an initial particle with momentum $\mathbf{p}$ and z component of spin m to be scattered into the direction $\mathbf{p}'$ and observed with z component of spin m'. (For obvious reasons f_{+-} and f_{-+} are referred to as spin-flip amplitudes and f_{++} and f_{--} as spin-nonflip amplitudes.) The most general initial and final spin states are given by two component spinors χ and χ' and, according to (A.96), the amplitude for observing the corresponding process $(\mathbf{p}', \chi' \leftarrow \mathbf{p}, \chi)$ is just the number $\chi'^{\dagger} F(\mathbf{p}' \leftarrow \mathbf{p})\chi$.

A.7.3 The In and Out spinors

In this section we give a useful alternative interpretation of the amplitude matrix $F(\mathbf{p}' \leftarrow \mathbf{p})$. To this end we consider particles incident in some definite spin state, which we now label by the normalized spinor χ^{in}; and in terms of χ^{in} we define a second spinor,

$$\chi^{out} = F(\mathbf{p}' \leftarrow \mathbf{p})\chi^{in} \tag{A.98}$$

What we shall show is that χ^{out} is precisely the actual (unnormalized) spinor of those particles which emerge with momentum $\mathbf{p}'$ if the initial momentum and spins were $\mathbf{p}$ and χ^{in}. To see this we focus attention on those particles emerging with momentum $\mathbf{p}'$. The result (A.96) for the cross section $(\mathbf{p}', \chi' \leftarrow \mathbf{p}, \chi^{in})$ can be rewritten as

$$\begin{aligned} \frac{d\sigma}{d\Omega}(\mathbf{p}', \chi' \leftarrow \mathbf{p}, \chi^{in}) &= |\chi'^{\dagger} F(\mathbf{p}' \leftarrow \mathbf{p})\chi^{in}|^2 \\ &= |\chi'^{\dagger}\chi^{out}|^2 \end{aligned} \tag{A.99}$$

which shows that the probability of those particles emerging in the direction $\mathbf{p}'$ being found with spins χ' is proportional to $|\chi'^{\dagger}\chi^{out}|^2$, for any χ'. But according to the elementary principles of quantum mechanics this means simply that χ^{out} is the actual spin state of these particles.

The spinor χ^{out} is not normalized; on the contrary,

$$\begin{aligned} \|\chi^{out}\|^2 = \sum_{\xi'} |\chi^{out}_{\xi'}|^2 &= \sum_{\xi'} |\sum_{\xi} f_{\xi'\xi}(\mathbf{p}' \leftarrow \mathbf{p})\chi^{in}_{\xi}|^2 \\ &= \sum_{\xi'} \frac{d\sigma}{d\Omega}(\mathbf{p}', \xi' \leftarrow \mathbf{p}, \chi^{in}) \end{aligned} \tag{A.100}$$

This sum will be recognized as the cross section $(\mathbf{p}' \leftarrow \mathbf{p}, \chi^{in})$ that is measured if we use spin-insensitive counters, which accept all particles irrespective of their spin state. Thus the result is simply that

$$\|\chi^{out}\|^2 = \frac{d\sigma}{d\Omega}(\mathbf{p}' \leftarrow \mathbf{p}, \chi^{in}) \quad \text{[out spins not monitored]} \tag{A.101}$$

A.8 Time-Independent Formulation of Quantum Scattering

So far we have set up a time-dependent description of collisions in which two particles scatter elastically, the so called single-channel processes. The collisions were first described in terms of the scattering operator S. The matrix-elements of S were then decomposed in terms of the scattering amplitude, and the differential cross section was expressed in terms of the amplitude.

Our principal remaining problem in one-channel scattering is to setup methods for the actual computation of the amplitude in terms of a given interaction. All such methods, fall within the so-called time-independent scattering theory. This formalism is built around the so-called stationary scattering states and two operators, the Green's operator $G(z)$ and the T operator $T(z)$.

In the time-independent formulation of the quantum scattering process we solve the time independent schrödinger equation

$$(H_0 + V)|\psi\rangle = E|\psi\rangle \tag{A.102}$$

with

$$H_0|\psi_{in}\rangle = E|\psi_{in}\rangle \tag{A.103}$$

where $|\psi_{in}\rangle$ is the incoming state $(E > 0)$. We assume the potential V to be zero far away from the target, therefore in asymptotic region, the energy eigenstate just describe a free-particle motion. The formal solution to this problem can be expanded as a sum of an incident and a scattered wave according to

$$|\psi\rangle = |\psi_{in}\rangle + |\psi_{out}\rangle \tag{A.104}$$

where the incident state vector $|\psi_{in}\rangle$ satisfies

$$[G^0]^{-1}(z)|\psi_{in}\rangle = 0 \tag{A.105}$$

while $|\psi\rangle$ satisfies

$$G^{-1}(z)|\psi\rangle = 0 \tag{A.106}$$

Here G^0 and G are the *Green's function* or *resolvent* for H^0 and H, respectively. The Green's function for an arbitrary Hamiltonian H is defined to be

$$G(z) = (z - H)^{-1} \tag{A.107}$$

for any z, real or complex, for which the inverse exists.

The knowledge of the Green's operator $G(z)$, for all z, of a Hamiltonian H is equivalent to knowledge of a complete solution of the corresponding eigenvalue

problem. The Green's operator $G(z)$ is analytic except on the spectrum of H. For each discrete eigenvalue, $G(z)$ has a pole whose position is precisely the eigenvalue and whose residue determines the corresponding eigenvector (or subspace of eigenvectors in the case of degeneracy). When H has a continuous spectrum (as it always does in scattering theory), $G(z)$ has a *branch cut* running along the real axis from 0 to ∞; that is, the value of $\langle\chi|G(z)|\psi\rangle$ at any $E > 0$ approached from above ($z = E + i0$) is different from its value at the same point approached from below ($z = E - i0$).

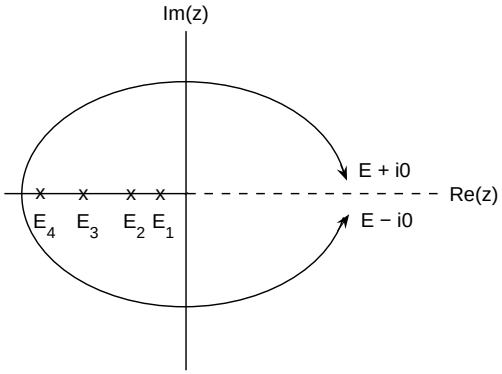

Fig. A.3: The Green's operator $G(z)$ is analytic except for poles at the bound states $z = E_1, E_2, \cdots$ and a cut from 0 to ∞.

A.8.1 Lippmann-Schwinger equation for $G(z)$

Knowledge of $G(z)$ for all z is equivalent to a complete solution of the eigenvalue problem of H. Needless to say, finding $G(z)$ is precisely as hard as solving the eigenvalue problem, and, generally, one cannot hope to find $G(z)$. For this reason it is useful to have an equation that relates the unknown $G(z)$ to some known operator. The usual choice for the latter is the free Green's operator $G^0(z)$. The equation relating G and G^0 is called the *resolvent equation* or *Lippmann-Schwinger equation for* $G(z)$. It is derived from the simple operator identity

$$A^{-1} = B^{-1} + B^{-1}(B - A)A^{-1}$$

If we set $A = z - H$ and $B = z - H^0$ this becomes:

$$G(z) = G^0(z) + G^0(z)VG(z) \tag{A.108}$$

or, if we interchange A and B

$$G(z) = G^0(z) + G(z)VG^0(z) \tag{A.109}$$

The free Green's operator G^0 is, explicitly known. In the momentum representation, it is diagonal and is given by

$$\langle \mathbf{p}'|G^0(z)|\mathbf{p}\rangle = \langle \mathbf{p}'|(z-H)^{-1}|\mathbf{p}\rangle = \frac{1}{z-E_p}\delta(\mathbf{p}-\mathbf{p}') \tag{A.110}$$

obviously, this allows us to calculate the matrix elements of $G^0(z)$ in any other representation.

To conclude this part on the definition and general properties of Green's operator we note that since $H = H^\dagger$ it is easily seen that

$$G(z^*) = [G(z)]^\dagger \tag{A.111}$$

and similarly for $G^0(z)$. This important identity asserts that the value of the function G at the point z^* is the same as the adjoint of its value at the point z.

A.8.2 The T operator

In scattering theory it is convenient to introduce another operator $T(z)$, which is defined in terms of $G(z)$ as

$$T(z) = V + VG(z)V \tag{A.112}$$

It is clear that as an analytic function of z the operator $T(z)$ has the same properties as $G(z)$. That is, $T(z)$ is analytic for all z not in the spectrum of H. When z approaches the energy of a bound state, $T(z)$ has a pole, and on the positive real axis $T(z)$ has a branch cut.

Using the Lippmann-Schwinger equation for G (A.108) one can show easily that

$$G^0(z)T(z) = G(z)V \tag{A.113}$$

and

$$T(z)G^0(z) = VG(z) \tag{A.114}$$

As a first application of these identities we can find an expression for G in terms of T. By replacing VG by TG^0 in the Lippmann-Schwinger equation for G, we find that

$$G(z) = G^0(z) + G^0(z)T(z)G^0(z) \tag{A.115}$$

This means that knowledge of T implies knowledge of G. Because the converse is obviously true (by the definition of T), we see that the information contained in T is precisely equivalent to that in G.

Using the identity (A.113) we can replace GV in (A.112) by G^0T to obtain the equation

$$T(z) = V + VG^0(z)T(z) \tag{A.116}$$

which gives T in terms of the known operator G^0. This equation is known as the Lippmann-Schwinger equation for $T(z)$, and is the starting point of many methods for calculating T. In particular, when V is *sufficiently weak* one can

hope to obtain a reliable solution by iteration, starting with the so-called Born approximation $T \approx V$. Inserting this into the right-hand side of (A.116) gives as the second approximation $T \approx V + VG^0V$; and continuing this procedure produces the infinite series,

$$T = V + VG^0V + VG^0VG^0V + \dots \tag{A.117}$$

This series (which may or may not converge) is known as the Born series.

Using (A.113), the equation (A.106) can easily be solved for the scattered wave in terms of the unperturbed Green's function G^0 and the T-matrix, yielding

$$|\psi_{out}\rangle = G^0T|\psi_{in}\rangle \tag{A.118}$$

Equation (A.115) is very useful when we study quantum scattering in low-dimension. Another formula on which we will rely heavily is the Lupu-Sax formula [41]

$$T_{H,V}(z) = \left[1 - T_{H',V}[G_H(z) - G_{H'}(z)]\right]^{-1} T_{H',V}(z) \tag{A.119}$$

which relates the T-matrix of the scatter V in the background Hamiltonian H to the T-matrix for the same scatter but in a different background Hamiltonian H'.

Finally we note that the identity (A.111) for G leads to a corresponding result for T

$$T(z^*) = [T(z)]^\dagger \tag{A.120}$$

A.8.3 Relation to the Møller operators

For a collision with the *in* asymptote labelled by the normalized vector $|\psi_{in}\rangle = |\phi\rangle$, the actual state at $t = 0$ is given by

$$|\psi\rangle = \Omega_+|\psi_{in}\rangle = \Omega_+|\phi\rangle = \lim_{t\to-\infty} U(t)^\dagger U^0(t)|\phi\rangle \equiv |\phi+\rangle \tag{A.121}$$

Similarly, if the *out* asymptote were going to be $|\psi_{out}\rangle = |\phi\rangle$, then the actual state at $t = 0$ would have to be

$$|\psi\rangle = \Omega_-|\psi_{out}\rangle = \Omega_-|\phi\rangle = \lim_{t\to+\infty} U(t)^\dagger U^0(t)|\phi\rangle \equiv |\phi-\rangle \tag{A.122}$$

Rewriting $U^\dagger(t)U^0(t)$ as the integral of its derivative, led to the result (which we write for Ω_-)

$$|\phi-\rangle = |\phi\rangle + i \lim_{\epsilon\to0^+} \int_0^\infty d\tau e^{-\epsilon\tau} U(\tau)^\dagger V U^0(\tau)|\phi\rangle \tag{A.123}$$

Here the damping factor $e^{-\epsilon\tau}$ is introduced such that we can replace the proper vector $|\phi\rangle$ by improper plane-wave state $|\mathbf{p}\rangle$ (an essential step in the discussion of the stationary scattering state in subsection A.8.5) and the integral still converges.

By inserting a complete set of states $|\mathbf{p}\rangle$ we obtain

$$|\phi-\rangle \equiv \Omega_-|\phi\rangle = |\phi\rangle + i \lim_{\epsilon\to 0^+} \int d^3p \int_0^\infty d\tau [e^{-\epsilon\tau} U(\tau)^\dagger V U^0(\tau)] |\mathbf{p}\rangle\langle\mathbf{p}|\phi\rangle \quad \text{(A.124)}$$

Now, the free evolution operator $U^0(\tau)$ acting on $|\mathbf{p}\rangle$ gives just $\exp(-iE_p\tau)$. Thus, the operator in brackets in the integrand can be replaced by

$$[\cdots] = \exp[-i(E_p - i\epsilon - H)\tau]V$$

and the integral over τ performed

$$\int_0^\infty d\tau[\cdots] = -i(E_p - i\epsilon - H)^{-1}V = -iG(E_p - i\epsilon)V$$

Substituting back into (A.124) we obtain

$$|\phi-\rangle \equiv \Omega_-|\phi\rangle = |\phi\rangle + \lim_{\epsilon\to 0^+} \int d^3p G(E_p - i\epsilon)V|\mathbf{p}\rangle\langle\mathbf{p}|\phi\rangle \quad \text{(A.125)}$$

With the same method one can show

$$|\phi+\rangle \equiv \Omega_+|\phi\rangle = |\phi\rangle + \lim_{\epsilon\to 0^+} \int d^3p G(E_p + i\epsilon)V|\mathbf{p}\rangle\langle\mathbf{p}|\phi\rangle \quad \text{(A.126)}$$

A.8.4 Relation to the scattering operator

In this section we establish expression for the scattering operator S in terms of $G(z)$ and $T(z)$, from which we establish the relevance of the operators $G(z)$ and $T(z)$ to scattering theory. Our starting point is the equation

$$\begin{aligned}\langle\chi|S|\phi\rangle &= \langle\chi|\Omega_-^\dagger\Omega_+|\phi\rangle \\ &= \lim_{t\to+\infty}\lim_{t'\to-\infty}\langle\chi|\left(e^{iH^0t}e^{-iHt}\right)\left(e^{iHt'}e^{-iH^0t'}\right)|\phi\rangle \quad \text{(A.127)}\end{aligned}$$

The order in which we take the limits $t \to +\infty$ and $t' \to -\infty$ is immaterial. In particular, we can take the two limits simultaneously; that is, we can set $t' = -t$ and simply let $t \to +\infty$, to give

$$\langle\chi|S|\phi\rangle = \lim_{t\to+\infty}\langle\chi|\left[e^{iH^0t}e^{-2iHt}e^{iH^0t}\right]|\phi\rangle \quad \text{(A.128)}$$

writing this expression as the integral of its derivative, in this case

$$\frac{d}{dt}[\cdots] = -i\left\{e^{iH^0t}Ve^{-2iHt}e^{iH^0t} + e^{iH^0t}e^{-2iHt}Ve^{iH^0t}\right\} \quad \text{(A.129)}$$

gives

$$\begin{aligned}\langle\chi|S|\phi\rangle &= \langle\chi|\phi\rangle - i\int_0^\infty dt\langle\chi|\{\cdots\}|\phi\rangle \\ &= \langle\chi|\phi\rangle - i\lim_{\epsilon\to0^+}\int_0^\infty dt e^{-\epsilon t}\langle\chi|\{\cdots\}|\phi\rangle \quad \text{(A.130)}\end{aligned}$$

If we now replace the proper vectors $|\chi\rangle$ and $|\phi\rangle$ by momentum eigenstates $|\mathbf{p}'\rangle$ and $|\mathbf{p}\rangle$ the free evolution operators in the integrand simplify and we get

$$\begin{aligned}\langle\mathbf{p}'|S|\mathbf{p}\rangle &= \delta_3(\mathbf{p}'-\mathbf{p}) \\ &\quad -i\lim_{\epsilon\to 0^+}\int_0^\infty dt\langle\mathbf{p}'|\left\{Ve^{i(E_{p'}+E_p+i\epsilon-2H)t}+e^{i(E_{p'}+E_p+i\epsilon-2H)t}V\right\}|\mathbf{p}\rangle \\ &= \delta_3(\mathbf{p}'-\mathbf{p}) \\ &\quad +\frac{1}{2}\lim_{\epsilon\to 0^+}\langle\mathbf{p}'|\left\{VG\left(\frac{E_{p'}+E_p}{2}+i\epsilon\right)+G\left(\frac{E_{p'}+E_p}{2}+i\epsilon\right)V\right\}|\mathbf{p}\rangle\end{aligned} \tag{A.131}$$

If we next replace VG by TG^0, and GV by G^0T, the free Green's operators acting on the momentum eigenstates can be replaced by their eigenvalues to give

$$\begin{aligned}&= \delta_3(\mathbf{p}'-\mathbf{p})+\lim_{\epsilon\to 0^+}\left\{\frac{1}{E_{p'}-E_p+i\epsilon}+\frac{1}{E_p-E_{p'}+i\epsilon}\right\} \\ &\qquad\qquad \times\langle\mathbf{p}'|T\left(\frac{E_{p'}+E_p}{2}+i\epsilon\right)|\mathbf{p}\rangle \\ &= \delta_3(\mathbf{p}'-\mathbf{p})-2\pi i\delta(E_{p'}-E_p)\lim_{\epsilon\to 0^+}\langle\mathbf{p}'|T(E_p+i\epsilon)|\mathbf{p}\rangle\end{aligned} \tag{A.132}$$

This is one of the central results of time-independent scattering theory. Comparing it with equation (A.19) we see that

$$\frac{1}{4\pi^2\mu}f(\mathbf{p}'\leftarrow\mathbf{p}) = t(\mathbf{p}'\leftarrow\mathbf{p}) = \langle\mathbf{p}'|T(E_p+i0)|\mathbf{p}\rangle \tag{A.133}$$

where we have used the notation $f(E+i0)$ to denote the limit of $f(E+i\epsilon)$ as $\epsilon\to 0^+$. The matrix $t(\mathbf{p}'\leftarrow\mathbf{p})$ is called the on-shell T matrix. It is defined only for $E_{p'}=E_p$, and is in fact the $\mathbf{p}',\mathbf{p}$ matrix element of the operator $T(z)$ for the particular values $z=E_p+i0$ and $E_{p'}=E_p$. For this reason $\langle\mathbf{p}'|T(z)|\mathbf{p}\rangle$ is known as the off-shell T matrix. The off-shell matrix is more general than $t(\mathbf{p}'\leftarrow\mathbf{p})$, since it is defined for an arbitrary complex numbers and independent momenta $\mathbf{p}$ and $\mathbf{p}'$.

A.8.5 The stationary scattering states

The stationary scattering states are improper eigenvectors of the Hamiltonian $H=H^0+V$ and are denoted by $|\mathbf{p}+\rangle$ and $|\mathbf{p}-\rangle$. In particular, the wave function $\langle\mathbf{x}|\mathbf{p}+\rangle$ is just the familiar scattering wave function, often denoted $\psi^+_{\mathbf{p}}(\mathbf{x})$, of elementary collision theory,

$$\langle\mathbf{x}|\mathbf{p}+\rangle\xrightarrow[r\to\infty]{}(2\pi)^{-3/2}\left(e^{i\mathbf{p}\cdot\mathbf{x}}+f\frac{e^{ipr}}{r}\right) \tag{A.134}$$

The scattering amplitude can be expressed in terms of $|\mathbf{p}+\rangle$ or $|\mathbf{p}-\rangle$ and any means of computing $|\mathbf{p}\pm\rangle$ therefore provides a method for calculating the amplitude. These method fall into two (closely connected) categories: those using

integral equations and those using differential equations. The integral method depends on the fact that the wave functions $\langle \mathbf{x}|\mathbf{p}\pm\rangle$ satisfy integral equations, closely related to the Lippmann-Schwinger equation for the operator $T(z)$. The differential method instead uses the fact that the vectors $|\mathbf{p}\pm\rangle$ are eigenvectors of H and, hence, that the wave functions $\langle \mathbf{x}|\mathbf{p}\pm\rangle$ satisfy the time-independent Schrödinger equation. The later is most useful when the potential is spherically symmetric, since in this case the wave function can be decomposed into angular-momentum eigenfunctions and the Schrödinger equation reduces to a set of ordinary differential equations.

The stationary scattering states $\langle \mathbf{x}|\mathbf{p}\pm\rangle$ are defined as

$$|\mathbf{p}\pm\rangle \equiv \Omega_{\pm}|\mathbf{p}\rangle \tag{A.135}$$

To understand the significance of this definition we consider an orbit with *in* asymptote labelled by $|\phi\rangle$, which we expand in terms of plane waves as

$$|\phi\rangle = \int d^3p\phi(\mathbf{p})|\mathbf{p}\rangle \tag{A.136}$$

In this case the actual state at $t = 0$ is

$$\begin{aligned} |\phi+\rangle = \Omega_{+}|\phi\rangle &= \int d^3p\phi(\mathbf{p})\Omega_{+}|\mathbf{p}\rangle \\ &= \int d^3p\phi(\mathbf{p})|\mathbf{p}+\rangle \end{aligned} \tag{A.137}$$

In other words, the actual state $|\phi+\rangle$ has the same expansion in terms of $|\mathbf{p}+\rangle$ as does its *in* asymptote $|\phi\rangle$ in terms of $|\mathbf{p}\rangle$. Similarly, if an orbit has out asymptote

$$|\chi\rangle = \int d^3p\chi(\mathbf{p})|\mathbf{p}\rangle \tag{A.138}$$

then the actual state at $t = 0$ is

$$|\chi-\rangle = \int d^3p\chi(\mathbf{p})|\mathbf{p}-\rangle \tag{A.139}$$

These two results give the primary significance of the improper vectors $|\mathbf{p}\pm\rangle$. They are the natural vectors for expanding the actual state at $t = 0$ to display explicitly its relation to the momentum expansions of the *in* and *out* asymptotes. Due to (A.13) one can show easily that the vectors $|\mathbf{p}\pm\rangle$ are eigenvectors of the full Hamiltonian

$$H|\mathbf{p}\pm\rangle = H\Omega_{\pm}|\mathbf{p}\rangle = \Omega_{\pm}H^0|\mathbf{p}\rangle = E_p\Omega_{\pm}|\mathbf{p}\rangle = E_p|\mathbf{p}\pm\rangle \tag{A.140}$$

The eigenvalue of H acting on $|\mathbf{p}\pm\rangle$ is the same as that of H^0 acting on $|\mathbf{p}\rangle$: $E_p = p^2/2m$. This means that the wave function $\langle \mathbf{x}|\mathbf{p}\pm\rangle$ satisfy the time-independent Schrödinger equation. Besides we have

$$U(t)|\mathbf{p}+\rangle = e^{-iE_pt}|\mathbf{p}+\rangle \tag{A.141}$$

$$U^0(t)|\mathbf{p}\rangle = e^{-iE_p t}|\mathbf{p}\rangle \tag{A.142}$$

Note that $U^0(t)|\mathbf{p}\rangle$ is not the asymptote of the actual orbit $U(t)|\mathbf{p}\rangle$. Nonetheless, they do satisfy the asymptote condition when "smeared" by the integral $\int d^3p\phi(\mathbf{p})$ into proper states.

$$\begin{aligned} U(t)|\phi+\rangle &\xrightarrow[t\to-\infty]{} U^0(t)|\phi\rangle \qquad [\text{any proper } |\phi\rangle] \\ U(t)\int d^3p\phi(\mathbf{p})|\mathbf{p}+\rangle &\xrightarrow[t\to-\infty]{} U^0(t)\int d^3p\phi(\mathbf{p})|\mathbf{p}\rangle \end{aligned} \tag{A.143}$$

or

$$\int d^3p\phi(\mathbf{p})[U(t)|\mathbf{p}+\rangle] \xrightarrow[t\to-\infty]{} \int d^3p\phi(\mathbf{p})[U^0(t)|\mathbf{p}\rangle] \tag{A.144}$$

By expanding $|\phi\pm\rangle$ and $|\phi\rangle$ in equation (A.125) and (A.126) in terms of the momentum wave function $\phi(\mathbf{p}) = \langle\mathbf{p}|\phi\rangle$ we obtain

$$\int d^3p\phi(\mathbf{p})|\mathbf{p}\pm\rangle = \int d^3p\phi(\mathbf{p})[|\mathbf{p}\rangle + G(E_p \pm i0)V|\mathbf{p}\rangle] \tag{A.145}$$

since this hold for any $\phi(\mathbf{p})$ we conclude that

$$|\mathbf{p}\pm\rangle = |\mathbf{p}\rangle + G(E_p \pm i0)V|\mathbf{p}\rangle \tag{A.146}$$

The relation (A.146) can be used to establish an expression for the on-shell T matrix in terms of $|\mathbf{p}+\rangle$ or $|\mathbf{p}-\rangle$. Since we already know that $t(\mathbf{p}' \leftarrow \mathbf{p})$ is the same thing as $\langle\mathbf{p}'|T(E_p + i0)|\mathbf{p}\rangle$ we begin by considering the vector

$$\begin{aligned} T(E_p \pm i0)|\mathbf{p}\rangle &= [V + VG(\pm)V]|\mathbf{p}\rangle \\ &= V[1 + G(\pm)V]|\mathbf{p}\rangle \end{aligned} \tag{A.147}$$

Using (A.146) we then obtain the important identities

$$T(E_p \pm i0)|\mathbf{p}\rangle = V|\mathbf{p}\pm\rangle \tag{A.148}$$

Multiplying the first of these by the bra $\langle\mathbf{p}'|$ gives

$$t(\mathbf{p}' \leftarrow \mathbf{p}) = \langle\mathbf{p}'|V|\mathbf{p}+\rangle \tag{A.149}$$

To obtain an equivalent expression in terms of $|\mathbf{p}+\rangle$ we use the identity (A.120), $T(z)^\dagger = T(z^*)$ to rewrite the second identity (A.148) (with $\mathbf{p}$ replaced by $\mathbf{p}'$) as

$$\langle\mathbf{p}'|T(E_{p'} + i0) = \langle\mathbf{p}' - |V \tag{A.150}$$

This leads at once to the result

$$t(\mathbf{p}' \leftarrow \mathbf{p}) = \langle\mathbf{p}' - |V|\mathbf{p}\rangle \tag{A.151}$$

These results allow one to calculate the scattering amplitude from either of the stationary states $|\mathbf{p}+\rangle$ or $|\mathbf{p}-\rangle$.

Returning to the equation (A.146) for $|\mathbf{p}\pm\rangle$ we note that, just as with the T operator in subsection A.8.2, it is convenient to replace the explicit expression in terms of $G(z)$ by an implicit expression in terms of $G^0(z)$. This can be done in two simple steps: we replace GV by G^0T, and then we use (A.148) to replace $T|\mathbf{p}\rangle$ by $V|\mathbf{p}\pm\rangle$. This gives

$$|\mathbf{p}\pm\rangle = |\mathbf{p}\rangle + G^0(E_p \pm i0)V|\mathbf{p}\pm\rangle \tag{A.152}$$

This equation, which is, of course, an integral equation for the wave function $\langle\mathbf{x}|\mathbf{p}\pm\rangle$, is called the *Lippmann-Schwinger equation for* $|\mathbf{p}\pm\rangle$.

The equation (A.152) can be also written as

$$(1 - G^0V)|\mathbf{p}\pm\rangle = |\mathbf{p}\rangle$$

from this we obtain a Born series for $|\mathbf{p}+\rangle$,

$$|\mathbf{p}+\rangle = |\mathbf{p}\rangle + G^0V|\mathbf{p}\rangle + \dots \tag{A.153}$$

If we then use (A.149) to calculate the on-shell T matrix, we obtain

$$t(\mathbf{p}' \leftarrow \mathbf{p}) = \langle\mathbf{p}'|V|\mathbf{p}\rangle + \langle\mathbf{p}'|VG^0V|\mathbf{p}\rangle + \dots \tag{A.154}$$

which is precisely the Born series resulting from iterating the Lippmann-Schwinger equation for $T(z)$.

From the Lippmann-Schwinger equation for $|\mathbf{p}\pm\rangle$ it follows that the wave function $\langle\mathbf{x}|\mathbf{p}\pm\rangle$ satisfy the integral equation

$$\langle\mathbf{x}|\mathbf{p}\pm\rangle = \langle\mathbf{x}|\mathbf{p}\rangle + \int d^3x' V(\mathbf{x}')\langle\mathbf{x}|G^0(E)|\mathbf{x}'\rangle\langle\mathbf{x}'|\mathbf{p}\pm\rangle \tag{A.155}$$

We can use this equation to establish the behavior of the wave function for large r; where $\langle\mathbf{x}|\psi\rangle$ is just a plane wave plus a spherical outgoing wave.

To use the above equation we must calculate the Green's function $\langle\mathbf{x}|G^0(E)|\mathbf{x}'\rangle$. We know that

$$G^0(E)|\mathbf{p}\rangle = \frac{1}{E + i0 - E_p}|\mathbf{p}\rangle, \quad E_p = \frac{\mathbf{p}^2}{2\mu} \tag{A.156}$$

Thus, by inserting a complete set of states $|\mathbf{p}\rangle$ into the required spatial matrix element, we find that

$$\begin{aligned}\langle\mathbf{x}|G^0(E)|\mathbf{x}'\rangle &= \int d^3p \langle\mathbf{x}|G^0(E)|\mathbf{p}\rangle\langle\mathbf{p}|\mathbf{x}'\rangle \\ &= \frac{1}{(2\pi)^3}\int d^3p \frac{e^{i\mathbf{p}\cdot(\mathbf{x}-\mathbf{x}')}}{E + i0 - E_p}\end{aligned} \tag{A.157}$$

If we choose the direction of $(\mathbf{x} - \mathbf{x}')$ as polar axis, the exponent becomes $ip|\mathbf{x} - \mathbf{x}'|\cos\theta$ and the angular integral can be performed to give

$$\begin{aligned}&= \frac{-i}{4\pi^2|\mathbf{x} - \mathbf{x}'|}\int_0^\infty pdp \frac{e^{ip|\mathbf{x}-\mathbf{x}'|} - e^{-ip|\mathbf{x}-\mathbf{x}'|}}{E + i0 - E_p} \\ &= \frac{i\mu}{2\pi^2|\mathbf{x} - \mathbf{x}'|}\int_{-\infty}^\infty dp \frac{pe^{ip|\mathbf{x}-\mathbf{x}'|}}{p^2 - 2\mu(E + i0)}\end{aligned} \tag{A.158}$$

This integral can be evaluated by contour integration. The final result is

$$\langle \mathbf{x}|G^0(E)|\mathbf{x}'\rangle = -\frac{\mu}{2\pi}\frac{e^{i\sqrt{2\mu(E+i0)}|\mathbf{x}-\mathbf{x}'|}}{|\mathbf{x}-\mathbf{x}'|} \tag{A.159}$$

For the incident plane wave $|\psi_{in}\rangle = |\mathbf{p}\rangle$ we have

$$E = \frac{\mathbf{p}^2}{2\mu} \quad \rightarrow \quad [2\mu(E+i0)]^{1/2} = +p. \tag{A.160}$$

Substitution of these results into (A.155) gives

$$\langle \mathbf{x}|\mathbf{p}+\rangle = \langle \mathbf{x}|\mathbf{p}\rangle - \frac{\mu}{2\pi}\int d^3x' \frac{e^{+ip|\mathbf{x}-\mathbf{x}'|}}{|\mathbf{x}-\mathbf{x}'|} V(\mathbf{x}')\langle \mathbf{x}'|\mathbf{p}\pm\rangle \tag{A.161}$$

To see what happens when $r = |\mathbf{x}|$ is large, we suppose for simplicity that $V(\mathbf{x}) \equiv 0$ for r greater than some a (although our result actually holds just as long as $V = o(r^{-3-\epsilon})$ as $r \rightarrow \infty$). In this case the integral is confined to $r' < a$, and for large r we can expand $|\mathbf{x}-\mathbf{x}'|$ in powers of (r'/r),

$$|\mathbf{x}-\mathbf{x}'| = \left(\mathbf{x}^2 - 2\mathbf{x}\cdot\mathbf{x}' + \mathbf{x}'^2\right)^{\frac{1}{2}} = r\left[1 - \frac{\mathbf{x}\cdot\mathbf{x}'}{r^2} + o\left(\frac{r'}{r}\right)^2\right] \tag{A.162}$$

The expansion (A.161) then becomes

$$\begin{aligned}\langle \mathbf{x}|\mathbf{p}\pm\rangle = \langle \mathbf{x}|\mathbf{p}\rangle - \frac{\mu e^{\pm ipr}}{2\pi r}\int d^3x' exp(\mp ip\widehat{x}\cdot\mathbf{x}')V(\mathbf{x}')\langle \mathbf{x}'|\mathbf{p}\pm\rangle \\ \times\left[1 + o\left(\frac{a}{r} + \frac{pa^2}{r}\right)\right] \\ \xrightarrow[r\,\rightarrow\,\infty]{} \quad (2\pi)^{-3/2}\left[e^{i\mathbf{p}\cdot\mathbf{x}} - (2\pi)^2\mu\langle \pm p\widehat{x}|V|\mathbf{p}\pm\rangle\frac{e^{\pm ipr}}{r}\right]\end{aligned} \tag{A.163}$$

From (A.148) we obtain

$$-(2\pi)^2\mu\langle p\widehat{x}|V|\mathbf{p}+\rangle = -(2\pi)^2\mu t(p\widehat{x} \leftarrow \mathbf{p}) = f(p\widehat{x} \leftarrow \mathbf{p}) \tag{A.164}$$

Thus we can rewrite (A.163) for $\langle \mathbf{x}|\mathbf{p}+\rangle$ as

$$\langle \mathbf{x}|\mathbf{p}+\rangle \quad \xrightarrow[r\,\rightarrow\,\infty]{} \quad (2\pi)^{-3/2}\left[e^{i\mathbf{p}\cdot\mathbf{x}} + f(p\widehat{x} \leftarrow \mathbf{p})\frac{e^{ipr}}{r}\right] \tag{A.165}$$

This establishes that our definition of the amplitude $f(\mathbf{p}' \leftarrow \mathbf{p})$ in terms of $\langle \mathbf{p}'|S|\mathbf{p}\rangle$ is, in fact, the same as the traditional definition in terms of the asymptotic form of the stationary scattering wave function.

A.9 Identical Particles

So far we assumed that both particles, involved in the scattering process, are (at least in principle) distinguishable. This means that we can discriminate between the 2 scattering diagrams in Fig. A.4 which both give rise to the same "signal" in the detector, if both particles are identical. The first diagram corresponds to a scattering amplitude $f(k,\theta)$ and the second to $f(k,\pi-\theta)$. As an example we consider the scattering of two electrons. Oppositely polarized electrons essentially remain distinguishable. If the detector D counts electrons of any spin then the probability for both processes just add up

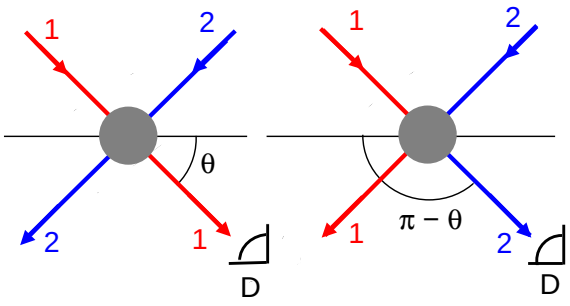

Fig. A.4: Two scattering processes leading to the same final state for two identical particles.

$$\frac{d\sigma}{d\Omega} = |f(\theta)|^2 + |f(\pi-\theta)|^2 \tag{A.166}$$

If beams (1) and (2) are both polarized spin up or down, then the detector cannot distinguish between the incident particles and we have to take the symmetrization into account. The two-particle wavefunction must obey

$$\psi(\mathbf{x}_1,\mathbf{x}_2) = \alpha\psi(\mathbf{x}_2,\mathbf{x}_1) \tag{A.167}$$

with $\alpha = 1$ for bosons and $\alpha = -1$ for fermions. When we impose this symmetrization condition for the relative wavefunction, we obtain

$$\psi(\mathbf{x}) = \alpha\psi(-\mathbf{x}) \tag{A.168}$$

where $\mathbf{x}$ is the relative coordinate $\mathbf{x} = \mathbf{x}_1 - \mathbf{x}_2$. The (anti)symmetrized asymptotic wavefunction can be written as

$$\psi(\mathbf{x}) \xrightarrow[r\to\infty]{} \frac{1}{(2\pi\hbar)^{3/2}} \frac{e^{ikz} + \alpha e^{-ikz}}{\sqrt{2}} + \frac{1}{(2\pi\hbar)^{3/2}} \frac{f(k,\theta) + \alpha f(k,\pi-\theta)}{\sqrt{2}} \frac{e^{ikr}}{r} \tag{A.169}$$

For bosons the amplitudes have to be added

$$\frac{d\sigma}{d\Omega}_b = |f(\theta) + f(\pi - \theta)|^2 \tag{A.170}$$

while for fermions they have to be subtracted

$$\frac{d\sigma}{d\Omega}_f = |f(\theta) - f(\pi - \theta)|^2 \tag{A.171}$$

At an angle $\theta = \pi/2$ this implies

$$\begin{aligned} \frac{d\sigma}{d\Omega}_b \left(\frac{\pi}{2}\right) &= 4|f\left(\frac{\pi}{2}\right)|^2 \\ \frac{d\sigma}{d\Omega}_f \left(\frac{\pi}{2}\right) &= 0 \end{aligned} \tag{A.172}$$

so that identical fermions never scatter at an angle of $\pi/2$, while the differential cross section for boson scattering is twice the classical value for this angle.

Using the parity of the Legendre polynomials

$$P_l(\cos(\pi - \theta)) = P_l(-\cos\theta) = (-1)^l P_l(\cos\theta) \tag{A.173}$$

we can deduce that the only partial waves contributing to the cross section for bosons correspond to even values of l, those for fermions to odd values of l. We take this into account when we follow the same procedure, that leads to (2.28) and see that the symmetrization principle doubles the contribution of the even partial waves for bosons and cancels the contribution of the odd ones and vice versa for fermions

$$\sigma(k) = \frac{8\pi}{k^2} \sum_{l\,\text{even}} (2l+1) \sin^2 \delta_l(k) \quad \text{for bosons} \tag{A.174}$$

$$\sigma(k) = \frac{8\pi}{k^2} \sum_{l\,\text{odd}} (2l+1) \sin^2 \delta_l(k) \quad \text{for fermions} \tag{A.175}$$

B. SCATTERING THEORY IN FREE SPACE: MULTIMODE REGIME

So far we have discussed only processes in which structureless particles undergo an elastic collision. However, almost all process of experimental interest do include collisions involving several particles (composite or neutral) and including inelastic processes such as excitation and disintegration. A typical example from atomic physics is the set of processes:

$$\begin{array}{cc} e + H \rightarrow e + H & \text{(elastic scattering)} \\ e + H \rightarrow e + H^* & \text{(excitation)} \\ e + H \rightarrow e + e + p & \text{(ionization or breakup)} \end{array}$$

(where H^* denotes any of the excited states of hydrogen); or in nuclear physics:

$$\begin{array}{cc} p + {}^{12}C \rightarrow p + {}^{12}C & \\ p + {}^{12}C \rightarrow n + {}^{12}N & \text{(charge exchange)} \\ p + {}^{12}C \rightarrow p + {}^{3}He + {}^{9}Be, \text{ etc} & \end{array}$$

or in particle physics:

$$\begin{array}{c} \Pi^- + p \rightarrow \Pi^- + p \\ \Pi^- + p \rightarrow K^0 + \Lambda^0 \\ \Pi^- + p \rightarrow \Pi^- + K^0 + \Pi^0 + p, \text{ etc} \end{array}$$

Each of the different sets of final particles in each of these examples is called a *channel*, and processes of this kind are called *multichannel* processes.

In this chapter we set up a description of the collision process in terms of asymptotic free states and define a unitary S operator that maps each *in* state onto the corresponding *out* state.

B.1 Channels

To illustrate the essential features of multichannel scattering we assume a system of N spinless particles, which interact via short-range two-body potentials. A channel α is specified by the grouping of the N particles into n_α freely moving fragments with $2 \leq n_\alpha \leq N$, each fragment being either one of the original N particles or a definite bound state of some subset (we do not include among the channels the bound states of all N particles for which $n_\alpha = 1$. These remain bound at all times and do not communicate with the scattering states, in which we are interested.)

Particles	a b c
Bound States	(bc) $(bc)^*$ (ac) and (possible bound states of all three particles)

Tab. B.1: The Model Three Particle System.

Channel number	0	1	2	3
Channel	$a+b+c$	$a+(bc)$	$a+(bc)^*$	$b+(ac)$

Tab. B.2: Possible Channels.

To illustrate the essential features of multichannel scattering lets discuss a system of three spinless particles, a, b and c, which interact via short-range two-body potentials. We shall suppose that the particles b and c have two bound states, a ground state (bc) and an excited state $(bc)^*$; that a and c have one bound state (ac); and that, apart from possible bound states of all three particles, there are no other bound states. For example, we can think of a, as a proton, b as a neutron and c as some stable nuclear "core" such as ^{16}O; in this case the (bc) bound state is ^{17}O, the (ac) state is ^{17}F, and we have a simple model for the scattering of protons off ^{17}O.

For definiteness we suppose that we are interested in the disintegration process

$$a+(bc) \to a+b+c \tag{B.1}$$

However, the given initial state $a+(bc)$ will in general lead to several different final states in addition to the particular one of interest. The possible grouping of the particles a, b and c into stable subsystems or channels are shown in Table B.2.

The process of interest (B.1) leads from an *in* state in channel 1 to an *out* state in channel 0. Clearly, however, an *in* state in channel 1 can generally lead to *out* state, in any of the four channels 0, 1, 2, or 3,

$$\begin{array}{cc} a+(bc) \to a+b+c & \text{(break up)} \\ a+(bc) \to a+(bc) & \text{(elastic scattering)} \\ a+(bc) \to a+(bc)^* & \text{(excitation)} \\ a+(bc) \to b+(ac) & \text{(rearrangement)} \end{array} \tag{B.2}$$

In exactly the same way the final state of interest can arise from several different initial states. In fact, a final state in any one of the four channels 0, 1, 2, or

3 can arise from an initial state in any of the same four channels. Therefore, there are 16 qualitatively distinct processes to be considered.

A schematic view of multichannel scattering, which illustrates the name channel, is shown in Fig. B.1. The various possible *in* channels are shown as tube, or channels, through which a fluid of probability can flow into a junction. This junction represents the actual collision, and from it lead the various possible *out* channels. In practice the *in* states always lies in a definite channel, which means that all of the fluid enters by one channel. The corresponding *out* state is usually a superposition of the various possible channels and the fluid therefore leaves through several channels in some definite proportions.

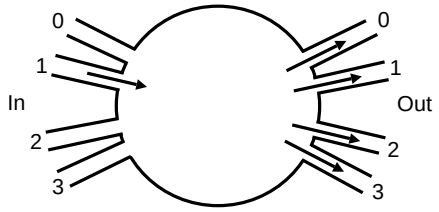

Fig. B.1: A Schematic view of multichannel scattering as a quantum-mechanical irrigation system.

In practice, experiments are performed with initial states whose energy and momentum are rather well defined. Since energy and momentum are conserved, this means that at certain energies some of the channels may not be accessible. For example, the original process of interest (B.1), cannot occur when the incident kinetic energy is insufficient to overcome the binding energy of (bc). In fact, in our model there are four *threshold* energies, at each of which one of the four channels "opens up". Thus, if we suppose that the energies of the three bound states (bc), $(bc)^*$, and (ac) occur in the order

$$E_{(bc)} < E_{(bc)^*} < E_{(ac)} < 0$$

then for energies below $E_{(bc)}$ there may be bound states of all three particles but there are no scattering states. In the energy range between $E_{(bc)}$ and $E_{(bc)^*}$ we can scatter a off (bc) but no inelastic processes can occur, thus, only elastic scattering of $a + (bc)$ is possible and, as we shall see, it is given by an amplitude with all the general properties (invariance properties, partial-wave decomposition, etc.) of the elastic amplitude of App. A. For energies between $E_{(bc)^*}$ and $E_{(ac)}$ excitation is possible, and there are two open channels allowing four possible processes. At $E_{(ac)}$ the channel $b + (ac)$ opens up and there are then three open channels and nine possible processes. And finally at $E = 0$, the disintegration channel $a + b + c$ opens up, therefore in the case of $E \geq 0$ there are four open channels, and all 16 processes are possible.

Our simple model should make clear all of the essential descriptive ideas related to the concept of a channel. In general a channel is simply a set of particles (elementary or composite) that can enter or leave a collision. In nonrelativistic theory one deals with systems of a fixed number of elementary particles, $i = 1, ..., N$. We shall always take as channel 0 that in which all N particles move freely. The remaining channels $\alpha = 1, 2, ...$ are groupings of the particles into n_α stable fragments ($2 \leq n_\alpha < N$) each of which is either one of the original particles or some definite bound state of some of them. The reason that the fragment must be stable is that the channels specify the grouping of particles in the asymptotic free states, which are defined as $t \to \pm\infty$. Since only a stable particle can live an infinitely long time, it is clear that -in principle at least- it makes no sense to speak of a channel containing unstable fragments.

Nonetheless, scattering experiments are done with unstable particles. The atomic physicist measures cross sections for excitation of atoms, even though the excited atom will eventually decay back to its ground state. One of the nuclear physicist's most important tools is the unstable neutron; and almost all elementary particles are unstable -many with exceedingly short lifetime. The point is that whenever one speaks of a scattering experiment involving unstable incident or outgoing fragment, the lifetime of these fragments, however short, is nonetheless much longer than the characteristic time of the actual collision. Thus, one can wait for what is (as regards the collision) an "infinitely" long time and still observe the unstable fragments well before they decay.

In this work we shall always assume that for any process under consideration all initial and final fragments of interest are stable. It should be emphasized that to identify a channel it is necessary to specify both the grouping of the particles and the internal state of each group. Thus, in our three-particle example, the channels

$$\begin{gathered} a + b + c \\ a + (bc) \\ b + (ac) \end{gathered}$$

are distinguishable by the arrangement of the particles into groups, while the channels

$$\begin{gathered} a + (bc) \\ a + (bc)^* \end{gathered}$$

have the same grouping and are distinguished by different internal states of (bc) and $(bc)^*$.

The number of channels for a given system can be either finite or infinite. In our model, which can be regarded as typical of nuclear physics in this respect, the number is finite. But when there are attractive Coulomb forces the number is generally infinite. (For example, the $e - H$ system has an infinite number of channels, since the hydrogen atom has infinitely many bound states.) For simplicity of discussion we shall suppose that the number of channels, $\alpha = 0, 1, ..., n$, is finite, although very little is changed when n becomes infinite.

It should also be emphasized that there are various different possible choices for the zero of energy. In the preceding discussion we have taken the energy when all three particles are well separated and stationary as our zero. Theoretically, this is the most natural choice (in nonrelativistic problems) since the total energy is then just the sum of all kinetic energies plus all potentials (each of which goes to zero for large separation). However it should be borne in mind that for an experimental starting, for example, in the channel $a + (bc)$, a very natural choice for zero-point would be the energy of a and (bc) when well separated and stationary. This choice differs from the previous one by the amount $E_{(bc)}$.

B.2 Channel Hamiltonian and Asymptotic States

In this section we discuss the quantum-mechanical evolution of a collision experiment. The discussion will proceed as a natural generalization of the one-channel discussion of App. A. In particular, the three essential results that lead up to the introduction of the S operator -the asymptotic condition, the orthogonality theorem and asymptotic completeness- are close analogues of the corresponding results of the one channel case.

The time development of any state is determined by the Hamiltonian which we take to have the form

$$H = \sum_{i=1}^{N} \frac{\mathbf{p}_i^2}{2m_i} + \sum_{i=1}^{N-1} \sum_{j=i+1}^{N} V_{ij}(\mathbf{x}_{ij}) \equiv H^0 + V \tag{B.3}$$

where $\mathbf{x}_{ij} = \mathbf{x}_i - \mathbf{x}_j$ and H^0 is the sum of the N kinetic energies. In terms of this Hamiltonian the general orbit of the system has the usual form ($\hbar = 1$)

$$U(t)|\psi\rangle \equiv e^{-iHt}|\psi\rangle \tag{B.4}$$

where now, of course, $|\psi\rangle$ is any vector in the N-particle Hilbert space $\mathcal{H} = \mathcal{L}^2(\mathcal{R}^{3N})$ defined by wave functions of the N coordinates,

$$\psi(\mathbf{x}_1, ..., \mathbf{x}_N) \equiv \psi(\widetilde{x})$$

Here we have introduced a tilde to denote the set of all particle coordinates

$$\widetilde{x} \equiv (\mathbf{x}_1, ..., \mathbf{x}_N).$$

Returning to our three-particle model, the Hamiltonian, takes the form

$$H = H^0 + V = \frac{\mathbf{p}_a^2}{2m_a} + \frac{\mathbf{p}_b^2}{2m_b} + \frac{\mathbf{p}_c^2}{2m_c} + V_{ab}(\mathbf{x}_{ab}) + V_{ac}(\mathbf{x}_{ac}) + V_{bc}(\mathbf{x}_{bc}) \tag{B.5}$$

Let us now consider a scattering orbit originating in channel 0; that is, which originated as three freely moving particles, $a + b + c$. For such an orbit we naturally expect that

$$e^{-iHt}|\psi\rangle \quad \xrightarrow[t \to -\infty]{} \quad e^{-iH^0 t}|\psi_{in}\rangle \tag{B.6}$$

for some *in* state $|\psi_{in}\rangle$. We shall see that this result, and a corresponding result for *out* asymptotes are indeed true for the appropriate states $|\psi\rangle$, and that they are true for exactly the same reason as before - as the three particles move apart all of their interactions cease to have any effect.

Suppose however we consider an orbit $U(t)|\psi\rangle$ which originated in channel 1, $a + (bc)$. When the two particles a and (bc) move apart (as we follow the orbit back in time) the interactions V_{ab} and V_{ac} between the particle a and the two particles b and c become ineffective. On the other hand the interaction V_{bc} between b and c can never lose its importance. Indeed, it is only because of $V_{(bc)}$ that the bound state (bc) remains bound. Thus, for an orbit that originated in channel 1, the part of H that is effective long before the collision is not H^0 but, rather, the "channel 1 Hamiltonian"

$$H^1 = \frac{\mathbf{p}_a^2}{2m_a} + \frac{\mathbf{p}_b^2}{2m_b} + \frac{\mathbf{p}_c^2}{2m_c} + V_{bc} \tag{B.7}$$

and for such an orbit we must expect that

$$e^{-iHt}|\psi\rangle \quad \xrightarrow[t \to -\infty]{} \quad e^{-iH^1 t}|\psi_{in}\rangle \tag{B.8}$$

for some $|\psi_{in}\rangle$.

It is important to note that if the orbit $U(t)|\psi\rangle$ does originate in channel 1, then the wave function of $|\psi_{in}\rangle$ must describe a state in which the position $\mathbf{x}_a$ of particle a and $\overline{\mathbf{x}}_{bc}$ of the center of mass of (bc) move arbitrarily, but the *relative motion* of b and c is fixed as that appropriate to the bound state (bc); that is,

$$\langle \widetilde{x}|\psi_{in}\rangle = \chi(\mathbf{x}_a, \overline{\mathbf{x}}_{bc})\phi_{(bc)}(\mathbf{x}_{bc}) \tag{B.9}$$

Here $\chi(\mathbf{x}_a, \overline{\mathbf{x}})$ describes the motion of the incident particles a and (bc) and is an arbitrary normalizable function of $\mathbf{x}_a$ and the center of mass $\overline{\mathbf{x}}_{bc}$ of b and c. On the other hand $\phi_{(bc)}(\mathbf{x}_{bc})$ is uniquely determined as the wave function for the internal motion of the bound state (bc). Thus, not every vector in $\mathcal{H}$ can label an *in* asymptote of channel 1; only those vectors in the subspace $\mathcal{L}^1 \subset \mathcal{H}$ made up from wave functions of the form (B.9) can label an *in* asymptote of channel 1. This subspace $\mathcal{L}^1$ is called the *channel 1 subspace* and consist of those vectors that can label *in* or *out* asymptote in channel 1.

The action of the channel Hamiltonian H^1 on the vectors of $\mathcal{L}^1$ is especially simple. By going into the relative and center of mass coordinates of the particles b and c we can write

$$H^1 = \frac{\mathbf{p}_a^2}{2m_a} + \frac{\overline{\mathbf{p}}_{bc}^2}{2M_{bc}} + (\frac{\mathbf{p}_{bc}^2}{2m_{bc}} + V_{bc}) \tag{B.10}$$

$$\tag{B.11}$$

where $\overline{\mathbf{p}}_{bc}$ and $\mathbf{p}_{bc}$ are the total and relative momentum operators for b and c, while M_{bc} and m_{bc} are their total and reduced masses. It is clear that the

asymptotic behavior (B.8) can be rewritten as

$$e^{-iHt}|\psi\rangle \xrightarrow[t \to -\infty]{} e^{-iH^1 t}|\psi_{in}\rangle = \exp\left[-i\left(\frac{\mathbf{p}_a^2}{2m_a} + \frac{\overline{\mathbf{p}}_{bc}^2}{2M_{bc}} + E_{(bc)}\right)t\right]|\psi_{in}\rangle \tag{B.12}$$

That is, the asymptotic behavior is just that of two freely moving particles - of masses m_a and $M_{bc} = (m_b + m_c)$ - except for the additional phase factor $exp(-iE_{(bc)}t)$. Here $E_{(bc)}$ is the eigenenergy of the relative Hamiltonian corresponding to the bound state $\phi_{(bc)}(\mathbf{x}_{bc})$; that is

$$\left(\frac{\mathbf{p}_{bc}^2}{2m_{bc}} + V_{bc}\right)\phi_{(bc)}(\mathbf{x}_{bc}) = E_{(bc)}\phi_{(bc)}(\mathbf{x}_{bc}) \tag{B.13}$$

Exactly parallel consideration apply to all other channels. In the general N-particle case, for a channel α, the corresponding channel Hamiltonian H^α is obtained by deleting from H those potentials that link different fragments,

$$H^\alpha = H - \sum{}' V_{ij} \tag{B.14}$$

Where $\sum'$ denotes a sum over all pairs ij for which particles i and j belong to different fragments of channel α - when the two particles i and j move apart (as we follow the orbit back in time) the interactions V_{ij} become ineffective -.

The *in* and *out* asymptotes in channel α are identified by wave functions in the subspace $\mathcal{L}^\alpha$ comprising those functions with the form

$$\chi(\mathbf{y}_1, ..., \mathbf{y}_{n_\alpha})\phi_1(z_1)...\phi_{n_\alpha}(z_{n_\alpha})$$

where χ is an arbitrary function of the centers of mass $\mathbf{y}_1, ..., \mathbf{y}_{n_\alpha}$ of the n_α fragments. The term $\phi_\nu(z_\nu)$ is the bound-state wave function of the ν^{th} fragment with internal coordinates z_ν. (If the ν^{th} fragment happens to be a single particle, then $\phi_\nu \equiv 1$.)

B.2.1 Asymptotic condition

If the particle interactions $V_{ij}(\mathbf{x}_{ij})$ all satisfy our usual assumptions, then for every vector $|\psi_{in}\rangle$ in any channel subspace $\mathcal{L}^\alpha$ there is a vector $|\psi\rangle$ that satisfies

$$e^{-iHt}|\psi\rangle \quad \xrightarrow[t \to -\infty]{} \quad e^{-iH^\alpha t}|\psi_{in}\rangle \tag{B.15}$$

and which is given in terms of a channel Møller operator $\mathbf{\Omega}_+^\alpha$ as

$$|\psi\rangle = \mathbf{\Omega}_+^\alpha|\psi_{in}\rangle = \lim_{t \to -\infty} e^{iHt}e^{-iH^\alpha t}|\psi_{in}\rangle \tag{B.16}$$

and similarly for every $|\psi_{out}\rangle$ in $\mathcal{L}^\alpha$ as $t \to +\infty$, with $|\psi\rangle = \mathbf{\Omega}_-^\alpha|\psi_{out}\rangle$. It should be emphasized that there are separate Møller operators $\mathbf{\Omega}_\pm^\alpha$ for each channel α and that they are defined by the limit (B.16) only for those vectors in $\mathcal{L}^\alpha$. In fact, we shall find that $\mathcal{L}^\alpha$ is the largest space on which we need to define $\mathbf{\Omega}_\pm^\alpha$.

The asymptotic condition guarantees that every vector in the channel subspace $\mathcal{L}^\alpha$ labels a possible *in* or *out* asymptotic in channel α. If $|\psi_{in}\rangle$ is in $\mathcal{L}^\alpha$ then the vector

$$|\psi\rangle = \mathbf{\Omega}_+^\alpha |\psi_{in}\rangle \tag{B.17}$$

is that actual state of the system which has developed from the *in* state labelled by $|\psi_{in}\rangle$ in channel α. Similarly, if $|\psi_{out}\rangle$ is in $\mathcal{L}^\alpha$, then

$$|\psi\rangle = \mathbf{\Omega}_-^\alpha |\psi_{out}\rangle \tag{B.18}$$

is the state that will develop into the *out* state $|\psi_{out}\rangle$ in channel α.

With this result we can calculate the probability that a system that enters a collision in channel α with *in* asymptote $|\phi\rangle$ (in $\mathcal{L}^\alpha$) be observed to leave in channel α' with *out* asymptote $|\phi'\rangle$ (in $\mathcal{L}^{\alpha'}$). If the *in* state was $|\phi\rangle$ in channel α, then the actual state at $t = 0$ would be $\mathbf{\Omega}_+^\alpha|\phi\rangle$. If the *out* state was going to be $|\phi'\rangle$ in channel α', then the actual state at $t = 0$ would have to be $\mathbf{\Omega}_-^{\alpha'}|\phi'\rangle$. The required probability amplitude is just the overlap of these two states

$$w(\phi', \alpha' \leftarrow \phi, \alpha) = |\langle\phi'|\mathbf{\Omega}_-^{\alpha'\dagger}\mathbf{\Omega}_+^\alpha|\phi\rangle|^2 \tag{B.19}$$

B.2.2 Orthogonality and asymptotic completeness

Just as in single-channel scattering any state that has developed from some *in* asymptote (or will develop into some *out* asymptote) should be orthogonal to any bound state of all N particles. In addition, we would expect that any two states that have developed from *in* asymptotic in (or will develop into *out* asymptotes of) different channels should be mutually orthogonal. These results are the content of the orthogonality theorem.

Orthogonality Theorem. Let $|\phi\rangle$ be any bound state of all N particles and let

$$\begin{aligned} |\psi\rangle &= \mathbf{\Omega}_+^\alpha|\psi_{in}\rangle \\ |\psi'\rangle &= \mathbf{\Omega}_+^{\alpha'}|\psi'_{in}\rangle \end{aligned} \tag{B.20}$$

with $|\psi_{in}\rangle$ in $\mathcal{L}^\alpha$ and $|\psi'_{in}\rangle$ in $\mathcal{L}^{\alpha'}$ and $\alpha \neq \alpha'$. Then

$$\langle\phi|\psi\rangle = \langle\phi|\psi'\rangle = \langle\psi|\psi'\rangle = 0$$

and likewise with $\mathbf{\Omega}_+^\alpha$ replaced by $\mathbf{\Omega}_-^\alpha$ (and "in" by "out") in (B.20).

By defining $\mathcal{B}$ to be the subspace spanned by the bound states of all N particles and $\mathcal{R}_\pm^\alpha$ to be the ranges of $\mathbf{\Omega}_\pm^\alpha$, i.e., $\mathcal{R}_+^\alpha$ is the subspace of all states that originated in the *in* channel α, while $\mathcal{R}_-^\alpha$ is the subspace of all states that will terminate in the *out* channel α, the theorem can be stated alternatively as:

$$\mathcal{B}\perp\mathcal{R}_+^\alpha\perp\mathcal{R}_+^{\alpha'} \quad [\text{all} \quad \alpha, \alpha'; \quad \alpha \neq \alpha']$$

and similarly,

$$\mathcal{B}\perp\mathcal{R}_-^\alpha\perp\mathcal{R}_-^{\alpha'} \quad [\text{all} \quad \alpha, \alpha'; \quad \alpha \neq \alpha'].$$

So far we have discussed only those scattering orbits that have developed from a definite *in* channel, or will develop into some definite *out* channel. These are certainly not the most general kind of scattering orbits. For example, suppose that $|\psi^1\rangle$ and $|\psi^2\rangle$ are states that have developed from *in* asymptotes in two different channels, $\alpha = 1$ and $\alpha = 2$ (say),

$$|\psi^1\rangle = \mathbf{\Omega}_+^1 |\psi_{in}^1\rangle$$

and

$$|\psi^2\rangle = \mathbf{\Omega}_+^2 |\psi_{in}^2\rangle$$

Then the superposition principle asserts that the vector $|\psi\rangle = |\psi^1\rangle + |\psi^2\rangle$ defines an allowed physical state, and we can ask the question: **what is the asymptotic form of the orbit defined by $|\psi\rangle$?** Now, we know that as $t \to -\infty$

$$e^{-iHt}|\psi^1\rangle \quad \longrightarrow \quad e^{-iH^1 t}|\psi_{in}^1\rangle$$

and

$$e^{-iHt}|\psi^2\rangle \quad \longrightarrow \quad e^{-iH^2 t}|\psi_{in}^2\rangle$$

Adding these two results we immediately see that the orbit defined by $|\psi^1\rangle + |\psi^2\rangle$ has the asymptotic form

$$e^{-iHt}(|\psi^1\rangle + |\psi^2\rangle) \quad \longrightarrow \quad e^{-iH^1 t}|\psi_{in}^1\rangle + e^{-iH^2 t}|\psi_{in}^2\rangle$$

That is, this orbit originates as a *superposition of states* in the two *in* channels 1 and 2.

Having once recognized the existence of orbits that originate as a superposition of two *in* channels, we must obviously expect that the most general scattering orbit would be one which originated as a superposition of all possible *in* channels.

$$e^{-iHt}|\psi\rangle \quad \xrightarrow[t \to -\infty]{} \quad e^{-iH^0 t}|\psi_{in}^0\rangle + \cdots + e^{-iH^n t}|\psi_{in}^n\rangle \tag{B.21}$$

where each ψ_{in}^α lies in the appropriate channel subspace $\mathcal{L}^\alpha$ and

$$|\psi\rangle = \mathbf{\Omega}_+^0 |\psi_{in}^0\rangle + \cdots + \mathbf{\Omega}_+^n |\psi_{in}^n\rangle \tag{B.22}$$

In the asymptotic form (B.21) it is natural to regard each term $exp(-iH^\alpha t)|\psi_{in}^\alpha\rangle$ as the component of the *in* asymptote in the channel α. The general *in* asymptote can be identified by giving the sequence

$$|\psi_{in}\rangle = \left\{|\psi_{in}^0\rangle, \ldots, |\psi_{in}^n\rangle\right\} \tag{B.23}$$

in the space

$$\mathcal{H}_{as} = \mathcal{L}^0 \oplus \cdots \oplus \mathcal{L}^n \tag{B.24}$$

where each $|\psi_{in}^{\alpha}\rangle$ identifies the component of the incoming asymptotic behavior in the corresponding channel α. The new space $\mathcal{H}_{as}$, which we call the space of asymptotic states, is (in an obvious sense) bigger than $\mathcal{H}$, since $\mathcal{L}^0$ alone is equal to $\mathcal{H}$.

In the same way we should expect the general scattering orbit to evolve as $t \to +\infty$ into a superposition of all possible out channels

$$e^{-iHt}|\psi\rangle \quad \xrightarrow[t \to +\infty]{} \quad e^{-iH^0 t}|\psi_{out}^0\rangle + \cdots + e^{-iH^n t}|\psi_{out}^n\rangle \tag{B.25}$$

with

$$|\psi\rangle = \mathbf{\Omega}_-^0|\psi_{out}^0\rangle + \cdots + \mathbf{\Omega}_-^n|\psi_{out}^n\rangle \tag{B.26}$$

This asymptotic form is, of course, identified by the sequence

$$|\psi_{out}\rangle = \left\{|\psi_{out}^0\rangle, \ldots, |\psi_{out}^n\rangle\right\} \tag{B.27}$$

in space $\mathcal{H}_{as}$.

It should be noted that in practice the *in* state always lies in one definite channel α and, hence, is given by a sequence

$$\{0, \ldots, 0, |\psi_{in}^{\alpha}\rangle, 0, \ldots, 0\} \tag{B.28}$$

On the other hand the *out* state is usually a superposition of several channels and has the general form (B.27) with several nonzero components (except of course in the special case where all inelastic processes are energetically impossible). According to (B.22), we can define a linear operator $\mathbf{\Omega}_+$ on our new space $\mathcal{H}_{as}$ as

$$\begin{aligned} \mathbf{\Omega}_+|\psi_{in}\rangle &= \mathbf{\Omega}_+\left\{|\psi_{in}^0\rangle, \ldots, |\psi_{in}^n\rangle\right\} \\ &= \mathbf{\Omega}_+^0|\psi_{in}^0\rangle + \cdots + \mathbf{\Omega}_+^n|\psi_{in}^n\rangle \end{aligned} \tag{B.29}$$

which maps $\mathcal{H}_{as}$ into $\mathcal{H}$ and for each *in* asymptote labelled by $|\psi_{in}\rangle$, the corresponding actual state at $t = 0$ is just $|\psi\rangle = \mathbf{\Omega}_+|\psi_{in}\rangle$. Similarly, we can define $\mathbf{\Omega}_-$ so that the actual state at $t = 0$ corresponding to any out asymptotic $|\psi_{out}\rangle$ is just $|\psi\rangle = \mathbf{\Omega}_-|\psi_{out}\rangle$.

Asymptotic Completeness. A multichannel scattering theory is asymptotically complete if the scattering states $|\psi\rangle$ [satisfying (B.21) and (B.25)] together with the bound states should span the space $\mathcal{H}$ of all states. In this case $\mathcal{H}$ can be written as the direct sum

$$\mathcal{H} = \mathcal{B} \oplus \mathcal{R}$$

Where $\mathcal{B}$ is the space spanned by the bound states of all N particles, while $\mathcal{R}$ is the space spanned by the scattering states, which has to be the direct sum:

$$\mathcal{R} = \mathcal{R}_+^0 \oplus \cdots \oplus \mathcal{R}_+^n = \mathcal{R}_-^0 \oplus \cdots \oplus \mathcal{R}_-^n \tag{B.30}$$

and $\mathcal{R}_{\pm}^{\alpha}$ is the subspace of all states that originated as (or will develop into) an asymptotic state in channel α.

Asymptotic completeness for a three-body system with suitable potentials was proved by Faddeev in 1965 [96] and his proof was extended to the N-body case by Hepp in 1969 [97].

It should be emphasized that the subspace $\mathcal{R}_{+}^{\alpha}$ and $\mathcal{R}_{-}^{\alpha}$ are not in general the same. Indeed, if it were true that $\mathcal{R}_{+}^{\alpha} = \mathcal{R}_{-}^{\alpha}$, then every orbit that came from the *in* channel α must necessarily evolve into the same *out* channel α; that is, no inelastic processes could occur. The observed fact that inelasticity *does* occur implies that each $\mathcal{R}_{+}^{\alpha}$ overlaps several of the spaces $\mathcal{R}_{-}^{0}, \ldots, \mathcal{R}_{-}^{n}$ and vice versa.

The two decompositions of $\mathcal{R}$ on the direct sums (B.30) express the fact that every scattering state can be written as a superposition of states each of which originated in a definite *in* channel α, and also as a superposition of states each of which will develop into a definite *out* channel α. This implies that every scattering orbit has *in* and *out* asymptotes of the forms (B.23) and (B.27).

Provided the theory is asymptotically complete, $\mathbf{\Omega}_{\pm}$ are actually isometric from $\mathcal{H}_{as}$ onto $\mathcal{R}$, the space of scattering states, that is, its domain is $\mathcal{H}_{as}$, its range $\mathcal{R}$, and it preserves the norm. The situation is as follows:

$$\mathcal{H}_{as} \xrightarrow[\mathbf{\Omega}_{+}]{isometric} \mathcal{R} \xleftarrow[\mathbf{\Omega}_{-}]{isometric} \mathcal{H}_{as} \tag{B.31}$$

or, in terms of vectors,

$$|\psi_{in}\rangle \xrightarrow[\mathbf{\Omega}_{+}]{} |\psi\rangle \xleftarrow[\mathbf{\Omega}_{-}]{} |\psi_{out}\rangle \tag{B.32}$$

The analogy with the single-channel problem is now complete. In particular, we can invert

$$|\psi\rangle = \mathbf{\Omega}_{-}|\psi_{out}\rangle \tag{B.33}$$

to give

$$|\psi_{out}\rangle = \mathbf{\Omega}_{-}^{\dagger}|\psi\rangle = \mathbf{\Omega}_{-}^{\dagger}\mathbf{\Omega}_{+}|\psi_{in}\rangle \tag{B.34}$$

Thus, if we define the scattering operator

$$\mathbf{S} = \mathbf{\Omega}_{-}^{\dagger}\mathbf{\Omega}_{+} \tag{B.35}$$

then S maps each *in* asymptote onto the corresponding *out* asymptote

$$|\psi_{out}\rangle = \mathbf{S}|\psi_{in}\rangle \tag{B.36}$$

Since S is isometric from $\mathcal{H}_{as}$ onto $\mathcal{H}_{as}$, it is actually unitary.

The probability amplitude for a system that enters a collision with *in* asymptote given by $|\phi\rangle$ in $\mathcal{H}_{as}$ to be observed leaving with out asymptote $|\phi'\rangle$ is just the matrix element $\langle\phi'|\mathbf{S}|\phi\rangle$,

$$w(\phi' \leftarrow \phi) = |\langle\phi'|\mathbf{S}|\phi\rangle|^2 \tag{B.37}$$

or

$$w(\phi' \leftarrow \phi) = |\langle \phi' | \mathbf{\Omega}_-^\dagger \mathbf{\Omega}_+ | \phi \rangle|^2 \tag{B.38}$$

In practice, the experimental initial state is prepared in a definite channel and the *in* asymptote $|\phi\rangle$ has the form

$$|\phi\rangle = \{0, \ldots, 0, |\phi\rangle, \ldots, 0\}$$

with $|\phi\rangle$ in a definite $\mathcal{L}^\alpha$. The corresponding *out* state $\mathbf{S}|\phi\rangle$ is naturally not (in general) in any definite channel. However, in practice one always monitors for a final state that *does* lie in a definite channel, that is, in practice we are interested in a $|\phi'\rangle$ of the form

$$|\phi'\rangle = \{0, \ldots, 0, |\phi'\rangle, \ldots, 0\}$$

with $|\phi'\rangle$ in a definite $\mathcal{L}^{\alpha'}$. For these states we have

$$\mathbf{\Omega}_+ |\phi\rangle = \mathbf{\Omega}_+^\alpha |\phi\rangle \tag{B.39}$$

and

$$\mathbf{\Omega}_- |\phi'\rangle = \mathbf{\Omega}_-^\alpha |\phi'\rangle \tag{B.40}$$

Thus, for such states the probability (B.37) can be written as

$$w(\phi', \alpha' \leftarrow \phi, \alpha) = |\langle \phi' | \mathbf{\Omega}_-^{\alpha'\dagger} \mathbf{\Omega}_+^\alpha | \phi \rangle|^2 \tag{B.41}$$

This is precisely the result quoted in (B.19) and serves to emphasize that if one is interested solely in the computation of transition probabilities between two different channels, it is actually unnecessary to introduce $\mathcal{H}_{as}$. It is only if we wish to express the required probability amplitudes as matrix elements of a single unitary operator S that this space is needed.

B.3 The Momentum-Space Basis Vectors

The momentum-space basis of H_{as} is a generalization of the basis of plane-wave states $|\mathbf{p}\rangle$ used in the one-particle case, and of the corresponding states $|\mathbf{p}_1, \mathbf{p}_2\rangle \equiv |\overline{\mathbf{p}}, \mathbf{p}\rangle$ in the two-particle problem. For simplicity we discuss first our simple model of three particle a, b, c introduced in the previous sections.

Since $\mathcal{H}_{as}$ is the direct sum of the channel spaces $\mathcal{L}^\alpha$ we can begin by constructing a basis for each $\mathcal{L}^\alpha$. We start with the channel 0, in which a, b, and c all move freely, and for which the general asymptote is labelled by an arbitrary wave function $\chi(\mathbf{x}_a, \mathbf{x}_b, \mathbf{x}_c)$ of all these positions. The appropriate basis is clearly given by the three particle momentum eigenstates:

$$|\mathbf{p}_a, \mathbf{p}_b, \mathbf{p}_c; 0\rangle \equiv |\widetilde{p}, 0\rangle \tag{B.42}$$

with corresponding wave functions

$$\langle \widetilde{x} | \widetilde{p}, 0\rangle = (2\pi)^{-9/2} \exp\left[i(\mathbf{p}_a \cdot \mathbf{x}_a + \mathbf{p}_b \cdot \mathbf{x}_b + \mathbf{p}_c \cdot \mathbf{x}_c)\right] \tag{B.43}$$

and normalization

$$\langle \widetilde{p}', 0|\widetilde{p}, 0\rangle = \delta_3(\mathbf{p}'_a - \mathbf{p}_a)\delta_3(\mathbf{p}'_b - \mathbf{p}_b)\delta_3(\mathbf{p}'_c - \mathbf{p}_c) \equiv \delta_9(\widetilde{p}' - \widetilde{p}) \tag{B.44}$$

[$\widetilde{p}$ stands for the set $(\mathbf{p}_a, \mathbf{p}_b, \mathbf{p}_c)$ and 0 is the channel number $\alpha = 0$.] These vectors are, of course, eigenvectors of the free Hamiltonian,

$$H^0|\widetilde{p}, 0\rangle = \left(\frac{\mathbf{p}_a^2}{2m_a} + \frac{\mathbf{p}_b^2}{2m_b} + \frac{\mathbf{p}_c^2}{2m_c}\right)|\widetilde{p}, 0\rangle \equiv E_p^0|\widetilde{p}, 0\rangle \tag{B.45}$$

In channel 1, $a + (bc)$, the asymptotes are identified by wave functions

$$\chi(\mathbf{x}_a, \overline{\mathbf{x}}_{bc})\phi_{(bc)}(\mathbf{x}_{bc}) \tag{B.46}$$

where χ is an arbitrary function of the position $\mathbf{x}_a$ and the center of mass $\overline{\mathbf{x}}_{bc}$ of b and c, while $\phi_{(bc)}$ is the bound-state wave function of (bc). Since $\phi_{(bc)}$ is fixed these functions can be spanned by products of plane waves in $\mathbf{x}_a$ and $\overline{\mathbf{x}}_{bc}$ with the fixed function $\phi_{(bc)}(\mathbf{x}_{bc})$. The appropriate basis vectors are:

$$|\mathbf{p}_a, \overline{\mathbf{p}}_{bc}; 1\rangle \equiv |\widetilde{p}, 1\rangle \tag{B.47}$$

with wave functions

$$\langle \widetilde{x}|\widetilde{p}, 1\rangle = (2\pi)^{-3} \exp\left[i(\mathbf{p}_a \cdot \mathbf{x}_a + \overline{\mathbf{p}}_{bc} \cdot \overline{\mathbf{x}}_{bc})\right] \phi_{(bc)}(\mathbf{x}_{bc}) \tag{B.48}$$

and normalization

$$\langle \widetilde{p}', 1|\widetilde{p}, 1\rangle = \delta_3(\mathbf{p}'_a - \mathbf{p}_a)\delta_3(\overline{\mathbf{p}}'_{bc} - \overline{\mathbf{p}}_{bc}) \equiv \delta_6(\widetilde{p}' - \widetilde{p}) \tag{B.49}$$

These vectors represent states in which particle a moves with momentum $\mathbf{p}_a$, while b and c are bound together into the bound state (bc), whose CM moves with momentum $\overline{\mathbf{p}}_{bc}$.

The energy operator for asymptotic states in channel 1 is the channel Hamiltonian H^1, and the vectors $|\widetilde{p}, 1\rangle$ are, of course, eigenvectors of this operator,

$$H^1|\widetilde{p}, 1\rangle = \left(\frac{\mathbf{p}_a^2}{2m_a} + \frac{\overline{\mathbf{p}}_{bc}^2}{2M_{bc}} + E_{(bc)}\right)|\widetilde{p}, 1\rangle \equiv E_{\widetilde{p}}^1|\widetilde{p}, 1\rangle \tag{B.50}$$

where $E_{(bc)}$ is the internal energy of the bound state (bc). Thus, the improper vectors $|\widetilde{p}, 1\rangle$ will represent *in* and *out* states of definite energy $E_{\widetilde{p}}^1$ in channel 1.

The momentum basis vectors for the other channels are constructed in exactly the same way.

The construction of the corresponding bases of $\mathcal{L}^\alpha$ in the general N-particle problem is entirely straightforward and need not be spelled out here. We mention only that, since the general channel α has n_α freely moving fragments, the corresponding basis vector has the form $|\widetilde{p}, \alpha\rangle$ where $\widetilde{p}$ labels the n_α momenta of these fragments.

Since $\mathcal{H}_{as}$ is the direct sum

$$\mathcal{H}_{as} = \mathcal{L}^0 \oplus \cdots \oplus \mathcal{L}^n \tag{B.51}$$

we can obtain an orthonormal basis of $\mathcal{H}_{as}$ by combining any orthonormal bases of $\mathcal{L}^0, \ldots, \mathcal{L}^n$. In particular, the vectors $|\widetilde{p}, \alpha\rangle$ (α fixed, all $\widetilde{p}$) are an (improper) orthonormal basis of $\mathcal{L}^\alpha$ and, hence, the set of vectors

$$\{0, \ldots, 0, |\widetilde{p}, \alpha\rangle, 0, \ldots, 0\} \equiv |\widetilde{p}, \alpha\rangle \quad [\alpha = 0, \ldots, n; \text{ all } \widetilde{p}] \tag{B.52}$$

is the desired momentum basis of $\mathcal{H}_{as}$. It should be noted that to span $\mathcal{H}_{as}$ we must include all momenta and all channels.

The basis vector (B.52) represents an asymptote with momenta $\widetilde{p}$ lying completely in the channel α. We use the same symbol $|\widetilde{p}, \alpha\rangle$ both for the basis vectors of $\mathcal{L}^\alpha$ in $\mathcal{H}$, and for the sequence in $\mathcal{H}_{as}$. In practice it will always be clear which kind of vector is being used, and this imprecise usage will cause no confusion. With this convention the orthonormality of our basis of $\mathcal{H}_{as}$ is expressed as

$$\langle \widetilde{p}', \alpha' | \widetilde{p}, \alpha \rangle = \delta_{\alpha'\alpha} \delta(\widetilde{p}' - \widetilde{p}) \tag{B.53}$$

where the factor $\delta_{\alpha'\alpha}$ reflects the orthogonality (as vectors of $\mathcal{H}_{as}$) of any two vectors belonging to different channels. With respect to this basis the S operator becomes a matrix with elements $\langle \widetilde{p}', \alpha' | \mathbf{S} | \widetilde{p}, \alpha \rangle$ and knowledge of all of these elements is equivalent to knowledge of $\mathbf{S}$. Similarly, an operator equation like the unitarity equation $\mathbf{S}^\dagger \mathbf{S} = 1$ becomes the matrix equation

$$\sum_{\alpha''} \int d\widetilde{p}'' \langle \widetilde{p}', \alpha' | \mathbf{S}^\dagger | \widetilde{p}'', \alpha'' \rangle \langle \widetilde{p}'', \alpha'' | \mathbf{S} | \widetilde{p}, \alpha \rangle = \delta_{\alpha'\alpha} \delta(\widetilde{p}' - \widetilde{p}) \tag{B.54}$$

To conclude this section we remark that so far we have assumed that all particles are spinless and that all bound states have zero orbital angular momentum. The inclusion of either kind of angular momentum into our formalism is completely straightforward. Suppose, for instance, that in our three-particle model the particle a has spin s and that the state (bc) has orbital angular momentum l. Let us then consider an asymptotic state (either *in* or *out*) in which a and (bc) move freely. There are various possible orientations of the spin of particle a, and similarly, of the orbital momentum of (bc); and it is natural to regard these as being different "spin" orientations *all within the same channel*. Thus, we denote as channel 1 *all* free states of a and (bc), and the corresponding momentum eigenvectors we label

$$|\mathbf{p}_a, \overline{\mathbf{p}}_{bc}, m_a, m_{bc}; 1\rangle \tag{B.55}$$

where $\mathbf{p}_a$ and $\overline{\mathbf{p}}_{bc}$ are the momenta of the two fragments, m_a is the z component of the spin of particle a, and m_{bc} is the z component of the orbital angular momentum of (bc). The corresponding wave function has the form

$$(2\pi)^{-3} \exp\left[i(\mathbf{p}_a \cdot \mathbf{x}_a + \overline{\mathbf{p}}_{bc} \cdot \overline{\mathbf{x}}_{bc})\right] \chi^{m_a} \phi(r_{bc}) Y_l^{m_{bc}}(\widehat{\mathbf{x}}_{bc}) \tag{B.56}$$

where χ^{m_a} is the appropriate spinor for particle a, and the last two factors are the radial and angular wave functions of the (bc) bound state.

It should be clear that, at this stage, fragments with spin (either intrinsic or "orbital") are no more than a slight notational complication, and we shall, for the most part, proceed under the simplifying assumption that none of the fragments in any channel have angular momentum.

B.4 Conservation of Energy and the On-Shell T Matrix

We are now in a position to establish conservation of energy, which follows in almost exactly the same way as in the one-channel case. By using the intertwining relations

$$H\mathbf{\Omega}_{\pm}^{\alpha} = \mathbf{\Omega}_{\pm}^{\alpha} H^{\alpha} \quad [\text{on } \mathcal{L}^{\alpha}] \tag{B.57}$$

which follow at once from the definition

$$\mathbf{\Omega}_{\pm}^{\alpha} = \lim_{t \to \mp\infty} e^{iHt} e^{-iH^{\alpha}t} \quad [\text{on } \mathcal{L}^{\alpha}] \tag{B.58}$$

exactly as in App. A, one can show easily that, the S-matrix element $\langle \widetilde{p}', \alpha' | \mathbf{S} | \widetilde{p}, \alpha \rangle$ between initial and final states of energies $E_{\widetilde{p}}^{\alpha}$ and $E_{\widetilde{p}'}^{\alpha'}$ -which we shall abbreviate as E and E' when there is no danger of confusion - is zero unless the initial and final energies are equal; that is, $\mathbf{S}$ conserves energy and its matrix elements contain the expected factor $\delta(E' - E)$.

In addition to conserving energy, $\mathbf{S}$ also conserves total momentum. This is because all potentials involve only the relative positions and the system is therefore translationally invariant. This means that $\mathbf{S}$ commutes with the total momentum operator $\overline{\mathbf{p}} = \sum \mathbf{p}_i$ and, hence, that its matrix elements contain a factor $\delta_3(\overline{\mathbf{p}}' - \overline{\mathbf{p}})$. In fact, we can go further: By using as independent variables the overall CM position $\mathbf{X}$ and any suitable choice of $N-1$ relative coordinates we can factor the space $\mathcal{H}$ (and similarly $\mathcal{H}_{as}$) as

$$\mathcal{H} = \mathcal{H}_{CM} \otimes \mathcal{H}_{rel} \tag{B.59}$$

Here, just as in the two-particle case, $\mathcal{H}_{CM}$ describes the motion of the overall CM, and $\mathcal{H}_{rel}$ the relative motion of the particles. The Hamiltonian can then be written as

$$H = H_{CM} + H_{rel} \tag{B.60}$$

where $H_{CM} = \overline{\mathbf{p}}^2/2M$ and M is the total mass of the system; and just as in two-particle scattering, the S operator factors as

$$\mathbf{S} = 1_{CM} \otimes S \tag{B.61}$$

The operator S describes the relative motion and is the scattering operator one would obtain directly from the Hamiltonian H_{rel}. Just as in the one-channel case all of the physically interesting information is contained in S and much of our subsequent analysis will be in terms of S.

Returning to the matrix elements of $\mathbf{S}$, by combining the consequences of energy and momentum conservation, one obtains

$$\langle \widetilde{p}', \alpha' | \mathbf{S} | \widetilde{p}, \alpha \rangle = \delta_{\alpha'\alpha} \delta(\widetilde{p}' - \widetilde{p}) - 2\pi i \delta(E' - E) \delta_3(\overline{\mathbf{p}}' - \overline{\mathbf{p}}) t(\underline{p}', \alpha' \leftarrow \underline{p}, \alpha) \tag{B.62}$$

Here the *on-shell* T matrix $t(\underline{p}', \alpha' \leftarrow \underline{p}, \alpha)$ depends only the sets of initial and final *relative* momenta, which we denote with a single underscore as $\underline{p}$ and $\underline{p}'$. (That is, $\underline{p}$ denotes the set of $n_\alpha - 1$ suitably chosen relative momenta for the

fragments of channel α.) It is defined only on the energy shell $E' = E$, i.e., for those $\underline{p}$ and $\underline{p}'$ consistent with conservation of energy. It can, of course, be computed directly from the operator S of the relative motion, whose matrix elements $\langle \underline{p}', \alpha' | S | \underline{p}, \alpha \rangle$ have a decomposition similar to (B.62), but without the factor $\delta_3(\overline{\mathbf{p}}' - \overline{\mathbf{p}})$.

The interpretation of the decomposition (B.62) is much the same as in the one-channel case. The first term is the S matrix for no scattering and leaves all momenta and channels unchanged. The second represents the actual scattering; it conserves total energy and total momentum but can in general change the relative momenta and the channel.

The fact that S can only connect states of the same energy leads to important restrictions on what we can call the "channel structure" of the S matrix. To illustrate this, let us return to our three-particle model with its four channels $\alpha = 0, ..., 3$. We can regard the discrete channel indices α' and α in $\langle \underline{p}', \alpha' | S | \underline{p}, \alpha \rangle$ or $t(\underline{p}', \alpha' \leftarrow \underline{p}, \alpha)$ as labelling the rows and columns of a matrix in "channel space", each element of which is a function of the momenta $\underline{p}'$ and $\underline{p}$. In our model we have a matrix with up to four rows and columns. However, at certain energies the dimension is actually less than four as we now discuss. For definiteness we shall confine our attention to the CM frame (that is, we discuss the S matrix of the relative motion), and we now imagine the energy to be increased from some large negative value.

All states in a given channel have energy at least as great as the channel's threshold energy. Thus for energies less than the lowest threshold $E_{(bc)}$ there are no states in any channel and hence, no S matrix. When the energy increases into the range $E_{(bc)} \leq E < E_{(bc)^*}$ there are states in channel 1 but none in any other. Thus, in this energy range, S is a 1×1 "channel-space" matrix

$$\langle \mathbf{p}', 1 | S | \mathbf{p}, 1 \rangle \tag{B.63}$$

which has many of the properties of the one-channel S matrix. For example, if we choose an angular momentum basis of the channel 1 subspace and assume rotational invariance, then exactly the arguments of section A.6 show that

$$\langle E', l', m'; 1 | S | E, l, m; 1 \rangle = \delta(E' - E) \delta_{l'l} \delta_{m'm} e^{2i\delta_l(E)} \qquad (E_{(bc)} \leq E < E_{(bc)^*}) \tag{B.64}$$

where the phase shift $\delta_l(E)$ is real.

If we now increase the energy into the range $E_{(bc)^*} \leq E < E_{(ac)}$ there are states in channel 1 and 2 but in no others. Thus, S becomes a 2×2 "channel-space" matrix:

$$\begin{pmatrix} \langle \mathbf{p}', 1 | S | \mathbf{p}, 1 \rangle & \langle \mathbf{p}', 1 | S | \mathbf{p}, 2 \rangle \\ \langle \mathbf{p}', 2 | S | \mathbf{p}, 1 \rangle & \langle \mathbf{p}', 2 | S | \mathbf{p}, 2 \rangle \end{pmatrix} \tag{B.65}$$

clearly, as we increase the energy past each threshold the corresponding channel opens up and the matrix gains one dimension. Finally, when $E \geq 0$ all channels are open and the S matrix has its full complement of four rows and four columns.

In conclusion, note the relative motion in any two-body channel is specified by a single momentum: the relative momentum of the two fragments. Thus, as

long as only two-body channels are open, each element $\langle \underline{p}', \alpha' | S | \underline{p}, \alpha \rangle$ is in fact labelled by just two momenta $\mathbf{p}'$ and $\mathbf{p}$, as indicated for example in (B.65). In this energy range the multichannel S matrix is more complicated than that of the one-channel problem only inasmuch as it has more than one element. Once the channels with three or more bodies open up, the corresponding matrix elements depend on several variables and the situation is markedly more complicated.

B.5 Cross Section

We must now set about computing the observable cross sections in terms of the on-shell T matrix. Since it is an experimental fact that almost all processes of current interest have two-body initial states, we shall confine our discussion to such processes, and consider a process leading from a two-body *in* channel α to an arbitrary *out* channel α' (with n' bodies). In our three-particle model we could consider any of the processes (B.2). Finally, we work in the CM frame, considering just the relative motion, and take an initial state $|\phi\rangle$ in $\mathcal{L}^\alpha$, prescribed by its momentum-space wave function $\phi(\mathbf{p})$ in the relative momentum $\mathbf{p}$ of the two initial particles which we assume to be well peaked about the mean incident momentum $\mathbf{p}_0$. The corresponding *in* asymptote must, of course, be written as

$$|\psi_{in}\rangle = |\phi\rangle = \{0, \ldots, 0, |\phi\rangle, 0, \ldots, 0\}$$

where $|\phi\rangle$ occupies the α^{th} position.

The probability that, with the given *in* state $|\psi_{in}\rangle = |\phi\rangle$ in channel α, the final particles be observed in channel α' with their momenta in some prescribed volume Δ' about some $\underline{p}'$ in the $(3n'-3)$-dimensional space of the relative momenta of this channel is given by

$$\begin{aligned} w(\Delta', \alpha' \leftarrow \phi, \alpha) &= \int_{\Delta'} d\underline{p}' |\langle \underline{p}', \alpha' | S | \phi \rangle|^2 \\ &\approx \int_{\Delta'} d\underline{p}' |\langle \underline{p}', \alpha' | S | \mathbf{p}, \alpha \rangle|^2 \end{aligned} \tag{B.66}$$

In principle, Δ' can be an arbitrary volume in the space of the final momenta. In the case that the final channel is a two-body channel, then $\underline{p}'$ reduces to a single momentum $\mathbf{p}'$ (the relative momentum of the two final particles) the natural choice for Δ' is the familiar cone defined by an element of solid angle about any fixed direction.

We can replace the S-matrix element by the appropriate multiple of the on-shell T matrix. (For elastic scattering, $\alpha' = \alpha$, this requires that we avoid the forward direction; for inelastic scattering this restriction is unnecessary.) One can obtain for the effective cross section of the target for scattering the packet ϕ into the volume Δ' in channel α' [1]

$$d\sigma(\Delta', \alpha' \leftarrow \phi, \alpha) = (2\pi)^4 \mu \int_{\Delta'} d\underline{p}' \int d^3p \frac{1}{p_\parallel} \delta(E' - E) |t(\underline{p}', \alpha' \leftarrow \mathbf{p}, \alpha)|^2 |\phi(\mathbf{p})|^2 \tag{B.67}$$

where μ denotes the reduced mass of the initial two particles in channel α and $p_\parallel$ is the component of $\mathbf{p}$ along $\mathbf{p}_0$. Provided the *in* wave packet is sufficiently well peaked about its mean momentum (which we now call $\mathbf{p}$) the integral over p disappears as the normalization integral for ϕ and we obtain an answer that is independent of the shape of ϕ and so can be written as

$$d\sigma(\Delta', \alpha' \leftarrow \mathbf{p}, \alpha) = (2\pi)^4 \frac{\mu}{p} \int_{\Delta'} d\underline{p}' \delta(E' - E) |t(\underline{p}', \alpha' \leftarrow \mathbf{p}, \alpha)|^2 \qquad \text{(B.68)}$$

Here we just discuss the simplest case of a two-body final channel [e.g. any of the first three processes in (B.2)]. In this case the final relative momenta $\underline{p}'$ reduce to a single momentum $\mathbf{p}'$ and the volume Δ' is a volume in the corresponding three-dimensional space. Because of energy conservation there is no interest in measurement of the magnitude of $\mathbf{p}'$, and the smallest interesting volume Δ' is the familiar cone defined by the infinitesimal solid angle $d\Omega$. For this case (B.68) becomes

$$d\sigma(\Delta', \alpha' \leftarrow \mathbf{p}, \alpha) = (2\pi)^4 \frac{\mu}{p} d\Omega \int_0^\infty p'^2 dp' \delta(\frac{p'^2}{2\mu'} + W_{\alpha'} - \frac{p^2}{2\mu} - W_\alpha) \otimes |t(\mathbf{p}', \alpha' \leftarrow \mathbf{p}, \alpha)|^2 \qquad \text{(B.69)}$$

Since the energy E in a two-body channel α is $\frac{p^2}{2\mu} + W_\alpha$, where W_α denotes the channel threshold. Rewriting the left-hand side in the familiar form $(d\sigma/d\Omega)d\Omega$ this given

$$\frac{d\sigma}{d\Omega}(\mathbf{p}', \alpha' \leftarrow \mathbf{p}, \alpha) = (2\pi)^4 \mu\mu' \frac{p'}{p} |t(\mathbf{p}', \alpha' \leftarrow \mathbf{p}, \alpha)|^2 \qquad \text{(B.70)}$$

$$(\alpha \,\text{and}\, \alpha' \,\text{two} - \text{body channels})$$

In the case of elastic scattering, $\alpha' = \alpha$, this result reduces to

$$\frac{d\sigma}{d\Omega}(\mathbf{p}', \alpha' \leftarrow \mathbf{p}, \alpha) = (2\pi)^4 \mu^2 |t(\mathbf{p}', \alpha' \leftarrow \mathbf{p}, \alpha)|^2 \qquad \text{(B.71)}$$

which has exactly the form of the one-channel result and includes the later as a special case. For inelastic processes, $\alpha' \neq \alpha$, the result (B.70) differs from (B.71) in two respects. The reduced masses μ and μ' may be different [as, for example, in the rearrangement collision $a + (bc) \to b + (ac)$]. And the initial and final momenta may be different, since p' is fixed by energy conservation to satisfy

$$\frac{p'^2}{2\mu'} + W_{\alpha'} = \frac{p^2}{2\mu} - W_\alpha$$

For example, in the excitation process $a + (bc) \to a + (bc)^*$,

$$p' = [p^2 - 2\mu(E_{(bc)^*} - E_{(bc)})]^{1/2} \qquad \text{(B.72)}$$

It is convenient, as in the one-channel case, to introduce a *scattering amplitude*, defined as

$$f(\mathbf{p}', \alpha' \leftarrow \mathbf{p}, \alpha) = -(2\pi)^2(\mu'\mu)^{1/2} t(\mathbf{p}', \alpha' \leftarrow \mathbf{p}, \alpha) \tag{B.73}$$

in terms of which the cross section for any process with two-body initial and final states is

$$\frac{d\sigma}{d\Omega}(\mathbf{p}', \alpha' \leftarrow \mathbf{p}, \alpha) = \frac{p'}{p} |f(\mathbf{p}', \alpha' \leftarrow \mathbf{p}, \alpha)|^2 \tag{B.74}$$

To conclude this section we remark that if we take the whole of the momentum space of channel α' for the volume Δ', then we obtain the *total cross section for scattering into channel* α', which we denote $\sigma(\alpha' \leftarrow \mathbf{p}, \alpha)$. (In particular, for $\alpha' = \alpha$ this is the *total elastic cross section.*) If we then sum this over all final channels α we obtain the *total cross section*,

$$\sigma(p, \alpha) = \sum_{\alpha'} \sigma(\alpha' \leftarrow \mathbf{p}, \alpha) = (2\pi)^4 \frac{\mu}{p} \sum_{\alpha'} \int d\underline{p}' \delta(E' - E) |t(\underline{p}', \alpha' \leftarrow \mathbf{p}, \alpha)|^2 \tag{B.75}$$

while if we restrict this sum to $\alpha' \neq \alpha$, we obtain the *total inelastic cross section.*

B.6 Rotational Invariance

If our multichannel system is rotationally invariant, then the rotational operator R commutes with the Hamiltonian H and H^α. It follows that it commutes with $\Omega_\pm^\alpha$ and, hence, with S,

$$S = R^\dagger S R \tag{B.76}$$

If all of the particles and their bound states are spinless, the effect of the rotation R on the channel basis vectors $|\underline{p}, \alpha\rangle$ is just

$$R|\underline{p}, \alpha\rangle = |\underline{p}_R, \alpha\rangle \tag{B.77}$$

where $\underline{p}_R$ denotes the effect of rotating all of the relative momenta p. Thus, taking matrix elements of (B.76), we obtain the very natural result

$$\langle \underline{p}', \alpha' | S | \underline{p}, \alpha \rangle = \langle \underline{p}'_R, \alpha' | S | \underline{p}_R, \alpha \rangle \tag{B.78}$$

and corresponding equalities for the T matrix $t(\underline{p}', \alpha' \leftarrow \underline{p}, \alpha)$. If any of the fragments of channels α and α' have spins (due either to the intrinsic spins of the original particles, or to the orbital momentum of the bound states), then this result is complicated by the transformation properties of the spin indices.

As, in the one-channel case, the simplest way to exploit rotational invariance is to work in an angular-momentum basis. This is especially simple if we consider an energy at which only two-body channels are open and suppose further that none of the bodies have spin. In this case the angular-momentum basis (of the relative motion) in each channel is a simple orbital basis with vectors $|E, l, m; \alpha\rangle$. Rotational invariance implies that the corresponding S matrix has the form

$$\langle E', l', m'; \alpha | S | E, l, m; \alpha \rangle = \delta(E' - E) \delta_{l'l} \delta_{m'm} s^l_{\alpha'\alpha}(E) \tag{B.79}$$

That is, the scattering for given E and l is determined by an $n \times n$ matrix $s^l(E)$ in "channel-space", n being the number of open channels at the energy E.

The passage between the momentum and angular-momentum bases proceeds exactly as in the one-channel case. Corresponding to the definition

$$f_l(E) = \frac{s_l(E) - 1}{2ip} \tag{B.80}$$

of the one-channel amplitude, we define the multichannel partial-wave amplitude as

$$f^l_{\alpha'\alpha}(E) = \frac{s^l_{\alpha'\alpha}(E) - \delta_{\alpha'\alpha}}{2i(p_{\alpha'}p_\alpha)^{1/2}} \tag{B.81}$$

Here p_α denotes the momentum in channel α when the total energy is E - that is,

$$p_\alpha = [2m_\alpha(E - W_\alpha)]^{1/2} \tag{B.82}$$

where W_α is the the threshold of channel α - and the Kronecker delta $\delta_{\alpha'\alpha}$ is to ensure that the amplitude is related to the matrix elements of the operator $S - 1$ in the normal way. With our definition, the multichannel partial-wave series has the simple form (for α and α' both two-body channels)

$$f(\mathbf{p}', \alpha' \leftarrow \mathbf{p}, \alpha) = \sum_l (2l + 1) f^l_{\alpha'\alpha}(E) P_l(\cos\theta) \tag{B.83}$$

The unitarity of S implies that the $n \times n$ matrix $s^l(E)$ of (B.79) is a unitary matrix. Since the dimension of this matrix depends on the energy, it is of some interest to discuss the unitary equation as a function of energy. We start with the energy E just above the threshold of the lowest channel (which we label $\alpha = 1$), and imagine E to be increased steadily past the various threshold W_α (which we label in order of increasing energy). When $W_1 \leq E \leq W_2$, the matrix $s^l(E)$ is a one-dimensional unitary matrix and hence has a single element of modulus one $|s^l_{11}| = 1$, or

$$s^l_{11}(E) = e^{2i\delta_l(E)} \quad [W_1 \leq E < W_2] \tag{B.84}$$

with $\delta_l(E)$ real. If we consider the partial-wave amplitude defined in (B.81) this means that the quantity $p_1 f^l_{11}$ lies on the unitary circle (see Fig. B.2).

When E moves above the first inelastic threshold, $s^l(E)$ becomes a 2×2 unitary matrix; and more generally, when E moves above W_n (still assume to be a two-body threshold) $s^l(E)$ becomes an $n \times n$ matrix satisfying

$$s^l(E)^\dagger s^l(E) = 1 \tag{B.85}$$

If we consider the $(1, 1)$ matrix element of this equation, we see that

$$|s^l_{11}|^2 + |s^l_{21}|^2 + \cdots + |s^l_{n1}|^2 = 1 \tag{B.86}$$

Clearly, as soon as there is any inelsticity, the original elastic element s^l_{11} must have modulus *less than* one, $s^l_{11} < 1$ or

$$s^l_{11}(E) = \epsilon_l(E) e^{2i\delta_l(E)} \tag{B.87}$$

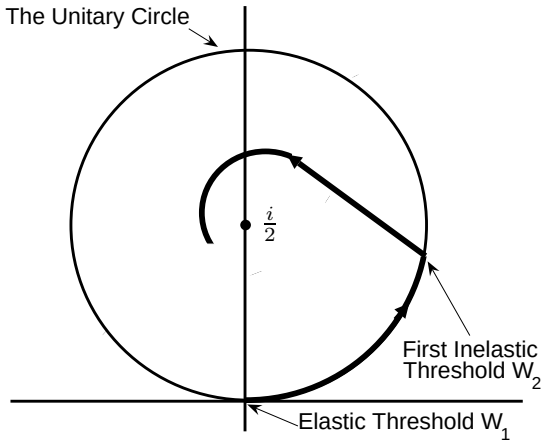

Fig. B.2: Typical behavior of the elastic partial-wave amplitude as a function of energy.

where δ_l is still real but ϵ_l, which is called the *inelasticity factor*, satisfies

$$0 \leq \epsilon_l(E) < 1$$

Alternatively we can write,

$$s^l_{11}(E) = e^{2i\eta_l(E)} \tag{B.88}$$

with η_l complex. In this form we can say that inelasticity forces the "phase shift" η_l to have a positive imaginary part. The result means that the elastic partial-wave amplitude moves *inside* the unitary circle as shown in Fig. B.2 .

The result (B.87) is easily understood. Much as in the one-channel case, $|s^l_{11}|^2$ is the ratio of outgoing to ingoing flux in channel 1, when the incident beam is pure l wave in channel 1. As long as only channel 1 is open, this ratio must be one; but as soon as other competing channels open up it must be less than one.

It is clear from (B.86), and its equivalent with 1 replaced by α, that every element $s^l_{\alpha'\alpha}$ must have modulus less than one. In particular, for any elastic element the number $p_\alpha f^l_{\alpha\alpha}$ must lies inside the unitary circle. However only the first amplitude f^l_{11} has a purely elastic interval.

Once a three-body channel opens up the situation becomes more complicated. The basis vectors for the relative motion in a three-body channel are labelled by E, l, m plus an internal energy (a continuous variable) and two internal angular momenta. The discussion of such channel is obviously much more difficult. Thus, if we return to (B.86) and suppose that the channel α has three bodies, then the simple term $|s^l_{\alpha 1}|^2$ is replaced by an integral and sum over the additional labels. However, this new term is still positive and our conclusion that $|s^l_{11}| \leq 1$ remains valid.

B.7 Time-Reversal Invariance

The discussion of parity invariance for multichannel scattering is little different from that for the one-channel case, and need not be spelled out here. However, in the case of time-reversal invariance, the multichannel problem offers some striking new possibilities.

If the dynamics are invariant under time reversal then we can show just as before that $S = T^\dagger S^\dagger T$ and, hence, that

$$\langle \chi | S | \phi \rangle = \langle \phi_T | S | \chi_T \rangle \tag{B.89}$$

For example, if all particles are spinless, T invariance simply implies that

$$\langle \underline{p}', \alpha' | S | \underline{p}, \alpha \rangle = \langle -\underline{p}, \alpha | S | -\underline{p}', \alpha' \rangle \tag{B.90}$$

The interesting new feature of this result is that it relates the amplitudes for two qualitatively different processes, $\alpha' \leftarrow \alpha$ and $\alpha \leftarrow \alpha'$.

B.8 Fundamentals of Time-Independent Multichannel Scattering

In the previous sections, we have set up the time-dependent theory of multichannel scattering. In this section we discuss the corresponding time-independent theory. Its main purpose is to furnish a means for the actual computation of the T matrix for given interaction; and for this reason it is the time independent theory that is the day to day concern of the practising physicist.

In one-channel scattering we saw that the time-independent formalism centers around the Green's operators $G(z)$ and $G^0(z)$, the T operator $T(z)$, and the stationary scattering states $|\mathbf{p}\pm\rangle$. Both $T(z)$ and $|\mathbf{p}\pm\rangle$ were given in terms of $G^0(z)$ by Lipmann-Schwinger equation, which provided essentially equivalent approaches to finding the quantity of real interest, the on-shell T matrix.

In this chapter we shall see how the one-channel results extend to the multichannel case. Superficially at least, the most important complication is that all quantities acquire additional channel labels. As we have already seen the single free Hamiltonian H^0 of the one-channel case is replaced by a family of "free" channel Hamiltonians H^α, describing the "free" evolution in the various different channels. In place of the single free Green's operator $G^0(z)$, there is a family of channel Green's operators $G^\alpha(z) = (z - H^\alpha)^{-1}$. In place of the stationary states $|\mathbf{p}\pm\rangle$, there is a family of stationary states $|\underline{p}, \alpha\pm\rangle$. In place of the single T operator there is a double family of T operators $T^{\beta\alpha}(z)$, one for each pair of channels α and β.

B.8.1 The stationary scattering states

In single-channel the stationary states $|\mathbf{p}\pm\rangle$ were eigenvectors of the full Hamiltonian H defined as $\Omega_\pm|\mathbf{p}\rangle$. We define multichannel stationary scattering states as

$$|\underline{p}, \alpha\pm\rangle = \Omega^\alpha_\pm |\underline{p}, \alpha\rangle \tag{B.91}$$

where as usual $\underline{p}$ denotes a set of $(n_\alpha - 1)$ relative momenta of the n_α bodies in channel α and $|\underline{p}, \alpha\rangle$ is the corresponding "free" plane-wave state. Using the intertwining relations (B.57) we can immediately see that these states are eigenstates of the full Hamiltonian H with energy $E = E^\alpha_{\underline{p}}$. (This means that their wave functions $\langle \underline{x}|\underline{p}, \alpha\pm\rangle$ satisfy the time-independent Schrödinger equation, which provides one route to the actual computation of the states.) In the same loose sense as applied to the single-channel case, $|\underline{p}, \alpha+\rangle$ ($|\underline{p}, \alpha-\rangle$) can be regarded as the actual state at $t = 0$ coming from an *in* asymptote (would evolve into an *out* asymptote) in channel α with momenta $\underline{p}$.

Just as in the one-channel case we can derive an expression for $|\underline{p}, \alpha\pm\rangle$ in terms of $|\underline{p}, \alpha\rangle$ and the Green's operator. We first note, in the now familiar way, that for a proper normalizable vector $|\phi\rangle$ in the channel α subspace,

$$\begin{aligned}\Omega^\alpha_\pm|\phi\rangle &= \lim_{t\to\mp\infty} e^{iHt}e^{-iH^\alpha t}|\phi\rangle \\ &= |\phi\rangle + i\int_0^{\mp\infty} dt e^{iHt}V^\alpha e^{-iH^\alpha t}|\phi\rangle \end{aligned} \tag{B.92}$$

where we have introduced the channel α scattering potential

$$V^\alpha = H - H^\alpha \tag{B.93}$$

This consists of all potentials that link different freely moving fragments in channel α; that is, V^α is precisely that part of the potential which becomes ineffective as the particles move apart in channel α. If V^α were zero, an *in* state in channel α would not be scattered.

The known convergence of the integral (B.92) allows as to insert the familiar damping factor $e^{\pm\epsilon t}$ with the limit $\epsilon \to 0^+$; and in this form we can apply (B.92) to the improper states $|\underline{p}, \alpha\rangle$ to give

$$|\underline{p}, \alpha\pm\rangle = |\underline{p}, \alpha\rangle + \lim_{\epsilon\to 0^+} i\int_0^{\mp\infty} dt e^{\pm\epsilon t}e^{iHt}V^\alpha e^{-iH^\alpha t}|\underline{p}, \alpha\rangle \tag{B.94}$$

Since $|\underline{p}, \alpha\rangle$ is an eigenvector of the channel Hamiltonian H^α with energy $E = E^\alpha_{\underline{p}}$ this gives

$$|\underline{p}, \alpha\pm\rangle = |\underline{p}, \alpha\rangle + \lim_{\epsilon\to 0^+} i\int_0^{\mp\infty} dt e^{-i(E\pm i\epsilon - H)t}V^\alpha|\underline{p}, \alpha\rangle \tag{B.95}$$

or

$$|\underline{p}, \alpha\pm\rangle = |\underline{p}, \alpha\rangle + G(E \pm i0)V^\alpha|\underline{p}, \alpha\rangle \tag{B.96}$$

where we have introduced the full Green's operator $G(z) = (z-H)^{-1}$. The result (B.96) is the analogue of the one channel result $|\mathbf{p}\pm\rangle = |\mathbf{p}\rangle + G(E \pm i0)V|\mathbf{p}\rangle$, and with its help we can obtain expressions for the on shell T matrix. The momentum-space S-matrix elements can be written as

$$\langle \underline{p}', \beta|S|\underline{p}, \alpha\rangle = \langle \underline{p}', \beta|\Omega^{\beta\dagger}_-\Omega^\alpha_+|\underline{p}, \alpha\rangle = \langle \underline{p}', \beta - |\underline{p}, \alpha+\rangle \tag{B.97}$$

Now, using (B.96) we can write $|\underline{p}, \alpha+\rangle$ as

$$|\underline{p}, \alpha+\rangle = |\underline{p}, \alpha-\rangle + [G(E+i0) - G(E-i0)]V^\alpha|\underline{p}, \alpha\rangle \tag{B.98}$$

which can be substituted into (B.97) to give

$$\langle \underline{p}', \beta|S|\underline{p}, \alpha\rangle = \delta_{\beta\alpha}\delta(\underline{p}' - \underline{p}) + \langle \underline{p}', \beta - |[G(E+i0) - G(E-i0)]V^\alpha|\underline{p}, \alpha\rangle \tag{B.99}$$

Finally, since the bra $\langle \underline{p}', \beta - |$ is an eigenvector of H with eigenvalue $E' = E^\beta_{\underline{p}'}$, the factor in brackets comes outside as

$$[\frac{1}{E - E' + i0} - \frac{1}{E - E' - i0}] = -2\pi i\delta(E' - E)$$

to give

$$\langle \underline{p}', \beta|S|\underline{p}, \alpha\rangle = \delta_{\beta\alpha}\delta(\underline{p}' - \underline{p}) - 2\pi i\delta(E' - E)\langle \underline{p}', \beta - |V^\alpha|\underline{p}, \alpha\rangle \tag{B.100}$$

That is, the on-shell T matrix is given by

$$t(\underline{p}', \beta \leftarrow \underline{p}, \alpha) = \langle \underline{p}', \beta - |V^\alpha|\underline{p}, \alpha\rangle \tag{B.101}$$

Similarly, if we were to rewrite the bra $\langle \underline{p}', \beta - |$ of (B.97) in terms of $\langle \underline{p}', \beta + |$ we would find the alternative result

$$t(\underline{p}', \beta \leftarrow \underline{p}, \alpha) = \langle \underline{p}', \beta|V^\beta|\underline{p}, \alpha+\rangle \tag{B.102}$$

These two expressions are the multichannel versions of the one-channel results (A.149) and (A.151). The version in (B.101) contains the scattering potential V^α of the initial channel α and is therefore referred to as the *"prior" version*. That in (B.102) has the potential V^β appropriate to the final channel β and is called the *"post" version*.

B.8.2 The Lippmann-Schwinger equations

It is clear from the result (B.101) and (B.102) that knowledge of the states $|\underline{p}, \alpha+\rangle$ or $|\underline{p}, \alpha-\rangle$ implies knowledge of the on-shell T matrix. Just as in the one-channel case the explicit expressions $|\underline{p}, \alpha\pm\rangle = |\underline{p}, \alpha\rangle + G(\pm)V^\alpha|\underline{p}, \alpha\rangle$ are of little direct use since they require knowledge of the full Green's operator $G(z)$. And, again, just as in the one-channel case, they can be converted into implicit Lippmann-Schwinger equation in terms of certain "free" Green's operators, as we now show.

The first step in establishing the Lippmann-Schwinger equation is to use the familiar identity

$$A^{-1} = B^{-1} + B^{-1}(B - A)A^{-1}$$

with $A = (z - H)$ and $B = (z - H^\alpha)$. This gives the resolvent equations

$$G(z) = G^\alpha(z) + G^\alpha(z)V^\alpha G(z) \tag{B.103}$$

where, we have defined the Channel Green's operators $G^\alpha(z)$ corresponding to the "free" channel Hamiltonian H^α, as

$$G^\alpha = (z - H^\alpha)^{-1} \tag{B.104}$$

Returning to (B.96) we multiply through by $G^\alpha V^\alpha$ to give

$$G^\alpha V^\alpha |\underline{p}, \alpha\pm\rangle = G^\alpha V^\alpha |\underline{p}, \alpha\rangle + G^\alpha V^\alpha G V^\alpha |\underline{p}, \alpha\rangle \tag{B.105}$$

Since by (B.103) $G^\alpha V^\alpha G = (G - G^\alpha)$, this reduces to the important result

$$G^\alpha(E \pm i0) V^\alpha |\underline{p}, \alpha\pm\rangle = G(E \pm i0) V^\alpha |\underline{p}, \alpha\rangle \tag{B.106}$$

Finally substitution into (B.96) gives the desired Lippmann-Schwinger equation

$$|\underline{p}, \alpha\pm\rangle = |\underline{p}, \alpha\rangle + G^\alpha(E \pm i0) V^\alpha |\underline{p}, \alpha\pm\rangle \tag{B.107}$$

This equation, which is an integral equation for the corresponding wave function, and the Schrödinger equation provide the two principle approaches to the computation of the stationary scattering states.

It should be emphasized that the multichannel Lippmann-Schwinger equation is considerably harder to handle than its single-channel equivalent. Some of the difficulties are readily apparent. For example, the Green's operator on the right is the channel Green's operator $G^\alpha(z) = (z - H^\alpha)^{-1}$. Except for the case $\alpha = 0$ (all particles free), H^α contains some potentials and the corresponding Green's operator G^α cannot, in general, be exactly calculated (in contra-distinction to the one-channel situation where G^0 is known exactly). A less obvious though more profound, difficulty is that where the one-channel equation is (or can be easily converted to) a *non-singular* integral equation, the multichannel equations are in general highly singular. This makes both the theoretical study and practical use of the equations much more difficult.

B.8.3 The T operators

Just as in the one-channel case, the time-independent multichannel theory has two essentially equivalent formulations, one in terms of the stationary scattering states, the other in terms of the T operators. Having established the former, we can now easily set up the latter.

We start with the expression

$$t(\underline{p}', \beta \leftarrow \underline{p}, \alpha) = \langle \underline{p}', \beta - |V^\alpha| \underline{p}, \alpha\rangle \tag{B.108}$$

into which we substitute

$$|\underline{p}, \beta-\rangle = |\underline{p}, \beta\rangle + G(E - i0) V^\beta |\underline{p}, \beta\rangle \tag{B.109}$$

This gives

$$t(\underline{p}', \beta \leftarrow \underline{p}, \alpha) = \langle \underline{p}', \beta | [V^\alpha + V^\beta G(E + i0) V^\alpha] |\underline{p}, \alpha\rangle \tag{B.110}$$

or

$$t(\underline{p}', \beta \leftarrow \underline{p}, \alpha) = \langle \underline{p}', \beta | T^{\beta\alpha}(E + i0) | \underline{p}, \alpha \rangle \tag{B.111}$$

where we have defined the T operator,

$$T^{\beta\alpha}(z) = V^{\alpha} + V^{\beta} G(z) V^{\alpha} \tag{B.112}$$

As anticipated here is a double family of T operators $T^{\beta\alpha}(z)$. The on-shell T matrix for a transition from channel α to channel β is given by the on-shell matrix elements of the *appropriate* $T^{\beta\alpha}(z)$ between the free states $|\underline{p}', \beta\rangle$ and $|\underline{p}, \alpha\rangle$.

One feature of the definition (B.112) of $T^{\beta\alpha}(z)$ that deserves comment is the apparent asymmetry between the indices α and β. There seem no obvious reason why it is the potential V^{α} and not V^{β} that appears in the first term. Indeed, if we had started with the "post" form $\langle \underline{p}', \beta | V^{\beta} | \underline{p}, \alpha + \rangle$ for the on-shell T matrix, we would have been led to a result similar to (B.111) but with the T operator

$$\widetilde{T}^{\beta\alpha}(z) = V^{\beta} + V^{\beta} G(z) V^{\alpha} \tag{B.113}$$

If the channel α and β have different grouping of the particles, then the channel Hamiltonians H^{α} and H^{β} are different and hence, $V^{\alpha} \neq V^{\beta}$. Thus, the two T operators $T^{\beta\alpha}(z)$ and $\widetilde{T}^{\beta\alpha}(z)$ are generally different. Nevertheless both leads to the same on-shell T matrix, since

$$\begin{aligned} \langle \underline{p}', \beta | (T^{\beta\alpha} - \widetilde{T}^{\beta\alpha}) | \underline{p}, \alpha \rangle &= \langle \underline{p}', \beta | (V^{\alpha} - V^{\beta}) | \underline{p}, \alpha \rangle \\ &= \langle \underline{p}', \beta | (H^{\beta} - H^{\alpha}) | \underline{p}, \alpha \rangle \\ &= (E' - E) \langle \underline{p}', \beta | \underline{p}, \alpha \rangle \end{aligned} \tag{B.114}$$

which is zero on the energy shell.

As one would expect, the explicit definition (B.112) of $T^{\beta\alpha}(z)$ can be replaced by an implicit Lippmann-Schwinger equation. To do this we multiply (B.112) on the left by $G^{\beta}(z)$ to give

$$G^{\beta}(z) T^{\beta\alpha}(z) = (G^{\beta} + G^{\beta} V^{\beta} G) V^{\alpha} = G(z) V^{\alpha} \tag{B.115}$$

substitution back into (B.112) gives the desired equation

$$T^{\beta\alpha}(z) = V^{\alpha} + V^{\beta} G^{\beta}(z) T^{\beta\alpha}(z) \tag{B.116}$$

B.8.4 Asymptotic form of the wave function; Collision without rearrangement

In this section we discuss the multi-channel analogue of the one-channel asymptotic form (A.165). This is quite complicated in general, and we shall therefore consider just a few simple examples. We begin by considering our three-particle model with light particles a and b and a heavy fixed particle c. We allow for several bound states $(bc)_1, \ldots, (bc)_n$ and $(ac)_1, \ldots, (ac)_{n'}$, and perhaps also some bound states of a and b. There are then n channels of the form

$$a + (bc)_1, \ldots, a + (bc)_n \tag{B.117}$$

and n' of the form

$$b + (ac)_1, \ldots, b + (ac)_{n'} \tag{B.118}$$

In addition, there is the channel 0 $(a + b + c)$ and perhaps further channels of the form $(ab) + c$.

We shall consider a process in which particle a is incident with momentum $\mathbf{p}$ on the ground state $(bc)_1$. We label this channel as channel 1, and the corresponding stationary state is then $|\mathbf{p}, 1+\rangle$. This has wave function $\langle \mathbf{x}_a, \mathbf{x}_b | \mathbf{p}, 1+\rangle$ depending on the two variables $\mathbf{x}_a$ and $\mathbf{x}_b$, and the question immediately arises: **Do we want the asymptotic behavior as $\mathbf{x}_a \to \infty$, or $\mathbf{x}_b \to \infty$, or perhaps both?** In fact, all of these cases are of interest, as can readily be seen. If $\mathbf{x}_a \to \infty$ with $\mathbf{x}_b$ fixed, then the wave function should show the effects of those channels in which particles a moves far away from b and c (and which are open at the energy considered). However, we would not expect to see those channels in which a is captured $[a + (bc)_1 \to b + (ac)_i]$, nor those in which a and b move off together $[a + (bc)_1 \to (ab)_i + c]$. Thus, as $\mathbf{x}_a \to \infty$ with x_b fixed, the wave function $\langle \mathbf{x}_a, \mathbf{x}_b | \mathbf{p}, 1+\rangle$ should consist of an incident plane wave in channel 1 plus outgoing waves in the channels $a + (bc)_i$ and $a + b + c$. Instead, if we let $\mathbf{x}_b \to \infty$ with $\mathbf{x}_a$ fixed, then we should see the outgoing waves in the channels $b + (ac)_i$ and $a + b + c$, but not the others.

We begin with the case that $\mathbf{x}_a \to \infty$ with $\mathbf{x}_b$ fixed. We proceed in close analogy with the one-channel analysis of Section A.8, starting from the Lippmann-Schwinger equation

$$|\mathbf{p}, 1+\rangle = |\mathbf{p}, 1\rangle + G^1(E + i0)V^1|\mathbf{p}, 1+\rangle \tag{B.119}$$

To get at the wave function $\langle \mathbf{x}_a, \mathbf{x}_b | \mathbf{p}, 1+\rangle$ we need to know the spatial matrix elements $\langle \mathbf{x}_a, \mathbf{x}_b | G^1(z) | \mathbf{x}'_a, \mathbf{x}'_b \rangle$ of the channel 1 Green's operator. In the one-channel case we evaluated the matrix element $\langle \mathbf{x} | G^0(z) | \mathbf{x}' \rangle$ of the free Green's operator by inserting a complete set of eigenvectors $|\mathbf{p}\rangle$ of the free Hamiltonian H^0. In the present case we seek analogous eigenvectors of the channel 1 Hamiltonian, which we write as

$$H^1 = \frac{\mathbf{p}_a^2}{2m_a} + \frac{\mathbf{p}_b^2}{2m_b} + V_{bc} \equiv \frac{\mathbf{p}_a^2}{2m_a} + H_{(bc)} \tag{B.120}$$

Here the second term is the Hamiltonian of particle b in the field of the fixed particle c. From this it is clear that we can take as eigenfunctions of H^1 the products,

$$(2\pi)^{-3/2} e^{i\mathbf{p}\cdot\mathbf{x}_a} \phi_\alpha(\mathbf{x}_b) \tag{B.121}$$

where $\phi_\alpha(x_b)$ denotes any of the eigenfunctions of $H_{(bc)}$ with energy E_α. These are of two types; there are the n bound states $(bc)_1, \ldots, (bc)_n$ with wave functions $\phi_1(\mathbf{x}_b), \ldots, \phi_n(\mathbf{x}_b)$. Also, there are the continuum states, which for example we could choose to be the outgoing wave scattering states of b in the field of c. In either case the function (B.121) are eigenfunctions of H^1 with energy $(\mathbf{p}^2/2m_a) + E_\alpha$.

When $\phi_\alpha(\mathbf{x}_b)$ is one of the bound-state wave functions $\phi_1, \ldots, \phi_n$, the function (B.121) is precisely the free wave function of the channel $a + (bc)_\alpha$. The same is *not* true of the continuum functions; in this case the function (B.121) is not the free wave function of any channel. Therefore, the basis of eigenfunctions (B.121) of the channel Hamiltonian H^1 is, a curious hybrid. The discrete part consists of free channel wave functions $\langle \mathbf{x}_a, \mathbf{x}_b | \mathbf{p}, \alpha \rangle$ where α runs over all channels with the arrangement $a + (bc)_\alpha$. The continuous part consists of functions that have no simple relation to any channels. In fact, one shall be mainly interested in the discrete part of the basis, and it is for this reason that we identify the functions $\phi_\alpha(\mathbf{x}_b)$ with the same label α as used to identify channels. However, it must be remembered that this α runs over *some of the channels* (specifically those with the same arrangement as channel 1), and it also runs over a continuous range corresponding to the continuum states of b in the potential V_{bc}. To emphasize this point we shall write "sums" over α with the symbol $(\int + \sum)$.

Now we can insert a complete set of the states (B.121) into the required Green's function, to give

$$\langle \mathbf{x}_a, \mathbf{x}_b | G^1(z) | \mathbf{x}'_a, \mathbf{x}'_b \rangle = (\pi)^{-3} \int d^3p \Big(\int + \sum_\alpha \Big) \frac{e^{i\mathbf{p}\cdot(\mathbf{x}_a - \mathbf{x}'_a)} \phi_\alpha(\mathbf{x}_b) \phi_\alpha(\mathbf{x}'_b)^*}{z - (p^2/2m_a) - E_\alpha} \tag{B.122}$$

The integral over $\mathbf{p}$ can be performed, exactly as in the one-channel case. Each term in the sum over α has a pole at $p = [2m_a(z - E_\alpha)]^{1/2}$; and for the case $z = E + i0$ the result is

$$\langle \mathbf{x}_a, \mathbf{x}_b | G^1(E+i0) | \mathbf{x}'_a, \mathbf{x}'_b \rangle = -\frac{m_a}{2\pi} \Big(\int + \sum_\alpha \Big) \frac{e^{ip_\alpha |\mathbf{x}_a - \mathbf{x}'_a|} \phi_\alpha(\mathbf{x}_b) \phi_\alpha(\mathbf{x}'_b)^*}{|\mathbf{x}_a - \mathbf{x}'_a|} \tag{B.123}$$

where $p_\alpha \equiv [2m_a(E - E_\alpha)]^{1/2}$ is the momentum of particle a if the target (bc) is left with energy E_α. In particular, we shall want the Green's function for $r_a \gg r'_a$, in which case,

$$\langle \mathbf{x}_a, \mathbf{x}_b | G^1(E + i0) | \mathbf{x}'_a, \mathbf{x}'_b \rangle \xrightarrow[\mathbf{x}_a \to \infty]{} -\frac{m_a}{2\pi} \Big(\int + \sum_\alpha \Big) \frac{e^{ip_\alpha r_a}}{r_a} e^{-ip_\alpha \widehat{\mathbf{x}}_a \cdot \mathbf{x}'_a} \times \phi_\alpha(\mathbf{x}_b) \phi_\alpha(\mathbf{x}'_b)^* \tag{B.124}$$

We are now ready to establish the asymptotic form of the stationary wave functions. From the Lippmann-Schwinger equation (B.119) it follows that

$$\langle \mathbf{x}_a, \mathbf{x}_b | \mathbf{p}, 1+ \rangle = \langle \mathbf{x}_a, \mathbf{x}_b | \mathbf{p}, 1 \rangle + \int d^3x'_a \int d^3x'_b \langle \mathbf{x}_a, \mathbf{x}_b | G^1(E + i0) | \mathbf{x}'_a, \mathbf{x}'_b \rangle \times V^1(\mathbf{x}'_a, \mathbf{x}'_b) \langle \mathbf{x}'_a, \mathbf{x}'_b | \mathbf{p}, 1+ \rangle \tag{B.125}$$

Substituting (B.124) for the Green's function we obtain

$$\xrightarrow[\mathbf{x}_a \to \infty]{} (2\pi)^{-3/2} [e^{i\mathbf{p}\cdot\mathbf{x}_a} \phi_1(\mathbf{x}_b) - (2\pi)^2 m_a \Big(\int + \sum_\alpha \Big) \frac{e^{ip_\alpha r_a}}{r_a} \times \phi_\alpha(\mathbf{x}_b) \langle p_\alpha \widehat{\mathbf{x}}, \alpha | V^1 | \mathbf{p}, 1+ \rangle] \tag{B.126}$$

or

$$\langle \mathbf{x}_a, \mathbf{x}_b | \mathbf{p}, 1+\rangle \xrightarrow[\mathbf{x}_a \to \infty]{} (2\pi)^{-3/2}[e^{i\mathbf{p}\cdot\mathbf{x}_a}\phi_1(\mathbf{x}_b) + (\int + \sum_\alpha) f(p_\alpha \widehat{\mathbf{x}}_a, \alpha \leftarrow \mathbf{p}, 1)\frac{e^{ip_\alpha r_a}}{r_a}\phi_\alpha(\mathbf{x}_b)] \quad \text{(B.127)}$$

This result is a natural generalization of the well-known one-channel result (A.165). The first is the expected incident plane wave in channel 1; the second term has a sum over α. This sum includes n discrete values, corresponding to the bound states $(bc)_1, \ldots, (bc)_n$, plus continuous values corresponding to the continuum states of the target (bc). For the moment we focus attention on the n discrete terms. Each of these is the product of three factors: an amplitude, a spherically spreading wave for particle a, and the target function $\phi_\alpha(\mathbf{x}_b)$. Since the momentum of the spherical wave is:

$$p_\alpha = [2m_a(E - E_\alpha)]^{1/2} \quad \text{(B.128)}$$

we see that each term in the sum represents the particle a travelling outwards with energy $E - E_\alpha$ having excited the target to the state $(bc)_\alpha$ with energy E_α.

If the total energy E is less than E_α, then the momentum (B.128) in channel α is pure imaginary. In this case the contribution of channel α to the asymptotic form (B.127) vanishes exponentially as $r_a \to \infty$. Thus, the sum in (B.127) can be taken to include only those channels that are open at energy E. In particular, if the energy is below that necessary to disintegrate the target, the "sum" in (B.127) is a genuine sum with no contribution from the continuum.

If the incident energy is sufficient to break up the target, then the "sum" in the asymptotic form (B.127) includes an integral over the continuum states. It can be shown that these terms represent outgoing waves in the breakup channel $a + b + c$. It is also not hard to extend these results to more general systems, in which both projectile and target are composites made up of several particles (atom-atom collisions, for example). However, we shall not go into these cases.

The cross sections for elastic scattering and for excitation can easily be read off from the asymptotic form (B.127). The first term represents a steady *incident flux per unit area* $= (2\pi)^{-3}\frac{p}{m}$, in channel 1. The α^{th} term in the sum represents a *scattered flux per unit solid angle* $= (2\pi)^{-3}|f(\mathbf{p}_\alpha, \alpha \leftarrow \mathbf{p}, 1)|^2\frac{p_\alpha}{m}$ in channel α. Thus we obtain

$$\frac{d\sigma}{d\Omega}(\mathbf{p}_\alpha, \alpha \leftarrow \mathbf{p}, 1) = \frac{\text{scattered flux/solid angle}}{\text{incient flux/area}} = \frac{p_\alpha}{p}|f(\mathbf{p}_\alpha, \alpha \leftarrow \mathbf{p}, 1)|^2 \quad \text{(B.129)}$$

as expected.

B.8.5 Asymptotic form of the wave function; Rearrangement collisions

So far we have considered the behavior of the stationary wave function $\langle \underline{x}|\mathbf{p}, 1+\rangle$ as the coordinate of the original projectile approaches infinity, with all target coordinates fixed. As expected this displayed the effects of these channels with the

same arrangement as that of the incident channel 1. If we wish to see the effects of rearrangement collision, then we must let some of the target coordinates go to infinity. Here we shall consider the same three-particle model as above with a incident on the ground state $(bc)_1$, and examine the wave function as $\mathbf{x}_b$ goes to infinity with $\mathbf{x}_a$ fixed. This should display the effects of the rearrangement collisions

$$a + (bc)_1 \to b + (ac)_\beta$$

The analysis of this case is quite similar to the previous one. The first step is to obtain some analogue of the Lippmann-Schwinger equation (B.119) in terms of the final Channel Green's operator $G^\beta(z) = (z - H^\beta)^{-1}$, where H^β is the Hamiltonian of the final channel under consideration,

$$H^\beta = \frac{\mathbf{p}_b^2}{2m_b} + \frac{\mathbf{p}_a^2}{2m_a} + V_{ac} \tag{B.130}$$

We start with the original Lippmann-Schwinger equation

$$|\mathbf{p}, 1+\rangle = |\mathbf{p}, 1\rangle + G^1(E + i0)V^1|\mathbf{p}, 1+\rangle \tag{B.131}$$

and rewrite G^1 in terms of G^β as

$$G^1 = G^\beta + G^\beta(V^\beta - V^1)G^1 \tag{B.132}$$

This gives

$$|\mathbf{p}, 1+\rangle = |\mathbf{p}, 1\rangle + G^\beta V^1|\mathbf{p}, 1+\rangle + G^\beta(V^\beta - V^1)G^1V^1|\mathbf{p}, 1+\rangle \tag{B.133}$$

Since $G^1V^1|\mathbf{p}, 1+\rangle$ in the last term is the same as $|\mathbf{p}, 1+\rangle - |\mathbf{p}, 1\rangle$, this gives

$$|\mathbf{p}, 1+\rangle = G^\beta V^\beta|\mathbf{p}, 1+\rangle + |o\rangle \tag{B.134}$$

where

$$|o\rangle = |\mathbf{p}, 1\rangle - G^\beta(V^\beta - V^1)|\mathbf{p}, 1\rangle \tag{B.135}$$

It can be shown that the vector $|o\rangle$ is orthogonal to all vectors in the channels of interest, i.e., the channels $b + (ac)_\beta$. Therefore it need not concern us here and we shall omit it from the next few equations. The first term in (B.134) can be treated by the techniques of the previous section.

To evaluate the spatial matrix elements of $G^\beta(z)$ we need a set of eigenfunctions for the channel Hamiltonian H^β of (B.130). These have the form

$$(2\pi)^{-3/2}e^{i\mathbf{p}\cdot\mathbf{x}_b}\chi_\beta(\mathbf{x}_a)$$

where $\chi_\beta(\mathbf{x}_a)$ stands for any of the (ac) bound-state wave functions or the corresponding continuum functions. This gives an expression for the matrix

elements of G^β analogous to (B.124) for G^1 (but with $\mathbf{x}_a, m_a$, and ϕ_α replaced by $\mathbf{x}_b, m_b$, and χ_β). Substitution into the expression (B.134) for $|\mathbf{p}, 1+\rangle$ gives

$$\langle \mathbf{x}_a, \mathbf{x}_b | p, 1+\rangle \xrightarrow[\mathbf{x}_b \to \infty]{} (2\pi)^{-3/2} [-(2\pi)^2 m_b (\int + \sum_\beta) \frac{e^{ip_\beta r_b}}{r_b} \chi_\beta(\mathbf{x}_a) \times \langle p_\beta \hat{\mathbf{x}}_b, \beta | V^\beta | \mathbf{p}, 1+\rangle] \quad \text{(B.136)}$$

Bearing in mind that for the rearrangement

$$a + (bc)_1 \to b + (ac)_\beta$$

the amplitude is

$$f(\mathbf{p}_\beta, \beta \leftarrow \mathbf{p}, 1) = -(2\pi)^2 (m_a m_b)^{1/2} t(\mathbf{p}_\beta, \beta \leftarrow \mathbf{p}, 1) \quad \text{(B.137)}$$

we can rewrite (B.136) in the final form

$$\langle \mathbf{x}_a, \mathbf{x}_b | p, 1+\rangle \xrightarrow[\mathbf{x}_b \to \infty]{} (2\pi)^{-3/2} \left(\frac{m_b}{m_a}\right)^{1/2} (\int + \sum_\beta) f(p_\beta \hat{\mathbf{x}}_b, \beta \leftarrow \mathbf{p}, 1) \times \frac{e^{ip_\beta r_b}}{r_b} \chi_\beta(\mathbf{x}_a) \quad \text{(B.138)}$$

where $p_\beta = [2m(E - E_\beta)]^{1/2}$.

This result has exactly the expected form; there is no incident wave. The discrete part of the sum runs over those open channels with the arrangement $b + (ac)$ (the closed-channel terms go to zero exponentially and can be dropped) and each term represents the particle b moving out in a spherical wave leaving particle a in the bound state $\chi_\beta(\mathbf{x}_a)$. Finally, it can be shown that the continuum terms represent the channel $a + b + c$ as before.

The relevant cross sections can be read off from (B.138). The scattered flux per unit solid angle in any of the discrete channels β is

$$(2\pi)^{-3} \frac{m_b}{m_a} |f(\mathbf{p}_\beta, \beta \leftarrow \mathbf{p}, 1)|^2 \frac{p_\beta}{m_b}$$

while the incident flux in channel 1 is $(2\pi)^{-3} p/m_a$ as before. Thus,

$$\frac{d\sigma}{d\Omega}(\mathbf{p}_\beta, \beta \leftarrow \mathbf{p}, 1) = \frac{p_\beta}{p} |f(\mathbf{p}_\beta, \beta \leftarrow \mathbf{p}, 1)|^2 \quad \text{(B.139)}$$

as expected.

B.9 Multichannel Scattering with Identical Particles

In this section we proceed to the general multichannel problem and shall find that the scattering theory for systems of identical particles can be obtained from

that for distinct particles by the use of symmetrizing projectors, much as in the single-channel case.

We consider an arbitrary system of N particles, at least some of which are identical, and which has Hamiltonian H. We can, of course, imagine H to be the Hamiltonian of N *distinct* particles (the fact that H commutes with the relevant permutation operators does not prevent this) in which case we already understand the corresponding scattering theory as follows.

The general state, which is labelled by an arbitrary function of the N variables x_i, can be written as a superposition of the bound states (of all N particles) and scattering states. The latter are the states of interest and can themselves be classified according to the channels from which they have evolved as $t \to -\infty$ (or to which they will evolve as $t \to +\infty$).

The general scattering state can be expressed as a superposition of states each coming from some definite *in* channel, and similarly of states each going into some definite *out* channel.

For an arbitrary wave function ψ the orbit $e^{-iHt}\psi$ does not represent an allowed orbit of the actual system (with identical particles) since ψ does not have the required symmetry. However, we have only to multiply by the appropriate projector Λ to obtain an orbit that does. Under the action of Λ the situation described in the previous paragraph changes. In particular, the number of channels is reduced in two ways.

The first change can be easily understood by considering the example of electron-Hydrogen scattering. Here, for every channel with the grouping

$$e_1 + (e_2 p)$$

there is a second channel of the form

$$e_2 + (e_1 p)$$

obtained by permuting the two electrons. If the electrons are distinguishable these two channels are physically distinct. In reality, however, the electrons are indistinguishable and the distinction between the two channels is without physical meaning. Nonetheless, in the formalism that we choose to adapt, the two channels are mathematically distinct, wave functions of the former having the form

$$\chi(x_1)\phi(x_2)$$

(where χ is an arbitrary wave packet, and ϕ is the hydrogen bound-state wave function) while those of the latter have the form

$$\chi(x_2)\phi(x_1)$$

In general, whenever a channel has two or more identical particles distributed among its freely moving fragments there is a whole family of channels obtained simply by permuting identical particles among the different fragments. These

channels, while mathematically distinct, are physically indistinguishable, any one of them can be used to identify the same physical situation.

To illustrate the second reduction in the number of channels we consider the slightly more complicated example of electron-helium scattering. The point is that if the three electrons are distinguishable then there are channels in which the electrons of the helium atom have a symmetric bound-state wave function. As soon as we act with the anti-symmetrizing projector these wave functions are annihilated, corresponding to the obvious fact that the real helium atom has only anti-symmetric states. In enumerating the channels of a system containing identical particles we shall count only those channels in which the particles of each fragment have the correct allowed symmetry. By the same token we shall always use channel wave functions which are properly symmetrized with respect to the internal coordinates of each fragment. Thus, the wave function describing an electron incident on a helium atom will have the form

$$\chi(x_1)\phi(x_2, x_3)$$

where $\chi(x_1)$ is the incident wave packet and $\phi(x_2, x_3)$ is the properly antisymmetric helium wave function.

B.9.1 Transition probabilities and cross section

Having classified the channels of our $N-$particle system we can now set up a time-dependent description of the collision process and compute the various scattering probabilities. If we multiply the appropriate results for distinct particles by the symmetrizer Λ we immediately obtain the asymptotic condition for identical particles. An orbit that originates in channel α has the form

$$\Lambda e^{-iHt}|\psi\rangle \xrightarrow[t \to -\infty]{} \Lambda e^{-iH^\alpha t}|\psi_{in}\rangle \quad [|\psi\rangle = \Omega_+^\alpha |\psi_{in}\rangle] \tag{B.140}$$

while an orbit which is going to terminate in channel α has the form

$$\Lambda e^{-iHt}|\psi\rangle \xrightarrow[t \to +\infty]{} \Lambda e^{-iH^\alpha t}|\psi_{out}\rangle \quad [|\psi\rangle = \Omega_-^\alpha |\psi_{out}\rangle] \tag{B.141}$$

Suppose now that we wish for the probability that an *in* state $|\phi\rangle$ in channel α lead to the *out* state $|\phi'\rangle$ in channel α'. If the *in* state was given by $|\psi_{in}\rangle = |\phi\rangle$ in $\mathcal{L}^\alpha$, then according to (B.140) the actual state at $t = 0$ is

$$a\Lambda\Omega_+^\alpha|\phi\rangle \tag{B.142}$$

where a is some normalization factor. If the *out* asymptote were going to be $|\phi'\rangle$ in $\mathcal{L}^{\alpha'}$, then according to (B.141) the actual state at $t = 0$ would have to be

$$a'\Lambda\Omega_-^{\alpha'}|\phi'\rangle \tag{B.143}$$

with a' the appropriate normalization factor. The required transition amplitude is just the overlap of these two functions, and hence,

$$w(\phi', \alpha' \leftarrow \phi, \alpha) = (a'a)^2|\langle\Lambda\Omega_-^{\alpha'}\phi'|\Lambda\Omega_+^\alpha\phi\rangle|^2$$

$$= (a'a)^2 |\langle \Lambda \Omega_-^{\alpha'} \phi' | \Omega_+^{\alpha} \phi \rangle|^2$$
$$\propto |\sum_{\Pi} \eta_{\Pi} \langle \Pi \Omega_-^{\alpha'} \phi' | \Omega_+^{\alpha} \phi \rangle|^2 \tag{B.144}$$

The interpretation of this result is completely natural. The first term inside the sum (that coming from $\Pi = 1$) is the amplitude one would obtain for the process if the particles were all distinct; the other terms are the amplitudes for the various "exchange" processes differing from the original one by permutations of the final (identical) particles. Since the particles are really indistinguishable, the actual amplitude is obtained by summing all of these amplitudes, multiplied by the appropriate factors ± 1 if the particles are fermions.

To determine the constant of proportionality in (B.144) we determine the normalization factors a and a' in the states (B.142) and (B.143). The calculation of these factors in general (i.e., with arbitrary numbers of particles of arbitrarily many different types and with arbitrary channels α and α') is straightforward but tedious. For important special case of a collision between a single particle and a target containing N particles of the same type as the projectile (this includes the important examples of collisions between an electron and N-electron atom, and between a nucleon and an N-body nucleus with proton and neutrons treated as identical using the isospin formalism), for processes in which the *in* and *out* channels have the same arrangements (i.e., only elastic scattering and excitation), the normalization factors a and a' are $(N+1)^{1/2}$. Therefore we have

$$w(\phi', \alpha' \leftarrow \phi, \alpha) = (N+1)^2 |\langle \Lambda \Omega_-^{\alpha'} \phi' | \Omega_+^{\alpha} \phi \rangle|^2$$
$$= (\frac{1}{N!})^2 \left| \sum_{\Pi} \eta_{\Pi} \langle \Pi \Omega_-^{\alpha'} \phi' | \Omega_+^{\alpha} \phi \rangle \right|^2 \tag{B.145}$$

To simplify the sum in (B.145) it is convenient to rewrite each of the permutations Π of the $N+1$ particles $0, 1, \ldots, N$ in the form

$$\Pi = \Pi' \Pi''$$

where Π' exchanges 0 with one of the variables $0, \ldots, N$ leaving all others alone, while Π'' is a permutation of $1, \ldots, N$ only. The sum over the $(N+1)!$ permutations Π can then be replaced by a sum over the $(N+1)$ permutations Π' and the $N!$ permutations Π''. Now, the wave function on which Π operates is already symmetrized with respect to particles $1, \ldots, N$ and so each of the $N!$ different permutations Π'' produces the same result. Summing over these exactly cancels the factor $1/N!$ outside to give

$$w(\phi', \alpha' \leftarrow \phi, \alpha) = \left| \sum_{\Pi}{}' \eta_{\Pi} \langle \Pi \Omega_-^{\alpha'} \phi' | \Omega_+^{\alpha} \phi \rangle \right|^2 \tag{B.146}$$

where now $\sum'$ denotes a sum over the $N+1$ permutations that exchange the original projectile 0 with one of the particles $0, \ldots, N$ leaving all other particles undisturbed.

Finally we can divide the sum $\sum'$ into one term corresponding to $\Pi = 1$ and the remaining N terms in which particle 0 changes place with one of the target particles $1, \ldots, N$. Since the wave function on which Π acts is already symmetrized with respect to particles $1, \ldots, N$ then last N terms are all the same and we arrive at the final result.

$$w(\phi', \alpha' \leftarrow \phi, \alpha) = \left| \langle \Omega_-^{\alpha'} \phi' | \Omega_+^{\alpha} \phi \rangle + \eta N \langle \Pi_{01} \Omega_-^{\alpha'} \phi' | \Omega_+^{\alpha} \phi \rangle \right|^2 \tag{B.147}$$

where as usual $\eta = \pm 1$ depending on whether the particles are bosons or fermions and Π_{01} denotes the permutation which just exchanges particles 0 and 1.

From this result we can immediately proceed to the calculation of the observed cross section. We assume spinless particles and target for simplicity. We obtain

$$\frac{d\sigma}{d\Omega}(\mathbf{p}', \alpha' \leftarrow \mathbf{p}, \alpha) = \frac{p'}{p} |\widehat{f}(\mathbf{p}', \alpha' \leftarrow \mathbf{p}, \alpha)|^2 \tag{B.148}$$

where

$$\widehat{f}(\mathbf{p}', \alpha' \leftarrow \mathbf{p}, \alpha) = f_{di}(\mathbf{p}', \alpha' \leftarrow \mathbf{p}, \alpha) + \eta N f_{ex}(\mathbf{p}', \alpha' \leftarrow \mathbf{p}, \alpha) \tag{B.149}$$

Here f_{di} is the amplitude one would calculate for the "direct" process

$$\text{direct}: \quad 0 + (12 \cdots N)_\alpha \to 0 + (12 \cdots N)_{\alpha'} \tag{B.150}$$

on the assumption that the particles are distinct; that is

$$f_{di}(\mathbf{p}', \alpha' \leftarrow \mathbf{p}, \alpha) = f(\mathbf{p}', \alpha' \leftarrow \mathbf{p}, \alpha) \tag{B.151}$$

if, as usual, we use f to denote the amplitude calculated for distinct particles. The amplitude f_{ex} is the corresponding "exchange" amplitude for the ejection of particle 1 with momentum $\mathbf{p}'$ and the simultaneous capture of particle 0

$$\text{exchange}: \quad 0 + (12 \cdots N)_\alpha \to 1 + (02 \cdots N)_{\alpha'} \tag{B.152}$$

$$f_{ex}(\mathbf{p}', \alpha' \leftarrow \mathbf{p}, \alpha) = f(\mathbf{p}', \widetilde{\alpha}' \leftarrow \mathbf{p}, \alpha) \tag{B.153}$$

where $\widetilde{\alpha}'$ denotes the exchange channel of (B.152). Since the original particle 0 can exchange with any one of the N equivalent particles in the target, the amplitude f_{ex} appears multiplied by N in the expression (B.149) for $\widehat{f}$.

C. ALKALI ATOMS IN A MAGNETIC GUIDE:MATRIX ELEMENTS

The matrix elements of the Hamiltonian (8.10) can be calculated analytically by exploiting the recurrence relation of the associated Laguerre polynomials [94, 95]. The matrix reads

$$\langle i \mid \ H \mid j\rangle = \frac{1}{2}[\langle i \mid \mathbf{p}^2 \mid j\rangle + \langle i \mid r\sin\theta\cos\varphi(S_x+\alpha I_x) \mid j\rangle + \langle i \mid r\sin\theta\sin\varphi \times(S_y+\alpha I_y) \mid j\rangle - 2\langle i \mid r\cos\theta(S_z+\alpha I_z) \mid j\rangle + \beta\langle i \mid \mathbf{I}\cdot\mathbf{S} \mid j\rangle] \quad \text{(C.1)}$$

Here $i=(n,l,m_i,m_s)$, $j=(n',l',m_i',m_s')$,

$$\begin{aligned}\langle i \mid \mathbf{p}^2 \mid j\rangle &= [-\hbar^2\langle R_n^\zeta \mid (\frac{\partial^2}{\partial r^2}+\frac{2}{r}\frac{\partial}{\partial r}) \mid R_{n'}^\zeta\rangle\langle Y_l^m \mid Y_{l'}^{m'}\rangle \\ &\quad + \langle R_n^\zeta \mid \frac{1}{r^2} \mid R_{n'}^\zeta\rangle\langle Y_l^m \mid L^2 \mid Y_{l'}^{m'}\rangle]\langle m_i,m_s \mid m_i',m_s'\rangle \quad \text{(C.2)}\end{aligned}$$

with $m=M-m_i-m_s$ and $m'=M-m_i'-m_s'$,

$$\begin{aligned}\langle i \mid r\sin\theta\cos\varphi(S_x+\alpha I_x) \mid j\rangle &= \langle R_n^\zeta \mid r \mid R_{n'}^\zeta\rangle\langle Y_l^m \mid \sin\theta\cos\varphi \mid Y_{l'}^{m'}\rangle \\ &\quad \times\langle m_i,m_s \mid (S_x+\alpha I_x) \mid m_i',m_s'\rangle \quad \text{(C.3)}\end{aligned}$$

$$\begin{aligned}\langle i \mid r\sin\theta\sin\varphi(S_y+\alpha I_y) \mid j\rangle &= \langle R_n^\zeta \mid r \mid R_{n'}^\zeta\rangle\langle Y_l^m \mid \sin\theta\sin\varphi \mid Y_{l'}^{m'}\rangle \\ &\quad \times\langle m_i,m_s \mid (S_y+\alpha I_y) \mid m_i',m_s'\rangle \quad \text{(C.4)}\end{aligned}$$

$$\begin{aligned}\langle i \mid r\cos\theta(S_z+\alpha I_z) \mid j\rangle &= \langle R_n^\zeta \mid r \mid R_{n'}^\zeta\rangle\langle Y_l^m \mid \cos\theta \mid Y_{l'}^{m'}\rangle \\ &\quad \times\langle m_i,m_s \mid (S_z+\alpha I_z) \mid m_i',m_s'\rangle \quad \text{(C.5)}\end{aligned}$$

and

$$\langle i \mid \mathbf{I}\cdot\mathbf{S} \mid j\rangle = \langle R_n^\zeta \mid R_{n'}^\zeta\rangle\langle Y_l^m \mid Y_{l'}^{m'}\rangle\langle m_i,m_s \mid \mathbf{I}\cdot\mathbf{S} \mid m_i',m_s'\rangle \quad \text{(C.6)}$$

C.1 Radial Matrix Elements

The Laguerre polynomials satisfy the following recursion relation

$$rL_n^l = -(n+l)L_{n-1}^l + (2n+l+1)L_n^l - (n+1)L_{n+1}^l \quad \text{(C.7)}$$

This yields the following relation for the basis functions $R_n^{(\zeta)}$

$$rR_n^{(\zeta)} = -(n+1)R_{n+1}^{(\zeta)} + (2n+1)R_n^{(\zeta)} - nR_{n-1}^{(\zeta)} \tag{C.8}$$

From which we obtain

$$\zeta\langle R_n^{(\zeta)} \mid \frac{1}{r^2} \mid R_{n'}^{(\zeta)}\rangle = \delta_{n,n'} \tag{C.9}$$

$$\begin{aligned} 4\zeta\langle R_n^{(\zeta)} \mid \frac{\partial^2}{\partial r^2} + \frac{2}{r}\frac{\partial}{\partial r} \mid R_{n'}^{(\zeta)}\rangle &= n'(n'-1)\delta_{n,n'-2} - 2(n'^2+n'+1)\delta_{n,n'} \\ &\quad + (n'+1)(n'+2)\delta_{n,n'+2} \end{aligned} \tag{C.10}$$

$$\zeta^2\langle R_n^{(\zeta)} \mid \frac{1}{r} \mid R_{n'}^{(\zeta)}\rangle = -n'\delta_{n,n'-1} + (1+2n')\delta_{n,n'} - (1+n')\delta_{n,n'+1} \tag{C.11}$$

$$\begin{aligned} \zeta^3\langle R_n^{(\zeta)} \mid R_{n'}^{(\zeta)}\rangle &= (n'-1)n'\delta_{n,n'-2} - 4n'^2\delta_{n,n'-1} + (2+6n'(1+n'))\delta_{n,n'} \\ &\quad - 4(1+n')^2\delta_{n,n'+1} + (1+n')(2+n')\delta_{n,n'+2} \end{aligned} \tag{C.12}$$

$$\begin{aligned} \zeta^4\langle R_n^{(\zeta)} \mid r \mid R_{n'}^{(\zeta)}\rangle = &-(n'-2)(n'-1)n'\delta_{n,n'-3} + 3(n'-1)n'(2n'-1)\delta_{n,n'-2} \\ &-3n'(1+5n'^2)\delta_{n,n'-1} + 2(1+2n')(3+5n'(1+n'))\delta_{n,n'} \\ &-3(1+n')(6+5n'(2+n'))\delta_{n,n'+1} + 3(1+n')(2+n')(3+2n')\delta_{n,n'+2} \\ &-(1+n')(2+n')(3+n')\delta_{n,n'+3} \end{aligned} \tag{C.13}$$

C.2 Angular Matrix Elements

For the angular matrix elements the following relations are needed

$$\cos\theta \mid Y_l^m\rangle = \sqrt{\frac{(l-m)(l+m)}{(2l-1)(2l+1)}} \mid Y_{l-1}^m\rangle + \sqrt{\frac{(l-m+1)(l+m+1)}{(2l+1)(2l+3)}} \mid Y_{l+1}^m\rangle \tag{C.14}$$

$$\begin{aligned} \sin\theta e^{\pm i\varphi} \mid Y_l^m\rangle = &\pm\sqrt{\frac{(l\mp m)(l\mp m-1)}{(2l-1)(2l+1)}} \mid Y_{l-1}^{m\pm1}\rangle \\ &\mp\sqrt{\frac{(l\pm m+2)(l\pm m+1)}{(2l+3)(2l+1)}} \mid Y_{l+1}^{m\pm1}\rangle \end{aligned} \tag{C.15}$$

From which we obtain

$$\langle Y_l^m \mid \cos\theta \mid Y_{l'}^{m'} \rangle = \sqrt{\frac{(l'-m')(l'+m')}{(2l'-1)(2l'+1)}}\delta_{l,l'-1}\delta_{m,m'} + \sqrt{\frac{(l'-m'+1)(l'+m'+1)}{(2l'+1)(2l'+3)}}\delta_{l,l'+1}\delta_{m,m'} \quad \text{(C.16)}$$

$$\langle Y_l^m \mid \sin\theta e^{\pm i\varphi} \mid Y_{l'}^{m'} \rangle = \pm\sqrt{\frac{(l' \mp m')(l' \mp m'-1)}{(2l'-1)(2l'+1)}}\delta_{l,l'-1}\delta_{m,m'+1} \mp \sqrt{\frac{(l' \pm m'+2)(l' \pm m'+1)}{(2l'+1)(2l'+3)}}\delta_{l,l'+1}\delta_{m,m'-1} \quad \text{(C.17)}$$

$$\langle Y_l^m \mid \sin\theta\cos\varphi \mid Y_{l'}^{m'} \rangle = \tfrac{1}{2}\langle Y_l^m \mid \sin\theta e^{i\varphi} \mid Y_{l'}^{m'} \rangle + \tfrac{1}{2}\langle Y_l^m \mid \sin\theta e^{-i\varphi} \mid Y_{l'}^{m'} \rangle \quad \text{(C.18)}$$

$$\langle Y_l^m \mid \sin\theta\sin\varphi \mid Y_{l'}^{m'} \rangle = \frac{1}{2i}\langle Y_l^m \mid \sin\theta e^{i\varphi} \mid Y_{l'}^{m'} \rangle - \frac{1}{2i}\langle Y_l^m \mid \sin\theta e^{-i\varphi} \mid Y_{l'}^{m'} \rangle \quad \text{(C.19)}$$

C.3 Spin Matrix Elements

For spin matrix elements the following relations are needed

$$I_x \mid m_i\rangle = \frac{\hbar}{2}\sqrt{(i+m_i+1)(i-m_i)} \mid m_i+1\rangle + \frac{\hbar}{2}\sqrt{(i-m_i+1)(i+m_i)} \mid m_i-1\rangle \quad \text{(C.20)}$$

$$I_y \mid m_i\rangle = \frac{\hbar}{2i}\sqrt{(i+m_i+1)(i-m_i)} \mid m_i+1\rangle - \frac{\hbar}{2i}\sqrt{(i-m_i+1)(i+m_i)} \mid m_i-1\rangle \quad \text{(C.21)}$$

$$I_z \mid m_i\rangle = \hbar m_i \mid m_i\rangle \quad \text{(C.22)}$$

i is integer or half-integer and $-i \le m_i \le i$. From these equations we obtain

$$\langle m_i \mid I_x \mid m_i'\rangle = \frac{\hbar}{2}\sqrt{(i+m_i+1)(i-m_i)}\delta_{m_i,m_i'+1} + \frac{\hbar}{2}\sqrt{(i-m_i+1)(i+m_i)}\delta_{m_i,m_i'-1} \quad \text{(C.23)}$$

$$\begin{aligned}\langle m_i \mid I_y \mid m_i' \rangle &= \frac{\hbar}{2i}\sqrt{(i+m_i+1)(i-m_i)}\delta_{m_i,m_i'+1} \\ &\quad - \frac{\hbar}{2i}\sqrt{(i-m_i+1)(i+m_i)}\delta_{m_i,m_i'-1} \qquad \text{(C.24)}\end{aligned}$$

$$\langle m_i \mid I_z \mid m_i' \rangle = \hbar m_i \delta_{m_i,m_i'} \qquad \text{(C.25)}$$

For S-Matrix elements we should just put $s = 1/2$ instead of i in above equations.

$$\begin{aligned}\langle m_i, m_s \mid \mathbf{I}\cdot\mathbf{S} \mid m_i', m_s' \rangle &= \langle m_i \mid I_x \mid m_i' \rangle \langle m_s \mid S_x \mid m_s' \rangle \\ &\quad + \langle m_i \mid I_y \mid m_i' \rangle \langle m_s \mid S_y \mid m_s' \rangle \\ &\quad + \langle m_i \mid I_z \mid m_i' \rangle \langle m_s \mid S_z \mid m_s' \rangle \qquad \text{(C.26)}\end{aligned}$$

D. BOSE-FERMI MAPPING THEOREM

In 1940 Nagamiya noted [102] that in the "fundamental sector" $z_1 \leq z_2 \leq \ldots \leq z_N$ the ground state wave function of a spatially uniform, 1D hard-core Bose gas can be written as an ideal Fermi gas determinant, continuation into other permutation sectors being effected by imposing overall Bose symmetry under all permutations $z_i \leftrightarrow z_j$ in spite of the fermionic *anti*symmetry under permutations of *orbitals* (*not* coordinates) in the fundamental sector. After that in 1960 the Fermi-Bose mapping method which is much more general was introduced independently by Girardeau [52] and Stachowiak [103]. The mapping theorem holding also in the presence of external potentials and/or finite two-particle or many-particle interactions in addition to the hard core interaction [52]. It also applies to the 1D time-dependent many-body Schrödinger equation and has been used to treat some time-dependent interference properties of the 1D hard core Bose gas [104, 105, 106, 107, 108]

We now briefly review the mapping theorem. In general the N-boson Hamiltonian is assumed to have the structure

$$H_{1D} = -(\hbar^2/2m)\sum_{j=1}^{N}\partial_{z_i}^2 + V(z_1,\ldots,z_N) \tag{D.1}$$

where the real, symmetric function V contains all external potentials (e.g., a longitudinal trap potential) as well as any finite interaction potentials *not including* the Hard-sphere repulsion, which is instead treated as a constraint on allowed wave functions $\psi_B(z_1,\ldots,z_N)$

$$\psi_B = 0 \quad \text{if } |z_j - z_k| < a, \quad (1 \leq j < k \leq N) \tag{D.2}$$

Let $\psi_F(z_1,\ldots,z_N)$ be a fermionic solution of $H_{1D}\psi = E\psi$ which is antisymmetric under all pair exchanges $z_j \leftrightarrow z_k$, hence all permutations. One can consider ψ_F to be either the wave function of a fictitious system of "spinless fermions", or else that of a system of real, spin-aligned fermions. Define a "unit antisymmetric function" [52]

$$A(z_1,\ldots,z_N) = \prod_{1\leq j<k\leq N} sgn(z_k - z_j), \tag{D.3}$$

where $sgn(z)$ is the algebraic sign of the coordinate difference $z = z_k - z_j$, i.e., it is $+1\,(-1)$ if $z > 0\,(z < 0)$. For given antisymmetric ψ_F, define a bosonic wave function ψ_B by

$$\psi_B(z_1,\ldots,z_N) = A(z_1,\ldots,z_N)\psi_F(z_1,\ldots,z_N) \tag{D.4}$$

which defines the Fermi-Bose mapping. ψ_B satisfies the hard core constraint (D.2) if ψ_F does, is totally symmetric (bosonic) under permutations, obeys the same boundary conditions as ψ_F, and $H_{1D}\psi_B = E\psi_B$ follows from $H_{1D}\psi_F = E\psi_F$ [52, 109]. In the case of periodic boundary conditions (no trap potential, spatially uniform system) one must add the proviso that the boundary conditions are only preserved under the mapping if N is odd, but the case of even N is accommodated by imposing periodic boundary conditions on ψ_F but *anti*periodic boundary conditions on ψ_B.

The mapping theorem leads to explicit expressions for all many-body energy eigenstates and eigenvalues under the assumption that the only two-particle interaction is a zero-range hard repulsion, represented by the $a \to 0$ limit of the hard-core constraint, the "TG gas". Such solutions were obtained in Sec. 3 of [52] for periodic boundary conditions and no external potential.

E. BOUNDARY CONDITIONS

In the limit r tends to zero, $\mathbf{u}$ in (5.17) goes to zero. This boundary condition can be satisfied easily by putting $\mathbf{u}(r=0)=\mathbf{0}$ and $\mathbf{u}_{-j}=\mathbf{u}_j$ in the vicinity of $r=0$. The latter is needed for approximating the derivatives $\frac{d^2}{dx^2}u(r(x))$ and $\frac{d}{dx}u(r(x))$ near the point $r=0$.

The boundary condition for u approximating the asymptotic form (5.10) at large r can be written in the form

$$\mathbf{u}_j+\alpha_j^{(1)}\mathbf{u}_{j-1}+\alpha_j^{(2)}\mathbf{u}_{j-2}+\alpha_j^{(3)}\mathbf{u}_{j-3}+\alpha_j^{(4)}\mathbf{u}_{j-4}=\mathbf{g}_j \qquad j=N-2,N-1,N \tag{E.1}$$

where α_j's are diagonal $N_\theta\times N_\theta$ matrices and $\mathbf{g}_j$ is a N_θ-dimensional vector. The above boundary conditions are constructed by eliminating the unknown amplitudes $f_{nn'}$ from the asymptotic equations (5.10) written for a few r_js neighboring to the point $r_N=R$. This gives the values for the coefficients α_j's and $\mathbf{g}_j$. In general for up to four open channels we have

$$\left[\alpha_j^{(l)}\right]_{mm'}=(-1)^i\left(T_j^{l-1,m}+T_j^{l,m}\right)\frac{r_j}{r_{j-l}}\frac{\phi_{n_e}(\rho_j^m)}{\phi_{n_e}(\rho_{j-l}^m)}e^{ik_{n_e}(|z_j^m|-|z_{j-l}^m|)}\delta_{mm'} \qquad (l=1,2,3,4) \tag{E.2}$$

and

$$[\mathbf{g}_j]_m=2\sqrt{\lambda_m}r_j\phi_{n_e}(\rho_j^m)e^{ik_{n_e}|z_j^m|}\sum_{n=0}^{n_e}\sum_{l=0}^{4}(-1)^i e^{-ik_{n_e}|z_{j-l}^m|}e^{ik_n z_{j-l}^m} \times(T_j^{l-1,m}+T_j^{l,m})\frac{\phi_n(\rho_{j-l}^m)}{\phi_{n_e}(\rho_{j-l}^m)} \tag{E.3}$$

For the case of bosonic (fermionic) collisions we must consider just the even (odd) part of the equation (E.3), i.e. we just need to replace the term $e^{ik_n z_{j-l}^m}$ by $\cos k_n z_{j-l}^m$ ($i\sin k_n z_{j-l}^m$). Here $\phi_n(\rho)=\phi_{n,0}(\rho,\varphi)$ is the eigenfunction of the transverse trapping Hamiltonian [see (5.6)], $\rho_j^m=r_j\sin\theta_m$, $z_j^m=r_j\cos\theta_m$, n is the channel number of the initial state, and n_e is the number of transversely excited open channels. The complex numbers $T_j^{i,m}$'s are given through

$$T_j^{l,m}=\delta_{l,0}+\delta_{l,1}(a_j^m+b_j^m+c_j^m)+\delta_{l,2}(a_j^m b_{j-1}^m+a_j^m c_{j-1}^m+b_j^m c_{j-1}^m) +\delta_{l,3}a_j^m b_{j-1}^m c_{j-2}^m \tag{E.4}$$

If $n_e < 1$ (single-mode regime) $a_j^m = 0$, otherwise

$$\begin{aligned} a_j^m = \{&\Xi_{0,j}^m - (1 + b_j^m + c_j^m)\Xi_{0,j-1}^m + (b_j^m + c_j^m + b_j^m c_{j-1}^m)\Xi_{0,j-2}^m \\ &- b_j^m c_{j-1}^m \Xi_{0,j-3}^m\} \times \{\Xi_{0,j-1}^m - (1 + b_j^m + c_j^m)\Xi_{0,j-2}^m \\ &+ (b_j^m + c_j^m + b_j^m c_{j-1}^m)\Xi_{0,j-3}^m - b_j^m c_{j-1}^m \Xi_{0,j-4}^m\}^{-1} \end{aligned} \tag{E.5}$$

if $n_e < 2$, $b_j^m = 0$, otherwise

$$\begin{aligned} b_j^m = &\left\{\Xi_{1,j}^m - (1 + c_j^m)\Xi_{1,j-1}^m + c_j^m \Xi_{1,j-2}^m\right\} \\ &\times \left\{\Xi_{1,j-1}^m - (1 + c_j^m)\Xi_{1,j-2}^m + c_j^m \Xi_{1,j-3}^m\right\}^{-1} \end{aligned} \tag{E.6}$$

if $n_e < 3$, $c_j^m = 0$, otherwise

$$c_j^m = \left\{\Xi_{2,j}^m - \Xi_{2,j-1}^m\right\} \times \left\{\Xi_{2,j-1}^m - \Xi_{2,j-2}^m\right\}^{-1} \tag{E.7}$$

where $\Xi_{n,j}^m = e^{i(k_n - k_{n_e})|z_j^m|} \frac{\phi_n(\rho_j^m)}{\phi_{n_e}(\rho_j^m)}$. k_n and k_{n_e} are given by (5.9).

F. FAST IMPLICIT MATRIX ALGORITHM

Following the idea of the LU decomposition [61] and the sweep method [62] (or the Thomas algorithm [63]), we search the solution of the system of N vector equations with any coefficient being a $N_\theta \times N_\theta$ matrix (5.24) in the form

$$\mathbf{u}_j = C_j^{(1)}\mathbf{u}_{j+1} + C_j^{(2)}\mathbf{u}_{j+2} + C_j^{(3)}\mathbf{u}_{j+3}, \qquad j = 1, ..., N-3 \tag{F.1}$$

Here we define $\mathbf{u}(r(x_j))$ as $\mathbf{u}_j$ for simplicity. The C_js are unknown $N_\theta \times N_\theta$ matrices. To find the solution, first we should calculate the unknown C_j matrices. The plan is the following: Due to (F.1) we have

$$\mathbf{u}_{j-p} = C_{j-p}^{(1)}\mathbf{u}_{j-p+1} + C_{j-p}^{(2)}\mathbf{u}_{j-p+2} + C_{j-p}^{(3)}\mathbf{u}_{j-p+3}, \qquad p = 1, 2, 3\ , \tag{F.2}$$

then one obtains

$$\mathbf{u}_{j-1} = C_{j-1}^{(1)}\mathbf{u}_j + C_{j-1}^{(2)}\mathbf{u}_{j+1} + C_{j-1}^{(3)}\mathbf{u}_{j+2} \tag{F.3}$$

$$\mathbf{u}_{j-2} = \left[C_{j-2}^{(1)}C_{j-1}^{(1)} + C_{j-2}^{(2)}\right]\mathbf{u}_j + \left[C_{j-2}^{(1)}C_{j-1}^{(2)} + C_{j-2}^{(3)}\right]\mathbf{u}_{j+1} + C_{j-2}^{(1)}C_{j-1}^{(3)}\mathbf{u}_{j+2} \tag{F.4}$$

and

$$\begin{aligned}\mathbf{u}_{j-3} \;=\; & \left[C_{j-3}^{(1)}C_{j-2}^{(1)}C_{j-1}^{(1)} + C_{j-3}^{(1)}C_{j-2}^{(2)} + C_{j-2}^{(2)}C_{j-1}^{(1)} + C_{j-2}^{(3)}\right]\mathbf{u}_j \\ & + \left[C_{j-3}^{(1)}C_{j-2}^{(1)}C_{j-1}^{(2)} + C_{j-3}^{(1)}C_{j-2}^{(3)} + C_{j-2}^{(2)}C_{j-1}^{(2)}\right]\mathbf{u}_{j+1} \\ & + \left[C_{j-3}^{(1)}C_{j-2}^{(1)}C_{j-1}^{(3)} + C_{j-2}^{(2)}C_{j-1}^{(3)}\right]\mathbf{u}_{j+2}\end{aligned} \tag{F.5}$$

By substituting u_j defined by (F.3-F.5) into (5.24) one can calculate $\mathbf{u}_j$ in terms of $\mathbf{u}_{j+1}$, $\mathbf{u}_{j+2}$, and $\mathbf{u}_{j+3}$. Then, by comparing with (F.1) we find a recurrence formula for calculating the unknown matrices C_j:

$$\begin{aligned}-DC_j^{(1)} = {} & \mathbf{A}_{j-3}^j\left[C_{j-3}^{(1)}C_{j-2}^{(1)}C_{j-1}^{(2)} + C_{j-3}^{(1)}C_{j-2}^{(3)} + C_{j-3}^{(2)}C_{j-1}^{(2)}\right] \\ & + \mathbf{A}_{j-2}^j\left[C_{j-2}^{(1)}C_{j-1}^{(2)} + C_{j-2}^{(3)}\right] + \mathbf{A}_{j-1}^j C_{j-1}^{(2)} + \mathbf{A}_{j+1}^j\end{aligned} \tag{F.6}$$

$$\begin{aligned}-DC_j^{(2)} \;=\; & \mathbf{A}_{j-3}^j\left[C_{j-3}^{(1)}C_{j-2}^{(1)}C_{j-1}^{(3)} + C_{j-3}^{(2)}C_{j-1}^{(3)}\right] \\ & + \mathbf{A}_{j-2}^j C_{j-2}^{(1)}C_{j-1}^{(3)} + \mathbf{A}_{j-1}^j C_{j-1}^{(3)} + \mathbf{A}_{j+2}^j\end{aligned} \tag{F.7}$$

and

$$-DC_j^{(3)} = \mathbf{A}_{j+3}^j. \tag{F.8}$$

Here

$$\begin{aligned} D &= \mathbf{A}_{j-3}^j \left[C_{j-3}^{(1)} C_{j-2}^{(1)} C_{j-1}^{(1)} + C_{j-3}^{(1)} C_{j-2}^{(2)} + C_{j-3}^{(2)} C_{j-1}^{(1)} + C_{j-3}^{(3)} \right] \\ &\quad + \mathbf{A}_{j-2}^j \left[C_{j-2}^{(1)} C_{j-1}^{(1)} + C_{j-2}^{(2)} \right] + \mathbf{A}_{j-1}^j C_{j-1}^{(1)} + \mathbf{A}_j^j + 2(\epsilon I - V_j) \end{aligned} \tag{F.9}$$

By using the left-side boundary conditions and (F.1) one can calculate the C_j matrices for $j = 1$, 2, and 3. Then by using (F.9-F.6) we calculate all the matrices C_j. Subsequently by using the right-side boundary conditions (E.1) and recurrence formula (F.1) we first calculate $\mathbf{u}_j$ for $j = N-2, N-1$, and N and then $\mathbf{u}_j$ for $j = 1, ..., N-3$.

G. ACKNOWLEDGMENTS

The financial support for doing the work which appears in this thesis has been provided by the **Ministry of Science, Research and Technology of Iran**, in the form of a scholarship. This provided me with the wonderful opportunity to study without being concerned about my finances.

I would like to express my deepest appreciation to my advisor Prof. **Peter Schmelcher**, I began working with him about four years ago and during this time I have learned an immense amount from him.

I am grateful to prof. **Vladimir Melezhik** for helpful discussion and for teaching me numerical methods.

I would like to thank Dr. **Igor Lesanovsky** who was a PhD student of Peter's group when I began working there. Discussion with him was really worthful for me.

I like to thank Prof. **Jochen Schirmer** for accepting to be the second examiner of this work.

Special thanks to all the members of groups of Prof. **Schmelcher**, Prof. **Schmiedmayer**, and Prof. **Pan** particularly **Bernd Hezel**, **Florian Lenz**, **Torsten Straßel**, **Dennis Heine**, **Budhaditya Chatterjee**, **Sascha Zöllner**, **Christoph Petri**, and **Florian Koch**.

I would like to thank my parents and my brother. They have been a great source of support and encouragement throughout of my life.

I am very grateful to my wife **Azam** and my children **Pourya** and **Yekta** for everything. I would like to dedicate this dissertation to my family.

BIBLIOGRAPHY

[1] J.R. Taylor, *Scattering Theory*, Wileg, New York (1972)

[2] L.E. Ballentine, *Quantum Mechanics*, Prentice-Hall International, Inc. (1990)

[3] L.I. Schiff, *Quantum Mechanics* (3rd ed.), McGraw-Hill, New York (1968)

[4] C. Maschler, Diploma Thesis, Universität Innsbruck

[5] O. Alon, M.Sc. Thesis, Technion - Israel Institute of Technology

[6] N. Moiseyev, Phys. Rep. 302, 211 (1998)

[7] S. Inouye et. al, Nature, 392, 151 (1998).

[8] G.A. Gamow, Zs. f. Phys. 51, 204; 52 (1928) 510; R.W. Gurney, E.U. Condon, Phys. Rev. 33, 127 (1929).

[9] A. Schutte, et al., J. Chem. Phys. 62, 600 (1975); J. Chem. Phys. 63, 3081 (1975)

[10] I. Eliezer, H.S. Taylor, J.K. Williams, J. Chem. Phys. 47, 2165 (1967). For a study by complex scaling see: N. Moiseyev, C.T. Corcoran, Phys. Rev. A 20, 814 (1979)

[11] R. G. Newton, *Scattering theory of waves and particles*, Springer (1982)

[12] D.C. Sorensen, *Parallel numerical algorithms - Implicitly restarted Arnoldi/Lanczos methods for large scale eigenvalue calculations*, Kluwer (Dordrecht) (1995)

[13] James W. Demmel, Stanley C. Eisenstat, John R. Gilbert, Xiaoye S. Li, and Joseph W. H. Liu. *A supernodal approach to sparse partial pivoting.* SIAM J. *Matrix Analysis and Applications*, 20(3):720-755 (1999)

[14] T. Pang, *An Introduction to Computational Physics*, Cambridge University Press (1999)

[15] R. Grimm, M. Weidemüller, and Y.B. Ovchinnikov, Adv. At. Mol. Opt. Phys. **42**, 95 (2000).

[16] R. Folman *et al.*, Adv. At. Mol. Opt. Phys. 42, 95 (2000).

[17] J. Reichel, Appl. Phys. B: Laser Opt. 74, 469 (2002).

[18] J. Fortagh *et al.*, Rev. Mod. Phys. 79, 235 (2007).

[19] E.L. Bolda, E. Tiesinga and P.S. Julienne, Phys. Rev. A 66, 013403 (2002).

[20] R. Stock, I.H. Deutsch and E.L. Bolda, Phys. Rev. Lett. 91, 183201 (2003).

[21] V.A. Yurovsky, Phys. Rev. A 71, 012709 (2005).

[22] R. Stock and I.H. Deutsch, Phys. Rev. A 73, 032701 (2006).

[23] V.A. Yurovsky and Y.B. Band, Phys. Rev. A 75, 012717 (2007).

[24] P. Naidon *et al*, New J. Phys. 9, 19 (2007).

[25] S.G. Bhongale, S.J.J.M.F. Kokkelmans and I.H. Deutsch, arXiv:0712.2070 v1, physics:atom-ph.

[26] V.A. Yurovsky, M. Ol'shanii and D.S. Weiss, Adv. At. Mol. Opt. Phys. 55, 61 (2007).

[27] M. Olshanii, Phys. Rev. Lett. 81, 938 (1998).

[28] T. Bergeman, M.G. Moore, and M. Olshanii, Phys. Rev. Lett. 91, 163201 (2003).

[29] C. Mora, R. Egger, A.O. Gogolin, and A. Komnik, Phys. Rev. Lett. 93, 170403 (2004).

[30] C. Mora, R. Egger, and A.O. Gogolin, Phys. Rev. A 71, 052705 (2005).

[31] C. Mora, A. Komnik, R. Egger, and A.O. Gogolin, e-print arXiv:cond-mat/0501641.

[32] B.E. Granger and D. Blume, Phys. Rev. Lett. 92, 133202 (2004).

[33] T. Kinoshita, T. Wenger and D.S. Weiss, Science 305, 1125 (2004).

[34] B. Paredes et al, Nature 429, 277 (2004).

[35] K. Günter et al, Phys. Rev. Lett. 95, 230401 (2005).

[36] J.I. Kim, J. Schmiedmayer, and P. Schmelcher, Phys. Rev. A 72, 042711 (2005).

[37] V. Peano, M. Thorwart, C. Mora, and R. Egger, New J. Phys. 7, 192 (2005).

[38] J.I. Kim, V.S. Melezhik, and P. Schmelcher, Phys. Rev. Lett. 97, 193203 (2006).

[39] J.I. Kim, V.S. Melezhik, and P. Schmelcher, Rep. Progr. Theor. Phys. Supp. 166, 159 (2007).

[40] V.S. Melezhik, J.I. Kim, and P. Schmelcher, Phys. Rev. A 76, 053611 (2007).

[41] A. Lupu-Sax, PhD Thesis, Harvard University (1998).

[42] M.G.E. da Luz, A.S. Lupu-Sax and E.J. Heller, Phys. Rev. E 56, 2496 (1997)

[43] M.G. Moore, T. Bergeman and M. Olshanii, J. Phys. IV 116, 69 (2004), Lecture courses Les Houches School on '*Quantum Gases in Low Dimensions*' (2003).

[44] M. D. Girardeau, H. Nguyen, and M. Olshanii, arXiv:cond-mat/0403721v1 (2004)

[45] S. Saeidian, V.S. Melezhik, and P. Schmelcher, Phys. Rev. A 77, 042721 (2008).

[46] T. M. Apostol, *Introduction to Analytical Number Theory* (Springer, 1976)

[47] D. S. Petrov, M. Holtzmann, and G. V. Shlyapnikov, Phys. Rev. Lett. 84, 2551 (2000)

[48] V. Dunjko, V. Lorent, and M. Olshanii, Phys. Rev. Lett. 86. 5413 (2001)

[49] R. Roth and H. Feldmeier, Phys. Rev. A 64, 043603 (2001)

[50] H. Suno, B.D. Esry, and C.H. Greene, Phys. Rev. Lett. 90, 053202 (2003)

[51] D.C. Mattis, *The Many-Body Problem* (World Scientific Publishing Co. Pte. Ltd., Singapore, 1993)

[52] M.D. Girardeau, J. Math. Phys. (N.Y.) 1, 516 (1960)

[53] C. Ticknor, C.A. Regal, D.S. Jin and J.L. Bohn, Phys. Rev. A 69, 042712 (2004)

[54] R.V. Krems, Phys. Rev. Lett. 96, 123202 (2006)

[55] V.S. Melezhik, J. Kim and P. Schmekcher, Phys. Rev. E 76, 066213 (2007)

[56] R. Stock, A. Silberfarb, E.L. Bolda and I.H. Deutsch, Phys. Rev. Lett. 94, 023202 (2005)

[57] Z. Idziaszek and T. Calarco, Phys. Rev. Lett. 96, 013201 (2006)

[58] V.S. Melezhik, J. Comput. Phys. 92, 67 (1991).

[59] V.S. Melezhik and Chi-Yu Hu, Phys. Rev. Lett. 90, 083202 (2003).

[60] V.S. Melezhik, Phys. Lett. A 230, 203 (1997).

[61] W.H. Press, S.A. Teukolsky, W.T. Vetterling, and B.P. Flannery, *Numerical Recipes*, Cambridge University Press, 1992.

[62] I.M. Gelfand and S.V. Fomin, *Calculus of Variations*, Dover Publications, 2000.

[63] G.N. Bruse et al., Petrol. Trans. AIME 198, 79 (1953).

[64] C.J. Pethick and H. Smith, *Bose-Einstein Condensation in Dilute Gases*, Cambridge University Press (2002)

[65] L. Pitaevskii and S. Stringari, *Bose-Einstein Condensation*, Oxford Science Publications (2003)

[66] W. Ketterle, D.S. Durfee and D.M. Stamper-Kurn, Proceedings Enrico Fermi summer school on '*Bose-Einstein condensation*', Varenna, Italy (1998)

[67] A. Leggett, Rev. Mod. Phys. 73, 307 (2001)

[68] F. Dalfovo, S. Giorgini, L.P. Pitaevskii and S. Stringari, Rev. Mod. Phys. 71, 463 (1999)

[69] R. Folman *et al*, Adv. At. Mol. Phys. 48, 263 (2002)

[70] J. Reichel, Appl. Phys. B 74, 469 (2002)

[71] J. Fortagh and C. Zimmermann, Science 307, 860 (2005)

[72] W. Ketterle and D.E. Pritchard, Appl. Phys. B 54, 403 (1992)

[73] T. Bergeman, G. Erez and H.J. Metcalf, Phys.Rev. A 35, 1535 (1987)

[74] J.D. Weinstein and K.G. Libbrecht, Phys. Rev. A 52, 4004 (1995)

[75] T.H. Bergeman *et al*, J. Opt. Soc. Am. B 6, 2249 (1989)

[76] I. Lesanovsky, and P. Schmelcher, Phys. Rev. A 71, 032510 (2005)

[77] K. Berg-Sorensen, M.M. Burns, J.A. Golovchenko and L.V. Hau, Phys. Rev. A 53, 1653 (1996)

[78] L. Vestergaard Hau, J.A. Golovchenko, and M. Burns, Phys. Rev. Lett. 75, 1426 (1995)

[79] J. P. Burke, Jr., Chris H. Greene, and B. D. Esry, Phys. Rev. A 54, 3225 (1996)

[80] R. Blümel, K. Dietrich , Phys. Rev. A 43, 22 (1991)

[81] E.A. Hinds and C. Eberlein, Phys. Rev. A 61, 033614 (2000)

[82] E.A. Hinds and C. Eberlein, Phys. Rev. A 64, 039902(E) (2000)

[83] R. M. Potvliege and V. Zehnlé, Phys. Rev. A 63, 025601 (2001)

[84] I. Lesanovsky and P. Schmelcher, Phys. Rev. A 70, 063604 (2004)

[85] J. Bill, M.-I. Trappe, I. Lesanovsky and P. Schmelcher, Phys. Rev. A 73, 053609 (2006)

[86] S. Saeidian, I. Lesanovsky and P. Schmelcher, Phys. Rev. A 74, 065402 (2006)

[87] S. Saeidian, I. Lesanovsky and P. Schmelcher, Phys. Rev. A 76, 023424 (2007)

[88] H. J. Metcalf and P. Van der Straten, *Laser cooling and traping*, Springer New York (1999)

[89] I. Lesanovsky, PhD thesis, Universität Heidelberg (2006)

[90] F. Gerbier *et al*, Phys. Rev. A 73, 041602R (2006)

[91] M. Greiner, O. Mandel, T. Esslinger, T.W. Hänsch and I. Bloch, Nature 415, 39 (2002)

[92] C.A. Regal, M. Greiner and D.S. Jin, Phys. Rev. Lett. 92, 040403 (2004)

[93] B.H. Brandsen and C.J. Joachain, *Physics of Atoms and Molecules*, Longman Ltd (1983)

[94] M. Abramowitz and A. Stegun. *Handbook of mathematical functions*. Dover Publications Inc. New York, 5 edition, 1968.

[95] Wolfram research, The Wolfram function site: www.function.wolfram.com

[96] L.D. Faddeev, *Mathematical Aspects of the Three-Body Problem in Quantum Scattering Theory*. Israel Program for Scientific Translations, Jerusalem.

[97] K. Hepp, Helv. Phys. Acta, Vol. 42, p. 425.

[98] M.A. Baranov, K. Osterloh, and M. Lewnstein, Phys. Rev. Lett. 94, 070404 (1995)

[99] P.J. Lee, C.J. Williams, and P.S. Julienne, Phys. Rev. Lett. 85, 2721 (2000)

[100] V. Bretin, S. Stock, Y. Seurin, and J. Dalibard, Phys. Rev. Lett. 92, 050403 (2004)

[101] S. Stock, Z. Hadzibabic, B. Battelier, M. Cheneau and J. Dalibard, Phys. REv. Lett. 95, 190403 (2005)

[102] T. Nagamiya, Proc. Phys. Math. Soc. Japan 22, 705 (1940)

[103] H. Stachowiak, Acta Univ. Wratislaviensis 12, 93 (1960)

[104] M.D. Girardeau and E.M. Wright, Phys. Rev. Lett. 84, 5691 (2000)

[105] M.D. Girardeau and E.M. Wright, Phys. Rev. Lett. 84, 5239 (2000)

[106] M.D. Girardeau, K.K. Das, and E.M. Wright, Phys. Rev. A 66, 023604 (2002)

[107] K.K. Das, G.J. Lapeyre, and E.M. Wright, Phys. Rev. A 65, 063603 (2002)

[108] K.K. Das, M.D. Girardeau, and E.M. Wright, Phys. Rev. Lett. 89, 170404 (2002)

[109] M.D. Girardeau, Phys. Rev.139, B500 (1965), particularly Secs. 2, 3, and 6